The Younger Dryas climate change

was it caused by an extraterrestrial impact?

Annelies van Hoesel

UTRECHT STUDIES IN EARTH SCIENCES

No. 54

Promotor

Prof.dr. Martyn Drury	Universiteit Utrecht

Co-promotores

Dr. Wim Hoek	Universiteit Utrecht
Dr. Gill Pennock	Universiteit Utrecht

Examination committee

Prof.dr. Achim Brauer	Deutsches GeoForschungsZentrum
Prof.dr. Christian Koeberl	Universität Wien
Prof.dr. Hans Renssen	Vrije Universiteit Amsterdam
Prof.dr. Nick Schryvers	Universiteit Antwerpen
Prof.dr. Jan Smit	Vrije Universiteit Amsterdam

This research was funded by the Focus & Massa program at Utrecht University.

Cover illustration: TEM thin foil from a shocked quartz grain. Smooth microspherules attached-to a larger Si-rich microspherule. The Dinkel river cutting through the coversands at Lutterzand.

ISBN: 978-90-6266-356-9
USES: 54

The Younger Dryas climate change

was it caused by an extraterrestrial impact?

De Jonge Dryas klimaatverandering

werd deze veroorzaakt door een meteorietinslag?

(met een samenvatting in het Nederlands)

PROEFSCHRIFT

ter verkrijging van de graad van doctor aan de Universiteit Utrecht
op gezag van de rector magnificus, prof. dr. G.J. van der Zwaan,
ingevolge het besluit van het college voor promoties
in het openbaar te verdedigen

op woensdag 21 mei 2014 des middags te 12.45 uur

door

Annelies van Hoesel

geboren op 5 juli 1986 te Meppel

Promotor:
Prof. dr. M.R. Drury

Co-promotoren:
Dr. W.Z. Hoek
Dr. G.M. Pennock

Contents

Summary

The Younger Dryas is a brief cold period, corresponding to Greenland Stadial 1 (12,850 - 11,650 years ago; Hoek, 2008; Lowe et al., 2008), which interrupted the deglaciation at the end of the Weichselian Lateglacial in the northern hemisphere. During the Younger Dryas stadial, climate conditions in the northern hemisphere went from almost interglacial conditions (during the Allerød interstadial) back to almost full glacial conditions. The generally accepted hypothesis for the mechanism triggering this return to cold conditions involves re-routing of meltwater from the North American ice cap to the northern Atlantic or Arctic Ocean, disabling the thermohaline circulation and initiating climate cooling, although the exact size, source and route of the meltwater input are still debated. This mechanism is also held responsible for similar cold periods in the climate record.

In 2007, an new explanation for the Younger Dryas cold period was proposed: the Younger Dryas impact hypothesis. According to this hypothesis, one or more extraterrestrial objects hit, or exploded over, the Laurentide Ice Sheet at the onset of the Younger Dryas, resulting in destabilisation of the ice sheet, continent-wide wildfires, the Pleistocene megafaunal extinctions and decline of the prehistoric Clovis culture in North America. Through the destabilisation of the ice sheet, the impact hypothesis provides a unique trigger for the meltwater input that disrupted the ocean thermohaline circulation, and caused the return to cold conditions.
Evidence presented for the Younger Dryas impact hypothesis consisted of peak concentrations of various markers found in sedimentological profiles taken across the Allerød- Younger Dryas boundary at several sites in North America and Europe. These markers originally included magnetic grains with iridium, magnetic microspherules, charcoal, soot, carbon spherules, glass-like carbon containing nanodiamonds, and fullerenes with extraterrestrial helium. Further evidence included nanodiamonds, possibly also the shock-produced form called lonsdaleite, which was found in bulk sediments and in carbon spherules. The hypothesis received a mixed reception and is considered as controversial. Most reported Younger Dryas impact markers are not considered diagnostic evidence for impacts and subsequent studies failed to find peak concentrations in magnetic spherules and iridium or evidence for widespread synchronous wildfires, leaving nanodiamonds as the most promising line of evidence two years after the Younger Dryas impact hypothesis had first been proposed. No shock indicators, such as shocked quartz, which is indicative of a crater forming impact, were reported.

The main objective of this thesis is to test the hypothesis that abrupt climate change at the Allerød-Younger Dryas transition was related to an extraterrestrial impact. Multiple known Allerød-Younger Dryas boundary layers were dated, where necessary, and sampled for the

occurrence of nanodiamonds and shocked quartz. Most sites were located in northwestern and northern central Europe and often contained a palaeosol (either the Usselo or Finow palaeosol) or a thin peat layer. One site from North America, where markers were previously reported, was also investigated.

Although multiple sites have been investigated, both nanodiamonds and shocked quartz were found only in the Usselo horizon at Geldrop Aalsterhut, the Netherlands. These nanodiamonds were found in glass-like carbon, which is a known wildfire product. Assuming that the glass-like carbon was formed during the same fire that created the radiocarbon dated charcoal in the layer, the nanodiamonds post-date the Allerød-Younger Dryas boundary. Only one shocked quartz grain was found. However, based on the current evidence it is not possible to determine whether this shocked quartz grain is related to the Younger Dryas impact event. The grain can also result from a small-scale local impact in the vicinity of the site during the Lateglacial period or earlier, or may be eroded from an older impact layer and re-deposited into the source sediment for the coversand in which the Usselo horizon was formed.
Shocked quartz is a well-known impact indicator, whereas nanodiamonds, on the other hand, are not considered diagnostic of an impact as their formation mechanism is still not completely understood. As the nanodiamonds reported in the Allerød-Younger Dryas boundary layer were found in carbon spherules and glass-like carbon, it has been suggested that the nanodiamonds might have been formed during the wildfires rather than as a result of an impact. Analysis of multiple glass-like carbon and charcoal particles of different ages, however, shows no indication of nanodiamonds. Therefore, wildfire does not seem a convincing alternative explanation for the occurrence of nanodiamonds in the Allerød-Younger Dryas boundary.

In order to prove that a single impact event (multiple airbursts or just one impactor) caused the Younger Dryas, all markers found must be deposited synchronous and date to the onset of the Younger Dryas. This synchronous-site requirement presents five challenges to the Younger Dryas impact hypothesis. Firstly, the exact timing of the Younger Dryas onset is still uncertain and seems to vary regionally. Secondly, many of the terrestrial sites where Younger Dryas impact markers were found have been dated using radiocarbon dating, which introduces additional uncertainties. Thirdly, not all sites have been directly dated or their dates have a high uncertainty. Fourthly, at several sites the sampling thickness or the thickness of the peak in markers leads to a large uncertainty in sample age. Finally, and most critically, there is an age discrepancy of up to two centuries between sites where Younger Dryas impact markers have been found. If the markers are not of the same age, they cannot be related to the same event.

In conclusion, there is no convincing evidence for the occurrence of one or more climate changing extraterrestrial impacts or airbursts at the onset of the Younger Dryas at this point in time. The change in ocean circulation that has been held responsible for the Younger Dryas climate cooling thus probably had a more common trigger, possible inherent to the Earth's system.

Samenvatting

De Jonge Dryas is een korte koude periode aan het einde van de laatste ijstijd en correspondeert met het Greenland Stadial 1 (12.850 – 11.650 jaar geleden). Aan het begin van het Jonge Dryas stadiaal veranderde het klimaat van ongeveer de huidige temperatuur (tijdens het Allerød interstadiaal) terug naar glaciale condities. Deze klimaatverandering wordt over het algemeen toegeschreven aan smeltwater van de Noord Amerikaanse ijskap dat in de Noord Atlantische of Arctische oceaan terecht kwam en daarmee de Warme Golfstroom stopzette. Dit mechanisme wordt ook verantwoordelijk gehouden voor vergelijkbare koude periodes tijdens de laatste en voorgaande ijstijden.

In 2007 werd er een alternatieve hypothese voorgesteld: de Jonge Dryas impact hypothese. Volgens deze hypothese sloegen één of meerdere buitenaardse objecten in of explodeerde boven de Noord Amerikaanse ijskap. Dit zou geresulteerd hebben in destabilisatie van de ijskap, het uitsterven van de Pleistocene megafauna, en het verdwijnen van de Noord Amerikaanse Clovis cultuur. Door middel van de destabilisatie van de ijskap biedt de hypothese een unieke oorzaak voor het smeltwater dat de Warme Golfstroom zou hebben stopgezet waardoor het klimaat weer kouder werd en de Jonge Dryas ontstond.
Het bewijs voor de Jonge Dryas impact hypothese bestond uit piekconcentraties van verscheidene deeltjes gevonden in de Allerød-Jonge Dryas grens op verscheidene locaties. De gevonden deeltjes zijn: magnetische korrels met hoge iridium concentraties, magnetische microbolletjes, houtskool, roet, koolstof bolletjes, glasachtige houtskool met nanodiamanten, en koolstof fullerenen met buitenaards helium. Daarnaast werden nog nanodiamanten gevonden, waaronder mogelijk Lonsdaleïet, de hexagonale polymorf van diamant die voornamelijk door schokmetamorfose gevormd wordt. De meeste deeltjes die naar voren geschoven werden als bewijs voor de hypothese vormen echter geen hard bewijs voor een meteoriet inslag. Behalve de mogelijke Lonsdaleïet deeltjes werden er geen schokmetamorfe deeltjes, indicatief voor een kratervormende inslag, gerapporteerd. Daarnaast lukte het andere onderzoekers niet om de piekconcentraties in magnetische bolletjes en iridium te vinden, en ook het bewijs voor wijdverbreide bosbranden werd onderuit gehaald. Twee jaar nadat de Jonge Dryas impact hypothese werd voorgesteld waren daarom alleen de nanodiamanten overgebleven als veelbelovend bewijs.

Het doel van dit onderzoek is om de hypothese dat de klimaatverandering aan het begin van de Jonge Dryas veroorzaakt werd door een meteorietinslag te testen. Verschillende Allerød-Jonge Dryas overgangen werden bemonsterd, de meesten uit noordwest en noordcentraal Europa waar de Allerød-Jonge Dryas grens herkenbaar is aan een paleobodem (de Usselo en Finow bodems) of een dunne veenlaag. Waar nodig zijn de monsters gedateerd met behulp van de ^{14}C methode.

Slechts op één locatie zijn nanodiamanten en geschokte kwarts, een bekende indicator voor een meteorietinslag, gevonden, namelijk in de Usselo laag van Geldrop Aalsterhut (Nederland). De nanodiamanten werden gevonden in glasachtige koolstofdeeltjes, die echter ook door branden gevormd kunnen worden. Wanneer wordt aangenomen dat deze deeltjes door dezelfde bosbrand zijn gevormd als de gedateerde houtskooldeeltjes uit dezelfde laag, dan blijkt dat de nanodiamant-houdende deeltjes waarschijnlijk pas na het begin van de Jonge Dryas gevormd zijn. Er is slechts één geschokte kwarts korrel gevonden, waardoor het moeilijk vast te stellen is of deze korrel direct gerelateerd kan worden aan de Jonge Dryas impact hypothese. Hoewel de korrel door een meteorietinslag gevormd moet zijn, kan namelijk niet direct bepaald worden wanneer deze inslag heeft plaatsgevonden. Het is ook mogelijk dat de korrel vervormd is tijdens een kleine lokale inslag die eerder is opgetreden, of dat de korrel uit een veel oudere inslag laag komt en na erosie en transport in het dekzand terecht is gekomen.
Terwijl geschokte kwarts een bekende inslagindicator is, worden nanodiamanten niet gezien als doorslaggevend bewijs voor een inslag. Het is namelijk nog onduidelijk hoe nanodiamanten precies worden gevormd. Aangezien de nanodiamanten uit de Allerød-Jonge Dryas grens onder andere gevonden zijn in koolstof bolletjes en glasachtige koolstof, werd er voorgesteld dat deze nanodiamanten wellicht gevormd zijn tijdens een bosbrand en niet als gevolg van een meteoriet inslag. Analyse van glasachtige koolstof en houtskool deeltjes van andere ouderdommen laat echter zien dat nanodiamanten zeldzaam zijn in deze deeltjes. Bosbranden lijken daarmee dus geen aannemelijke alternatieve verklaring voor het voorkomen van nanodiamanten in de Allerød-Jonge Dryas grens.

Om vast te stellen dat een meteorietinslag verantwoordelijk is voor de koude Jonge Dryas periode is het niet alleen nodig om aan te tonen dat de gevonden deeltjes door een meteorietinslag gevormd moeten zijn. De gevonden deeltjes moeten daarnaast ook nog eens in de tijd gecorreleerd kunnen worden met het begin van de Jonge Dryas. Een vijftal problemen is hieraan gerelateerd. Ten eerste lijkt de Jonge Dryas klimaatverandering op verschillende locaties op een ander moment te beginnen. Ten tweede zijn veel van de locaties waar de bewijzen voor de Jonge Dryas impact hypothese zijn gevonden gedateerd met behulp van ^{14}C dateringen die eerst nog gekalibreerd moeten worden naar normale kalender jaren. Ten derde zijn niet alle locaties gedateerd en op sommige locaties die wel gedateerd zijn is de onzekerheid erg hoog. Ten vierde resulteert de dikte van de bemonsterde laag soms in een bredere spreiding in de mogelijke ouderdom. Als laatste, en wellicht het meest belangrijkst, is er een verschil in ouderdom tussen de gevonden bewijzen op verschillende locaties en wanneer de deeltjes niet dezelfde ouderdom hebben, kunnen ze moeilijk gerelateerd zijn aan eenzelfde inslag.

Uiteindelijk kan er geconcludeerd worden dat er momenteel geen bewijs is voor de hypothese dat één of meerdere meteorietinslagen verantwoordelijk zijn voor de Jonge Dryas koude periode. De oorzaak van de klimaatverandering aan het begin van de Jonge Dryas moet dus waarschijnlijk gewoon gezocht worden in een aardse oorzaak zoals de verandering in oceaanstroming.

Chapter 1

General introduction

1.1 The Younger Dryas cold period

Originally, the Younger Dryas (or Late Dryas) was identified as a palynological zone in Scandinavia (Jessen and Jonassen, 1935) and subsequently recognised in terrestrial records in other parts of Europe (e.g. van der Hammen, 1951). Although the terminology was based on terrestrial biostratigraphy, the classification later also included elements of climatostratigraphy and chronostratigraphy, and the Younger Dryas was recognised in marine records and ice cores (Björck et al., 1998). Based on radiocarbon dating of the biostratigraphic zone boundaries in southern Scandinavia, Mangerud et al. (1974) proposed a chronostratigraphy in which the Younger Dryas was dated to 11,000 – 10,000 ^{14}C yrs BP. However, differences in age arise when comparing biostratigraphic zones from one region to the other because of the transgressive nature of climate change and vegetation response in Europe (see Björck et al., 1998; Hoek, 2008; Lowe et al., 2008). These differences get even larger when comparing different parts of the world, for example because of the phase lagged climatic pattern between the northern and southern hemisphere (Lowe et al., 2008; Lowell and Kelly, 2008).

In this thesis, the Younger Dryas is referred to as the brief cold period which interrupted the deglaciation at the end of the Weichselian Lateglacial in the Northern hemisphere, and roughly corresponds to Greenland Stadial 1 (12.85 - 11.65 ka, Hoek, 2008; Lowe et al., 2008; Lohne et al., 2013) (see also figure 1.1). During the Younger Dryas, climate conditions in the northern hemisphere went from almost interglacial conditions (during the Allerød interstadial) back to almost full glacial conditions. Similar cold periods were also observed during some of the previous deglaciations and might be an intrinsic part of the deglaciation process (Sima et al., 2004; Carlson, 2008; Cheng et al., 2009; Broecker et al., 2010; Denton et al., 2010).

The climate change at the onset of the Younger Dryas occurred in a series of steps (Alley, 2000) and, although defined in terrestrial sequences, is best studied in the Greenland ice cores. The GISP2 ice core shows that sea salt, sulphate, and crustal fluxes increased dramatically over a decade at the onset of the Younger Dryas, reflecting significant re-organisation of the atmosphere (Mayewski et al., 1993). High-resolution ice core data with an annual resolution from the NGRIP ice core show an even more dramatic change: the transition in deuterium excess, another proxy for atmospheric re-organization, occurred in one year (Steffensen et al., 2008). Other proxies, however, show a more gradual change. The annual layer thickness of the NGRIP ice core, a proxy for precipitation rate, shows a 33% decrease in annual layer thickness over a

period of 152 years. The decrease in temperature at the NGRIP site, as recorded in the $\delta^{18}O$, even lasted over two centuries (Steffensen et al., 2008).
The cause of the Younger Dryas cold period is still not entirely understood (Broecker et al., 2010; Fiedel, 2011). Several hypotheses have been suggested, including a change in atmospheric circulation, a change in solar irradiation, and even a supernova or solar proton pulse (Renssen et al., 2000; Brakenridge, 2011; Fiedel, 2011; LaViolette, 2011). The main hypothesis for the mechanism triggering the Younger Dryas involves changes in the Atlantic Ocean meridional overturning circulation (or thermohaline circulation). Currently, deep water formation in the North Atlantic is aided by the presence of denser, high salinity water that sinks to deeper regions. During this process, heat is released to the atmosphere, effectively warming the atmosphere and resulting in a milder climate in western and northern Europe. The meridional overturning circulation was also active during the glacial periods. However, at times when meltwater from the ice caps to the North Atlantic increased, the input of fresh water decreased the salinity of the sea water, effectively stopping, or slowing, the deep water formation and resulting in cooling of the climate. When the fresh water input decreased, the salinity increased and the circulation was eventually re-established. This mechanism has been termed the salt oscillator and it was suggested that this mechanism was responsible for not only the Dansgaard-Oeschger cycles, but also the Younger Dryas cooling (Broecker et al., 1990; Mangerud et al., 2010). The exact route and origin of the meltwater that caused the Younger Dryas is, however, still uncertain.
Initially, it was suggested that rerouting of meltwater from pro-glacial Lake Agassiz from the Mississippi outlet to the Gulf or Lawrence, possibly in a catastrophic outflow, triggered the change in ocean circulation (Broecker et al., 1989). After problems with the eastern outflow hypothesis, a northern outflow of Lake Agassiz, through the Mackenzie valley to the Arctic Ocean was suggested (Tarasov and Peltier, 2005; Teller et al., 2005; Tarasov and Peltier, 2006; Condron and Winsor, 2012). Another option is that the cooling is not necessarily related to Lake Agassiz but involves general melting and iceberg calving of the northern hemisphere ice sheets, which is typical of deglaciation periods (Denton et al., 2010). There is thus still no consensus on the source of the meltwater that caused the Younger Dryas climate change (Broecker et al., 2010; Carlson and Clark, 2012; Lowell et al., 2013; Teller, 2013).

1.2 The Allerød-Younger Dryas boundary

The Allerød-Younger Dryas boundary layer can be identified in a wide range of sedimentary records, often based on changes in pollen (vegetation), oxygen isotopes and other indicators of climate change. In some cases, the Allerød-Younger Dryas boundary is clearly visible as a marker horizon, for example by the presence of the Black Mat (North America) or the buried Usselo soil horizon (Europe).

1.2.1 North America: the Black Mat

At two-thirds of the geoarchaeological sites spanning the Late Glacial-Holocene transition in the United States a dark grey to black organic rich layer, the so-called Black Mat, is present (Haynes Jr., 2008). The Black Mat includes palaeosols, algal mats and pond sediments that formed as a result of the higher water table during the Younger Dryas cold period. Radiocarbon dating places the start of the major deposition of the Black Mat at the onset of the Young Dryas, although Allerød ages have also been found for a few Black Mat sites (Haynes Jr., 2008). The Allerød-Younger Dryas boundary is thus situated at the base of the Black Mat. At some sites,

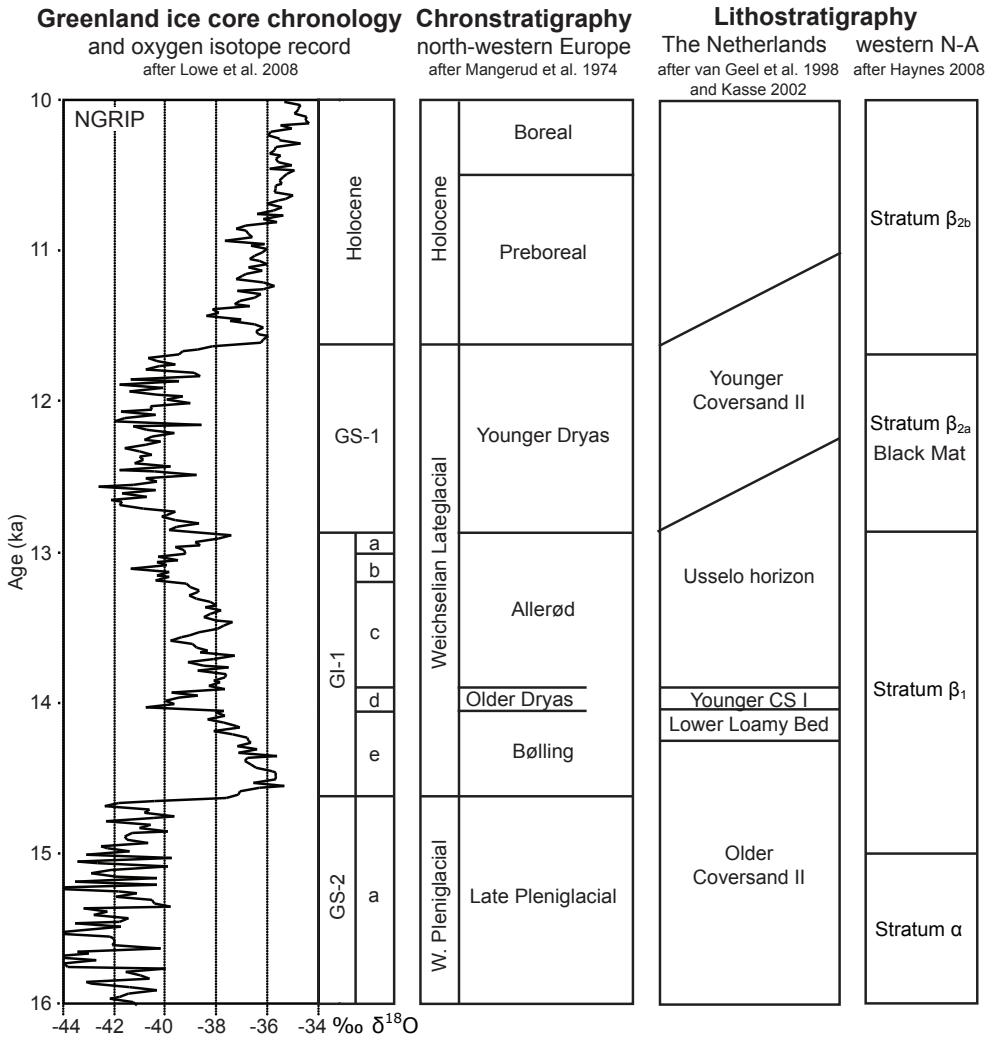

Figure 1.1. Typical lithostratigraphy in the north western European coversand area and Black Mat regions in North America in relation to the chronostratigraphy and the Greenland ice core chronology. Outside the Netherlands the Finow palaeosol can sometimes be found instead of the Usselo horizon.

the late Allerød was a period of erosion. At these sites, a hiatus of up to two millennia is present between the Black Mat and the underlying sediments. At other sites, the hiatus between the Black Mat and earlier deposits only spans a decade, or even less (Haynes Jr. et al., 1999).

1.2.2 Europe: the Usselo horizon

In the northern part of western and central Europe two palaeopedological marker horizons for the Allerød-Younger Dryas boundary exist: The Usselo horizon – also referred to as the Usselo layer, bed, or (palaeo)soil – and the Finow soil. The Usselo horizon is a 5 to 20 cm thick palaeosol in aeolian coversand deposits characterized by slight humus accumulation, the presence

of charcoal, and bleaching of the quartz grains (Kaiser et al., 2009). This horizon is often visible as a thin grey-ish top layer above the lighter, bleached part. The Finow soil represents a 5 to 30 cm thick brownish, charcoal-bearing weathering horizon in aeolian coversand deposits (Kaiser et al., 2009). About half of the Usselo and Finow paleosol horizons have conspicuous amounts of small macroscopic charcoal (0.1-0.5 mm) dispersed in the soil matrix (Kaiser et al., 2009). The Usselo horizon is found across the European sandbelt area, whereas the Finow soil is mostly confined to the Brandenburg area (north-eastern Germany) and the Torun basin (central Poland), where the two palaeosol types are found in close proximity of each other (Kaiser et al., 2009 figure 7).
The European sandbelt forms a continuous aeolian deposit found in the Netherlands to Russia; some deposits are also found in Great Britain. In the Netherlands, these deposits are divided into the Older and Younger Coversands (van Geel et al., 1989; Kasse, 2002; Kaiser et al., 2009). The Younger Coversands are divided into the Younger Coversand I, which formed around the Older Dryas, and the Younger Coversand II, which formed during the Younger Dryas (figure 1.1). During the warmer Allerød period, the return of forest vegetation stabilised the landscape and aeolian activity ceased (Hoek, 1997; Kasse, 2002). Soil formation in the higher and dryer parts of the coversand led to the formation of the Usselo and Finow soil horizons. In the wetter areas, thin peat layers were formed simultaneously (e.g. Kaiser et al., 2006). After the forest vegetation disappeared as a result of the Younger Dryas cold period, aeolian activity re-started and the soils were buried, forming a palaeosol. Extensive dating of the both palaeosols has shown that both horizons are not strictly of Allerød age, as has been assumed earlier, but also include Younger Dryas and even one or two early Holocene ages (Kaiser et al., 2009). The Usselo horizon and Finow soil thus provide marker horizons separating the pre- and post Allerød coversand deposits. The Usselo horizon differs from the Black Mat in that the top of the horizon coincides with the Allerød-Younger Dryas boundary rather than the base. It must be noted though, that the Usselo and Finow palaeosols were at the surface during their entire formation period and thus represent a time period of at least several hundred years, which, on average, includes both the late Allerød and early Younger Dryas. In addition, some mixing and disturbance of the sediment often occurred during and after the formation of the Usselo horizon (Kaiser et al., 2009).

1.3 The Younger Dryas impact hypothesis

According to the Younger Dryas impact hypothesis, one or more extraterrestrial objects hit, or exploded over, the Laurentide Ice Sheet at the onset of the Younger Dryas, possibly at a location near the current Great Lakes area (Firestone et al., 2007). Besides initiating several short term cooling mechanisms, the force and extreme heat generated by the impact, according to this hypothesis, would have destabilized the ice sheet, yielding enough meltwater to disrupt ocean circulation and hence initiate the observed climate cooling that led to the Younger Dryas period. This hypothesis (Firestone et al., 2007) thus provides a unique trigger for the generally accepted meltwater re-routing mechanism that was probably responsible for the Younger Dryas cooling. In addition, Firestone et al. (2007) claim that the Younger Dryas impact event resulted in extensive or continent-wide wildfires, the Pleistocene megafaunal extinctions and decline of the prehistoric Clovis culture in North America.
The research that eventually led to the formulation of the Younger Dryas impact hypothesis started in the 1990's with the dissertation research of William Topping. In 2001 he and Richard

Firestone published a paper that suggested that a supernova resulted in a catastrophic nuclear irradiation event 12.5 ka (Firestone and Topping, 2001). This hypothesis was based on anomalously young ^{14}C dates at paleoindian Clovis sites in the Great Lakes area, magnetic micrometeorite-like particles and spherules, cosmic ray tracks in chert, depletion in ^{235}U (uranium), and high ^{239}Pu (plutonium) concentrations (Firestone and Topping, 2001). Around the same time Tollmann (2001) suggested that an extraterrestrial impact at 13 ka had caused the megafaunal extinctions, extensive wildfires (first proposed by Kloosterman, 1976), as well as the Allerød warm period. The paper by Tollman (2001) is however highly speculative and only tenuously based on any evidence.

The supernova hypothesis by Firestone and Topping was criticized (Southon and Taylor, 2002) and in a response Firestone stated that "the event as published was too extreme to be reasonable" but that a smaller catastrophe might still have occurred (Firestone, 2002). In 2007 Firestone, together with 25 other researchers, presented the Younger Dryas impact hypothesis at the AGU Joint Assembly shortly followed by their paper (Firestone et al., 2007). The group investigated the Allerød-Younger Dryas boundary at multiple sites in North America, including six Black Mats, and one site in Europe, containing the Usselo horizon. The new evidence included peak concentrations of magnetic grains with iridium, magnetic microspherules, charcoal, soot, carbon spherules, glass-like carbon containing nanodiamonds, and fullerenes with extraterrestrial helium (Firestone et al., 2007). Further evidence included nanodiamond, possibly also its shock produced form called lonsdaleite, which were found in bulk sediments and in carbon spherules (Kennett et al., 2009b). The hypothesis received mixed receptions (Dalton, 2007; Kerr, 2007; Kerr, 2008; Kerr, 2009; Morrison, 2010) as many of the reported markers are not considered diagnostic evidence for an extraterrestrial impact (French and Koeberl, 2010). Furthermore, subsequent studies failed to find peak concentrations in magnetic spherules and iridium or evidence for widespread wildfires (Marlon et al., 2009; Paquay et al., 2009; Surovell et al., 2009), which left nanodiamonds as the most promising line of evidence two years after the Younger Dryas impact hypothesis had first been proposed. Nanodiamonds can, however, be formed under a wide range of circumstances and their occurrence and origin in natural sediments is not yet entirely understood (French and Koeberl, 2010). For example, it has been suggested that the nanodiamonds at the Allerød-Younger Dryas boundary might have been formed in wildfires (Paquay et al., 2009).

1.4 Aim and outline of this thesis

The main objective of this thesis is to test the hypothesis that abrupt climate change at the Allerød-Younger Dryas transition was related to an extraterrestrial impact as suggested by Firestone et al. (2007). To confirm that an extraterrestrial impact caused the Younger Dryas climate change a three-fold approach is necessary. It must be shown that:

1 the presented evidence is reproducible and diagnostic of an impact event;

2 the age of the sedimentary layers in which the markers were found point to the moment in time exactly at or just before the onset of the Younger Dryas;

3 the extraterrestrial impact event triggered the mechanism responsible for the Younger Dryas climate cooling.

The main focus of this thesis concerns the first two of these problem statements, namely testing whether there is evidence to support the claim that there was indeed an extraterrestrial impact event and whether this event occurred at the onset of the Younger Dryas. Advanced electron microscopy methods were used to investigated multiple known Allerød-Younger Dryas boundary layers from Europe, where necessary dated using AMS radiocarbon dating, for the occurrence of shocked quartz, a well-known impact indicator, and nanodiamonds. To investigate the origin of the nanodiamonds and their use as an impact indicator, charcoal and glass-like cabron particles were analysed using transmission electron microscopy. The results are presented in the following chapters.

Chapter 2 provides a detailed discussion of the different lines of evidence that have been used to support the Younger Dryas impact hypothesis, focusing on evidential reproducibility and use of the different markers as an impact indicator. In addition the nature of the proposed impact event, as well the related events – extensive wildfires, climate change, megafaunal extinctions and disappearance of the Clovis culture – are discussed.

Chapter 3 presents a case study of the Geldrop Aalsterhut fieldsite in the southern Netherlands. Using scanning and transmission electron microscopy, the Usselo horizon at this site was investigated for the occurrence of charcoal, glass-like carbon, carbon spherules, nanodiamonds and magnetic spherules. ^{14}C dating of 14 individual charcoal particles from the Usselo horizon provides insight in the use of ^{14}C dating to determine the age of the Usselo horizon and the results are compared to the ^{14}C ages of other sites where nanodiamonds have been reported.

Chapter 4 explores the origin of nanodiamonds, as well as the formation of glass-like carbon, through analysis of various charcoal and glass-like carbon particles of different ages. In addition several Allerød-Younger Dryas boundary layers, including an annually laminated lake record, were investigated for the occurrence of nanodiamonds.

Chapter 5 presents the results of an analysis of the quartz fraction of different Allerød-Younger Dryas boundary layers for the occurrence of shocked quartz using a new scanning electron microscopy approach.

Chapter 6 discusses the results of the previous chapters and elaborates on the origin of the Allerød-Younger Dryas boundary nanodiamonds and the timing of the proposed impact event.

Chapter 7 summarises the main conclusions of this thesis and provides suggestions for further research.

All microscopy work in this thesis was performed by the author, except for the colour-CL images in figure 5.6 which were made by Maartje Hamers. The charcoal reflectance analysis, which was done by Freek Braadbaart, who also provided the Rennes and Flevoland samples. Radiocarbon dating was performed by the Hans van der Plicht and the Groningen AMS facility. Alexander Andronikov kindly provided the Murray Springs samples. Recent carbon spherules were provided by Nick Scrhijvers.

Chapter 2

The Younger Dryas impact hypothesis: a critcal review.

The Younger Dryas impact hypothesis suggests that multiple extraterrestrial airbursts or impacts resulted in the Younger Dryas cooling, extensive wildfires, megafaunal extinctions and changes in human population. After the hypothesis was first published in 2007, it gained much criticism, as the evidence presented was either not indicative of an extraterrestrial impact or not reproducible by other groups. Only three years after the hypothesis had been presented, a requiem paper was published. Despite this, the controversy continues. New evidence, both in favour and against the hypothesis, continues to be published.

In this review we briefly summarize the earlier debate and critically analyse the most recent reported evidence, including magnetic microspherules, nanodiamonds, and iridium, shocked quartz, scoria-like objects and lechatelierite. The subsequent events proposed to be triggered by the impact event, as well as the nature of the event itself, are also briefly discussed. Although convincing evidence for the hypothesis that multiple synchronous impacts resulted in massive environmental changes at ~12,900 yrs ago remains debatable, we conclude that some evidence used to support the Younger Dryas impact hypothesis cannot fully be explained at this point in time.

This chapter has been published as part of: van Hoesel, A., Hoek, W.Z., Pennock, G.M., Drury, M.R. (2014) The Younger Dryas impact hypothesis: a critical review. Quaternary Science Reviews 83, 95-114.

2.1. Introduction

In 2007, a group of researchers led by Firestone (2007) proposed a unique mechanism for the onset of the Younger Dryas cold period that followed the Allerød interstadial near the end of the Last Glaciation (Hoek, 2008). According to the Younger Dryas impact hypothesis, one or more extraterrestrial objects hit, or exploded over, the Laurentide Ice Sheet - possibly at a location near the current Great Lakes area – at the onset of the Younger Dryas, ~12,900 yrs ago (Firestone et al., 2007). Besides initiating several short term cooling mechanisms, the force and extreme heat generated by this impact, according to this hypothesis, would have destabilized the ice sheet, yielding enough meltwater to disrupt ocean circulation and hence initiate the observed long term climate cooling. This hypothesis (Firestone et al., 2007) thus provides a unique trigger for the generally accepted meltwater re-routing mechanism which was probably responsible for the Younger Dryas cooling. This meltwater re-routing mechanism includes re-routing of meltwater to the northern Atlantic or Arctic Ocean, disabling the thermohaline circulation and initiating climate cooling (Broecker et al., 1989; Tarasov and Peltier, 2005; Broecker et al., 2010; Murton et al., 2010; Fiedel, 2011). In addition to the rapid climate change, Firestone et al. (2007) also claim that the Younger Dryas impact accounts for extensive wildfires, Pleistocene megafaunal extinctions and decline of the prehistoric Clovis culture in North America. Evidence presented for the Younger Dryas impact hypothesis (Younger Dryas impact hypothesis) consists of peak concentrations of various markers found in profiles taken across the Allerød- Younger Dryas boundary at several sites in North America and one in Europe. These markers included magnetic grains and microspherules, charcoal, carbon spherules and glass-like carbon, iridium concentrations, and fullerenes with extraterrestrial helium (Firestone et al., 2007).

Although the Younger Dryas impact hypothesis gained further support from a study in 2009 reporting nanodiamonds at the Allerød- Younger Dryas boundary (Kennett et al., 2009a; Kennett et al., 2009b), the hypothesis was received with scepticism and is still considered as controversial (Dalton, 2007; Kerr, 2007; Pinter and Ishman, 2008; Dalton, 2009; French and Koeberl, 2010; Kerr, 2010; Jones, 2013). Most reported Younger Dryas impact markers are not considered diagnostic evidence for impacts (French and Koeberl, 2010). These non-diagnostic markers include different forms of carbon, magnetic grains and spherules and fullerenes. Furthermore, researchers trying to reproduce the work often failed to find nanodiamonds or peaks in magnetic spherule concentration (Surovell et al., 2009; Daulton et al., 2010). Four years after publication of the hypothesis, a review paper titled "The Younger Dryas impact hypothesis: A requiem" argued against all of the evidence presented for the Younger Dryas impact hypothesis (Pinter et al., 2011). However, this "requiem" review paper left several questions unanswered: for example, the recent work on a South American site (Mahaney et al., 2010a; Mahaney et al., 2010b; Mahaney et al., 2011), although mentioned, is not discussed in any detail and the conclusion that the reported nanodiamonds were probably misinterpreted seems to ignore earlier reports by other independent researchers (Tian et al., 2011). In addition, convincing alternative explanations for the occurrence of these nanodiamonds in the Allerød- Younger Dryas boundary are lacking. In this review we address some of these outstanding questions in the light of the most recent research on the topic (e.g. Andronikov et al., 2011; Marshal et al., 2011; Bunch et al., 2012; Fayek et al., 2012; Israde-Alcántara et al., 2012; Pigati et al., 2012; Wittke et al., 2013) and discuss the arguments both in favour of and against the different lines of evidence in detail. The subsequent events supposedly triggered by the impact event and the nature of the event itself are also briefly discussed.

2.2. Summary of data for and against the Younger Dryas impact hypothesis

To substantiate their claim of an extraterrestrial impact at the Allerød- Younger Dryas boundary, Firestone et al. (2007) report evidence from a wide range of sites, predominantly in North America. Most of their sites contain the so-called Black Mat: a dark grey to black layer with high organic content formed during the early Younger Dryas (Haynes Jr., 2008). Other samples were taken from the rims of several of the Carolina Bays, elliptical depressions that Firestone et al. (2007) relate to the impact. An impact origin for the bays, however, is unlikely as the bays were not formed instantly, furthermore, there is evidence that the bays were formed before the Younger Dryas (Brooks et al., 2010; Pinter et al., 2011). Only one of the sites analysed by Firestone et al. (2007) is located outside of North America, namely Lommel (Belgium), where the Usselo horizon was sampled. The Usselo horizon is a buried soil horizon formed during the late Allerød to early Younger Dryas and is widespread in the European coversand area (Kaiser et al., 2009). Like the Black Mat, the Usselo horizon thus approximately marks the onset of the Younger Dryas in the sedimentary record. In later studies, sites located in South America and the Middle East were also investigated (Mahaney et al., 2010a; Bunch et al., 2012). Figure 2.1 gives an overview of all the sites at which Younger Dryas impact hypothesis markers have been reported. Firestone et al. (2007) report peak concentrations of a wide range of markers across the Allerød- Younger Dryas boundary. The main markers they report include "magnetic grains with iridium, magnetic microspherules, charcoal, soot, carbon spherules, glass-like carbon containing nanodiamonds, and fullerenes with ET [extraterrestrial] helium". Of the markers put forward by Firestone et al. (2007), only elevated iridium (Ir) concentrations are commonly used as an impact

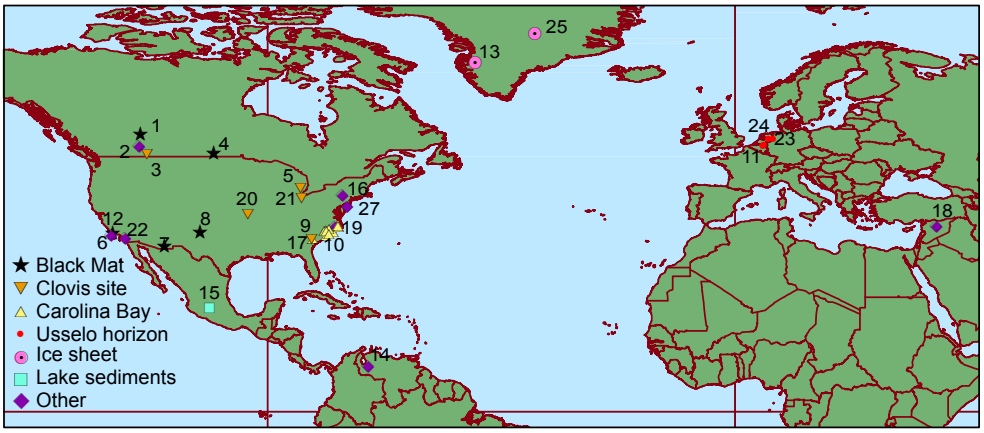

Figure 2.1. Overview of all the sites where different Younger DryasI markers have been reported. 1. Chobot[a,b,r] 2. Morley[a] 3. Wally's beach[a] 4. Lake Hind[a,b] 5. Gainey[a,r] 6. Daisy Cavea 7. Murray Springs[a,b,c,d,e,f,q,s] 8. Blackwater Draw[a,g,h,i,q,s] 9. Topper[a,b,g,h,i,q] 10. Carolina bays[a,g] 11. Lommel[a,g,i,q,s] 12. Arlington Canyon[d,k,l,q] 13. Kangerlussuaq[m] 14. Mucubaji[n] 15. Lake Cuitzeo[o,q] 16. Melrose[p,q,s] 17. Blackville[a,p,q] 18. Abu Hureyra[p,q] 19. Barber Creek[q] 20. Big Eddy[q] 21. Sheridan Cave[q,s] 22. Talega[q] 23. Lingen[q] 24. Ommen[q]. 25. GISP2[r] 26. Newtonville[s]. Different type of sites or sedimentary archives are indicated by different symbols.

[a]Firestone et al. (2007); [b]Kennett et al. (2009a); [c]Haynes et al. (2010); [d]Daulton et al. (2010); [e]Fayek et al. (2012); [f]Pigati et al. (2012); [g]Paquay et al. (2009); [h]Surovell et al. (2009); [i]LeCompte et al. (2012); [j]Tian et al. (2010); [k]Kennett et al. (2008, 2009b); [l]Scott et al. (2010); [m]Kurbatov et al. (2010); [n]Mahaney et al. (2009; 2010; 2011); [o]Israde-Alcantara et al. (2012); [p]Bunch et al. (2012); [q]Wittke et al. (2013b); [r]Petaev et al. (2013); [s]Wu et al. (2013)

indicator (Tagle and Hecht, 2006; French and Koeberl, 2010; Koeberl et al., 2012). Fullerenes with extraterrestrial helium on the other hand, are considered controversial and have not been confirmed independently at any known impact site (French and Koeberl, 2010). Charcoal, soot, carbon spherules and glass-like carbon are only indicative of biomass burning, regardless of what initiated the fires. As fullerenes, charcoal or soot cannot be used as supportive evidence for an impact, they are not discussed in further detail. Although carbon spherules and glass-like carbon are also not indicative of an impact either, they are briefly discussed as nanodiamonds have been reported to occur in these particles. This review focuses on the proposed impact markers that are currently still part of the debate: magnetic spherules, the recently reported scoria-like objects and lechatelierite, Ir and other platinum group elements (PGEs), shocked quartz, and nanodiamonds. In this section the occurrence of these markers and their relevance as indicators of the Younger Dryas impact event will be discussed in detail.

2.2.1. Magnetic microspherules

Spherules, both magnetic and non-magnetic, are known to occur in distal ejecta layers related to extraterrestrial impacts (French and Koeberl, 2010; Glass and Simonson, 2012), they are formed by melting of crustal material heated by an airburst or crater forming impact. Microspherules can, however, also form through volcanism, as meteorite ablation debris (cosmic spherules), and through various sedimentary, diagenetic and artificial processes (French and Koeberl, 2010; Glass and Simonson, 2012). The presence of microspherules is, therefore, not considered diagnostic evidence for an extraterrestrial impact (French and Koeberl, 2010). The impact origin of the microspherules needs to be confirmed by other lines of evidence, such as the presence of meteoritic components, evidence of shock metamorphism or a characteristic composition. Other, non-diagnostic, indications that a spherule-rich layer might be impact related are: the absence of similar spherules in the rest of the sedimentary sequence, the presence of rare splashform shapes indicative of melting, such as teardrops or dumbbells, the presence of vesicles in the spherules indicative of melting, crystallisation structures developed inward from the rim of the spherule, the absence of other volcanic material, a chemical composition similar to the target rock and the absence of exotic compositions (French and Koeberl, 2010; Glass and Simonson, 2012).

Firestone et al. (2007) reported a distinct peak in magnetic grain and microspherule concentrations across the Allerød- Younger Dryas boundary at most of their sites. Whereas magnetic grains are not reported at known impact layers and quickly left the Younger Dryas impact debate, the magnetic spherules remain one of the major markers used to support the Younger Dryas impact hypothesis (Bunch et al., 2012; Israde-Alcántara et al., 2012; LeCompte et al., 2012; Wittke et al., 2013). Scanning electron microscopy (SEM) imaging shows that these spherules often have dendritic or polygonal surface patterns. In addition to the patterned spherules, smooth spherules have also been reported as Allerød- Younger Dryas boundary spherules (Bunch et al., 2012; Israde-Alcántara et al., 2012).The patterned surfaces are interpreted as indicative of melting and rapid quenching, and therefore used to argue in favour of an impact-related origin Younger Dryas impact hypothesis (Bunch et al., 2012; Israde-Alcántara et al., 2012; LeCompte et al., 2012; Mahaney et al., 2013; Wittke et al., 2013).

LeCompte et al. (2012), using SEM, estimated which percentage of the total magnetic spherule count at the Allerød- Younger Dryas boundary contained quench-like surface microstructures. At the Blackwater Draw site 80% of spherules have quench structures while at the Topper site,

where spherule counts were lower, only 25% of spherules have quench textures. The authors do not explain this difference, but it might be just natural variation in spherule abundances. Only these quench-texture spherules in the Allerød- Younger Dryas boundary were taken into account in the spherule counts for the Allerød- Younger Dryas boundary by LeCompte et al. (2012). Unfortunately LeCompte et al. (2012) do not report the percentage of quench textured spherules within the sediment layers overlying and underlying the Allerød-Younger Dryas boundary but instead use the total spherule count as an upper limit for these layers. Therefore it is not known if the Allerød- Younger Dryas boundary percentages of quench textured spherules are anomalous for these sites or whether the older and younger layers contain the same percentage of quench-texture spherules and just fewer spherules in total. In order to state that the occurrence of quench texture spherules in the Allerød-Younger Dryas boundary is anomalous, and possibly indicative of a single event, the relative amount of quench spherules in the rest of the section should also be analysed.

The chemical composition of the magnetic spherules found at the Allerød-Younger Dryas boundary is another characteristic of the spherules which is used as an argument in favor of an impact related origin (Bunch et al., 2012; Israde-Alcántara et al., 2012; Wittke et al., 2013). Firestone et al. (2007) argue that geochemical analyses of their Allerød- Younger Dryas boundary spherules show that the spherules are non-volcanic in origin and suggest an extraterrestrial origin. The other studies (Bunch et al., 2012; Israde-Alcántara et al., 2012; Wittke et al., 2013) also argue that the Allerød-Younger Dryas boundary spherules are not of volcanic origin, and show that their spherules have a heterogeneous composition similar to that of impact ejecta. In addition Bunch et al. (2012) show that the rare earth elements (REEs) of the Allerød- Younger Dryas boundary magnetic spherules are terrestrial. They therefore argue that the Allerød- Younger Dryas boundary magnetic spherules must consist of crustal material that melted as a result of an extraterrestrial impact or airburst (Bunch et al., 2012; Israde-Alcántara et al., 2012; Wittke et

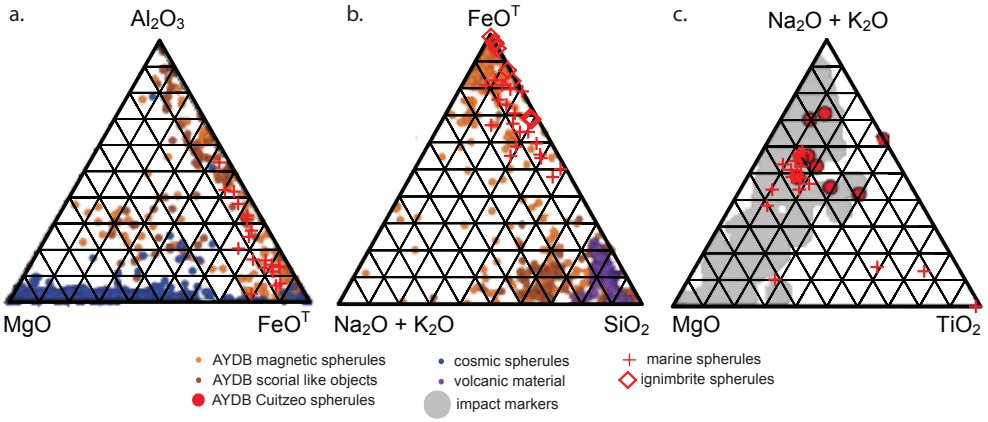

Figure 2.2. Comparison of the chemical composition of Allerød-Younger Dryas boundary magnetic spherules to other types of magnetic spherules: a. cosmic (Bunch et al. 2012, Fig. 3a) b. volcanic (Bunch et al. 2012, Fig. 3c) and c. impact material (Israde-Alcantara et al. 2012, Fig. 6c). We plotted the chemical composition of magnetic spherules from deep sea sediments of non-impact origin (Franke et al., 2007) and spherules found in volcanic ignimbrites (Grebennikov, 2011; Grebennikov et al., 2012) in these diagrams for comparison. This comparison shows that magnesium rich compositions associated with a cosmic origin are not found in spherules from the Allerød-Younger Dryas boundary, or in older sediments. The spherules from the older marine sediments as well as the ignimbrite spherules have a similar composition to the Allerød-Younger Dryas boundary magnetic spherules. This comparison shows that the Allerød-Younger Dryas boundary spherules are not unique to an impact and might have a different origin.

al., 2013). The data of Bunch et al. (2012) also show that the Allerød-Younger Dryas boundary objects (including the magnetic spherules) from the Abu Hureyra site differ in composition from those of the Melrose and Blackville site, suggesting a different source for the material.
The combination of microstructural features (quench textures) and composition of the magnetic spherules are thus used as arguments to support the Younger Dryas impact hypothesis. Other processes, such as meteorite ablation or volcanism, could, however, also be responsible for the melt and quench features (Weixin Xu et al., 1994; Franke et al., 2007; Itambi et al., 2010; Grebennikov, 2011; Grebennikov et al., 2012). Indeed, magnetic microspherules with dendritic surface patterns have also been found at other locations, in sediments of different ages. These spherules are arguably of volcanic or cosmic origin rather than impact related (Weixin Xu et al., 1994; Franke et al., 2007; Itambi et al., 2010; Grebennikov, 2011). In figure 2.2 we compare the composition of some of these non- Allerød-Younger Dryas boundary quench spherules to the composition of the Allerød-Younger Dryas boundary spherules. This comparison shows that some of these older magnetic spherules (Franke et al., 2007; Grebennikov, 2011) have a composition similar to those of the Allerød-Younger Dryas boundary magnetic spherules (figure 2.2). The marine spherules were found in three cores taken in the Southern Atlantic Ocean from sediments dated to approximately 65,000 and 120,000 yrs ago and are interpreted as volcanic in origin (Franke et al., 2007). No known impacts occurred at these times (Earth Impact Database, http://www.passc.net/EarthImpactDatabase/index.html, accessed January 2013). The composition and age of these marine magnetic spherules suggests that the combination of quench textures and composition of the Allerød-Younger Dryas boundary is not unique to the Allerød-Younger Dryas boundary spherules or impact spherules and therefore should not be used to argue in favour of an impact origin for the Allerød-Younger Dryas boundary material. In addition, Bunch et al. (2012) only compared the Allerød-Younger Dryas boundary spherules to silica-rich volcanic material, while iron-rich spherules have also been related to volcanic activity (Franke et al., 2007; Grebennikov, 2011; Grebennikov et al., 2012). The chemical composition of these ignimbrite spherules overlaps with some of the iron-rich Allerød-Younger Dryas boundary spherules (figure 2.2). Although there is no known large-scale volcanic activity at the onset of the Younger Dryas, there were two large volcanic eruptions in the centuries prior to the proposed timing of the Younger Dryas impact event: the Glacier Peak eruption in western North America (Gardner et al., 1998; Kuehn et al., 2009) and the Laacher See eruption in western Europe (Schmincke et al., 1999; Litt et al., 2003). It is possible that some of the volcanic material has been incorporated into the Black Mat, the Usselo Horizon or other sites investigated for Younger Dryas impact markers (see also section 5), although Wittke et al. (2013) report that they found no tephra in the Usselo horizon.
Another type of spherule reported as evidence for the Younger Dryas impact hypothesis is the framboidal type (Fayek et al., 2012; Israde-Alcántara et al., 2012). Framboids typically consist of spherical clusters of euhedral microcrystals (Sawlowicz, 1993a) and can have a wide range of possible origins, such as algae activity (Pinter et al., 2011) or anoxic conditions (Israde-Alcántara et al., 2012) and are thus not indicative of impacts. The larger framboidal spherules (>400 μm) found by Fayek et al. (2012) were contained in a glassy iron-oxide-rich matrix. Fayek et al. (2012) suggest that the framboids they found at Murray Springs are similar to those found in several types of chondritic meteorites and thus originated from a high velocity impact (Fayek et al., 2012). However, when they plotted in a graph and compared with known impact material (Fayek et al., 2012, figure 4), the chemistry of the Allerød-Younger Dryas boundary spherules does

not overlap with that of the plotted impact material, which suggests that the framboids are not impact related.

Pinter and Ishman (2008) argue that the peak concentrations in magnetic spherules at the Allerød-Younger Dryas boundary found by Firestone et al. (2007) have nothing to do with an extraterrestrial impact and suggested that the magnetic microspherules are consistent with the accumulation of micrometeoritic ablation fallout, or 'meteoritic rain', over a longer period of time. A cyclical high input in cosmic dust occurring roughly every 1,250 yrs rather than a long accumulation time has also been suggested as an explanation of the peak concentrations in the Allerød-Younger Dryas boundary (Fiedel, 2010), although this cycle has no known peak at the Allerød-Younger Dryas boundary (Franzén and Cropp, 2007). The Younger Dryas impact hypothesis proponents, however, show that the composition of their Allerød-Younger Dryas boundary spherules is inconsistent with that of cosmic spherules (Bunch et al., 2008; Israde-Alcántara et al., 2012; Wittke et al., 2013). The composition of the Allerød-Younger Dryas boundary spherules is, however, not unique to impact spherules either (figure 2.2).

Pigati et al. (2012) reported peak concentrations of magnetic spherules across the Allerød-Younger Dryas boundary. However, the high concentrations of magnetic microspherules were typical for all other black mats they analysed as well, regardless of age. These results strengthen the case of earlier studies, which suggest that the peak in magnetic spherules in the Allerød-Younger Dryas boundary might be related to the depositional environment rather than to an impact (Surovell et al., 2009; Haynes et al., 2010; Pinter et al., 2011). Bunch et al. (2012), however, suggest that the non Allerød-Younger Dryas boundary spherules found by Pigati et al. (2012) are likely to be of volcanic origin as there are several volcano's in the vicinity of these sites. Unfortunately, since Pigati et al. (2012) analysed their microspherules only for iridium and rare earth elements (see section 2.3), it is not possible to directly compare the geochemistry and morphology of their spherules to the reported Allerød-Younger Dryas boundary magnetic microspherules for similarities between magnetic spherules from different black mats.

2.2.1.1. Reproducibility of the peaks in magnetic spherule concentration

The reproducibility of the peaks in magnetic spherule concentrations was first questioned by Surovell et al. (2009), who investigated seven sites of similar age, including two sites that were also investigated by Firestone et al. (2007). Using the method of Firestone et al. (2007), they were unable to replicate the reported peaks in magnetic spherules but instead found peaks at non Allerød-Younger Dryas boundary levels at several sites. Based on their observations, Surovell et al. (2009) argue that the peaks in magnetic spherule as reported by Firestone et al. (2007) are related to changes in the depositional environment rather than an extraterrestrial impact. Two subsequent studies (Haynes et al., 2010; Pinter et al., 2011) also failed to replicate the results of Firestone et al. (2007) and echoed the conclusions of Surovell et al. (2009). LeCompte et al. (2012) investigated the discrepancy between the results of Surovell et al. (2009) and Firestone et al. (2007), conducting a blind study of the magnetic spherule concentrations at three Allerød-Younger Dryas boundary sites. Two of these sites, Blackwater Draw and Topper, were also investigated by both Firestone et al. (2007) and Surovell et al. (2009). The third site, Paw Paw Cove, was only investigated by Surovell et al. (2009). However, since LeCompte et al. (2012) analysed only one sample from the Allerød-Younger Dryas boundary at Paw Paw Cove, and no samples from above and below it, it is difficult to compare results for this site. Unlike Surovell et al. (2009), LeCompte et al. (2012) found high concentrations of magnetic spherules in the

Allerød-Younger Dryas boundary, even higher than those reported by Firestone et al. (2007). There thus seems to be a discrepancy in spherule counts between different sites.

In an attempt to explain this discrepancy in magnetic spherule counts, LeCompte et al. (2012) list five major reasons which might have contributed to the absence of peak spherule concentrations at the Allerød-Younger Dryas boundary as reported by Surovell et al. (2009). These reasons are summarised in table 2.1, which also includes other studies that investigated the magnetic spherule fraction. It is clear from the comparison in table 2.1 that there is no consistent trend between the reasons listed by LeCompte et al. (2012) and the discrepancy in spherule counts between studies. In addition, these reasons do not entirely explain why Surovell et al. (2009) or Pigati et al. (2012) found small numbers of magnetic spherules at some other stratigraphic levels. LeCompte et al. (2012) suggest that Surovell et al. (2009) might have found spherules of a diagenetic origin: further SEM work would be necessary to clarify this point. Although size-sorting seems an important factor, as LeCompte et al. (2012) did not manage to find any spherules before applying rigorous size sorting, Pigati et al. (2012), without size sorting report peaks in magnetic spherule concentration at the Allerød-Younger Dryas boundary. This shows that although LeCompte et al. (2012) failed to find any magnetic spherules without rigorous size sorting, size sorting does not entirely explain the discrepancy in spherule counts between studies. Furthermore, at the Topper site, LeCompte et al. (2012), who used a stronger magnet then the other studies, found three times as many spherules as Firestone et al. (2007). Even though the peak in spherule concentration was reproduced, there is thus still a discrepancy in exact spherule counts between studies. Part of this discrepancy might be related to the method used to extract the magnetic spherules,namely using a hand magnet wrapped in plastic to repeatedly extract the magnetic particles from a slurry until diminishing returns. Although this is an easy method, accessible to most research teams, some researcher consider it as much an art as it is science (Haynes et al., 2010). In addition, different results are obtained when a different magnet is used (LeCompte et al., 2012). To aid reproducibility and comparison between studies it might therefore be better to use an electromagnetic separator.

It is important to note that even if the discrepancy in spherule count can be explained, the Allerød-Younger Dryas boundary magnetic spherules are not a unique impact signature. Similar spherules have been found in marine sediments (figure 2.2) and black mats of different ages seem to effectively trap magnetic spherules, explaining the observed peak concentration in the Allerød-Younger Dryas boundary Black Mat (Pigati et al., 2012).

2.2.2. Scoria-like objects and lechatelierite

One line of evidence for the Younger Dryas impact hypothesis, which was not part of the original Younger Dryas impact hypothesis (Firestone et al., 2007), is the presence of vesicular (bubbly) melted siliceous glass, referred to as scoria-like objects (SLOs). These SLOs were found in the magnetic fraction at three sites, two in North America and one in Syria (Bunch et al., 2012) , suggesting that these objects also contain some magnetic minerals. Although scorias are volcanic in origin, similar shaped objects are formed during impacts or nuclear airbursts (Bunch et al., 2012). The composition of the scoria-like objects found in the Allerød-Younger Dryas boundary is similar to the local composition of the sediment cover, suggesting that they consist of molten material of local or regional origin (Bunch et al., 2012). This local origin of the molten material, as well as the large distance between the sites (1000-10000 km), led Bunch et al. (2012) to adopt at least two impact locations.

Table 2.1. Overview showing the presence or absence in peak concentration of magnetic spherules for several studies which were published before LeCompte et al. (2012). The methodology used in these studies is summarized in terms of five aspects that might affect the reproducibility of the magnetic spherule analysis according to LeCompte et al. (2012), who looked only at the Firestone et al. (2007) and Surovell et al. (2009) studies. 1. Allerød-Younger Dryas boundary (AYDB)sampling thickness. As the Allerød-Younger Dryas boundary is a very thin layer (Firestone et al., 2007), LeCompte et al. (2012) suggest that the magnetic spherules are diluted when sampling thickness increases and therefore more difficult to detect. 2. Aliquot size or amount of investigated material. As only small numbers of Allerød-Younger Dryas boundary spherules are present in the samples, it is easy to over, or underestimate the number of magnetic spherules due to natural variation in the sample, especially when looking at small samples. Thus assigning a "peak" concentration to small aliquots is also questionable on this basis. 3. Size sorting. At first LeCompte et al. (2012), did not size sort their samples and failed to find any magnetic spherules. Only after they implemented rigorous size sorting to their samples, did LeCompte et al. (2012) find high concentrations of magnetic spherules at the Allerød-Younger Dryas boundary. 4. Sphericity. Surovell et al. (2009) only looked for unfaceted, highly spherical spherules with a smooth glassy surface. However, other studies on the Allerød-Younger Dryas boundary magnetic spherules used less conservative criteria (Firestone, 2009; Israde-Alcántara et al., 2012; LeCompte et al., 2012), thus including more spherules in the count. 5. Scanning electron microscopy and chemical analyses. LeCompte et al. (2012) suggest only quench textured spherules and certain chemical composition should be included in the spherule count. + indicates that peak concentrations of magnetic spherules were found or that the study adhered to a certain part of the methodology. – indicates that peak concentrations of magnetic spherules were not found or that the study used a different methodology.

	peak concentrations		**methodology**				
study	**at AYDB**	**non-AYDB**	**1. sampling thickness**	**2. nr + size of aliquot**	**3. size sorting**	**4. perfect sphericity**	**5. SEM**
Firestone et al. (2007)	+	-	2-15 cm	≥ 1; 100-200 mg			no images reported
Surovell et al. (2010)	-	+	2-18 cm; most 5-10 cm	10-40 mg	-	+	-
Haynes et al. (2010)	+		0.5-1 cm	10 mg	+		-
Pinter et al. (2011)		+				+	+
Israde-Alcántara et al. (2012)	+	-	5-10 cm	≥ 1; 100-200 mg	+	-	+
Pigati et al. (2012)	+	+	≤ 2 cm	100 g (bulk)	-	+	-
Bunch et al. (2012)	+	-	5-15 cm		+	-	+
LeCompte et al. (2012)	+	-	4-15 cm	10-40 mg	"smaller than recommended size"	-	+

Both the SLOs and the magnetic spherules at these three locations are reported to contain lechatelierite (Bunch et al., 2012; Wu et al., 2013), a vesicular form of silica glass containing flow structures (Kieffer et al., 1976; Stöffler and Langenhorst, 1994; Grieve et al., 1996). During an impact, lechatelierite can be formed due to shock-melting of quartz at high pressures (>50GPa), followed by rapid quenching (Stöffler and Langenhorst, 1994). Inclusions of lechatelierite in tektites (impact related glass) are therefore considered evidence for an impact origin (Glass, 1990; French and Koeberl, 2010; Glass and Simonson, 2012). However, lechatelierite can also form during lightning strikes, a more local and small-scale phenomenon during which the high temperatures needed to melt the quartz (>1700 °C) are reached (French and Koeberl, 2010; Bunch et al., 2012). Bunch et al. (2012) argue that at their sites, the SLOs are not confined to a small area but are found over greater distances, and are therefore unrelated to lightning strikes. However, the scoria-like objects containing samples at Abu Hureyra and Blackville came from cores separated by only 4.5 m and 10 m respectively (Bunch et al., 2012). A core taken 2.2 km from the Blackville site, on the other hand, did not contain any scoria-like objects at the Allerød-Younger Dryas boundary. At Melrose scoria-like objects were also found in samples taken 28 m as well 28 km away from the original site. However, as Melrose contains no visible Allerød-Younger Dryas boundary and the two other locations near Melrose were not dated, it is possible that these samples do not date to the Allerød-Younger Dryas boundary. Exogenic fulgurites, formed when molten droplets are ejected from the soil during a lightning strike, though rare, have been found within a 5 m radius of a lighting strike (Mohling, 2004), suggesting that although it is unlikely that Bunch et al. (2012) found material originating from lightning strikes at three of their sites and only at the Allerød-Younger Dryas boundary, this is not necessarily impossible. Wittke et al. (2013) argue that the lack of excess magnetization of the Allerød-Younger Dryas boundary spherules exclude lighting as a possible formation mechanism. However, none of the lechatelierite-containing spherules or SLOs were analysed in this study.
If the lechatelierite inclusions are correctly identified and indeed unrelated to lighting strikes, this would indicate an impact related origin for both the scoria-like objects and magnetic spherules at these three locations, as suggested by Bunch et al. (2012). However, no other inclusions indicative of an impact, such as shocked quartz, other high-pressure polymorphs, or elevated concentrations of projectile-related elements, were reported at these sites. In addition, although multiple sites were reported in studies mentioning the lechatelierite (Wittke et al., 2013; Wu et al., 2013), the lechaterlierite was reported at only three sites investigated, the same as investigated by Bunch et al. (2012). More work is necessary to establish whether the scoria-like objects and lechatelierite are indeed related to an extraterrestrial airburst and whether they are found at the other Allerød-Younger Dryas boundary sites as well.

2.2.3. Iridium and other platinum group elements

Several types of meteorites are highly enriched (up to 1000 times) in the platinum group elements (PGEs) compared to the average continental crust. Following an impact, small amounts of this PGE-rich material are incorporated in the distal ejecta layer, resulting in a typical impact signature (Sawlowicz, 1993b; French and Koeberl, 2010). PGEs are therefore taken as a reliable impact marker (French and Koeberl, 2010). Because of difficulties in measuring very low PGE concentrations, the concentration of Ir (iridium), typically >1-2 ppb in the case of an impact signature, is often taken as representative for all PGEs, as it is the easiest to measure (Kyte et al., 1988; French and Koeberl, 2010). However, small amounts of Ir enrichment can also result

from terrestrial processes (Sawlowicz, 1993b; French and Koeberl, 2010), which complicates interpretation. It is therefore more reliable to measure all the PGEs rather than just Ir, which, on its own, cannot be considered a unique marker (Sawlowicz, 1993b; French and Koeberl, 2010).
Firestone et al. (2007) initially found elevated concentrations of Ir in the Allerød-Younger Dryas boundary layer at half of their sites (in bulk samples: <0.5 to 3.8 ppb with ±50-90% uncertainty; in the magnetic fraction: up to 117 ppb with ±10% uncertainty). However, upon retesting subsamples from the same sites only half of the elevated Ir concentrations were confirmed (Firestone et al., 2007). Different studies also report different Ir concentrations for the same site, for example at the Murray Springs site (see table 2.2). Ir concentrations thus not only vary between sites, but also within the same site. These varying results do not exclude an extraterrestrial origin, as impact signatures vary as well (Sawlowicz, 1993b). However, at Murray Springs, Haynes et al. (2010) showed that the background concentration at the site is variable as well, including Ir concentrations as high as those found in the Black Mat (33-72 ppb). The Ir concentrations at Murray Springs are therefore variable and not anomalous when compared to the background concentrations. The reported Ir concentrations at Murray Springs thus cannot be taken as evidence for an extraterrestrial source of the material.
Pigati et al. (2012) report peaks in magnetic spherules and Ir concentrations (bulk and magnetic) of different magnitudes at, or near, the base of several Allerød-Younger Dryas boundary Black Mats, as well as Black Mat-like deposits of different ages. They suggest that the peaks in magnetic spherule and Ir concentrations at the bottom of the Black Mat must therefore be inherent to the depositional environment in which Black Mat-like layers are formed. These inherent peak concentrations (Ir and magnetic spherules) in Black Mat-like deposits show that unless there were impacts at all these sites at different times, a peak in Ir concentrations (regardless of the exact amount) at the base of the Black Mat does not immediately imply that an extraterrestrial impact occurred, as suggested by Firestone et al. (2007) and Bunch et al. (2010). Moreover, Pigati et al. (2012) found high Ir concentrations of >1-2 ppb, not only in one of the Allerød-Younger Dryas boundary Black Mats but also in several black mats of different ages (>40 ka - 5.6 ka), both in the American Southwest and in Chile. This is consistent with the idea that isolated Ir analysis are not strong evidence for an impact and that other related elements, such as the rest of the PGEs, should be analysed in order to get a reliable indication of an impact (French and Koeberl, 2010). In addition, Petaev et al. (2013) found no Ir anomaly at the Allerød-Younger Dryas boundary in the GISP2 ice core, but found a peak in Pt concentrations. Their results suggest that the Ir concentrations found in some black mats might indeed have terrestrial origins, as suggested by Pigati et al. (2012). Based on the combination of high Pt with low Ir and Al concentrations, Petaev et al. (2013) suggest that the source of the Pt peak in the GISP2

Table 2.2. Ir concentrations of the Allerød-Younger Dryas boundary at Murray Springs (Arizona) within both the magnetic fraction and the bulk sediment as reported by different research teams.

Study	Ir concetration in magnetics (ppb)	Ir concentration in bulk sediment (ppb)
Firestone et al. (2007)	<0.1 - <11	<0.5 - 2.2
Paquay et al. (2009)	not reported	0.077
Haynes et al. (2010)	64[1]	not reported
Pigati et al. (2012)	1.03 - 129[2]	0.06 - 0.66

[1]Similar Ir concentrations were reported in the non Allerød-Younger Dryas boundary sediments as well.
[2]The highest concentration of Ir in the magnetic fraction (200 ppb) was reported 10 cm below the Allerød-Younger Dryas boundary.

ice core most likely has an extraterrestrial source, possibly a magmatic iron meteorite. Overholt and Melott (2013) have shown that the high ^{14}C and 10Be concentrations at the onset of the Younger Dryas could have been formed by a long-period comet. These higher concentrations can however also be caused by different processes. To properly show that there was a Younger Dryas impact, 26Al/10Be ratio's in the ice core must be measured (Overholt and Melott, 2013). However, the proposed increase in 26Al due to input from the impactor (Overholt and Melott, 2013) would be inconsistent with the conclusions of Petaev et al. (2013), who suggest a Al poor impactor.

An extensive study on the bulk sediment PGE concentrations within the Allerød-Younger Dryas boundary at several sites was conducted by Paquay et al. (2009). At all sites, the bulk PGE concentrations, including those of Ir, were similar to average continental crust values and lower than those reported by Firestone et al. (2007) or Haynes et al. (2010). Although at some sites the Ir concentrations reported by Paquay et al. (2009) peaked in the Allerød-Younger Dryas boundary, the values (max 0.117 ppb at Lake Hind) are still well below the >1-2 ppb threshold used to identify impact signatures (Kyte et al., 1988; French and Koeberl, 2010). In response, Firestone (2009) argues that Paquay et al. (2009) sampled without using the proper microstratigraphy, thereby diluting the Ir signal. However, Paquay et al. (2009) claim to have used subsamples of the Murray Springs samples that were used by Firestone et al. (2007). It therefore seems unlikely that the lack of evidence reported by Paquay et al. (2009) is entirely the result of the wrong sampling strategy. Furthermore, Paquay et al. (2009) also looked at the bulk Os isotope ratio, which has an even greater potential to identify small amounts of meteoritic material compared to the PGE method (Paquay et al., 2009; French and Koeberl, 2010). All measured 187Os/188Os ratios in the Allerød-Younger Dryas boundary were too high (mostly >1) to be consistent with the input of extraterrestrial material (Paquay et al., 2009). Another argument put forward against the work of Paquay et al. (2009) is that they only analysed the PGE and Os-isotope ratios in the bulk sediment rather than in the magnetic fraction (Bunch et al., 2010). The largest peaks in Ir have indeed been reported in the magnetic fraction rather than in the bulk sediment (Firestone et al., 2007; Haynes et al., 2010; Pigati et al., 2012). If the magnetic grains are the carriers of the Ir signal (Bunch et al., 2010), eliminating the Ir poor non-magnetic parts of the samples by only analysing the magnetic fraction, would increase the measured Ir relative to measurements of the bulk samples. In addition, analysing the magnetic fraction might concentrate any cosmic spherules present in the sample. As cosmic spherules may contain Ir concentrations of >1000 ppb (Sawlowicz, 1993b), concentrating this material by only looking at the magnetic fractions will increase the measured Ir concentration in the total magnetic fraction. Pigati et al. (2012), however, showed that the rare earth elements (REE) of the total magnetic grain fraction found at the Allerød-Younger Dryas boundary has a typical terrestrial profile, suggesting that cosmic spherules concentrations might be low. In addition, Wu et al. (2013) investigated the Os-isotope ratio in both bulk and magnetic fractions and reported no Os-isotope anomaly at most of their sites. They report low Os-isotope ratios in the bulk sediment at Lommel and Melrose. Total Os concentrations at these sites are however low and Wu et al. (2013) therefore suggest the Os might have a terrestrial source.

In summary, although Firestone et al. (2007) report peaks in Ir concentration at some of their sites, other researchers were not always able to reproduce these results (Paquay et al., 2009). Furthermore, it has been shown that the peaks in Ir concentration do not necessarily indicate an impact event (Haynes et al., 2010; Pigati et al., 2012) and analysis of other elements indicate

a terrestrial origin of the material (Paquay et al., 2009; Pigati et al., 2012). Although Petaev et al. (2013) suggest that the Pt peak they found in the Greenland ice sheet is related to a meteorite impact, no Pt has been reported at other sites yet. There is thus no unambiguous geochemical evidence that the Younger Dryas impact event took place.

2.2.4. Microstructures in quartz

Planar deformation features (PDFs) are thin (<1 μm), closely spaced (<10 μm), straight, parallel deformation planes in crystals which form during shock deformation and are sometimes referred to as 'shock lamellae' (Langenhorst, 2002; French and Koeberl, 2010; Hamers and Drury, 2011). They are most well known for their occurrence in quartz (also referred to as 'shocked quartz'), where they are oriented parallel to specific crystallographic planes. As PDFs are distinct and unique features, they are widely used as a diagnostic indicator of high shock pressures following an impact (Langenhorst, 2002; French and Koeberl, 2010; Hamers and Drury, 2011). Nevertheless, some non-shock lamellae in quartz have occasionally been misidentified as PDFs (Langenhorst, 2002; French and Koeberl, 2010). It is therefore important that the correct identification techniques and criteria are used in identifying PDFs. The only completely reliable method to distinguish PDFs from non-shock lamellae is transmission electron microscopy (TEM), but orientation measurements using a U-stage microscope or analysis using scanning electron microscopy (SEM) cathodoluminescence (CL) imaging also give good results (Boggs S. et al., 2001; French and Koeberl, 2010; Hamers and Drury, 2011).
In 2010, Mahaney et al. reported the occurrence of "shattered quartz, notably with prominent PDFs in the finer silt fractions" in a ~13 ka Black Mat-like layer in the Venezuelan Andes. Their interpretation was based on SEM observations of planar surface features, spaced 0.5-1.0 μm apart. Although the spacing of the features is consistent with PDFs, only one set of features was observed and none of the other features indicative of PDFs were reported. Further analysis, such as SEM-CL or TEM, is thus necessary to establish whether these features are indeed PDFs (e.g. French and Koeberl, 2010; Mahaney et al., 2010a; Hamers and Drury, 2011). In a follow-up paper, Mahaney et al. (2010b) stated that they found no irrefutable PDFs. Instead, Mahaney et al. (2010b) focus on the presence of closely spaced fractures oriented parallel to the surface of the quartz grains, as well as highly disrupted grain surfaces leading to extreme brecciation (Mahaney et al., 2010b). (Mahaney et al., 2010b)These features are however not considered as indicative of an extraterrestrial impact (French and Koeberl, 2010). As Mahaney et al. (2010b) have shown, these fractured and disrupted grain surfaces can form as a result of heating and are thus not necessarily the result of an impact. Even though Mahaney et al. (2010a) show no conclusive evidence for the occurrence of shocked quartz and Mahaney et al. (2010b) conclude that they find no irrefutable evidence for the occurrence of PDFs, the first paper (Mahaney et al., 2010a) has been cited by proponents of the Younger Dryas impact hypothesis to substantiate their claim that a large impact event occurred (Mahaney et al., 2011; Bunch et al., 2012; Israde-Alcántara et al., 2012; Mahaney et al., 2013).

2.2.5. Nanodiamonds

Nanodiamonds have been found in meteorites and in relation to impact craters (Hanneman et al., 1967; Carlisle and Bramant, 1991; Daulton et al., 1996; Hough et al., 1997; Koeberl et al., 1997; Gilmour, 1998; Masaitis, 1998; Karczemska et al., 2008; French and Koeberl, 2010).

Although micrometer to millimeter-sized shock-produced diamonds in craters have been used to establish an impact origin, no distal ejecta layers have been diagnosed based on nanodiamonds (< 5 nm) alone. Instead, the use of these nanodiamonds as a definite impact criterion is still debated since their formation mechanisms are still not always clear (French and Koeberl, 2010). In meteorites, several polymorphs of diamond have been reported, namely: the diamond cubic polymorph (3C diamond, spacegroup 227 – Fd_3m; hereafter referred to as 3C diamond; figure 2.3a), the most common form of diamond found on Earth and often referred to simply as cubic diamond; a relatively new form of diamond called n-diamond (structure uncertain, often thought to have a face center cubic (fcc) structure (figure 2.3b), see also (Konyashin et al., 2006; Dadsetani et al., 2010)); an hexagonal form of diamond named lonsdaleite (2H diamond, space group 194 – $P6_3/mmc$; figure 2.3c). The different crystal forms can be recognised using transmission electron microscopy (TEM) on the basis of their crystal structure and d-spacing (table 2.3), which are visible in high resolution images and diffraction patterns, or their electron energy loss spectrum (EELS) (Qin et al., 1998; Phelps, 1999; Daulton et al., 2010). Other, non-diamond forms of carbon include: graphite (figure 2.3d), the most common form of carbon on Earth; graphene (figure 2.3e), single one-atom thick sheets of carbon which form turbostratic carbon when disorderly stacked; and carbon onions, spherical nanoparticles consisting of concentric graphene shells (Banhart and Ajayan, 1996; Daulton et al., 2010). Graphane (figure

Figure 2.3. Schematic drawings of the different carbon-structures described. Open circles indicate the location of a carbon atom. a. Cubic diamond structure. b. fcc-unit cell, the structure suggested for n-diamond. c. Lonsdaleite structure. d. Graphite. e. A sheet of graphene. f. A sheet of graphane. Little grey circles indicate the location of hydrogen atoms. Hydrogen atoms pull the carbon atoms either slightly up or down, depending on their position, resulting in a slightly wrinkled sheet, compared to flat graphene sheets.

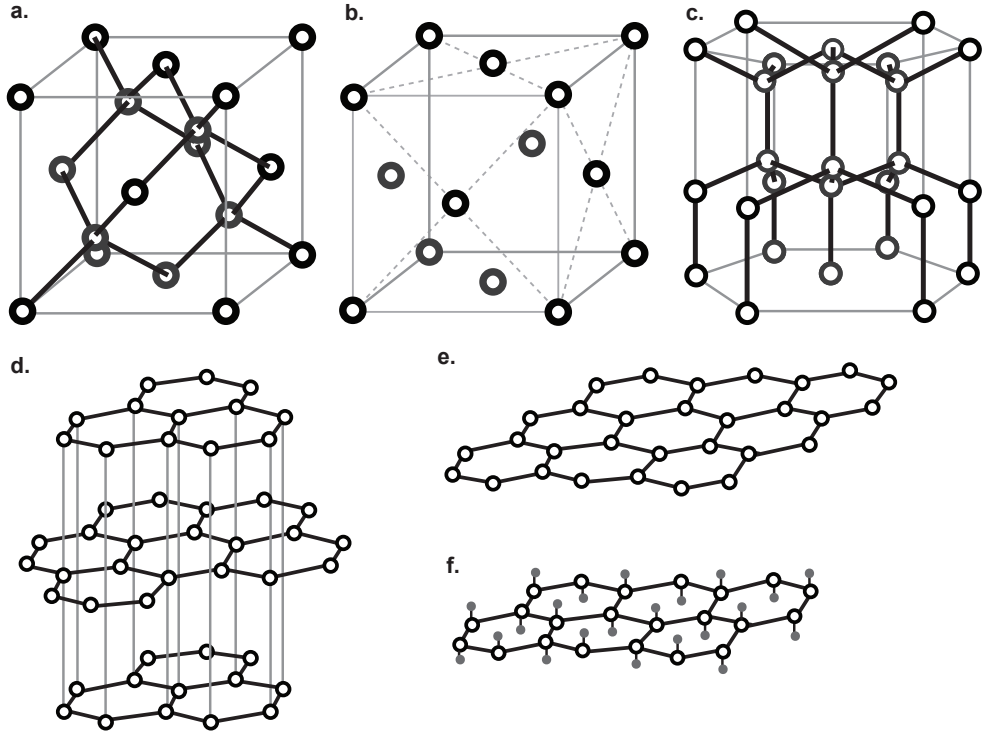

2.3f), a hydrogentated form of graphene, has also been observed in the llerød-Younger Dryas boundary (Daulton, et al. 2010).

The occurrence of nanodiamonds in the Allerød-Younger Dryas boundary was first reported by Firestone et al. (2007), who found a peak in a nuclear magnetic resonance (NMR) spectrum of glass like carbon which they interpreted as nanodiamond. However, according to Kerr (2008) and Pinter et al. (2011) the peak is too broad for diamond and at the wrong location, at 38 ppm rather than at 34 ppm (figure S11 in Firestone et al. (2007) and figure 4 in Cody et al. (2002)). Two years later, Kennett et al. (2009a), using TEM and selected area electron diffraction patterns (SADP), reported the occurrence of nanodiamonds in the Allerød-Younger Dryas boundary layer at several locations in North America. These nanodiamonds were found within, or adhered to, carbon spherules, as well as in the bulk sediment of the Black Mat. Two polymorphs of diamond were reported: 3C diamond and the relatively new structure called n-diamond. In a different study of the Black Mat at Arlington Canyon (Santa Rosa Island, California, USA), Kennett et al. (2009b) found not only 3C diamond and n-diamond, but also the hexagonal polymorph lonsdaleite in 'carbon elongates' and carbon spherules. Lonsdaleite can be formed through shock metamorphism and is therefore often considered as an indicator for shock (Hanneman et al., 1967). However, lonsdaleite can form through non-shock mechanisms as well (Frenklach et al., 1989; Daulton et al., 1996; Erlich and Hausel, 2002) and the utility of nanodiamond as an impact indicator is still debated because the relationship between nanodiamonds and impact events is still unclear (French and Koeberl, 2010).
Daulton et al. (2010), however, failed to find any nanodiamonds in samples from the Black Mat. Instead, they identified graphene and graphene/graphane aggregates within microcharcoal, carbon spherules, and glass-like carbon from the Black Mat as well as in older and modern samples. Moreover, Daulton et al. (2010) note that the diffraction patterns reported by Kennett et al. (2009b) do not show the unique 1.5 and 1.93 Å atomic spacing's found in the lonsdaleite

Table 2.3. Interplanar spacings, or d-spacings, for the different carbon crystal structures found in the Allerød-Younger Dryas boundary (Hirai and Kondo, 1991; Qin et al., 1998; Phelps, 1999; Daulton et al., 2010).

cubic diamond 3C diamond	n-diamond fcc-carbon (?)	lonsdaleite 6H diamond	graphite	graphene	graphane
			3.35		
2.06	2.06	2.18	2.13	2.13	
		2.06	2.03		2.02
		1.93			
			1.68		
			1.80		
		1.5	1.54		
1.26	1.26	1.26	1.23	1.23	
		1.16	1.16		1.17
		1.09	1.12		
1.08	1.08	1.08	1.07	1.07	
1.03	1.04	1.06	1.03		1.01
0.89		0.83	0.90	0.81	0.76

structure (Phelps, 1999). Daulton et al. (2010) therefore conclude that Kennett et al. (2009b) must have mistaken graphene/graphane aggregates for lonsdaleite and graphene aggregates for polycrystalline 3C diamond. Daulton et al. (2010) also report finding nanocrystalline copper, which they suggest might have been misidentified as n-diamond. In contrast, a group working on the European Allerød-Younger Dryas boundary section at Lommel, report the occurrence of nano to microscale diamonds (Tian et al., 2011). These diamonds include rounded nanodiamond and flake-like microdiamonds (both 3C diamond) in bulk samples from the Usselo horizon. No lonsdaleite or n-diamond structures were identified in this study. In Europe, nano- and microdiamonds have been identified in carbon spherules from modern European forest soils (Yang et al., 2008), but these came from different locations, namely Burghausen (Germany) and Spa (Belgium). The origin of these nanodiamonds is still unknown, the possibility of an impact event was suggested but has not been confirmed (Yang et al., 2008).

Both lonsdaleite and n-diamond have been reported in the Greenland ice sheet at Kangerlussuaq (Kurbatov et al., 2010) and in lacustrine sediments from Lake Cuitzeo, Central Mexico (Israde-Alcántara et al., 2012). Both of these studies included high-resolution TEM images that show the unique 1.93 Å lattice spacing corresponding to the (101) plane of lonsdaleite, but no corresponding diffraction patterns. Daulton (2012) suggests that the high-resolution image given by Kurbatov et al. (2010) is inconsistent with lonsdaleite and that the images in Israde-Alcántara et al. (2012) are also consistent with other materials. Kurbatov et al. (2010) state that the lonsdaleite and n-diamond they found in the Greenland ice are "morphologically and analytically indistinguishable" from those found in the Black Mat layer. The rounded lonsdaleite particles as reported in the Greenland ice (Kurbatov et al., 2010), however, are dissimilar to the "stacked diamond clusters" from the Black Mat layer at Arlington Canyon (Kennett et al., 2009b). Furthermore the particles are freely dispersed in the ice layer rather than found within carbon spherules. This dissimilarity suggests that if the Greenland Ice Sheet particles are indeed nanodiamonds, these might yet still have a different origin.

Pinter et al. (2011) note that the electron energy loss spectrum (EELS) given by Kurbatov et al. (2010, Fig. 8) as evidence for n-diamond is similar to the spectrum of amorphous carbon with sp2 bonded components rather than that of n-diamond. However, when compared to the spectra published by Konyashin et al. (2001, Fig. 3), the spectrum in Kurbatov et al. (2010) looks more similar to the spectrum of fcc-carbon (n-diamond) then to the spectrum of amorphous carbon. The EELS pattern of the Lake Cuitzeo nanodiamonds (Israde-Alcántara et al., 2012 fig. 9), on the other hand, appears closer to that of amorphous carbon. In both cases, however, high-resolution TEM and SADP analysis on other n-diamond particles as reported in the papers clearly show that those particles are polycrystalline (Kurbatov et al., 2010; Israde-Alcántara et al., 2012). Assuming both particles consist of carbon, the similarity of the EELS spectra of the reported nanodiamonds to the spectra of amorphous carbon in both cases is thus likely due to the relatively small size of the nanodiamonds compared the amorphous carbon coating on the thin film grid used to support samples resulting in a low signal to noise ratio. The particles reported might thus still be nanodiamonds, even though there is no clear EELS signal.

In summary, the proponents of the Younger Dryas impact hypothesis have claimed to have found 3C diamonds and n-diamonds in several North American Black Mats, the Greenland ice sheet and Central Mexico (Kennett et al., 2009a; Kennett et al., 2009b; Kurbatov et al., 2010; Israde-Alcántara et al., 2012) as well as a possible Allerød-Younger Dryas boundary in the Greenland ice sheet (Kurbatov et al., 2010). In addition they report lonsdaleite at some of

those sites, which is known as the hexagonal shock polymorph of diamond. Another group of researchers trying to reproduce the work on the North American Black Mats failed to find any nanodiamonds and suggested that Kennett et al. (2009a; 2009b) had misinterpreted the nature of the particles (Daulton et al., 2010). A different group working on the European Usselo horizon did report the occurrence 3C diamond, while failing to find n-diamond or lonsdaleite (Tian et al., 2011). Although the occurrence of 3C diamond in the Allerød-Younger Dryas boundary thus seems confirmed, the occurrence of n-diamond and lonsdaleite is still questioned (Daulton, 2012). In addition, although there are similarities, there are also differences in morphology of the nanodiamonds reported by the different groups (see also table 3.3), suggesting that the reported nanodiamonds might have different origins. In order to use the occurrence of the 3C diamonds and possibly lonsdaleite, it is thus important to discuss the possible origin of these nanodiamonds.

2.3. Events associated with the Younger Dryas impact hypothesis

2.3.1. Extensive wildfires

Based on the presence of charcoal, soot, and polycyclic aromatic hYounger Dryasrocarbons (PAHs) at many Allerød-Younger Dryas boundary sites, Firestone et al. (2007) argue that a fireball and superheated ejecta following the Younger Dryas impact resulted in continent-wide (Kennett et al., 2008) wildfires, possibly even reaching Europe. The environmental destruction brought by these wildfires would have affected the human and animal populations, while the soot in the atmosphere would have had a short term cooling effect (Firestone et al., 2007). Although soot and PAHs have been reported at the K/T boundary (Wolbach et al., 1985), the presence of extensive wildfires at a boundary reveals nothing about how the fire was ignited. Regional fires caused by small impacts do not differ much from natural fires (Svetsov, 2008) and wildfires frequently occurred during the Late Glacial, either naturally or initiated by humans (Pinter and Ishman, 2008; van der Hammen and van Geel, 2008; Daniau et al., 2010).
Marlon et al. (2009), using 35 charcoal records located across North America, found neither evidence for a charcoal peak at 12,900 yrs ago nor any continent-wide wildfire episode during the last glacial-interglacial transition (15,000 – 10,000 yrs ago). Kennett et al. (2009), argue that multiple ^{14}C-dating errors led Marlon et al. (2009) to miss the continent-wide charcoal peak and that this peak is present in other records as well. Yet other groups also failed to find charcoal peaks at 12,900 yrs ago (Gill et al., 2009; Daniau et al., 2010). Haynes et al. (2010) also report that they found no evidence for extensive biomass burning at any Clovis site in the San Pedro Valley of Arizona. In addition Haynes et al. (2010) argue that the peak in charcoal and vitreous carbon as reported by Firestone et al. (2007) at Murray Springs came from a sample located near a Clovis hearth and that three other samples from Murray Springs did not contain any charcoal.

[1]All uncalibrated radiocarbon years are presented as 14C yrs BP. Unless otherwise specified, calibrated radiocarbon ages (cal. yrs BP) are calibrated using the IntCal13 calibration curve (Reimer et al., 2013) and the OxcCalv4.2 calibration software (Bronk Ramsey, 2009).

Firestone et al. (2007) further argue that ammonium and nitrate spikes in the GISP2 ice core (Mayewski et al., 1993), as well as a major ammonium spike in the GRIP ice core (Fuhrer et al., 1996) are evidence for impact related biomass burning. However Melott et al. (2010) show that the nitrate spike at the Allerød-Younger Dryas boundary in the GISP2 record is too small for the hypothesised Younger Dryas impact event, although this might be related to the low sampling resolution. In addition, Mayewski et al. (1993) attributed this brief (100 yr) increase in the ammonium flux during the early Younger Dryas to the destruction of the Bølling-Allerød biomass. In the GRIP ice core, ammonium actually increases steadily during the Bølling-Allerød, reaching a maximum concentration during the early Younger Dryas (Fuhrer et al., 1996). Fuhrer et al. (1996) suggest that this trend in ammonium concentration parallels the build-up of biomass during the warming climate followed by plant material released during deglaciation. This increase of ammonium and biomass during the warming climate is in line with the worldwide charcoal records analysed by Daniau et al. (2010), which show a significant peak in biomass burning corresponding to the warming events, lagging the peak of the warm period by 100-200 years, then dropping during the cold periods. The high ammonium concentration in the ice cores therefore seems consistent with natural wildfires and does not indicate the occurrence of an extraterrestrial impact. Furthermore, the Pt peak found in the GISP2 ice core predates the ammonium and nitrite peaks by 30 years (Petaev et al., 2013). If the Pt peak is directly caused by to a Younger Dryas impact event, as suggested by Petaev et al. (2013), the wildfires are not, or vice versa.

2.3.2. Climate change

The cause of the Younger Dryas cold period is still not entirely clear (Broecker et al., 2010; Fiedel, 2011). In the past, it was thought that the Younger Dryas cooling might have been related to the eruption of the Laacher See volcano (11,063 ± 13 ^{14}C yrs BP; 12,995-12,890 cal. yrs BP[1]), but research on varved lake sediments showed that the eruption actually occurred 180-200 years prior to the onset of the Younger Dryas in Europe (Schmincke et al., 1999; Litt et al., 2003). The current main hypothesis for the cause of the Younger Dryas was first proposed by Broecker (1989). This hypothesis involved rerouting of drainage from the pro-glacial Lake Agassiz to the northern Atlantic Ocean, rather than the Gulf of Mexico, causing a shutdown of the thermohaline circulation, resulting in cooling of the region (Broecker et al., 1989; Broecker et al., 1990). More recently, it has also been proposed that meltwater flow into the Arctic ocean was responsible for the cooling (Tarasov and Peltier, 2005; Tarasov and Peltier, 2006; Bradley and England, 2008; Condron and Winsor, 2012). The exact size and origin of the freshwater discharge resulting in the Younger Dryas cooling is however still debated and we refer to Carlson and Clark (2012) for a detailed overview of the current hypothesis for the cause of the Younger Dryas. Alternative hypotheses for the Younger Dryas cooling include a decrease in summer insolation or a displaced jetstream (Renssen et al., 2000; Fiedel, 2011).

With the extraterrestrial impact hypothesis Firestone et al. (2007) offered a new alternative explanation: they note that in addition to the known short-term cooling effects of impacts, the Younger Dryas impact event would have destabilized the ice sheet, suddenly releasing meltwater into the North Atlantic. In effect, the Younger Dryas impact hypothesis provides a unique trigger for the generally accepted meltwater hypothesis. However, conceptual models have shown that Younger Dryas-like cold periods could be inherent to the climate system (Schulz et al., 2002; Sima et al., 2004) and more recently, evidence for Younger Dryas-like cooling

events during other glacial terminations have been found in Antarctic ice cores and Chinese stalagmites (Carlson, 2008; Cheng et al., 2009; Broecker et al., 2010; Denton et al., 2010). The existence of these similar events during earlier terminations indicates that the Younger Dryas cooling might not have been as unique as originally thought and would have happened with or without the interference of an extraterrestrial object. Furthermore, extraterrestrial impacts do not necessarily induce climate change, so even if an extraterrestrial object hit Earth at the onset of the Younger Dryas, this does not immediately imply that it accounted for the Younger Dryas cooling.

2.3.3. Megafaunal extinctions

During the end of the Last Glaciation, most of the megafaunal species became extinct. These extinctions occurred at different times in different continents: first in Australia around 45,000 yrs ago, after humans arrived at the continent, and finally in South America when climate started to change to interglacial conditions. The Eurasian extinction happened in two events, approximately 48,000-23,000 yrs ago and 14,000-10,000 yrs ago, the second interval roughly coinciding with the Allerød-Younger Dryas periods. Africa seems to have been little affected by the Late Pleistocene extinction episodes (Barnosky, 2008). The degree of abruptness, timing, and cause of the megafaunal extinctions are still under debate. Explanations for the megafaunal extinctions include human overkill, competition for resources, climate change, pandemic disease, or even a combination of several triggers (Barnosky, 2008; Haynes Jr., 2008; Fiedel, 2009; Ruban, 2009). Early proponents of the Younger Dryas impact hypothesis argued that the Younger Dryas impact was responsible for the megafaunal extinctions (Firestone et al., 2007; Kennett et al., 2008; Kennett et al., 2009b). However, Gill et al. (2009) show that a decline of Sporomiella (dung fungus) spores suggests that the major collapse of the North American megafauna happened between 14,800 and 13,700 cal. yrs BP (calibrated using Calib 5.0.2), well before the proposed Younger Dryas impact. Others, however, do not consider the use of sporomiella spore abundances as a percentage related to the pollen sum is the most appropriate method to investigate megafaunal abundances (Baker et al., 2013; Wood and Wilmshurst, 2013). Although the exact timing of the megafaunal extinctions in North America is still uncertain, it is not likely that the proposed Younger Dryas impact was the major cause of the extinctions (Ruban, 2009). Most likely, a combination of different factors, such as ecosystem changes associated with the Last Glacial Termination and human hunting, are the causes of megafaunal extinctions.

2.3.4. Disappearance of the Clovis culture in North America

Firestone et al. (2007) argue that major adaptive shifts in human culture, including the disappearance of the Clovis culture and an inferred population decline in North America, occurred at the onset of the Younger Dryas as a result of the Younger Dryas impact event. However, some regions show evidence of overlap between Clovis and post-Clovis cultures (Hamilton and Buchanan, 2009) and no population decline (Buchanan et al., 2008; Hamilton and Buchanan, 2009; Fiedel, 2010). Other studies however showed a population decline near the Allerød-Younger Dryas boundary (Anderson et al., 2008; Jones, 2008; Kennett and West, 2008). Whether or not there was a population decline at the onset of the Younger Dryas is thus still debated. Furthermore, if there was a population decline, other possible causes, such as climate

and environmental change or disappearance of prey, must be ruled out before the population decline can be conclusively related to an impact event.
A recent study reporting evidence in support of the Younger Dryas impact hypothesis from the Abu Hureyra site in Syria (Bunch et al., 2012), however, puts the effect of the proposed Younger Dryas impact on the human population into question. Abu Hureyra was inhabited almost continuously from 13,400 to 7,500 cal. yrs BP (IntCal09) (Colledge and Conolly, 2010). The scoria-like objects found at the site (Bunch et al., 2012) suggests that the proposed airburst must have happened relatively close to Abu Hureyra, seemingly without a large effect on the local population. The continuing population at Abu Hurerya is inconsistent with the suggestion that a similar airburst or airbursts caused a population decline over the North American continent.

2.4. Nature of the event

Based on the evidence they found, Firestone et al. (2007) suggested that a fragmented body, likely a comet (an icy body), colliding with Earth was responsible for the peak concentrations in certain markers and environmental changes. According to the original Younger Dryas impact hypothesis (Firestone et al., 2007) the comet fragments (< 2 km) either obliquely hit the 2 km thick Laurentide ice sheet, thereby disrupting the ice sheet but not producing a crater in the crust below, or exploded in the atmosphere above the ice sheet, resulting in an airburst much larger than the Tunguska event in 1908 (Svetsov and Shuvalov, 2008; Napier and Asher, 2009; Mignan et al., 2011), which devastated over 2,000 km2 of forest in Central Siberia during an explosion with an estimated equivalent energy of 5 Mton TNT (Mignan et al., 2011). It has also been suggested that the Corossol structure, a possible impact crater in the Gulf of Saint Lawrence (Higgins et al., 2011), is related to the Younger Dryas impact event (Israde-Alcántara et al., 2012). The uncertainty in the age of the Corossol structure is currently however quite large, ranging from 12.9 ka to 450 Ma. The lower limit of 12.9 ka is based on dates from a core through the crater infill. However, the core did not extend to the crater floor, so the crater could be older than 12.9 ka. The Corossol structure thus cannot be related to the Younger Dryas impact event with any certainty until better age control is established. The two other Canadian craters mentioned by Wu et al. (2013) can also not be tied to the Younger Dryas impact event. The age of the Bloody Creek structure, Nova Scotia (Canada), has not yet been determined (Spooner et al., 2009) and the Charity Shoal structure, Lake Ontario, is most likely of Ordovician age (Holcombe et al., 2013). No other craters of possible Allerød-Younger Dryas boundary age have been found thus far and it is considered unlikely that all evidence of an Allerød-Younger Dryas boundary impact crater would be completely erased in only ~13,000 years (French and Koeberl, 2010). The most recent papers on the Younger Dryas impact hypothesis, however, seem to favour the airburst model over an actual impact, although the type of impactor is not specified (Bunch et al., 2012; Israde-Alcántara et al., 2012; Wittke et al., 2013). In addition, Bunch et al. (2012) suggest that there must have been at least three airbursts rather than just one, one in Syria and two in North America. Wittke et al. (2013) suggest a comet that broke up in multiple fragments before encountering Earth, which further disintegrated when traveling through the Earth's atmosphere. This idea is similar to one of the original hypothesis in Firestone et al. (Firestone et al., 2007), except that multiple impact sites are involved.
Pinter and Ishman (2008) argue that even for a very high fireball, the thermal radiation is zero below the horizon, making it impossible for an impact over North America to have ignited

forests in Europe. In addition, large impactors are required to ignite continent-wide (>8 km diameter impactor) or global (>15 km impactor) wildfires (Durda and Kring, 2004; Svetsov, 2008). However, the total damage of small impactors can greatly increase when fragmentation occurs in the atmosphere (Svetsov, 2008). If multiple impacts or airbursts were spread over the globe, as suggested by Bunch et al. (2012), this would greatly increase the directly affected burn area, which could include the flight path and region beneath any airburst exposures. However, small impacts and airbursts do not necessarily ignite wildfires. For example, the Chelyabinski event (February 15, 2013), which had a total energy equivalent to 440 kton TNT, was only accompanied by shock wave, and the Carancas impact event (September 15, 2007), which had an estimated energy of 0.015-3 ton of TNT and left a small 13,5 m diameter crater (Kenkmann et al., 2009; Tancredi et al., 2009), also did not result in wildfires. In addition, there is no evidence for increased biomass burning or continent-wide wildfires at the onset of the Younger Dryas (see section 3.1).

Several researchers have also challenged the Younger Dryas impact hypothesis based on the type of impactor. Pinter and Ishman (2008) argue that the combined lines of evidence are incompatible with any single impactor or known impact event. Paquay et al. (2009), after eliminating the presence of increased concentrations of platinum-group elements (PGEs) in the Allerød-Younger Dryas boundary, suggested that the impactor might have been a PGE-poor type of achondritic meteorite. However, the probability of such an achondritic meteorite hitting Earth is low, and such meteorites are not known to contain nanodiamonds (Paquay et al., 2009). Nanodiamonds formation may have occurred in an impact related airburst through a CVD mechanism (Israde-Alcántara et al., 2012), thus excluding the need for a nanodiamonds rich impactor. Petaev et al (2013) agree that the impactor could not have been a chondritic meteorite, but, based on the Pt anomaly they found, they suggest a highly differentiated, possibly iron-poor, meteorite.

French and Koeberl (2010) note that in order to avoid visible surface deformation, any impactor fragments hitting the Laurentide ice sheet would need to be clustered in a size range of 30-50 m in diameter; such clusters are unknown in the solar system (French and Koeberl, 2010). Boslough et al. (2012) agree with French and Koeberl (2010) that the Younger Dryas impact

Table 2.4. Reproducibility of (peaks in) markers reported as evidence for the YDIH and their use as impact markers. See section 2 for a discussion of the details. Note that there is a discrepancy in reported findings of shocked quartz and that lechatelierite is a very recent finding. + indicates positive – indicates negative.

Markers	Found in impact layers?	Diagnostic?	Other explanations?	Reproduced?
magnetic microspherules	+	-	++	±
scoria-like objects	+	-	+	
lechatelierite	+	+	±	
iridium	+	+	+	-
shocked quartz	+	++	-	-
charcoal / soot	+	-	++	±
carbon spherules / glass-like carbon	-	-	++	±
cubic nanodiamonds	+	-	±	+
lonsdaleite	+	±	±	-
n-diamond	+	-	±	-

event as originally put forward in Firestone et al. (2007) is physically not possible and add that it is also "statistically impossible". Napier (2010), on the other hand, argues that it is theoretically possible for Earth to have encountered a swarm of debris from a fragmenting comet large enough to have caused a catastrophe around 12,900 yrs ago.
Bunch et al. (2012) proposed multiple impact epicentres near the three sites where they found lechatelierite (Abu Hureyra, Middle-East; Blackville and Melrose, North America) and possibly at other locations. The available dates for these three sites, however, have large uncertainties (see also section 5): the layers in which the lechatelierite was found could have been formed centuries to millennia apart. Even if the layers formed at different times, this does not necessarily imply that the sites are not impact related. Tunguska-sized airbursts are fairly common, occurring roughly every 220-1000 years, depending on the study (Revelle, 1997; Brown et al., 2002; Bland and Artemieva, 2006). Impacts on land by iron meteorites large enough to form 100 m diameter craters occur every 500 years (Bland and Artemieva, 2006). Craters this small might be easily obscured by erosion and sedimentation processes over several thousand years. If Bland and Artemieva (2006) are correct, the occurrence of several airburst and/or small impacts occurring decades to centuries apart might prove a plausible explanation for some of the markers found.

2.5. Summary

The Younger Dryas impact hypothesis (Younger Dryas impact hypothesis) consists of two essential parts, (1) an extraterrestrial impact occurring 12,820 ± 130 yrs ago that (2) resulted in continent-wide or worldwide wildfires, the Younger Dryas cooling, megafaunal extinctions, and the disappearance of the Clovis culture. There is no evidence that there were continent-wide wildfires at the onset of the Younger Dryas and it is still debated whether the megafaunal extinctions were indeed sudden or whether there was a gradual megafaunal population decline. Furthermore, wildfires were common and the climate change as well as the megafaunal extinctions can be explained without invoking an extraterrestrial impact. There is thus no evidence that the Younger Dryas impact event as presented by Firestone et al. (2007) took place. However, just because these large-scale environmental changes can be explained by terrestrial mechanisms does not mean that an extraterrestrial impact event could not have taken place around the same time. It is thus important to critically examine the different type of markers found (see table 2.4 for a summary).
It has been argued that material resulting from gradual processes has been interpreted as catastrophic, and terrestrial materials as extraterrestrial, while at the same time no unambiguous impact signatures were reported (Pinter et al., 2011). In addition, other groups failed to reproduce the results (e.g. Paquay et al., 2009; Surovell et al., 2009; Daulton et al., 2010). Proponents of the Younger Dryas impact hypothesis have reported more elaborate analyses, in response to some of the criticism directed at the Younger Dryas impact hypothesis, which have focused on magnetic spherules and nanodiamonds (e.g. Israde-Alcántara et al., 2012). Research on the magnetic spherules now includes SEM analysis showing patterned surfaces as well as chemical analysis (Bunch et al., 2012; Israde-Alcántara et al., 2012; Wittke et al., 2013). Some researchers even argue that only spherules with certain surface patterns and composition should be included (LeCompte et al., 2012), resulting in a discrepancy in the type of spherules counted in different studies. Based on the SEM results, Younger Dryas impact hypothesis proponents no longer consider the magnetic spherules as extraterrestrial but as terrestrial material that was melted into

droplets by an airburst fireball and dispersed in the atmosphere following the shockwave (Bunch et al., 2012; Israde-Alcántara et al., 2012; Wittke et al., 2013). There is however, an alternative explanation for the peak concentrations of magnetic spherules, as well as iridium, both of which tend to accumulate near the bottom of black-mat-type deposits of any age due to unknown processes (Pigati et al., 2012). In addition, other studies on magnetic spherules have shown that similar surface textures and composition are found in magnetic spherules of different origins (e.g. Franke et al., 2007; Grebennikov, 2011; Voldman et al., 2012) and are thus not unique to impact related spherules.

New evidence in the form of lechatelierite in magnetic spherules and scoria-like objects, found only at three sites, might point to an impact-related origin for the spherules at these locations only if lightning strikes are ruled out (French and Koeberl, 2010; Glass and Simonson, 2012). Nanodiamonds, one of the other important lines of evidence, have not been reported at the three sites said to contain lechatelierite, but nanodiamonds have been the focus of other studies at different locations (Kennett et al., 2009a; Kennett et al., 2009b; Tian et al., 2011; Israde-Alcántara et al., 2012). Although some researchers failed to find any diamonds, 3C diamonds are present at some of the sites. Whether the particles interpreted as being lonsdaleite and n-diamond are indeed diamond, is however still questioned (Daulton et al., 2010; Daulton, 2012). Although nanodiamonds can form through impact-related processes, nanodiamonds in distal ejecta layers are not considered diagnostic evidence for an impact (French and Koeberl, 2010). However, there is not much research on nanodiamonds in the geological record and other explanations for the origin of the Allerød-Younger Dryas boundary nanodiamonds are currently not much more convincing. It is therefore important to investigate other plausible nanodiamond formation mechanisms and occurrences in the geological record in order to convincingly rule out or confirm an impact-related origin.

Chapter 3

Case study Geldrop Aalsterhut: Nanodiamonds and wildfire evidence in the Usselo horizon post date the Allerød-Younger Dryas boundary.

The controversial Younger Dryas impact hypothesis suggests that at the onset of the Younger Dryas an extraterrestrial impact over North America caused a global catastrophe. The main evidence for this impact - after the other markers proved to be neither reproducible nor consistent with an impact - is the reported occurrence of several nanodiamond polymorphs, including the proposed presence of lonsdaleite, a shock polymorph of diamond. Magnetic spherules also remained the focus of the Younger Dryas impact studies. Using electron microscopy we examined the buried Usselo soil horizon at Geldrop-Aalsterhut (The Netherlands), which formed during the Allerød/ Early Younger Dryas and would have captured such impact material.

Our AMS radiocarbon dates of 14 individual charcoal particles are internally consistent and show that wildfires occurred well after the proposed impact. In addition we present evidence for the occurrence of cubic diamond in glass-like carbon. No lonsdaleite was found. The relation of the cubic nanodiamonds to glass-like carbon, which is produced during wildfires, suggests that these nanodiamonds might have formed after, rather than at the onset of the Younger Dryas. A preliminary analysis of the magnetic fraction also found no magnetic spherules. Our analysis thus provides no support for the Younger Dryas impact hypothesis.

The main part of this chapter has been published as: van Hoesel A., Hoek W.Z., Braadbaart F., van der Plicht J., Pennock G.M. and Drury M.R., 2012. Nanodiamonds and wildfire evidence in the Usselo horizon postdate the Allerød-Younger Dryas boundary. Proceedings of the National Academy of Sciences 109 (20), 7648-7653. Additional results from the analysis of the magnetic fraction have been added to the chapter version.

3.1 Introduction

The exact cause of the onset of the Younger Dryas stadial (~12,9 ka) is still debated (Fiedel, 2011). Firestone et al. (2007) proposed that an extraterrestrial impact over the North American ice sheet was not only the cause of the rapid cooling, but also resulted in worldwide high temperature biomass burning, North American megafaunal extinction, and the disappearance of the human Clovis culture. Evidence for this hypothesis has been under severe scrutiny ever since; most lines of evidence have proven to be not reproducible or not unique to an impact (see (Pinter et al., 2011) for an overview). Among the lines of evidence proposed by Firestone et al. (2007) were peak concentrations of magnetic grains and spherules. Although magnetic spherules are currently still one of the major lines of evidence (Bunch et al., 2012; Fayek et al., 2012; Israde-Alcántara et al., 2012), others failed to reproduce the results. Furthermore, magnetic spherules are not considered diagnostic for an impact event (Surovell et al., 2009; French and Koeberl, 2010; Pigati et al., 2012).

One of the more promising lines of evidence for the impact hypothesis is the reported occurrence of nanodiamonds in Allerød-Younger Dryas boundary sediments. At first, nanodiamonds were reported based on nuclear magnetic resonance (NMR) analysis of so-called 'glass-like' carbon - black, carbon-rich objects with an irregular shape and smooth reflective 'glassy' surfaces (Firestone et al., 2007). The peak in the NMR spectrum, however, might have been wrongly identified as diamond (Kerr, 2008). More convincing evidence of nanodiamonds was subsequently reported by Kennett et al. (2009a; 2009b). Using transmission electron microscopy (TEM) they claim to have found several nanodiamond polymorphs in so-called carbon spherules – black, carbon-rich spherical objects with a honeycomb-like or open interior structure – and in bulk samples from the Black Mat, a marker horizon in North America dated to the Allerød-Younger Dryas boundary. The polymorphs they reported include cubic (3C) diamond, lonsdaleite (2H diamond) and n-diamond (fcc-carbon). Lonsdaleite is especially of interest, as in nature it is reported only in meteorites (Hanneman et al., 1967) or in relation to impact craters (Gilmour, 1998; Masaitis, 1998), and is generally formed through shock deformation of graphite or diamond. Lonsdaleite has, therefore, been previously taken as evidence for shock impact formation (Gilmour, 1998), although it can also be created in low quantities during carbon vapor deposition (CVD) (Frenklach et al., 1989; Daulton et al., 1996). Furthermore, the presence of lonsdaleite in impact craters has been challenged and the use of nanodiamonds as a diagnostic criterion for an impact is still debated (Koeberl et al., 1997; Gilmour, 1998; Masaitis, 1998; French and Koeberl, 2010). Daulton et al. (2010), however, found no evidence of nanodiamonds in carbon spherules, glass-like carbon or micro-charcoal aggregates from the Black Mat and other, non Allerød-Younger Dryas age, strata. Instead, they found graphene- and graphene/graphane-oxide aggregates in all their samples. Moreover, Daulton et al. (2010) suggest that Kennett et al. (2009a; 2009b) did not find any nanodiamonds either but misinterpreted their diffraction data: mistaking graphene aggregates for cubic diamond and graphene/graphane aggregates for lonsdaleite. Later, the occurrence of n-diamond and lonsdaleite was also reported during a more extensive analysis on a layer of ice from the surface of the Greenland ice sheet (Kurbatov et al., 2010). The layer of ice in which these nanodiamonds were found was indirectly dated to the onset of the Younger Dryas, although Pinter et al. (2011) suggest the oxygen isotope signal might have been misinterpreted and actually points to a Holocene age. In Europe, cubic nanodiamonds were found in the Usselo horizon at Lommel, Belgium (Tian et al., 2011). However, no age-control was presented and no lonsdaleite or n-diamond was found. Recently, nanodiamonds similar to

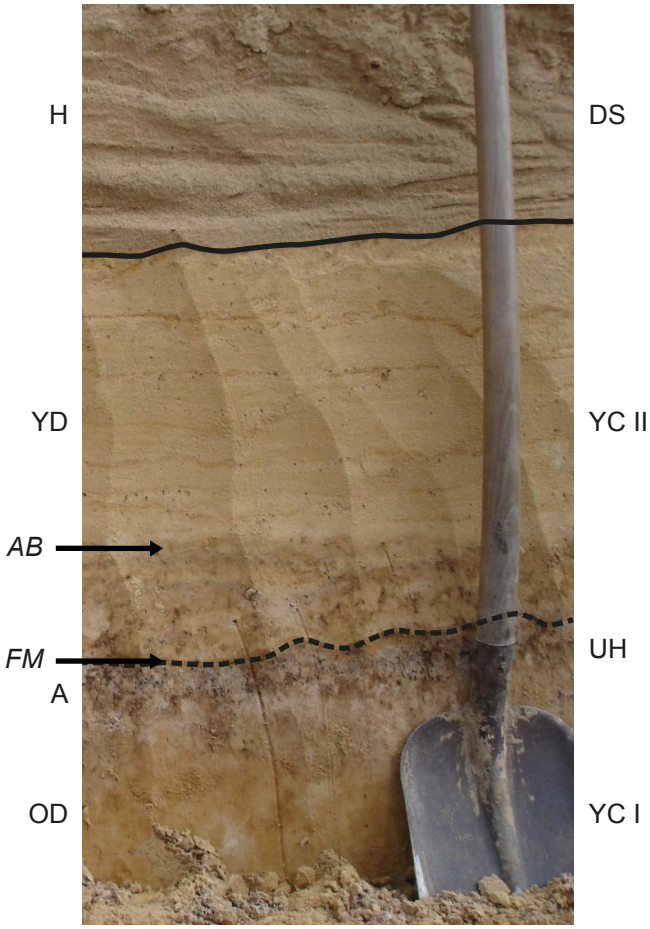

Figure 3.1. The Late Glacial - Holocene stratigraphy at Geldrop Aalsterhut. Approximate time periods are given on the left, stratigraphy on the right. From bottom to top: aeolian deposits belong to the Younger Coversands I (YC I) formed during the Older Dryas (OD) cold stadial. The Usselo horizon (UH), which formed in the top of the YC I during the warmer Allerød (A) interstadial and into the early part of the Younger Dryas (YD) cold stadial, is visible as a bleached layer with charcoal particles. The Younger Coversands II (YC II) were subsequently deposited on top of the UH due to continued aeolian activity as vegetation cover diminished during the Younger Dryas. There is an erosional boundary to the Holocene (H) driftsands (DS), which represent renewed aeolian activity due to human activity during the Middle Ages. The soil that had formed before Medieval times has been eroded at this location. Occupation horizons of the Federmesser (FM) and the Ahrensburg (AB) culture are indicated with arrows. The Ahrensburg occupation horizon at Geldrop has been dated within 10,600 - 9,800 14C yrs BP (Vermeersch, 2011). The Federmesser culture had mostly disappeared from the Benelux near the end of the Younger Dryas (De Bie and Vermeersch, 1998; Riede, 2008; Vermeersch, 2011). At Geldrop, their occupation horizon coincides with the Usselo horizon.

those found in the Greenland were found in Mexican lake sediments thought to represent the Allerød-Younger Dryas boundary (Israde-Alcántara et al., 2012). However, even if their age-depth model is correct, the 10 cm wide peak in nanodiamonds might reflect 5890 years of deposition (Israde-Alcántara et al., 2010). The occurrence and origin of nanodiamonds, and especially lonsdaleite, in the Younger Dryas boundary sediments is thus still uncertain.

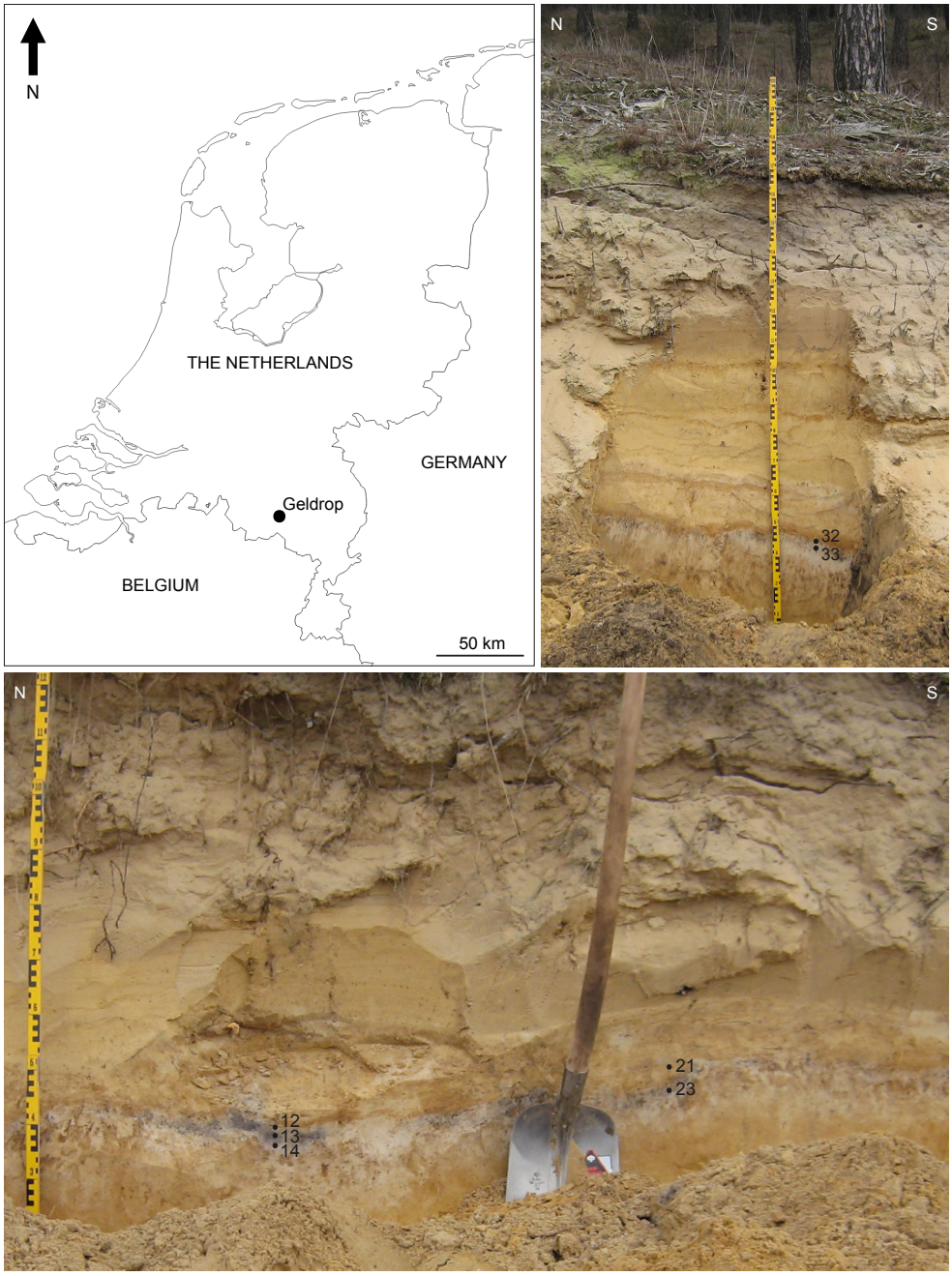

Figure 3.2. Location of the field site (Geldrop-Aalsterhut) and the charcoal samples from the Usselo Horizon used for ^{14}C dating. The section shown at the top is located approximately 20-m south of the section shown at the bottom. See Figure 1 for stratigraphy and Table 1 for specific depth of the samples.

In the North Western European coversand area, the onset of the Younger Dryas is often stratigraphically marked by the Usselo horizon, a buried/fossil soil horizon formed during the Allerød to early Younger Dryas (Kaiser et al., 2009). During the second half of the Younger Dryas the Usselo horizon was covered by the Younger Coversand II (Kasse, 2002) (figure 3.1). The Usselo horizon should thus have collected any impact material falling from the atmosphere during the Allerød to early Younger Dryas. Using electron microscopy techniques, we investigated the Usselo horizon at Geldrop-Aalsterhut (figure 3.2), The Netherlands, for the occurrence of nanodiamonds and also conducted a preliminary search for magnetic spherules. Bulk charcoal from the Usselo horizon at Geldrop has been previously dated (De Vries et al., 1958) to 11,020 ± 230 ^{14}C BP, 13,085 - 12,715 cal. yrs BP (sample GrN-603), and to 10,960 ± 85 ^{14}BP, calibrated 12,920 - 12,730 cal. yrs BP (sample GrN-1059). These ^{14}C dates are from the early days of radiocarbon dating, they were measured by radiometry and are thus imprecise compared to modern standards, in particular sample GrN-603. Here we report on new, more precise AMS (accelerator mass spectrometry) dates for 14 individual charcoal particles, twelve from the Usselo horizon and two from just above the horizon. In addition, the reflectance of several charcoal particles was measured using light microscopy to estimate the wildfire temperature (Braadbaart and Poole, 2008; McParland et al., 2009).

3.2 Methods

3.2.1 Fieldwork

Samples were taken during a one-day fieldwork at the archaeological site Geldrop Aalsterhut. Several pits were manually dug using shovels and cleaned with trowels to locate the best part of the Usselo horizon to sample. Samples of 200-800 g of sediment were taken by the corresponding and second author from three selected locations in two pits at several intervals within and above the charcoal-rich part of the Usselo horizon (see figure 3.2 and table 3.1). One bulk sample of the charcoal layer at the top of the Usselo horizon at Aalsterhut, AH-4, was sampled by a colleague together with the second and last author during an earlier field visit.

3.2.2 Radiocarbon dating

A total of 14 individual charcoal particles, >2 mm, from different samples (table 3.1) were hand picked and prepared for AMS radiocarbon dating using standard Acid-Alkali-Acid treatment and ultrasonic cleaning (Mook and Streurman, 1983) by which only charcoal structures remained while soot disaggregated. Radiocarbon ages were measured at the Groningen AMS facility (van der Plicht et al., 2000) and reported in conventional radiocarbon years (Mook and van der Plicht, 1999). Ages were calibrated to calendar years using the IntCal13 calibration curve (Reimer et al., 2013) and the OxCalv4.2 calibration software (Bronk Ramsey, 2009). Both the radiocarbon and calibrated ages are rounded to the nearest 5; all uncertainties are given within 1-sigma confidence.

3.2.3 Charcoal reflectance analysis

Several charcoal particles, >2mm, from sample AH-21 were embedded in resin blocks, polished and submitted to reflectance analysis for a preliminary estimate of the wildfire temperature following the procedure described in (Braadbaart and Poole, 2008). For each particle, 100 measurements of the reflections were taken at different locations using a Leitz motorized DMLA microscope.

3.2.4 Scanning electron microscopy analysis of the carbonaceous fraction

Subsamples of 100 g from samples AH-4, 14 and 33 were dried in the oven at 90 °C, and sieved into fractions of <63 μm, 63-355 μm, and >355 μm. The carbonaceous fraction, of 63-355 μm, was floated using sodiumpolytungstate heavy liquid with a density of 2000 kg/m3. Floatation in water, as used in the original study (Firestone et al., 2007; Kennett et al., 2009b), did not yield any carbon spherules. Carbon spherules and glass-like carbon were then picked under a light microscope (magnification 40x) based on their morphology; that is black spherical particles or black particles with an irregular shape and smooth reflective 'glassy' surface. The distinction between glass-like carbon and normal charcoal, however, was not always easy to make as there seems to be a gradual transition between the two with some charcoal particles having a partly 'glassy' surface. Representative particles from samples AH-14 and 33 were mounted on a stub and analyzed using an FEI XL30SFEG SEM (scanning electron microscope) equipped with an EDAX EDXS (energy dispersive X-ray spectrometry) detector located at the Electron Microscopy laboratory Utrecht (EMU).

3.2.5 Transmission electron microscopy analysis of the carbonaceous fraction

Carbon spherules (sample AH-4) and glass-like carbon particles (samples AH-14 and 33) were separately grouped for transmission electron microscopy (TEM) analysis. These were crushed in ethanol using an agate pestle and mortar, and part of the suspension dispersed on a holey carbon grid. TEM analysis was preformed using a FEI Tecnai 12 120kV and a Tecnai 20 FEG 200kV TEM equipped with an EDAX EDXS detector, both located at EMU. The TEM grids were sampled both in diffraction mode, to locate crystalline particles, and in image mode to locate individual particles. In this way, several hundreds of particles per grid were analyzed. Selected area diffraction patterns were used to identify the crystal structure of the particles, and EDX spectrometry was to check the carbon content.

3.2.6 Extraction and analysis of the magnetic fraction

One bulk sample (500 g) of the Usselo horizon was sieved for magnetic separation. The magnetic fraction <38 μm was separated in water using a Frantz magnetic separator at 0.8 A. The magnetic fractions of 38-53 μm and 53-75 μm were separated dry using a hand magnet. All fractions were analyzed under a light microscope for the presence of spherules. A small subsample from each fraction was then mounted on a carbon sticker on an SEM stub and carbon coated. Chemical analysis of the particles was made using EDX spectroscopy in the SEM.

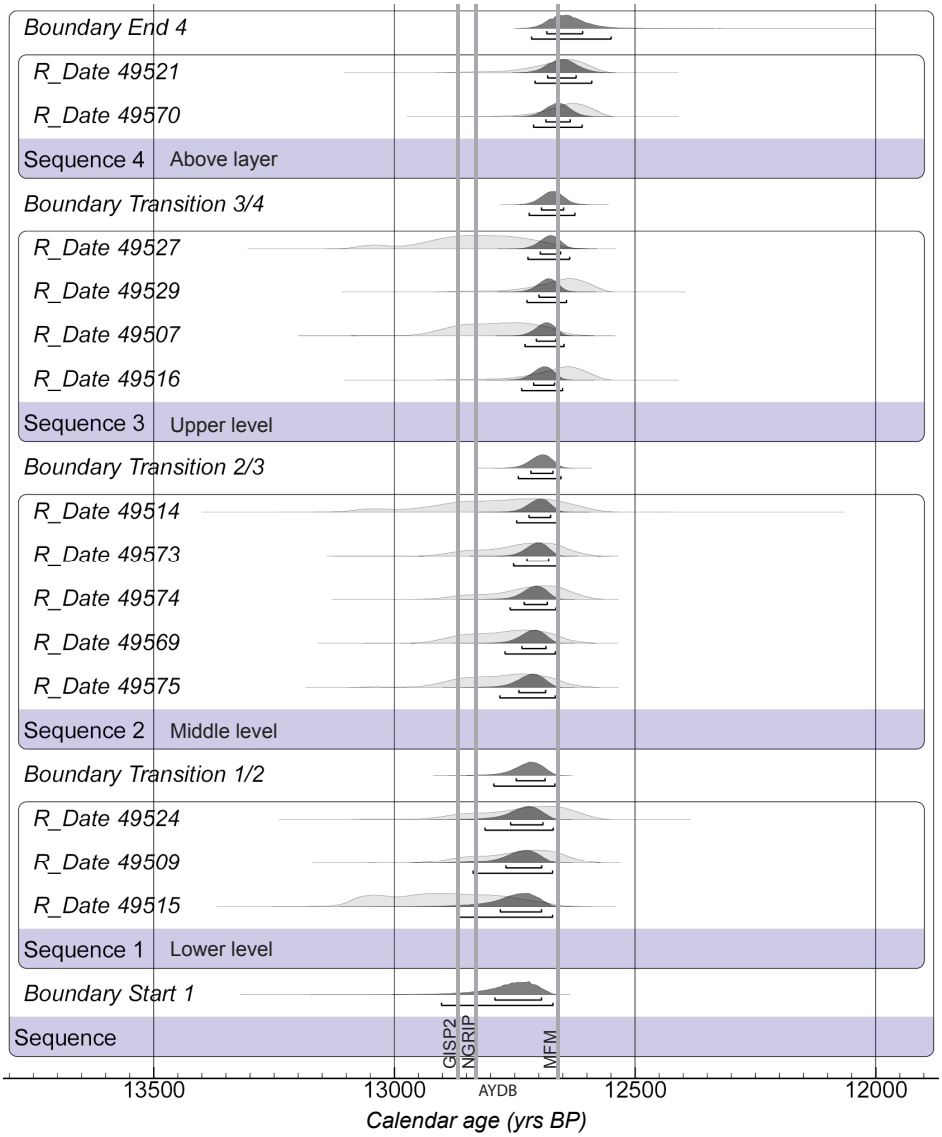

Figure 3.3. Modelled (dark gray) and unmodelled (light gray) calibrated age of the charcoal particles in calendar years B.P. Bayesian analysis was performed using the OxCal v4.1.7 program (Bronk Ramsey, 2009) and the IntCal09 calibration curve (Reimer et al. 2009). Dates were grouped according to their respective location within the charcoal-rich part of the Usselo horizon (see also Table 1 and Figure S1), boundaries between the levels are calculated by the model. The distribution of the modelled dates is much narrower than the single calibrated ages. Although the modelled dates show a trend toward younger dates at the top, they all overlap within two standard deviations. Furthermore, the boundaries between the different groups all overlap within one standard deviation, making them statistically the same. The Allerød-Younger Dryas boundary (AYDB) is indicated according to the Greenland Ice Sheet Project 2 and North Greenland Ice Core Project ice cores (Stuiver et al., 1995; Rasmussen et al., 2006) as well as the Meerfelder Maar (MFM) varved lake (Brauer et al., 1999). The timing of the onset of the Younger Dryas as derived from the ice cores most likely represent the timing of the alleged impact because the Greenland ice sheet would have recorded the destabilization of the thermohaline circulation to which the impact has been linked by Firestone et al. (2007).

3.3 Results

The AMS radiocarbon dates of carefully selected and cleaned individual charcoal particles from the charcoal rich top part of the Usselo horizon show no correlation with depth and range over 400 ^{14}C years (table 3.1.). The weighted average of the charcoal particles from the Usselo horizon is 10,870 ± 15 ^{14}C yrs BP (12,750 – 12,715 cal. yrs BP). Bayesian analysis (Bronk Ramsey, 2009) however, shows that the two particles found slightly above the horizon (AH21a,b), are part of the same population (figure 3.3); it is likely that they were distributed due to bioturbation. Including these two particles yields a slightly younger average of 10,845 ± 15 ^{14}C yrs BP (12,740 – 12,710 cal. yrs BP). Our radiocarbon ages are consistent with optically stimulated luminescence (OSL) ages from the same sites (Tebbens et al. 2013) and two centuries younger than the Black Mat layers in which hexagonal diamonds have been found (Kennett et al., 2009b), which have an average age of 11,070 ± 10 ^{14}C yrs BP (13,005 – 12,900 cal. yrs BP) (Kennett et al., 2009b). With the exception of one or two outliers in each dataset, the datasets show almost no overlap (figure 3.4); these outliers all have high standard deviations. When compared to other radiocarbon dated sites reported to contain nanodiamonds (Kennett et al., 2009a) our layer is of a similar age to Murray Springs (Haynes Jr., 2008) but older than Lake Hind (Firestone et al., 2007).

Charcoal particles from the Usselo horizon show a reflectance of 0.96 ± 0.06 %Ro, indicating a charring temperature of approximately 420 ± 10 °C, assuming a charring period of 1 hour

Table 3.1. AMS radiocarbon dates of the individual charcoal particles from the charcoal-rich top layer of the Usselo horizon at Geldrop-Aalsterhut (individually calibrated using IntCal13). The larger measurement errors are caused by the fact that the samples were very small, even for AMS. Samples were taken from different depths within the Usselo horizon at three different locations at Geldrop-Aalsterhut (see Figure 3.2.) The depth of the samples is indicated using the top of the Usselo horizon as a reference level (0 cm). See Figure 3.3. for a visual overview of the modelled and individually calibrated dates.

Sample name	Depth (cm	Sample nr. for AMS	^{14}C age BP	Cal. age BP
AH-21a	-5.0 – -4.0	GrA-49570	10,735 ± 45	12,715 - 12,657
AH-21b	-5.0 – -4.0	GrA-49521	10,765 ± 50	12,725 - 12,675
AH-12a	0.0 – 2.0	GrA-49516	10,765 ± 50	12,725 - 12,675
AH-12b	0.0 – 2.0	GrA-49507	10,920 ± 50	12,810 - 12,725
AH32a	0.0 – 2.0	GrA-49527	10,960 ± 60	12,885 - 12,735
AH-32b	0.0 – 2.0	GrA-49529	10,755 ± 55	12,725 - 12,660
AH-23a	0.0 – 2.0	GrA-49573	10,860 ± 45	12,760 - 12,705
AH-23b	0.0 – 2.0	GrA-49574	10,845 ± 45	12,750 - 12,700
AH-13a	2.0 – 4.0	GrA-49569	10,895 ± 45	12,790 - 12,720
AH-13b	2.0 – 4.0	GrA-49514	10,880 ± 110	12,885 - 12,690
AH-33a	2.0 – 4.5	GrA-49575	10,900 ± 50	12,795 - 12,720
AH-14a	4.0 – 5.5	GrA-49515	11,020 ± 75	12,985 - 12,795
AH-14b	4.0 – 5.5	GrA-49509	10,865 ± 55	12,775 - 12,705
AH-14c	4.0 – 5.5	GrA-49524	10,840 ± 75	12,785 - 12,690

The larger measurement errors are caused by the fact that the samples were very small, even for AMS. Samples were taken from different depth Usselo at three different locations (see figure. 3.1). The depth of the samples is indicated using the top of the Usselo horizon as a reference level (0 cm). See figure. 3.2 for a visual overview of the modelled and individually calibrated dates.

(Braadbaart and Poole, 2008). This temperature is consistent with the occurrence of carbon spherules and glass-like carbon found within the horizon (figure 3.5), which are both thought to form during low temperature wildfires (McParland et al., 2010; Scott et al., 2010). Glass-like carbon (up to 150 particles/100g) is more common in the Usselo horizon than carbon spherules (<10 particles/100g). Charcoal (figure 3.6) is, however, the most abundant form of charred material (>10,000 particles/100g). Although the charcoal particles, in most cases, have the characteristic cell structure of the precursor wood (figure 3.6d), the polished sections also showed parts where no remnant cells were observed (figure 3.6c).

TEM analysis of crushed glass-like carbon particles shows the presence of carbonaceous microparticles similar to those interpreted by Kennett et al. (2009b) as lonsdaleite (figure 3.7a,c). Diffraction rings, containing discrete spots (figure 3.7b,d), correspond to some of the known lonsdaleite spacings (Hanneman et al., 1967). The patterns, however, like the ones reported from the Black Mat (Kennett et al., 2009b), do not display rings associated with the unique 1.93 Å and 1.50 Å d-spacings associated with lonsdaleite (table 3.2). The diffraction patterns of these particles are therefore more consistent with graphene-graphane aggregates instead (Daulton et al., 2010). Some of the diffraction patterns (figure 3.7d) show a small number of grouped spots corresponding to the 1.54 Å and 1.79 Å d-spacings of graphite and might therefore be closer to turbostratic carbon or disordered graphite than the randomly stacked graphene/graphane aggregates.

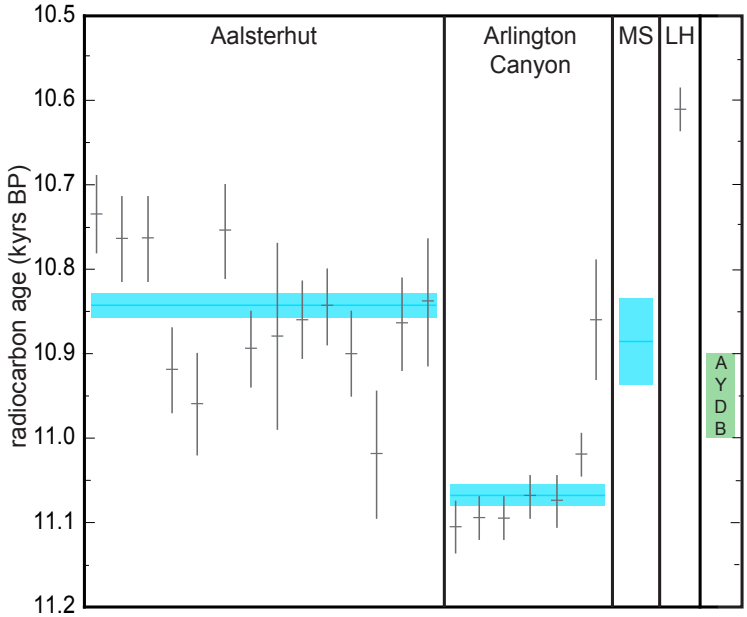

Figure 3.4. Individual radiocarbon ages (uncalibrated) and weighted average (blue bands) of the charcoal particles from the Usselo horizon at Aalsterhut compared to those of the Black Mat at Arlington Canyon, where the alleged hexagonal diamonds have been found (Kennett et al., 2009b). The age of the lower boundary of the Black Mat at Murray Springs (MS, average of 8 (Haynes Jr., 2008)) and Lake Hind (LH, single date (Firestone et al., 2007)), where cubic and n-diamonds have been found (Kennett et al., 2009a) are also included. For reference, the approximate age of the Allerød-Younger Dryas boundary (AYDB) is indicated in green (see discussion).

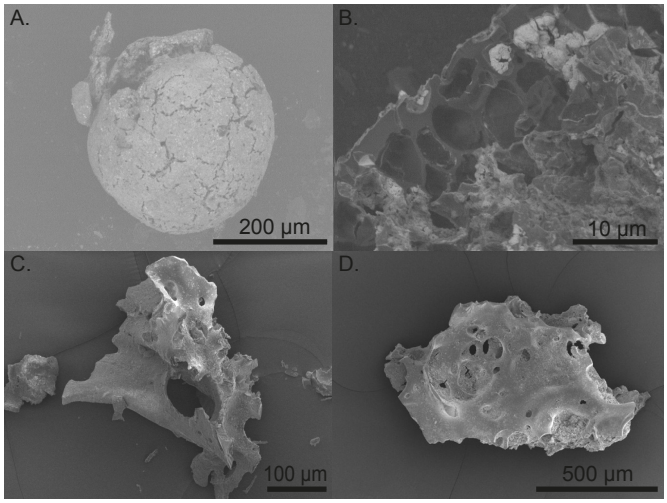

Figure 3.5. Secondary electron (SE) scanning electron microscopy (SEM) images of hand-picked carbon spherules (sample AH-33) and glass-like carbon (sample AH-4). (a) Complete carbon spherule and (b) close up of internal structure of a broken carbon spherule. Energy dispersive X-ray (EDX) spectrometry shows that the spherules contain 45-90 wt% carbon; the other dominant element is oxygen. Although smaller (<0.3 mm in size compared to <2.5 mm in size) these particles look similar to the carbon spherules found in the Black Mat (Firestone et al., 2007; Kennett et al., 2009b), as well as to charred fungal sclerotia (Scott et al., 2010). (c,d) Examples of 'glass-like carbon' showing smooth 'glassy' surfaces and irregular shapes. No remnant structure of the precursor wood, as in charcoal (figure 3.6A,B),is visible.

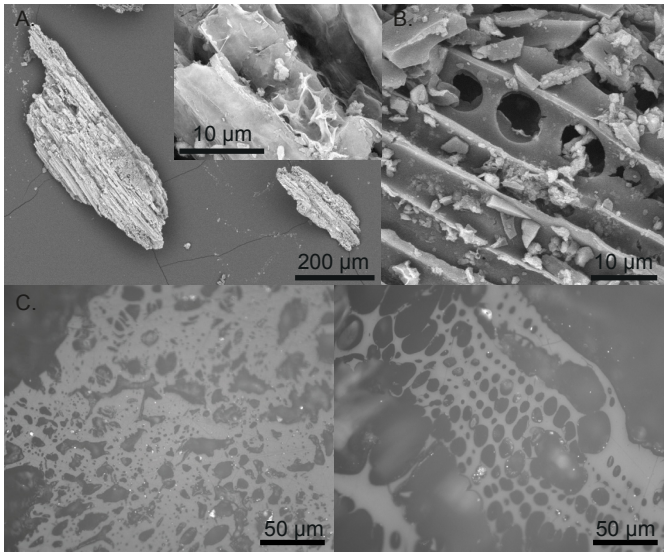

Figure 3.6. Charcoal from the Usselo horizon. (a) SE image of two charcoal particles from the charcoal part of the Usselo horizon (sample AH-4) showing remnant structure from the cell walls of the precursor wood. The inset shows a higher magnification image of the particle on the left, showing detail of small-scale structure. (b) SE image of a different charcoal particle showing the same structure. (c,d) Reflective light image of two polished charcoal particles (sample AH-21) analyzed for their reflectance. The polished sample (c) shows no evidence of remnant cell walls, while in (d) cell walls are observed.

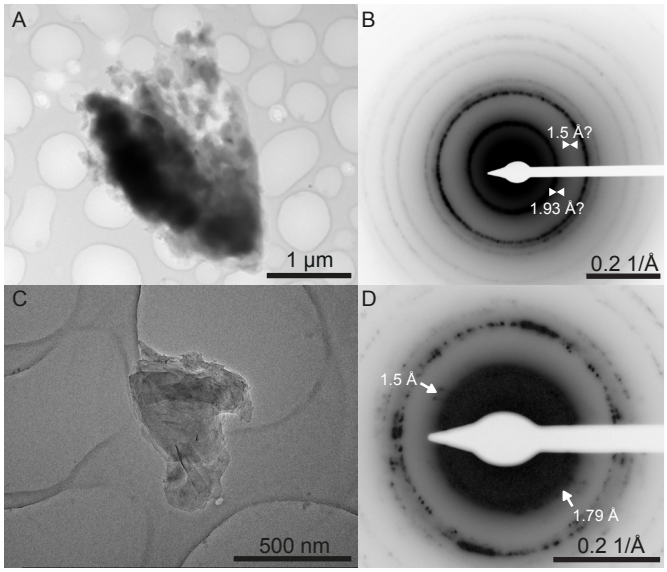

Figure 3.7. Bright field TEM images of carbonaceous microparticles within crushed glass-like carbon (a,b: sample AH-14; c,d: sample AH-33) and their associated diffraction patterns. Diffraction patterns are inverted for better visibility. (b) Diffraction pattern of (a) showing double diffraction rings corresponding to graphene/graphane aggregates, rather then lonsdaleite. The double triangles show the location of the missing 1.93 Å and 1.5 Å rings that should be present in the case of lonsdaleite. (d) Diffraction pattern of (c) showing discrete rings. The arrows indicate a few discrete spots corresponding to a d-spacing of 1.5 and 1.79 Å, which are known d-spacings of graphite. Measured d-spacings are given in table 3.2.

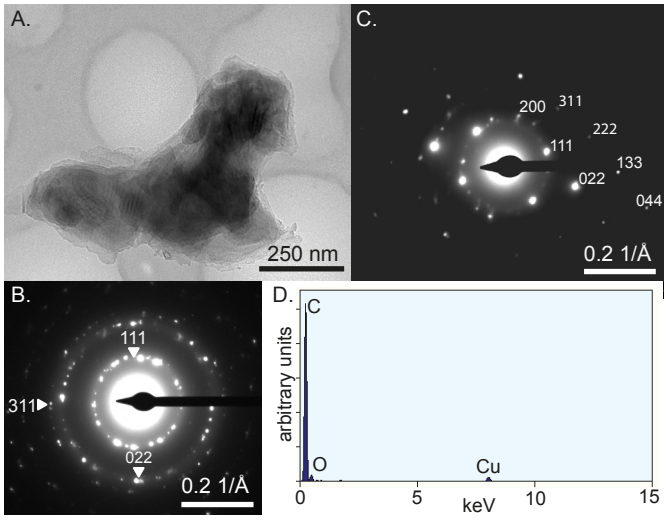

Figure 3.8. (a) Bright field TEM image of a polycrystalline diamond particle within crushed glass-like carbon from the lower part of the charcoal-rich layer (sample AH-14). (b) Diffraction pattern of the entire particle showing rings corresponding to the diamond d-spacings and (c) [011] SADP of a single diamond crystal from the particle in (a). (d) The EDX spectrum shows the carbonaceous nature of the particle, the small copper peak is from the copper grid used to support the holey carbon film.

Other, less common, polycrystalline particles show diffraction rings with d-spacings corresponding to cubic diamond (figure 3.8.), although the cubic diamond reflections are also close to those calculated for graphene (Daulton et al., 2010). The 400 reflection (0.89 Å) however, which has no equivalent in graphene (table 2.3), is weakly present. The selected area diffraction pattern (SADP) of a small part of the particle (~200 nm) in Figure 6A yields a diffraction pattern (figure 3.8c) similar to the [011] pattern of cubic diamond (Edington, 1975). Weak 200 'forbidden' reflections, forbidden for cubic diamond but not for fcc-carbon or n-diamond, are visible. They do not show up in the ring pattern and are, therefore, more likely the result of double diffraction within a cubic diamond crystal than an indicator for n-diamond.

SEM Analysis of the magnetic fraction showed that the magnetic grains have a variety of shapes and sizes. Figure 3.9 shows some examples of the magnetic grains found. Most of the grains are rounded (e.g. figure 3a), suggesting they have been transported, most likely as part of the coversand. Some of the grains showed different morphologies, including grains consisting of plate-like morphology, likely a titanohematite (figure 3.9c,d) and a small spherule-like particle made up of pyramids (figure 3.9e). No magnetic spherules were found. The composition of the magnetic grains within the different fractions is summarized in table 3.3. Most magnetic grains sconsist of magnetite, although Ti bearing grains were also observed. Sometimes, particles appeared to consist of non-magnetic grains coated with magnetic material (figure 3.9a,b).

Table 3.2. Measured d-spacings from the particles in figure 3.7 compared to the known d-spacings of Lonsdaleite as well as the graphitic forms of carbon. The spacings of the particles cleary match those of graphene and graphene/ graphane aggregates

Lonsdaleite		**Graphite**		**Graphene**		**Graphane**		**Measured**	
hkl	spacing	hkl	spacing	hkl	spacing	hkl	spacing	fig. 3.7a,b	fig. 3.7c,d
		002	3.35						
100	2.18	100	2.13	100	2.13			2.12	2.10
002	2.06	101	2.05			100	2.02		2.01
101	1.93	102	1.80						1.78*
		004	1.68						
102	1.50	103	1.54						1.54*
110	1.26	110	1.23	110	1.23			1.25	1.22
103	1.16	112	1.16			112	1.17		1.15
200	1.09	006	1.12						
112	1.08	200	1.07	200	1.07			1.07	1.07
004	1.03	202	1.03			200	1.01		1.03

*Just a few spots visible rather than full rings.

3.4 Discussion

3.4.1 Wildfires

Our radiocarbon dates suggest that wildfires at this location occurred after the Allerød-Younger Dryas transition. There are, however, uncertainties in the timing of the Younger Dryas onset

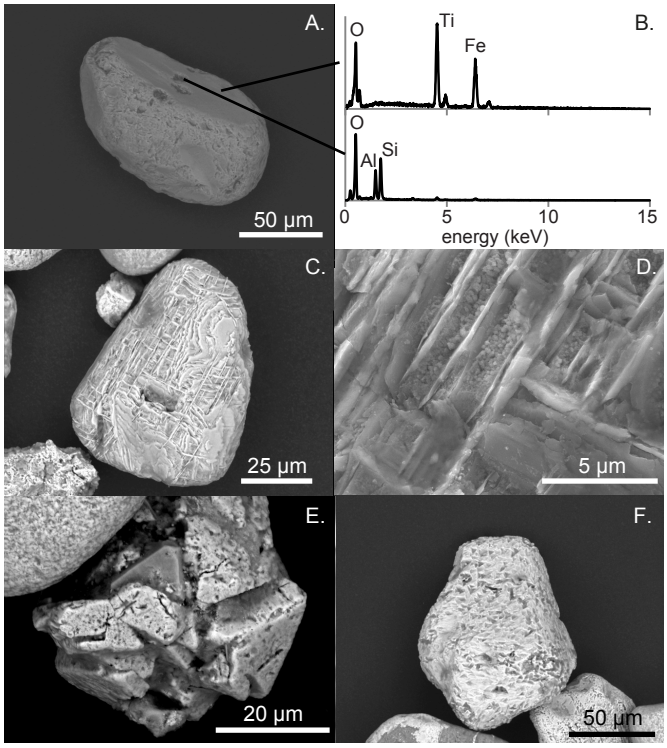

Figure 3.9. SEM back scatter electron images of magnetic grains from the Usselo horizon. (a) Typical rounded grain with some pits that show up darker in the BSE image. (b) EDX spectra of the surface of the grain in a (table 3.2 magnetic particles 38-53 µm #1c) as well as the darker pit (table 3.2 magnetic particles 38-53 µm #1b). The difference in composition between the overall surface and the pits suggest that the particle consist of a non-magnetic grain (Al-silicate) encrusted in magnetic material (possibly Ti-magnetite). (c) Grain with plate-like morphology, likely titanohematite (table 3.2 magnetic particles 38-53 µm #9). (d) Higher magnification image of the grain in (c). (d) Small semi-spherical grain consisting of pyramid shaped crystals (table 3.2 magnetic particles 38-53 µm #12). (f) Semi-rounded grain with pitted surface (table 3.2 magnetic particles 38-53 µm #8).

(Fiedel, 2011), as well as in the interpretation of wood-charcoal ages due to the 'inbuilt age' effect (Gavin, 2001). The inbuilt age occurs because consumption of the outer wood during a wildfire leaves charcoal with radiocarbon ages representing the older wood of the trees (Gavin, 2001). In addition many trees would have died as a result of wetter conditions during the early Younger Dryas (Hoek and Bohncke, 2002), possibly providing an older fuel source. Both these aspects of the inbuilt age result in the charcoal radiocarbon ages pre-dating the wild-fire event for an unknown number of years. Additional uncertainty arrises when callibrating the radiocarbon ages to calendar years because of uncertainties in the callibration curve (Reimer et al. 2013) and comparing ages calibrated using different calibration curves can lead to confusion and misinterpretation of results (see box 3.1). Therefore, radiocarbon ages of the Geldrop Aalsterhut site are directly compared to the onset of the Younger Dryas or the nanodiamond bearing layers at other sites rather than calibrating them first (e.g. figure 3.4).

The precise timing of the Younger Dryas onset is still ambiguous (Fiedel, 2011) and the calibration curve for this interval is not definitive (Reimer et al., 2009; Blockley et al., 2012). For North Western Europe the onset of the Younger Dryas chronozone, which is marked by a

Table 3.3. Geochemistry of the magnetic particles from the Usselo horizon obtained using SEM EDX. # indicates sample number.

Magnetic particles <38 micron													
#	Na2O	MgO	Al2O3	SiO2	P2O5	SO3	K2O	CaO	TiO2	Cr2O3	MnO	Fe2O3	NiO
02	6,03	5,70	2,49	21,23	1,36	2,64	0,82	1,50	1,26	5,86	3,32	37,20	10,58
03	12,29	6,32	9,94	9,66	3,84	5,57	1,17	2,15	5,25	1,26	3,12	34,40	5,04
04	2,74	2,80	5,70	15,82	0,80	2,24	0,67	1,15	41,28	0,71	4,16	19,13	2,80
06a	10,72	4,57	12,54	16,88	3,73	4,20	0,31	0,73	5,18	0,29	2,69	38,16	0,00
06b	10,48	5,63	12,53	20,44	4,32	5,46	1,30	1,71	7,60	0,54	2,42	25,71	1,86
07	9,19	2,09	9,58	22,76	2,56	3,82	0,31	1,08	5,41	1,08	5,84	33,18	3,09
08	10,35	4,15	12,32	19,07	2,83	3,60	1,32	1,60	5,64	0,60	2,77	31,04	4,71
10	29,07	0,00	4,25	22,60	1,35	34,72	2,08	0,00	1,74	0,00	4,19	0,00	0,00
12	8,92	2,15	10,89	18,07	3,00	2,28	0,64	0,83	5,44	0,63	3,61	40,47	3,06
13	0,00	2,06	1,41	2,62	0,55	1,00	0,75	1,42	56,48	0,34	2,48	28,33	2,56
13b	0,83	26,20	19,27	34,20	0,13	0,48	0,36	0,89	0,78	0,47	0,86	13,34	2,19
Magnetic particles 38-53 micron													
#	Na2O	MgO	Al2O3	SiO2	P2O5	SO3	K2O	CaO	TiO2	Cr2O3	MnO	FeO	NiO
01a	1,61	2,69	1,64	3,07	0,47	0,39	0,12	0,19	40,47	0,05	0,74	48,13	0,43
01b	2,16	4,13	18,27	57,66	0,80	0,94	1,47	0,32	5,86	0,00	0,26	7,64	0,50
01c	0,29	0,55	0,58	1,13	0,28	0,59	0,22	0,41	41,87	0,28	1,62	50,66	1,52
02	1,78	2,54	1,87	2,58	0,64	0,80	0,08	0,13	89,60	0,00	0,00	0,00	0,00
03a	2,86	3,98	2,91	54,37	26,49	2,45	0,08	0,00	0,45	0,32	1,14	1,65	3,30
03b	3,08	5,12	8,25	54,34	18,12	2,51	0,62	0,31	0,38	0,29	0,72	4,20	2,05
04a	1,56	2,55	1,98	3,53	0,48	0,46	0,00	0,18	51,20	0,00	1,69	36,06	0,30
04b	0,56	3,03	15,08	51,49	0,41	0,38	2,19	1,43	8,31	0,23	0,66	15,38	0,88
05	1,48	5,24	1,40	2,35	0,63	1,04	0,18	0,32	41,84	0,20	1,34	42,63	1,36
06	2,24	3,59	4,70	10,33	0,92	0,99	0,37	0,34	49,42	0,53	2,98	21,55	2,06
07	0,00	1,84	3,63	1,89	0,12	0,57	0,24	0,49	3,96	16,26	1,05	68,63	1,34
08	2,42	3,50	1,59	3,12	1,08	1,59	0,69	1,08	1,14	0,48	1,03	80,55	1,72
09	3,34	9,70	3,52	3,52	0,85	1,09	0,40	0,45	38,48	0,37	2,07	34,50	1,70
10a	0,58	0,87	0,67	2,14	0,09	0,53	0,50	2,19	10,10	15,04	5,51	56,52	5,27
10b	0,00	0,36	0,38	0,65	0,03	0,10	0,12	0,29	1,36	4,33	2,77	88,72	0,88
10c	2,05	3,83	2,60	5,03	0,94	1,60	0,56	0,94	1,18	17,57	4,99	57,86	0,85
14a	1,94	28,42	12,29	3,77	0,57	0,55	0,19	0,27	6,13	0,19	1,54	43,71	0,44
14b	1,18	32,66	33,12	1,76	0,47	0,41	0,11	0,33	1,20	0,38	0,73	27,63	0,00
Magnetic particles 53-75 micron													
#	Na2O	MgO	Al2O3	SiO2	P2O5	SO3	K2O	CaO	TiO2	Cr2O3	MnO	FeO	NiO
2	1,52	1,46	1,17	93,84	0,55	0,91	0,09	0,08	0,00	0,00	0,07	0,00	0,31
3	12,53	2,00	12,82	68,35	0,78	1,05	0,24	0,90	0,28	0,06	0,31	0,35	0,32
6	1,63	2,40	12,80	74,65	0,49	0,66	6,59	0,05	0,00	0,00	0,07	0,33	0,32
07a	1,70	4,13	14,24	42,09	0,77	1,00	0,25	5,86	0,20	0,09	3,16	6,84	0,68
07b	2,01	4,95	17,28	52,27	0,98	1,26	0,31	7,31	0,25	0,12	3,93	8,49	0,84

change in vegetation, was originally defined at 11,000 ^{14}C yrs BP (Mangerud et al., 1974). This age corresponds to the increase in atmospheric ^{14}C starting between 11,000 and 10,950 ^{14}C yrs BP, often referred to as the "radiocarbon cliff". This radiocarbon cliff is presumably related to the shutdown of the thermohaline circulation, and has been suggested as a global marker for the onset of the Younger Dryas (Goslar et al., 1995; Hajdas et al., 1998; Fiedel, 2011; Kaiser et al., 2012). In the Netherlands, the clear shift in vegetation marked by an abrupt increase in non-arboreal pollen from numerous palynological records related to the onset of the Younger Dryas occurred slightly later, around 10,950 ^{14}C yrs BP (Hoek, 1997). An even younger age for the onset of 10,900 ± 50 ^{14}C yrs BP has been adopted when dating the North American Black Mats (Haynes Jr., 2008). Therefore, we use a range of 11,000 to 10,900 ^{14}C yrs BP for the Allerød-Younger Dryas boundary (figure 3.4) in which the older half (11,000 – 10,950 ^{14}C yrs BP)

corresponds best to the northwestern European records (Mangerud et al., 1974; Hoek, 1997; Schaub et al., 2008; Hua et al., 2009; Kaiser et al., 2012).
Within two standard deviations, our individual radiocarbon ages do not all overlap, and show a gap of 45 ^{14}C yrs between the youngest and the oldest age (table 3.1). This gap is within the lifespan of an individual pine tree, which can grow up to 200 years old, and less than the minimum fire frequency in present day boreal forests of 50 – 200 years (van der Hammen and van Geel, 2008). When looking at the calibrated dates (table 3.1) however, there is no gap but an overlap of at least 10 cal. yrs within one standard deviation. Furthermore, when using Bayesian statistics (Bronk Ramsey, 2009), all ages overlap within one standard deviation (figure 3.3.) and they are thus statistically the same.
The charcoal in the Usselo horizon at Geldrop-Aalsterhut can thus easily represent a single episode of wildfire, with the charcoal particles dispersed through the top of the Usselo horizon by bioturbation. In that case, taking into account the inbuilt age, all radiocarbon ages pre-date the actual wildfire and the maximum age of the youngest charcoal particle (AH-21a, within two standard deviations), 10,835 ^{14}C yrs BP, provides a maximum (oldest) age estimate of the timing of the wildfire (Gavin, 2001). The wildfire thus occurred up to two centuries after the onset of the Younger Dryas (figure 3.4). The wildfire is therefore not only low temperature, but also does not fall within the same time window as the proposed impact, which is contrary to suggestions by Firestone et al. (2007). Moreover, when compared to the nanodiamond bearing layer at Arlington Canyon (Kennett et al., 2009b) our wildfire is clearly younger (figure 3.4) and, therefore, must represent a different event. Our findings are, however, in agreement with several studies in North America showing the absence of evidence for continent-wide wildfires (Gill et al., 2009; Marlon et al., 2009; Haynes et al., 2010), let alone intercontinental wildfires reaching Europe.
As our charcoal particles were derived from a palaeosol horizon, which accumulates material over a long time period, it can also be argued that the dated charcoal particles represent multiple wildfires, rather than just one episode of biomass burning. Within the respective dating uncertainties, some of the older charcoal particles might then be related to a wildfire occurring around the onset of the Younger Dryas. This does not however require a relation with the proposed impact, as frequent fires occurred naturally (van der Hammen and van Geel, 2008).

3.4.2 Origin of the nanodiamonds

When considering the extraterrestrial impact hypothesis there are several possibilities for the origin of the nano- and microdiamonds. They [1] originate from the impactor body, [2] formed through shock-transformation processes during the impact, [3] formed within the high temperature 'fireball' resulting from the airburst or impact, [4] could have arrived through continuous 'meteoritic rain' or [5] formed through a terrestrial process unrelated to an impact.
[1] Tian et al. (2011) report that nanodiamonds found in the Usselo horizon at Lommel contained terrestrial isotopic δ13 C and C/N ratios, while Kurbatov et al. (2010) note that the rounded n-diamonds they found in the Greenland ice sheet are 'unlike any diamonds found in meteorites'. These results suggest that these nanodiamonds did not originate from an impactor. In addition, a nanodiamond-bearing impactor would have been enriched in platinum group elements, which are absent in the Younger Dryas boundary layer (Paquay et al., 2009).
[2] The occurrence of lonsdaleite, although a rare but possible indicator of shock metamorphism, has not been independently confirmed. Lonsdaleite is, however, also absent in the K/T

(Cretaceous/Tertiary) boundary, where only shock produced cubic diamond was found (Gilmour et al., 1992; Hough et al., 1997). The morphology of the smaller (~20 nm) nanodiamonds found by Tian et al. (2011) however, suggest an isotropical growth mechanism for these diamonds rather than an anisotropic shock mechanism (Daulton et al., 1996). In addition, no other shocked minerals have been reported from the Allerød-Younger Dryas boundary.

[3] Isotropic growth is more consistent with CVD nanodiamond formation in the superheated fireball following an impact or airburst. The presence of carbon spherules and glass-like carbon in the Younger Dryas boundary sediments, and in which nanodiamonds have been found, may, however, be inconsistent with such extreme temperatures, as current research suggests carbon spherules and glass-like carbon form at temperatures below 500 °C (McParland et al., 2010; Scott et al., 2010). Furthermore the larger (>100 nm) flake-like or tabular nano- and microdiamonds, found in the Black Mat as well as the Usselo horizon, cannot easily form by isotropic growth.

[4] Nanodiamonds have been found in micrometeorites and some interplanetary dust particles (Dai et al., 2002), which continuously rain down on Earth. However, these nanodiamonds are small (<5 nm) and thus do not explain the larger diamonds found in our work and elsewhere (Kennett et al., 2009b; Tian et al., 2011). In addition, if the nanodiamonds are the result of continuous rain, it would be expected that they should be present throughout the records, whereas they are almost absent outside the proposed boundary layer (Kurbatov et al., 2010; Israde-Alcántara et al., 2012).

[5] If the evidence is not consistent with any of the possible extra-terrestrial or impact origins, nanodiamonds must have originated from some kind of terrestrial process. It has been suggested that they might have formed during the wildfires responsible for the charred material in the Younger Dryas boundary layer (Paquay et al., 2009). As wildfires are very common, this formation mechanism could also explain the age discrepancy. Artificial nanodiamonds have been grown using low pressure CVD at temperatures as low as 450 °C (Frenklach et al., 1989; Daulton et al., 1996; Cowley et al., 2004), although the experimental conditions differ from natural wildfire settings. Furthermore, particles with a cubic diamond structure as well as carbon onion structures, which can serve as nanoscopic pressure cells for diamond formation (Banhart and Ajayan, 1996; Banhart, 1997; Tomita et al., 2000), have been observed in wood that was experimentally charred at 700 °C and subsequently cooled in a nitrogen atmosphere (Ishimaru et al., 2001). In addition, cubic nanodiamonds (<5 nm) have recently been discovered in a candle flame and a natural gas flame (Su et al., 2011). Although most nanodiamonds burn up in the flame, this discovery suggests it might be possible for nanodiamonds to form during a combustion-type process under normal atmospheric conditions. These findings are contrary to the suggestions of Kurbatov et al. (2010) that nanodiamond formation requires extraordinary high temperature, pressure and redox conditions not naturally found at the Earth surface, leading them to adopt an extraterrestrial origin for the nanodiamonds in the Greenland ice sheet.

Although natural wildfires can reach temperatures as high as 900 °C, glass-like carbon and carbon spherules found in our study as well as the Black Mat (Firestone et al., 2007; Kennett et al., 2008; Kennett et al., 2009b) possibly indicate a low temperature formation (<550 °C or more likely <400 °C (McParland et al., 2010; Scott et al., 2010)). A wildfire temperature of ~420°C, as inferred from our reflectance analysis at Geldrop-Aalsterhut, also indicates that temperatures were slightly too low for known diamond forming mechanisms. It must however be noted that the final reflectance value depends not only on temperature, but also on the duration of charring (Braadbaart and Poole, 2008; McParland et al., 2009). If heating occurred during a period of <1 hour, the temperature would have been slightly higher than what we inferred from our

Table 3.4. Overview of different diamond polymorphs and morphologies (shape and size) as found within the Allerød-Younger Dryas boundary as reported by different researchers Results from the Cretaceous/Tertiar boundary nanodiamonds and recent carbon spherules have been added for comparison. K/T, Cretaceous/Tertiar.

		cubic diamond							n-diamond	lonsdaleite (2H diamond)		
		octahedral nano	rounded nano	flakes micro	irregular	polycrystalline hexagonal	polycrystalline rectangular	polycrystalline irregular	rounded nano	rounded nano	tabular nano	tabular micro
Younger Dryas Boundary	Kennett et al. 2009a carbon spherules bulk sediment		X						X			
	Kennett et al. 2009b carbon spherules carbon elongates				X				X			X[1]
	Daulton et al. 2010 carbon spherules glass-like carbon charcoal											
	Kurbatov et al. 2010 ice sheet[2]								X	X[3]	X[3]	
	Tian et al. 2010 bulk black material		X	X					X	X		
	Israda-Alcántara et al. 2012 bulk sediment		~									
	this study glass-like carbon							X				
K/T boundary [4]		X			X	X	X					
Recent carbon spherules[5]			X	X								

[1]Misses the 1.93 and 1.5 reflections typical for lonsdaleite. Daulton et al. (2010) suggested these are actually graphene/graphane aggregates misinterpreted as lonsdaleite.
[2]Ice layer not dated with absolute certainty. Pinter et al (2011) argue that the oxygen isotopes suggested a Holocene age rather then Late Glacial.
[3]Kurbatov et al. (2010) claim that the nanodiamonds they found are morphological and analytically indistinguishable from the lonsdaleite and n-diamondsfound across North America in Allerød-Younger Dryas boundary carbon spherules and sediments. Rounded or nanosized tabular lonsdaleite is however not reported by Kennett et al. (2009a; 2009b)
[4]Carlisle and Bramant (1991), Gilmour et al (1992), and Hough et al (1997)
[5]Yang et al. (2008).

Wittke et al. (2013) present evidence of a major cosmic impact at the onset of the Younger Dryas episode, including some markers found in the top of the well-known Usselo marker horizon. This is contrary to our extensive radiocarbon dating effort from this horizon (van Hoesel et al. 2012), which shows that the Usselo horizon at Aalsterhut post-dates the onset of the Younger Dryas. Furthermore, Wittke et al. (2013) misinterpret the origin of the Usselo horizon: this horizon is a well-defined paleosoil that formed during the Allerød and the early Younger Dryas in the top part of coversand. This coversand was deposited prior to the Allerød, during cold and dry conditions, and is part of the European Sandbelt. Wildfires were common and occurred throughout this period, rather than synchronously with the onset of the Younger Dryas (Kaiser et al. 2009).

Wittke et al. (2013) cite our paper on the Usselo Horizon at the Aalsterhut site and state that we neglected to address calibration issues when interpreting our radiocarbon dates. This is simply not true. Moreover, the statement that we used a value of 12,900 ± 30 cal. yrs BP for the onset of the Younger Dryas is incorrect: this age is not in our paper. We report an age range of 11,000-10,900 ^{14}C yrs BP. Using the older, discontinued IntCal04 calibration, this radiocarbon age range gives a calibrated age for the onset of the YD of 12,900 ± 30 cal. yrs BP. Wittke et al. (2013) compare some of our radiocarbon dates from the UH, calibrated using the presently recommended IntCal09 curve (Reimer et al., 2009), to a value for the onset of the Younger Dryas calibrated using a different (unspecified) calibration curve, thus creating a problem with calibration issues. Had Wittke et al. used the current IntCal09 calibration curve for the Younger Dryas dating, which yields 12,815 ± 90 cal. yrs BP, there would not be a calibration issue.

Calibration increases the uncertainty of the timing of the Younger Dryas due to a long lasting "plateau" in the calibration curve for this time period (Reimer et al., 2009). This is why we directly compared the radiocarbon ages, showing that the charcoal in the Usselo horizon at Aalsterhut is somewhat younger than the Allerød-Younger Dryas boundary. When using the calibrated ages, as Wittke et al. (2013) did, it can indeed be argued that our data are consistent with the Allerød-Younger Dryas boundary. However, this does not indicate that our site is consistent with the diamond-rich layer reported by Kennett et al. (2009), as suggested by Wittke et al. (2013). The Usselo Horizon, and associated wildfire, at Aalsterhut (10,870 ± 15 ^{14}C yrs BP or 12,785-12,650 cal. yrs BP; n=12, IntCal09) is clearly younger than the Black Mat where Kennett et al. (2009) found nanodiamonds (11,070 ± 10 ^{14}C yrs BP or 13,080-12,915 cal. yrs BP; n=7, IntCal09).

Accurate dating is imperative for establishing causal relationships between deposits and events and, in order to compare calibrated radiocarbon dates, these must be obtained using the same calibration curve. It is thus essential to report both the original radiocarbon ages and the calibration curve used.

Box 3.1. Response to Wittke et al. (2013) misinterpretation of the concept of the Usselo horizon and our interpretation of the ^{14}C ages at Geldrop Aalsterhut presented in this chapter and in van Hoesel et. al. (2012). Published previously in van Hoesel et al. (2013).

reflectance values. For example, for a charring period of only 10 minutes our value of 0.96 %Ro would indicate a temperature of ~460 ˚C (Braadbaart and Poole, 2008).
The carbon spherules found in the Younger Dryas boundary layer seem similar to charred fungal sclerotia formed under relatively low temperatures (<450 °C) (Scott et al., 2010). Although Daulton et al. (2010) do not report any nanodiamonds in similar carbon spherules, cubic nanodiamonds have been found in carbon spherules from modern forest soils (Yang et al., 2008). If the morphology of these carbon spherules to the charred fungal sclerotia is due to a similar low temperature origin, this might suggest a yet unknown low temperature formation of nanodiamonds. This similarity seems in agreement with our findings of nanodiamonds in glass-like carbon as well as the low wildfire temperature inferred from the charcoal. Although we cannot exclude the possibility that the nanodiamonds were adhered to the surface of the glass-like carbon and might thus be unrelated.
In summary, although some formation scenarios seem less likely than others, the exact formation mechanism of the nano- and microdiamonds found in the Younger Dryas boundary layer is still unknown. It is possible that several mechanisms have played a role. For example, a CVD-like process within an impact/airburst fireball or natural wildfire might have been responsible for the smaller rounded nanodiamonds reported (Kennett et al., 2009a; Kennett et al., 2009b; Kurbatov et al., 2010; Tian et al., 2011), while another process might be responsible for the larger flake-like and tabular nano- and microdiamonds (Kennett et al., 2009b; Tian et al., 2011, this study).
Finally, it must be noted that there is a wide range in diamond polymorphs and morphology reported from different locations and/or by different authors (see table 3.4). This also seems the case for the diamonds reported at the K/T boundary (Carlisle and Bramant, 1991; Gilmour et al., 1992; Hough et al., 1997). In addition, Daulton et al. (2010) report that no nanodiamonds were present at all in their Black Mat samples. This suggests that differences in sample preparation, analysis and interpretation might also affect the results. In addition sample size and relative abundances at different locations can be a problem. We analyzed several hundred particles in the TEM, representing only a fraction of the glass-like carbon in the samples, but only found less than a handful of possible nanodiamonds. We found no nanodiamonds in a small fraction of carbon spherules analyzed; this might, however, be related to the small sample size.

3.1.1 Magnetic fraction

Even though magnetic spherules were found at the nearby Lommel site, we found no magnetic spherules in our preliminary analysis of the magnet fraction at Geldrop Aalsterhut. The concentration of magnetic spherules reported at Lommel is however only 16 spherules per kilogram of sediment site (Firestone et al., 2007). If magnetic spherule concentrations at Geldrop Aalsterhut are similarly low, we should have found approximately 8 spherules. If we assume that the spherules are distributed heterogeneously in the Ussleo horizon, there is thus a small chance that we missed the spherules because they were not present in our subsample. If, however, there are indeed no magnetic spherules at Geldrop Aalsterhut, this would strengthen our conclusion that the nanodiamonds that have been found here are not related to the proposed Younger Dryas impact event.

3.5 Conclusions

Our work follows two lines of research on the carbonaceous fraction of the Usselo horizon, associated with the proposed Younger Dryas impact event and a preliminary study on the magnetic fraction. No magnetic spherules have been found in the Usselo horizon at Geldrop-Aalsterhut. TEM analysis of glass-like carbon shows that although cubic nanodiamonds are present, there is no sign of the shock polymorph lonsdaleite. Furthermore, although the formation of the Usselo horizon started during the Allerød, our critical dating places the wildfire episode up to two centuries after the proposed impact event and into the Younger Dryas. Moreover, our nanodiamonds are two centuries younger than the diamonds reported by Kennett et al. (2009b), indicating that unless two impacts happened in a short period of time, one or both of the cubic diamond populations must have a non-impact origin. As the glass-like carbon in which the nanodiamonds were found is known as a wildfire product, the nanodiamonds might in some way be related to wildfires instead. We therefore conclude that although our findings cannot exclude the possibility of an impact, we found no evidence in the Usselo horizon to support the Younger Dryas impact hypothesis.

Chapter 4

A TEM study of charcoal and glass-like carbon: insights in nanodiamond formation in the Allerød-Younger Dryas boundary layer.

Products of fire - such as charcoal, soot, glass-like carbon and carbon spherules - are widespread in the sedimentary and archaeological record. Though a common feature, not everything about these materials is known. For example, it is still not known how glass-like carbon is formed. Recently, nanodiamonds were reported in carbon spherules from the Black Mat in North America, a sediment layer marking the Allerød-Younger Dryas transition. These nanodiamonds were used as evidence for a hypothetical extraterrestrial impact, and have subsequently been reported in the Greenland ice sheet, bulk sediment samples, and glass-like carbon from the same layer. However, both carbon spherules and glass-like carbon are known wildfire products and it has therefore been suggested that the reported nanodiamonds are the result of wildfire rather than an extraterrestrial impact. We investigated various carbon spherules, charcoal, and glass-like carbon particles from the Allerød-Younger Dryas boundary as well as samples of different ages. Using TEM we evaluated the nano- and micro-structural differences between different carbon types and searched for the presence of nanodiamonds. In addition, we similarly analysed a varved lake-core section that spanned the Allerød-Younger Dryas boundary, which has better dating resolution than most other Allerød-Younger Dryas boundary layers investigated.

The most abundant carbon phase found in all samples is amorphous carbon. Of the organised phases, so-called graphene aggregates are the most common. The second most common organised phase of carbon is in the form of poorly defined carbon onions, similar to soot, as well as more distinct onion-like features. Although these more distinct onion-like features look similar to the microstructure of commercial glass-like carbon, we found them both in glass-like carbon and in charcoal. No nanodiamonds were found in the Allerød-Younger Dryas boundary samples or the charcoal and glass-like carbon samples of different ages. We thus found no evidence for widespread occurrence of nanodiamonds Allerød-Younger Dryas boundary, as suggested to be present according to the Younger Dryas impact hypothesis. Nor do we find evidence that nanodiamonds commonly form in wildfires.

4.1 Introduction

Nano- and microdiamonds have been found inside meteorites and in relation to impact craters (Hanneman et al., 1967; Carlisle and Bramant, 1991; Gilmour, 1998; Masaitis, 1998; French and Koeberl, 2010). Shock-produced diamonds (up to mm scale), which have clearly formed from shock metamorphism of graphite in the source rock, have been used to establish an impact origin of craters (Hough et al., 1995; Koeberl et al., 1997; French and Koeberl, 2010). Nano- and microdiamonds, however, form under a range of circumstances, both natural and artificial (Banhart and Ajayan, 1996; Tomita et al., 2000; Ishimaru et al., 2001; Schwander and Partes, 2011; Su et al., 2011) and the presence of nanodiamonds in distal ejecta layers is therefore not considered to be a diagnostic impact criterion (French and Koeberl, 2010). Nevertheless, nanodiamonds have been used as evidence for the Younger Dryas impact hypothesis (Kennett et al., 2009a; Kennett et al., 2009b; Kurbatov et al., 2010; Israde-Alcántara et al., 2012). This controversial hypothesis suggests that multiple simultaneous airbursts or impacts resulted in the Younger Dryas cold period (Firestone et al., 2007; Pinter et al., 2011; Bunch et al., 2012; van Hoesel et al., 2013). Using transmission electron microscopy (TEM), Kennett et al. (2009a; 2009b) report the presence of nano- and microdiamonds in carbon spherules from the Allerød-Younger Dryas boundary (~12.8 ka). Others, however, failed to find these nanodiamonds and suggested that other particles might have been mistaken for diamond (Daulton et al., 2010). Nano- and microdiamonds have also been reported in samples of similar age, including black carbon rich clusters from the Usselo horizon (Tian et al., 2011), chemical extracts of carbon-rich bulk sediment (Kennett et al., 2009a; Israde-Alcántara et al., 2012), the Greenland ice sheet (Kurbatov et al., 2010), and in glass-like carbon from the Allerød-Younger Dryas boundary (Firestone et al., 2007; Kerr, 2009; van Hoesel et al., 2012).

Of particular interest in the study of nanodiamonds at the Allerød-Younger Dryas boundary are glass-like carbon and carbon spherules – black, carbon-rich spherical objects with a honeycomb-like or open interior structure (an example is shown in figure 3.5a,b) – both of which are common and can form during wildfires (Hunt and Rushworth, 2005; McParland et al., 2010; Scott et al., 2010). Glass-like carbon, also known as glassy carbon or vitrified charcoal, is found in both sediments and archaeological contexts, and consists of black, carbon-rich objects with an irregular shape and a smooth, reflective 'glass-like' surface (best visible in light microscopy, see for example McParland et al. 2010 figure 1). While charcoal generally retains the structure of the precursor wood, glass-like carbon does not (as illustrated in figure 4.1). Instead, glass-like carbon has an irregular structure with relatively large holes or pits and a smooth surface. The distinction between charcoal and glass-like carbon is, however, not always clear, since glass-like carbon can also contain regions with remnant plant structure (McParland et al. 2010; also illustrated in figure 4.1d). Glass-like carbon forms in fires, but its exact formation mechanism is still unknown. The presence of glass-like carbon in archaeological contexts has generally been ascribed to high temperature or even melting (Marguerie and Hunot, 2007; McParland et al., 2010). McParland et al. (2010), however, showed that reflectance values of glass-like carbon are consistent with low-temperature formation.
While the archaeological glass-like carbon is thus likely formed at low temperatures, synthetic glass-like carbon, on the other hand, is produced from organic materials at high temperatures, typically 1000 - 2000 °C (Harris, 2004; Stroud et al., 2011). Synthetic glass-like carbon is described as a non-graphitising carbon – carbon that does not transform to graphite, even at

temperatures above 3000 ˚C – and is known for its thermal stability, impermeability to gasses and high resistance to chemical attack (Harris, 2004; Harris, 2005). Although synthetic glass-like carbon has been studied in the transmission electron microscope (TEM), little is known about the TEM scale microstructure of natural glass-like carbon.

Because some of the nanodiamonds reported at the Allerød-Younger Dryas boundary were found within carbon spherules and glass-like carbon, it has been suggested that these nanodiamonds could have formed in natural wildfires rather than during an airburst or impact (Paquay et al., 2009a; Tian et al., 2011; van Hoesel et al., 2012, see also section 3.4.2). Although this hypothesis for the origin of the nanodiamonds was disputed by Bunch et al. (2010), nanodiamonds have been reported in artificially charred wood (Ishimaru et al., 2001): small crystalline particles with lattice spacings consistent with diamond were observed within onion-like structures and a diamond-like nano-particle, possibly n-diamond, was reported outside the onion-like structures (Ishimaru et al., 2001).
Two TEM studies on natural charcoal, on the other hand, have not reported the occurrence of nanodiamond (Cohen-Ofri et al., 2007; Daulton et al., 2010). Both these studies identified amorphous carbon as the dominant phase of carbon within charcoal, but differ somewhat in the reported non-amorphous carbon phases. Daulton et al. (2010), who also investigated glass-like carbon and carbon spherules, report that the dominant crystalline phases of carbon are, in descending order of abundance: polycrystalline graphene aggregates, graphene/graphane aggregates and graphite. Graphene aggregates consist of randomly oriented sheets of graphene

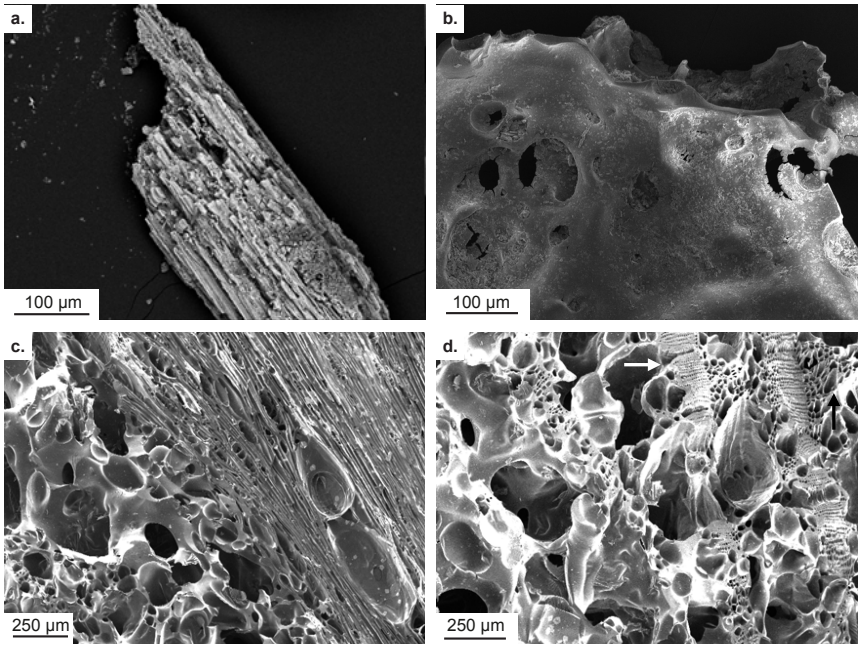

Figure 4.1. Examples of charcoal and glass-like carbon particles. A. SEM-BSE image of a charcoal particle from the Usselo horizon at Aalsterhut, clearly showing the remnant wood structure. B. SEM-SE image of a glass-like carbon particle from the Usselo horizon at Aalsterhut. C. SEM-SE image of the particle from Rennes showing both the remnant wood structure (top-right) and glass-like structure (bottom-left). D. SEM-SE image of the glass-like carbon in C. with areas still containing remnant wood structure (black arrows).

(a 2-dimensional planar molecule that forms the building block of graphite) that lack any correlation (Daulton et al., 2010). When graphene sheets are stacked normal to their plane, they form either graphite (ordered) or turbostratic carbon (randomly stacked). Graphane is a modified form of graphene with a slightly shorter edge length, and graphene/graphane aggregates are therefore detectable in TEM diffraction patterns through asymmetric doubled diffraction rings (Daulton et al., 2010). Based on their TEM images of modern charcoal, Cohen-Ofri et al. (2007) report a 'two-phase structure' consisting of organised and non-organised (seemingly amorphous) parts, with the organised part described as consisting of graphite-like microcrystalline sheets (Cohen-Ofri et al., 2007). Although Daulton et al. (2010) do not include any TEM images, making direct comparison difficult, the included electron energy loss spectroscopy (EELS) spectra and selected area diffraction patterns (SADP) of the graphene aggregates (Daulton et al., 2010) and the 'graphite like microcrystalline sheets' (Cohen-Ofri et al., 2007) look similar.
Cohen-Ofri et al. (2007) also report the occurrence of a so-called semi-ordered phase, rounded porous structures similar to onion-like carbon structures, and curled graphite-like structures. In high resolution TEM (HRTEM) imaging the semi-ordered structure – 'exfoliated graphene layers and small stacks of 2 to 3 layers, which result in only short-range order' (Cohen-Ofri et al., 2007) – shows some similarities to some of the less ordered onion-like structures reported in artificially charred wood (Hata et al., 2000) and glass-like carbon reported in a meteorite (Stroud et al., 2011). Carbon onions consist of concentric graphite rings with varying d-spacing (e.g. Banhart and Ajayan, 1996). The graphitic shells of the carbon onions reported by Hata et al. (2000) were spaced relatively far apart: 5-6 Å, almost twice the spacing of graphite 0002 fringes (3.4 Å). The porous structure that has been reported in natural and artificial charcoal (Ishimaru et al., 2001; Cohen-Ofri et al., 2007) consists of an onion-like structure in which the graphitic shells do not continue into the centre of the structure, but rather surround a 'pore'. This porous structure has also been observed in synthetic glass-like carbon (Harris, 2004). If we assume that the porous structure is three dimensional, then the centre of the onion in the 2D TEM image would correspond to the top and bottom sides of the onion and likely consist of one or more graphene sheets (see also Harris, 2013), while the centre of the 3D structure would be empty.

In this chapter a three-fold approach is used to test whether the nanodiamonds found in the Allerød-Younger Dryas boundary are valid evidence for the Younger Dryas impact hypothesis or whether they might have a different origin. First, using TEM, the occurrence of nanodiamonds in the Usselo horizon and Black mat at several sites is investigated to assess the lateral extent of the nanodiamonds as well as their reproducibility. Second, part of a lake core spanning the Allerød-Younger Dryas transition is analysed for nanodiamonds in order to put a better time constraint on the occurrence of nanodiamonds. Third, charcoal and glass-like carbon particles of different (non Allerød-Younger Dryas boundary) ages are examined using TEM and reflectance measurements to check whether nanodiamonds might be common in wildfire products and to get estimates of the temperature range in which they might form. In addition, comparing the different microstructures of charcoal and glass-like carbon found in our TEM analysis might provide insight into the origin of glass-like carbon.

4.2 Methods

Charcoal, carbon spherule, and glass-like carbon particles were collected at different locations (see table 4.1 for an overview). For Geldrop-Aalsterhut, the charcoal, carbon spherules and glass-like carbon particles were obtained as described in §3.2.3. Charcoal from the modern wildfire was collected from the surface at Strabrechtse Heide several days after the fire. The charcoal and glass-like carbon from Rennes are both part of the same charred particle of several centimetres in diameter, which was charred in a charcoal meiler at the Université de Rennes 1.
Some charcoal and glass-like carbon particles were embedded in resin blocks, polished and examined using reflectance analysis for a preliminary estimate of the wildfire temperature following the procedure of Braadbaart and Poole (2008). For each particle, 100 reflection measurements were taken using a Leitz motorized DMLA microscope.

For the TEM analysis of charcoal, glass-like carbon or carbon spherules, the particles were crushed in ethanol using an agate pestle and mortar and part of the suspension was dispersed on a holey carbon grid. Multiple particles of charcoal from Strabrechtse Heide and the glass-like carbon from Geldrop Aalsterhut were investigated. For the acid resistant residues of bulk sedi-

Table 4.1. Overview of the different type of samples and their origin. The glass-like carbon and charcoal from Rennes were both part of the same particle, which was half charcoal and half glassy. At Murray Springs, Lommel and Geldrop Aalsterhut nanodiamonds have been reported before (Kennett et al., 2009a; Tian et al., 2011; van Hoesel et al., 2012).

Location	Origin	Age
Glass-like carbon		
Flevoland (NL)	archaeological hearth	Early - Middle Holocene
Geldrop Aalsterhut (NL)	Usselo horizon	Late Allerød - Early Younger Dryas
Rennes (FR)	experimental	2006 AD
Carbon spherules		
Geldrop-Aalsterhut (NL)	Usselo horizon	Late Allerød - Early Younger Dryas
Western Europe	modern forest soil	< 2000 yrs
Charcoal		
Geldrop-Aalsterhut (NL)	Usselo horizon	Late Allerød - Early Younger Dryas
Rennes (FR)	experimental	2006 AD
Strabrechtse Heide (NL)	recent wildfire	2010 AD
Acid resistant residues		
Geldrop-Aalsterhut (NL)	Usselo horizon	Late Allerød - Early Younger Dryas
Geldrop-Aalsterhut (NL)	underlying coversand	Older Dryas
Lommel Maatheide (BE)	Usselo horizon	Late Allerød - Early Younger Dryas
Lutterzand (NL)	Usselo horizon	Late Allerød - Early Younger Dryas
Rosenberg (DE)	Medieval soil horizon	1000 - 1200 AD
Murray Springs (US)	Black Mat	Allerød-Younger Dryas boundary
Soppensee (CH)	lace core	Late Allerød - Early Younger Dryas

ment samples (see table 4.1) we used the chemical preparation method as described in Israde-Alcántara et al. (2012). From a Soppensee lake core from Switzerland (for more information: Hajdas and Michczyński, 2010), six continuous samples were taken above the Laacher See tephra, which was deposited approximately 200 years prior to the onset of the Younger Dryas (Litt et al., 2003), and across the Allerød-Younger Dryas boundary. Samples from the varved Soppensee lake core were of minimum sample size (4 grams) according to Israde-Alcántara et al. (2012), samples from different (palaeo)soil horizons were larger (12-16 grams).
Typically, one TEM grid per sample was investigated using TEM. TEM analysis was performed using a FEI Tecnai 12 120 kV TEM, and a Tecnai 20 FEG 200 kV TEM equipped with an EDAX EDXS detector. Both TEMs are located at Electron Microscopy Laboratory Utrecht (EMU). The TEM grids were analysed both in diffraction mode, to locate crystalline particles, and in image mode, to locate individual particles. Energy dispersive X-ray (EDX) spectroscopy was used to check the carbon content of selected particles. Selected area diffraction patterns (SADPs) were used to identify whether carbon particles were amorphous or crystalline. For some regions high resolution TEM (HRTEM) images were made to obtain more information on the structure of the particles.

4.3 Results

4.3.1 Charring temperature

Reflectance measurements and inferred charring temperature of several charcoal and glass-like carbon particles are given in table 4.2. The lowest reflectance measurements were measured in the charcoal from the Usselo horizon at Lommel and Geldrop-Aalsterhut, suggesting a wildfire temperature of ~420°C. The highest reflectance values were found in the charcoal from the modern wildfire, with values indicating a temperature range of 550-660 °C. It must be noted, though, that the reflectance of charcoal increases both with temperature and fire duration. As the estimated temperature is based on exposure for an hour, the actual temperature could be lower when the charring lasted longer, whereas the temperature would be higher if the fire was of shorter duration. For reflectance values of <1%R0, such as for Lommel and Aalsterhut, this temperature difference is only 15 °C, but for higher reflectance values this difference can be

Table 4.1. Reflectance of different charcoal and glass-like carbon particles and the estimated wildfire temperature. Estimated temperatures are based on an exposure time of 1 hour (Braadbaart et al., 2008). When exposed to the heat for longer durations, the actual temperatures will be lower than estimated here.

Location	Type	Reflectance (%R0)	Estimate temperature (°C)
Geldrop Aalsterhut	charcoal	0.96 ± 0.06	420
Lommel	charcoal	1.02 ± 0.15	420
Flevoland	glass-like carbon	1.63 ± 0.31	480
Strabrechtse Heide (1)	charcoal	3.15 ± 0.35	600
Strabrechtse heide (3)	charcoal	2.49 ± 0.37	550
Rennes	charcoal	2.56 ± 0.09	560
Rennes	glass-like carbon	2.58 ± 0.10	560

up to 75 °C (Braadbaart, 2008). In addition, post-depositional processes could result in lower reflectance values (Braadbaart et al., 2009).

4.3.2 Microstructural analysis

No evidence of a diamond phase was found in any of the samples in this study, except for the polycrystalline microdiamond particle already reported in chapter 3. Instead, TEM of the charred particles and acid-resistant residues of bulk sediment samples shows that the majority of the carbon is present as an amorphous phase (based on the SADPs, see figure 4.2c), consistent with the work of Cohen-Ofri (2007). The size and shape of these amorphous carbon flakes varies (e.g. figure 4.2a,b). Sometimes, a semi-ordered region was observed at the edge of an amorphous carbon flake (figure 4.2e), suggesting that carbon flakes with a typical amorphous diffraction pattern, usually taken across the entire flake, do not always completely lack local microstructure. The observed semi-ordered regions were beam sensitive and often converted to a non-organized or completely amorphous phase under electron radiation.
Organised carbon phases were less common but were observed in most samples. The most common non-amorphous carbon phases observed in this study are graphitic carbon flakes (section 4.3.2.1) and carbon onions (section 4.3.2.2). The latter can be divided into soot-like carbon onions and onion-like carbon structures resembling the pore structure observed in wood (Ishimaru et al., 2001; Cohen-Ofri et al., 2007). Non-carbon materials were also found in most samples, including calcite, Si-rich particles and several metal-oxides, particularly TiO2 (section 4.3.2.3).

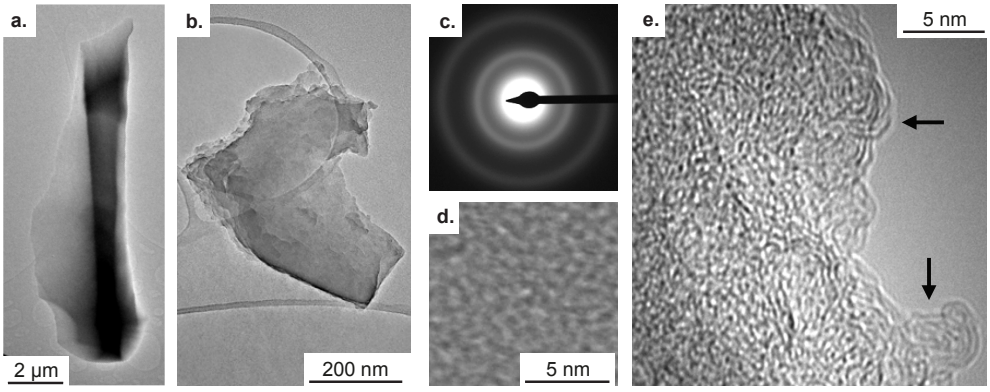

Figure 4.2. Examples of amorphous carbon. Images from the charcoal and glass-like carbon from Rennes. A. Typical larger amorphous carbon flake. B. Typical smaller amorphous carbon flake. C. Typical diffraction pattern for amorphous carbon. D. HRTEM image of amorphous carbon in B. E. Semi-ordered structure (arrows) visible in an HRTEM image of the edge of a carbon flake which was amorphous according to its diffraction pattern.

4.3.2.1 Graphitic carbon flakes

Most samples contained polycrystalline carbon in the form of graphitic carbon flakes (figure 4.3). The diffraction rings of these flakes have diameters consistent with the $\{10\bar{1}0\}$, $\{11\bar{2}0\}$ and $\{20\bar{2}0\}$ spacings of graphite, and sometimes a few isolated discrete spots consistent with the (0002) plane. The absence of $l \neq 0$ planes in the SADPs indicates that the flakes are similar to the graphene aggregates reported by Daulton et al. (2010). However, some of the graphitic carbon flakes consist of multiple layers (figure 4.3a), as evidenced by the presence of the (0002)

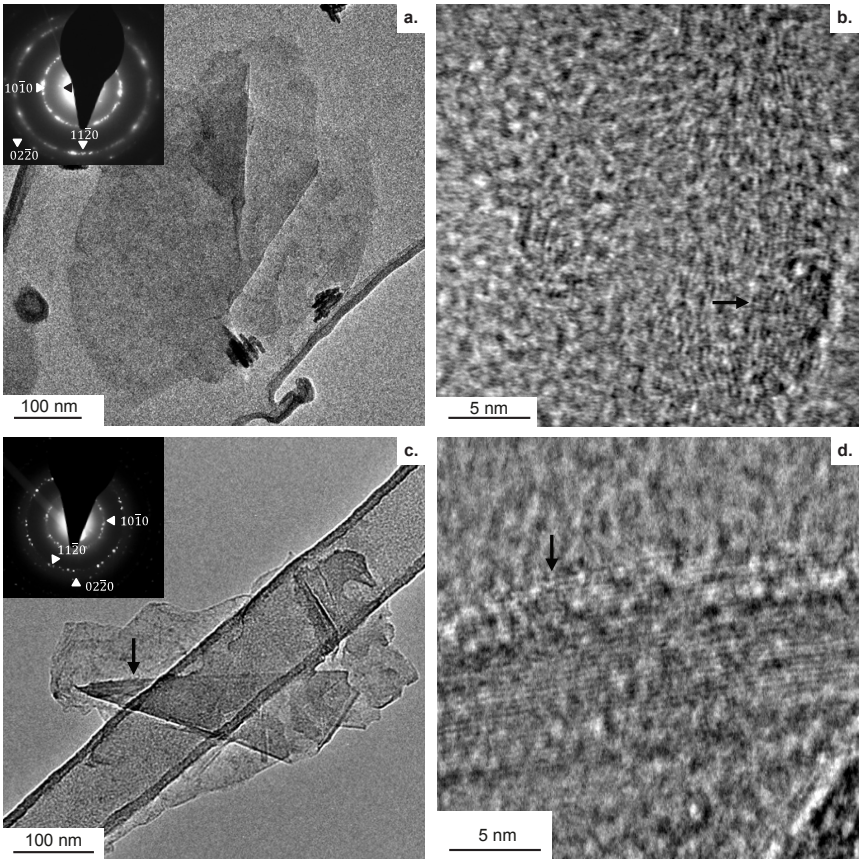

Figure 4.3. Graphitic carbon particles. A. TEM-BF image of a graphitic carbon particle, in charcoal from the recent wildfire at Strabrechtse Heide, that looks like several overlapping layers. The dark particles at the bottom right of the graphitic carbon shard are Ti-oxide particles. Inset shows the SADP of the graphitic particle, with rings corresponding to the d-spacings of graphene or graphite. The black arrow indicates the location of a few spots corresponding to the {0002} planes of graphite. B. HRTEM image of the graphitic particle in A showing fringes (0.36 nm) with distances slightly larger than the d-spacing for 0002 graphite planes (0.34 nm). C. TEM-BF image of a polycrystalline graphitic carbon particle in the acid resistant residue from the Soppensee lake core. The band running from the bottom-left to the top-right corner of the image is part of the holey carbon support film. The black arrow corresponds to the location of D. Inset shows the SADP with rings (white arrows) corresponding to the d-spacings of graphene or graphite. D. HRTEM image of the graphitic particle in C. Lattice fringes (0.37) at the edge (black arrow) are close to the d-spacing of 0002 graphite. Similar graphitic carbon flakes found in glass-like carbon from the Usselo horizon at Geldrop Aalsterhut are presented in figure 3.7.

spots in the diffraction pattern. Therefore the term graphitic carbon flakes, rather than graphene aggregates, is used in this work.

High resolution TEM (HRTEM) imaging of the graphitic carbon flakes shows that most of the flakes have no clear lattice fringes, possibly because most flakes were too thick or because of overlapping of different flakes. Sometimes lattice fringes with a spacing of ~0.35 nm (consistent with graphite) were observed, often near the edge of the flakes (figure 4.3d) where the thickness is generally less, but sometimes also in the centre of the flakes (figure 4.3b), as was also reported by Cohen-Ofri et al. (2007). Only one graphite microparticle was found (figure 4.4.) with lattice

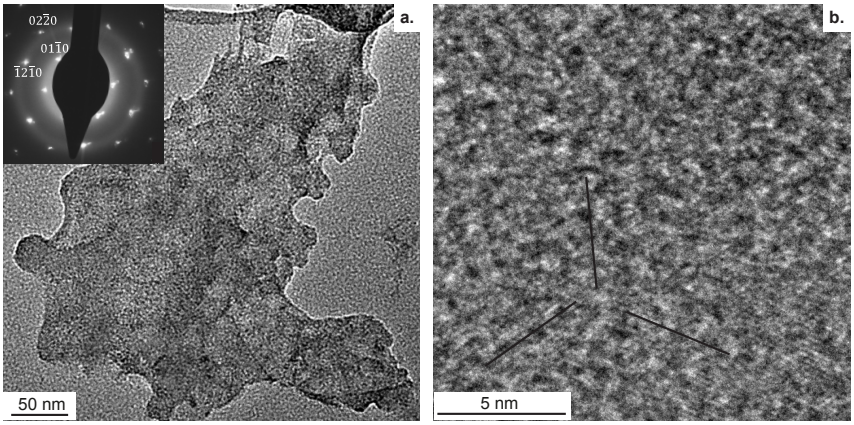

Figure 4.4. Graphite micro particle from the acid resistant residue of the medieval soil horizon at Rosenberg. A. TEM-BF image and corresponding diffraction pattern (inset) of the <0001> zone axis showing discrete spots from graphite and diffuse rings from the underlying holey carbon thin film. B. HRTEM image of the particle showing lattice fringes corresponding to the $\{10\bar{1}0\}$ planes of graphite.

spacings of 2.13 Å, consistent with the $\{10\bar{1}0\}$ lattice spacing of graphite as well as a diffraction pattern consistent with the 0001 zone-axis of graphite.

4.3.2.2 Carbon onion and pore structures

Some of the samples contained clusters of semi-spherical nanoparticles (figure 4.5) similar to soot particles (Harris, 2005; Su et al., 2011). Selected area diffraction of these clusters of particles show diffuse rings characteristic of amorphous carbon. HRTEM images show that these spherical particles are not amorphous but consist of poorly defined concentric graphite rings with a spacing slightly larger than that of graphite (~4 Å rather than 3.35 Å), consistent with the carbon onion structures reported by Hata et al. (2000). Most of these carbon onion structures are 15-25 nm wide, but larger onion structures of up to 35 nm in diameter were also observed. In charcoal from the recent wildfire, similar carbon onion structures were observed on the edge of an amorphous carbon shard (figure 4.5f). Most of the carbon onion structures were beam sensitive. With increased beam exposure, the onion structures altered to become more like the semi-ordered regions shown in figure 4.2d.

Other, better-defined, onion-like carbon structures are shown in figure 4.6. The carbon layering in these structures tends to be more continuous, often surrounding 'pores' (grey arrows) similar to the pore structure described in previous studies (Ishimaru et al., 2001; Cohen-Ofri et al., 2007). Based on the 2D TEM image it is not possible to see whether the centre is empty or consists of amorphous material. The onion-like pore structures in figure 4.6a-c,f consists of narrow (~5 layers) graphitic shells surrounding relatively large pores. In contrast, the graphitic shells in figure 4.6e are relatively thick, with minimal to no visible pores. The onion-like structures have various shapes, but small (<10nm), clearly defined carbon spherical onion structures are also present. The onion-like carbon structures in figure 4.6 are clearly more organised than the carbon onion structures shown in figure 4.5. Although the lattice fringes of the graphitic shells in the onion-like carbon structures in figure 4.6d are slightly better defined than the in porous onion-like structure in figure 4.6a, these particles have an SADP with diffuse rings, which is typical of amorphous material. The diffraction pattern of figure 4.6a, on the other hand, shows rings

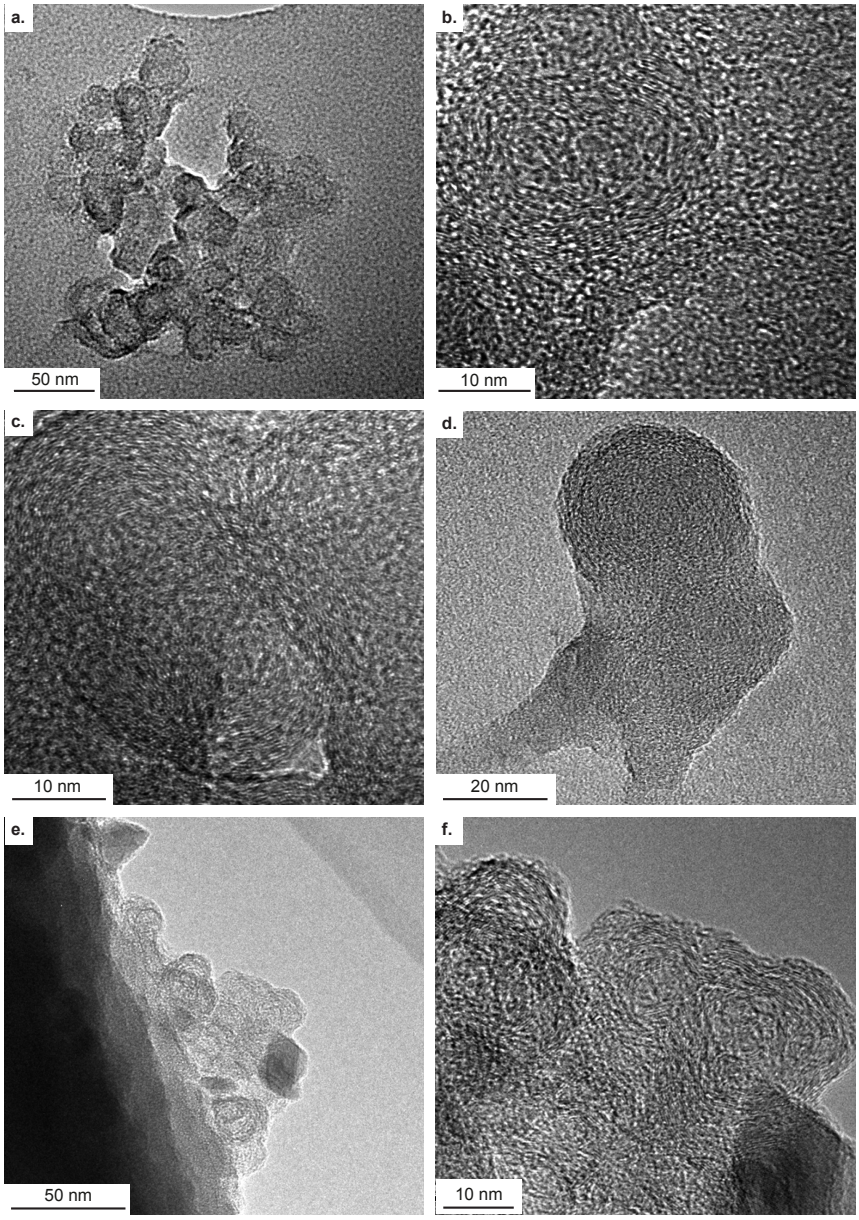

Figure 4.5. Groups of soot-like carbon onions. A. TEM-BF image of a group of semi-spherical features in charcoal from the recent wildfire at Strabrechtse Heide. B. HRTEM image of the semi-spherical features in A, showing an onion-like structure. C. HRTEM image of carbon onions in the acid resistant residue from the medieval soil horizon at Rosenberg. D. A few larger carbon onions in charcoal from the recent wildfire at Strabrechtse Heide. The largest onion (top) is 35 nm in diameter. E. Carbon onions at the edge of an amorphous carbon flake in charcoal from the recent wildfire at Strabrechtse Heide. F. HRTEM image of the carbon onions in E. The diamond-shaped nano-crystal in the bottom-right corner of the image is not carbon but a Co-rich nanocrystal.

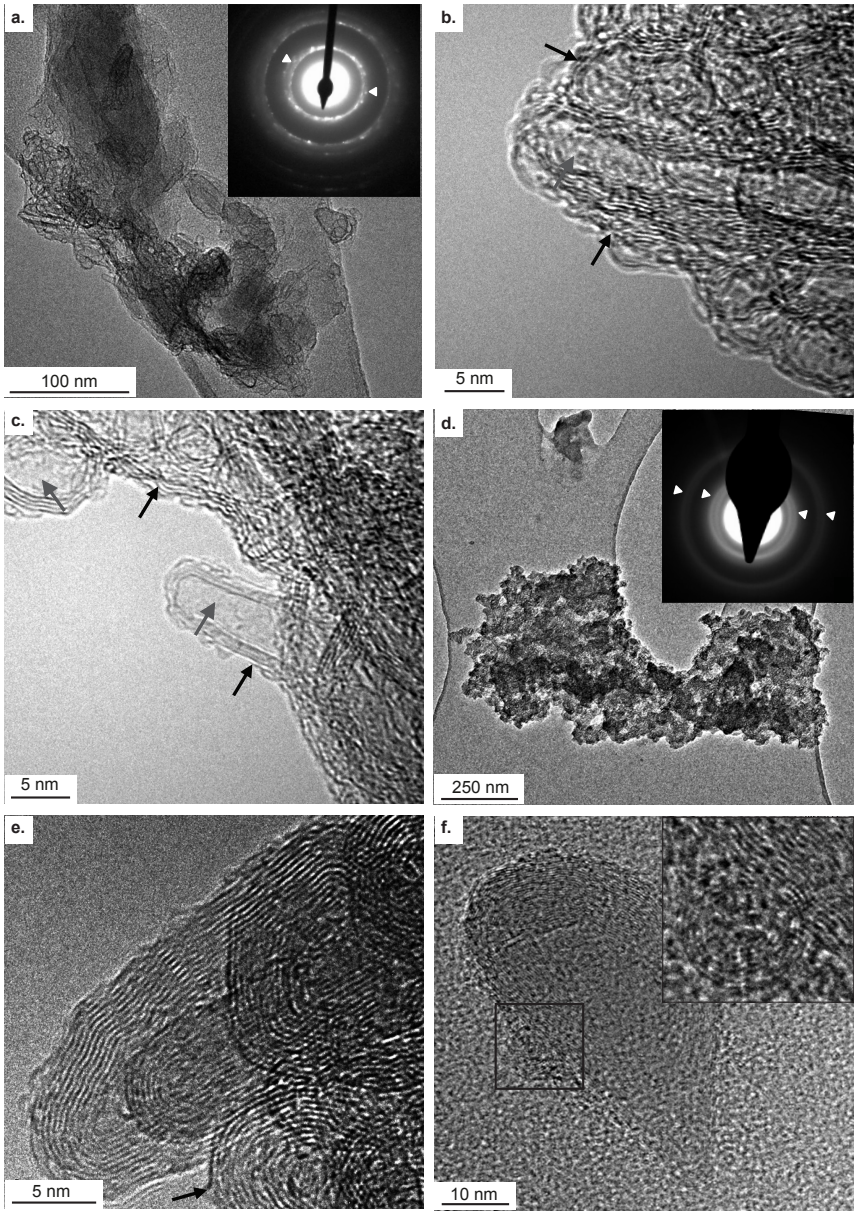

Figure 4.6. Groups of onion-like carbon with similarities to the pore structure observed in wood. A. Group of carbon particles in charcoal from the recent wildfire at Strabrechtse Heide. Inset shows diffraction pattern with doubled diffraction rings. B-C. HRTEM images of the group of particles in A showing that the particle consists of carbon ribbons (black arrows) with amorphous material (grey arrows) in between. Closed onion-like features are also observed. D. Group of onion-like carbon particles in the acid resistant residue from the medieval soil horizon at Rosenberg. Inset shows the diffraction pattern. E. HRTEM image of the particle in D. showing carbon-onion like features with thick shells. Spherical carbon onions are also observed (arrow indicates part of a spherical carbon onion in the image). F. Teardrop shaped carbon particle with a rim of graphitic shells and an amorphous centre found in the glass-like carbon from Rennes. Inset shows a HRTEM image of a small (7.5 nm diameter) carbon onion particle located at the edge of the larger particle.

consisting of discrete spots, consistent with an organised or crystalline structure and atypical for an amorphous material. Both SADPs show doubled asymmetric rings (white arrows) similar to those in the diffraction pattern of graphene/graphane aggregates as reported by Daulton et al. (2010). Unlike these graphene/graphane aggregates, however, the porous onion-like carbon also shows a few spots near 0.34 nm, the (0002) d-spacing of graphite. The microporous onion-like carbon in figure 6b,c also contains some longer carbon 'ribbons' that do not directly appear to be part of an onion-like structure.

4.3.3.3 Non-carbon crystalline materials present.
Most charcoal and glass-like carbon specimens contained Ca-rich particles, often in the form of polycrystalline calcite. In the recent charcoal sample from Rennes some of the polycrystalline calcite showed interesting ordering and morphology (figure 4.7). These Ca-rich nanoparticles were contained in elongated structures. EDX figure 4.7e shows that chemical composition of the particle in figure 4.7a is consistent with calcium carbonate. Based on the high C peak, it is suggested the calcite nanocrystals might be incorporated in a carbon matrix. The EDX spectra of the particle in figure 4.7c (taken above a hole in the carbon thin film), on the other hand, contains relatively more Ca than that in figure 4.7a.
Other non-carbon particles found include Si-rich (possibly phytholiths), Ti-rich and Fe-rich particles, and occasionally other metal-oxide particles were observed (figure 4.8). Interestingly, Ti-rich particles with a typically elongated shape (figure 4.8a) were abundant in all samples. A similar elongated particle was, however, found on a holey carbon grid with no sample dispersed on it, suggesting some sort of contamination. Rounded Ti-rich nanocrystals (figure 4.8c) were less abundant than elongated particles, but still present on multiple specimens.

4.4 Discussion

4.4.1 Lack of nanodiamonds

The lack of nanodiamonds in our samples from the Usselo horizon, the Black Mat and the part of the Soppensee record spanning the Allerød-Younger Dryas transition does not support the Younger Dryas impact hypothesis in which impact related nanodiamonds should be widespread. More interestingly, no nanodiamonds were found in the acid resistant residue of the Usselo horizon at Lommel, where nanodiamonds had been previously reported by Tian et al. (2011) or the Black Mat at Murray Springs, one of the sites where the nanodiamonds at the Allerød-Younger Dryas boundary were first discovered (Kennett et al., 2009a). This is in line with the results of Daulton et al. (2010), who did not find nanodiamonds in micro-charcoal aggregates from Murray Springs, nor in carbon spherules from Arlington Canyon, both sites where nanodiamonds have been reported previously (Kennett et al., 2009b). There are three possible explanations for this discrepancy between nanodiamond occurrences in different studies at the same site.
First, assuming similar sampling volumes were used, nanodiamonds might not be as abundant as Kennett et al. (2009a) suggested, or they could be inhomogeneously distributed through the sediment layer. Assuming that the nanodiamonds originally formed in the carbon spherules and glass-like carbon, a heterogeneous distribution of nanodiamonds would be quite likely, as carbon spherule concentration could also vary laterally to some extent. Due to the nature of TEM anal-

ysis, only small amounts of material can be examined, so it would be easy to miss particles that are heterogeneously distributed. However, sampling differences and a possible heterogeneous distribution of nanodiamonds do not explain why Kennett et al. (2009a) found nanodiamonds at all their sites, as they would be just as likely to miss the nanodiamonds.

Second, the nanodiamonds reported at Murray Springs might have been misidentified. Kennett et al. (2009a; 2009b) showed only diffraction patterns containing discrete rings corresponding to the d-spacings of diamond. However, the d-spacings of cubic diamond are close to those

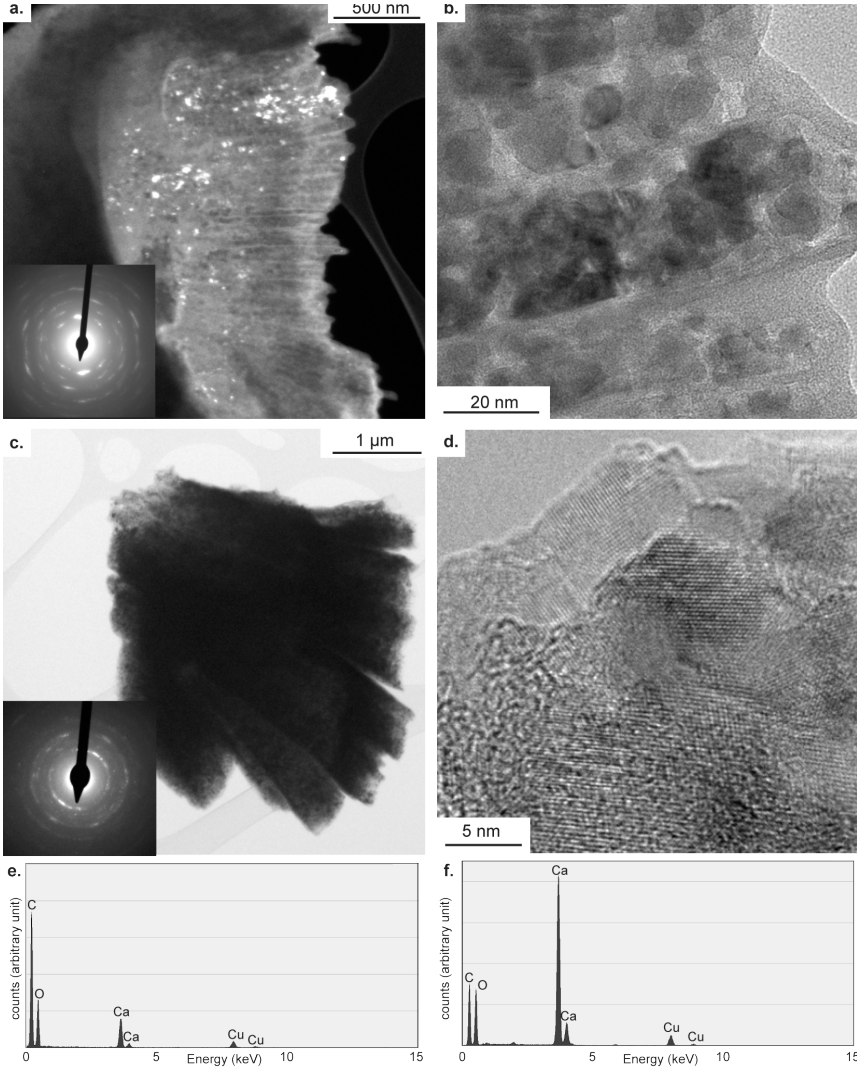

Figure 4.7. Ca-rich nanocrystals in charcoal from the recent wildfire at Strabrechtse Heide. A. TEM-DF image of a particle consisting nanocrystalline calcite ordered in west-east trending bands. Streaking in the diffraction patterns (inset) suggests that the orientation of the individual crystals is slightly variable. B. Higher magnification of the nano-crystalline calcite in the particle in A. C. Different polycrystalline Ca-rich particle. Inset shows the diffraction pattern. D. HRTEM image of nanocrystalline calcite in C. E. EDX spectrum of the particle in A, which is consistent with calcite. F. EDX spectrum of the particle in C. The low intensity of the oxygen peak suggests that it might be calciummonoxide rather than calcite. The Cu peak in the spectra is from the supporting TEM-grid.

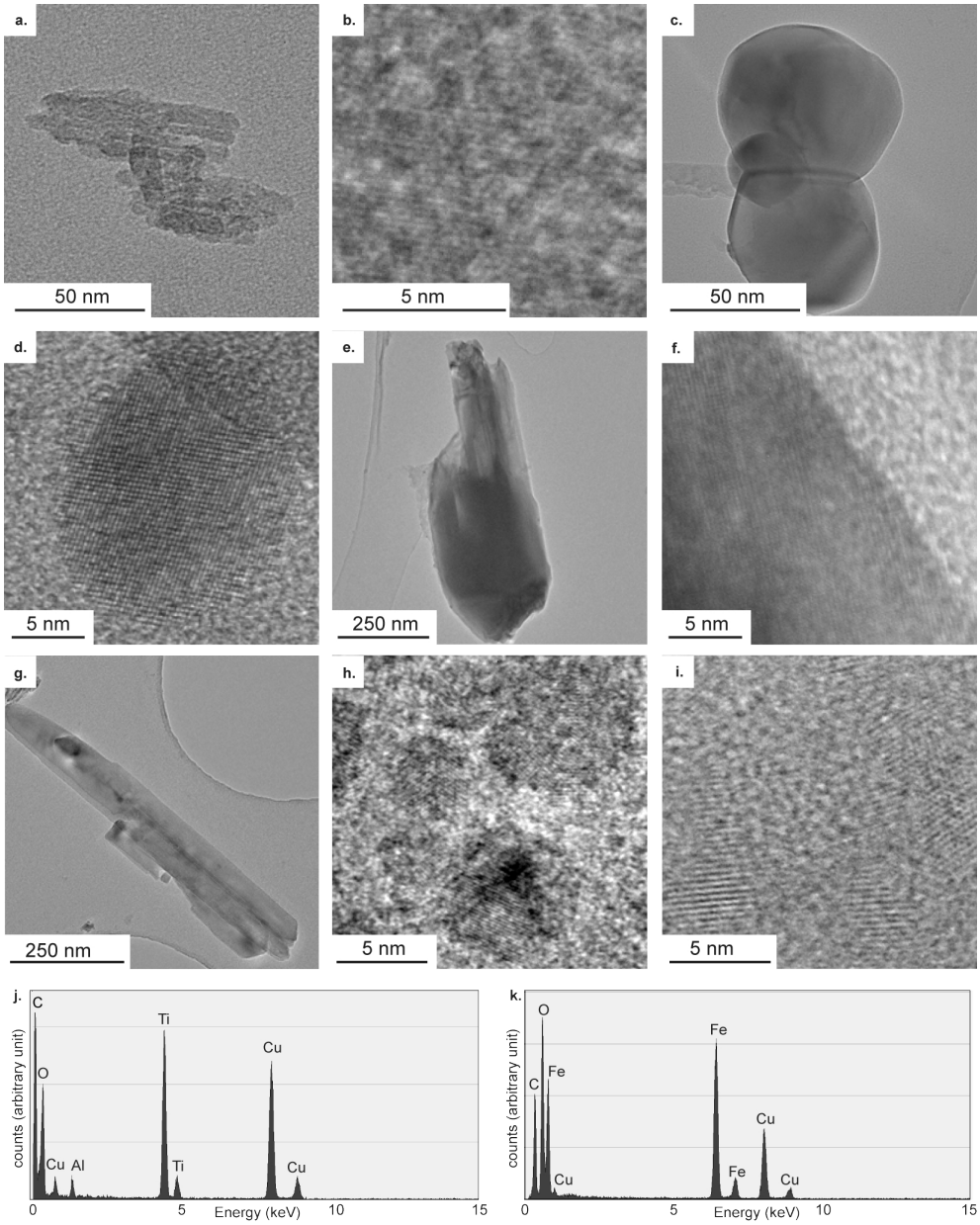

Figure 4.8. Examples (TEM-BF images) of crystalline metal(-oxides) present in the samples. A. Ti-rich particle with typical elongated shapes, found in all of the samples. B. HRTEM image of the particle in A, showing that the elongate shape follows the direction of one of the crystal planes. C. Typical rounded Ti-rich particles. D. Ti-rich nanocrystal. E. Larger Ti-rich particle. F. HRTEM image of E. G. Typical Fe-rich particle, usually much larger than the Ti-rich particles. H. Fe-rich nanocrystals. I. Al-rich nanocrystals. J. EDX spectrum of the Ti-rich particle in A. Usually these type of particles do not contain Al, it might be either a trace element within the Ti-rich particle or a separate nano-particle attached to it. K. EDX spectrum of the Fe-rich particle in G. The C peak in the EDX spectra is from the holey carbon film and the Cu peak from the supporting grid.

of graphene, which led Daulton et al. (2010) to suggest that the authors might have mistaken graphene aggregates for cubic diamond. More recent studies, on different locations, however, show more elaborate analysis of (cubic) diamond, including HRTEM, SADP of single crystals and EELS (Kurbatov et al., 2010, no results on cubic diamond reported; Tian et al., 2011; Israde-Alcántara et al., 2012). One of the studies (Kurbatov et al., 2010 figure 6) also reported HRTEM and a single crystal SADP of particles they interpret as lonsdaleite. According to Daulton et al. (2012), the HRTEM image of this particle is inconsistent with lonsdaleite or any other known carbon material, because no crystallographic orientation of lonsdaleite exists which displays two sets of {0002} planes. Measurement of the d-spacings from the HRTEM image (Kurbatov et al., 2010, figure 6b), using scale-bar provided for measurement calibration, gives d-spacings of approximately 1,27 Å, 1,26 Å and 1,18 Å (also lonsdaleit spacings, see table 2.3) rather than the reported values of 2,06 Å, 2,06 Å and 1,93 Å (a unique lonsdaleite spacing). It does appears that the image has been mislabeled, but unfortunately the correct scale is unkown (Allen West, pers. comm.). Furthermore, the diffraction pattern of lonsdaleite reported by Kurbatov et al. (2010, figure 6c) is consistent with that of the 0001 zone axis of graphite or a single graphene sheet (table 4.3, see also figure 4.4). Without further information on the crystals, such as SADPs of different zone axis or EELS, it is thus not possible to distinguish between graphite and lonsdaleite based solely on the 0001 diffraction pattern. It is thus possible that Kurbatov et al. (2010) misinterpreted graphite, or a single layer of graphene, as lonsdaleite.
Third, material might have been lost during the many steps involved during chemical preparation of the bulk samples. However, as other carbonaceous nano-particles, such as carbon onion structures, were found in the current study, the specimen preparation would have needed to exclude nanodiamonds but leave intact other carbon allotropes, which seems unlikely.

Because the nanodiamonds in the Allerød-Younger Dryas boundary were originally found in carbon spherules, which can form in wildfires (Eric, 2010), it has been suggested that the nanodiamonds might have formed in wildfires rather than during an impact (Paquay et al., 2009b; Tian et al., 2011; van Hoesel et al., 2012). However, in this study, no nanodiamonds were found in the charcoal and glass-like carbon samples of different ages. These results are consistent with other TEM studies of natural charcoal (Cohen-Ofri et al., 2007; Daulton et al., 2010). The lack of nanodiamonds in charcoal suggests that wildfires are an unlikely source of the abundant nanodiamonds reported at the Allerød-Younger Dryas. Nanodiamond (cubic diamond or n-diamond) has been reported earlier in charcoal of wood that has been experimentally carbonized at 700 °C (Ishimaru et al., 2001). Possibly the presence of nanodiamonds in their charcoal is related to the experimental procedure or the relatively high temperature compared to the samples examined here. Temperatures as high as 700 °C can be found in wildfires, but the reflectance measurements suggest that the temperatures at the Allerød Younger Dryas boundary wildfires at the examined locations were lower. A more elaborate discussion on the origin of the nanodiamonds can be found in §6.2.

4.4.2 Identification of the carbonaceous phases

In our study of the microstructure of charcoal, glass-like carbon, carbon spherules and acid resistant residues of bulk sediment we found that most of the carbonaceous material is present in an amorphous phase, which is consistent with earlier work on charcoal (Cohen-Ofri et al., 2007). We also found a semi-ordered phase (Hata et al., 2000; Cohen-Ofri et al., 2007), poorly defined

Table 4.3. D-spacings of graphite, graphene and lonsdaleite. D-spacings of the planes observed in the diffraction pattern of Figure 4.4a are in bold.

	d-spacing (Å)		
planes	**graphite**	**graphene**	**lonsdaleite**
0002	3.35		2.06
$10\bar{1}0$	**2.13**	**2.13**	**2.18**
$10\bar{1}1$	2.03		1.93
$10\bar{1}2$	1.80		1.50
0004	1.68		1.03
$10\bar{1}3$	1.54		1.16
$11\bar{2}0$	**1.23**	**1.23**	**1.26**
$11\bar{2}2$	1.16		1.08
0006	1.12		0.69
$20\bar{2}0$	**1.07**	**1.07**	**1.09**

carbon onion structures (Hata et al., 2000), microporous onion-like structures (Ishimaru et al., 2001; Cohen-Ofri et al., 2007), as well as graphitic carbon flakes with SADPs consistent with graphene aggregates (Daulton et al., 2010) and HRTEM images similar to the two-phase structure reported by Cohen-Ofri et al. (2007). The onion-like carbon structures were somewhat more common in the recent samples compared to the fossil charcoal samples. Differences between fossil and modern charcoal have been observed previously and are ascribed to the oxidation of the charcoal over time (Cohen-Ofri et al., 2007). However, considering the reflectance values of our samples (table 4.2), the differences could instead be related to a slightly higher temperature for the more recent samples.

Although Daulton et al. (2012) report that graphite is the third most abundant type of carbon they found, we only found one possible graphite particle (figure 4.4). The identification of this particle was based on a 0001 zone SADP. The {$10\bar{1}0$}, {$11\bar{2}0$} and {$20\bar{2}0$} d-spacings for graphite, graphene and lonsdaleite are, however, very close to each other (table 4.3). Because no further information, such as SADPs at different tilt or EELS, was obtained, it is not possible to distinguish between the different carbon polymorphs. However, as graphite is far more common than lonsdaleite, we consider graphite to be the most likely structure of the particle.

Distinguishing between the different microstructures based solely on SADPs is thus not straightforward, as was also shown by Daulton et al. (2012). Furthermore, not only do different carbon polymorphs have similar d-spacings (see also table 2.3 and 4.3), but particles with amorphous SADPs are sometimes semi-ordered (figure 4.2d) or consist of carbon onion structures (figure 4.5). More interestingly the microporous onion-like structures we found (figure 4.6) have diffraction patterns similar to the graphene/graphane aggregates reported by Daulton et al. (2010). This similarity in SADPs might suggest that the onion-like structures are made of both graphene and graphane sheets. The microstructure of the microporous onion-like structures is however clearly different from the graphene aggregates we found (figure 4.3). Harris (2013) investigated the microstructures in activated carbon using aberration corrected TEM, and found that the 'pores' in the structure contained not only hexagonal but also pentagonal carbon rings. These pentagonal carbon rings are slightly smaller than the hexagonal carbon rings, and their presence might thus explain the doubled diffraction lines rather than the presence of graphane.

The TEM analysis has shown that identification of the different carbon structures is difficult based on SADPs alone. The soot-like carbon onions (figure 4.5) give an SADP (not shown) with diffuse rings similar to that of amorphous carbon (figure 4.2). The porous onion-like carbon structures (figure 4.6a) have a diffraction pattern similar to that of the graphene/graphane aggregates reported by Daulton et al. (2010), and disordered or polycrystalline graphite in certain arrangements would also give diffraction patterns similar to those of the graphitic carbon flakes or graphene aggregates (figure 4.3). In addition, as discussed in §4.4.1, some of the d-spacings of different diamond polymorphs are very close to those of graphitic carbon, but diamond has a different EELS spectrum than graphitic carbon due to the different carbon bonding (Konyashin et al., 2001). It is thus important to combine careful analysis of (multiple) SADPs with HRTEM images and, where necessary, EELS spectra when identifying carbon structures found in charcoal.

4.4.3 Presence of non-carbon materials

Calcite in charcoal is formed when the natural occurring calcium oxalate monohydrate (also known as whewellite) in the plant decomposes to calcite during combustion between 460 and 500 °C. Decomposition of the calcite to calcium monoxide occurs at higher temperatures, between 730 and 750 °C (Frost and Weier, 2004; Regev et al., 2011). The temperature window for the occurrence of calcite (460-750 °C) is consistent with the temperature estimates from the reflectance measurements. Calcium oxalate monohydrate crystals in plants show various morphologies. The calcium-rich particle in figure 4.7c shows some resemblance to the druse-type crystal described in Franceschi and Nakata (2005), which suggest that the original plant morphology of the calcium oxalate monohydrate is retained during combustion.
The presence of an elongated Ti-rich particle on an empty TEM grid suggests that some of the Ti-rich particles (e.g. figure 4.8a) might be contamination. Other types of Ti-rich particles (e.g. figure 4.8c-e), however, were not found on the empty grid. As Ti is the ninth most common element in the Earth's crust and is present in plants (Dumon and Ernst, 1988; Buettner and Valentine, 2011), these other Ti-rich particles are therefore likely not contamination but part of the wood that was turned into charcoal. Daulton et al. (2010) also reported trace amounts of Ti-, Si-, and Ca-rich particles, and Fe- and Cu-oxides were also observed as trace elements in a TEM study of charcoal. The authors even suggested that some Cu nanocrystals might be mistaken for n-diamond, as the EDX signal for Cu-nanoparticles deposited on standard C-film supported by a Cu TEM grid will look similar to that of pure C on the same grid (Daulton et al., 2010). However most non-carbonaceous nanoparticles should be easy to distinguish from nanodiamond based on their d-spacings, EDX signal and EELS spectrum.

4.4.4 Glass-like carbon formation

Glass-like carbon has also been referred to as vitrified charcoal (Marguerie and Hunot, 2007; McParland et al., 2010). The term "vitrification" describes the transformation of a material into glass. This process is often associated with heating of the material to high temperatures, followed by rapid cooling, inhibiting the formation of crystal structure. However, based on reflectance measurements, McParland et al. (2010) showed that natural glass-like carbon is formed at relatively low temperatures (310-530 °C). In addition, they showed that the reflectance values of

the glass-like parts and parts with remnant wood structure ('charcoal parts') of the same particle had the same reflectance. The reflectance values of the charcoal and glass-like carbon parts of the particle from Rennes (table 4.2), also suggest that the reflectance of charcoal and glass-like carbon respond to temperature in the same way and that glass-like carbon formed in a low temperature regime (<560 °C).
The microstructure of the onion-like carbon porous structure from our recent charcoal particle (figure 4.6b,c) shows some resemblance to that of some carbon fibres (Fitz Gerald et al., 1991) and to the microstructure of commercial glass-like carbon produced through pyrolysis at 2800-3000°C (Harris, 2004). This similarity suggests that similar processes might be occurring during wildfires at much lower temperatures (<600°C), and also in charcoal particles with no glass-like appearance. It has been suggested that glass-like carbon might be the result of re-precipitation of tar – a dark, oily, viscous material, consisting mainly of hydrocarbons, produced by the destructive distillation of organic substances such as wood – in the wood structure (McParland et al., 2010) or charred conifer resin (Eric, 2010). The similarities in microstructures found within natural glass-like carbon and charcoal particles, however, suggest that glass-like carbon might be more related to charcoal. However, synthetic glass-like carbon can be made from a range of precursor material (Harris, 2004), but seems to contain similar a microstructure independent of the precursor material. Analysis of the other properties of charcoal and glass-like carbon would be necessary to see whether both types share more similar properties. In addition, Focused Ion Beam (FIB)-SEM in combination with TEM could give better insight in the microstructures, and their spatial relationships, of charcoal and glass-like carbon.

4.5 Conclusions

- No nanodiamonds were found in the samples from the Usselo horizon, the black mat or the lake core spanning the Allerød-Younger Dryas transition, which is inconsistent with the Younger Dryas impact hypothesis.

- No nanodiamonds were found in natural charcoal and glass-like carbon of different ages. Wildfires therefore do not seem a likely explanation for the presence of nanodiamonds in the Allerød-Younger Dryas boundary layer.

- TEM analysis of the charred particles shows that carbon is present in different forms: amorphous carbon flakes, graphitic carbon flakes, soot-like carbon onion structures, and porous onion-like carbon structures.

- No clear difference in microstructures was observed in the carbon particles in the charcoal and glass-like carbon samples, although the soot-like carbon onions seemed more common in charcoal and in the modern particles with a higher charring temperature.

Chapter 5

Shocked quartz in the Usselo horizon

The Younger Dryas impact hypothesis suggests that multiple airbursts or extraterrestrial impacts occurring at the end of the Allerød interstadial resulted in the Younger Dryas cold period. This hypothesis is considered controversial, as no reproducible, diagnostic impact evidence has been reported. Shocked quartz, or quartz grains containing planar deformation features, is considered a reliable indicator for the occurrence of an extraterrestrial impact. Although shocked quartz has been reported at a possible Allerød-Younger Dryas boundary layer in Venezuela, the identification of shocked quartz in this layer is ambiguous. To test whether shocked quartz is indeed present in the proposed impact layer, we investigated the quartz fraction of multiple Allerød-Younger Dryas boundary layers from the European sandbelt and from a Black Mat site from North America where proposed impact markers have been reported.

Grains were analysed using a combination of light and electron microscopy techniques. All samples contained a variable amount of grains with (sub)planar microstructures, often tectonic deformation lamellae. Only one grain containing planar deformation features was found, located in the Usselo horizon at Geldrop Aalsterhut, the Netherlands. Scanning electron microscopy cathodoluminescence and transmission electron microscopy imaging, however, show that the planar deformation features are healed and thus likely to be older than the Allerød-Younger Dryas boundary. We suggest that this grain was eroded from an older crater or distal ejecta layer and later re-deposited in the European sandbelt.

5.1 Introduction

In 2007, it was suggested that one or more extraterrestrial impacts or airbursts caused the onset of the Younger Dryas cold period (12.85-11.65 ka), megafaunal extinctions and a decline in human population (Firestone et al., 2007; Wittke et al., 2013b). This idea is also known as the Younger Dryas impact hypothesis and was initially based on elevated concentrations (compared to background) of several markers in the Allerød-Younger Dryas boundary layer at several sites in North America and one in Europe. These markers include, among others, iridium and magnetic spherules, and later also nanodiamonds, lechatelierite, and platinum (Kennett et al., 2009a; Kennett et al., 2009b; Bunch et al., 2012; Petaev et al., 2013). Most of the reported markers are however, either not reproducible by others or not considered as diagnostic evidence for an impact (French and Koeberl, 2010; Pinter et al., 2011; Pigati et al., 2012; van Hoesel et al., 2013).
Mahaney et al. (2010a) reported the occurrence of planar deformation features (PDFs) in quartz, or simply 'shocked quartz', in a black mat-like layer in the Venezuelan Andes, reported as representing the Allerød-Younger Dryas boundary. PDFs are thin (<1 μm), closely spaced (<10 μm), usually straight, parallel deformation planes in crystals, which form during shock deformation (Langenhorst, 2002; French and Koeberl, 2010; Hamers and Drury, 2011). PDFs are unique features, and shocked quartz is therefore widely used as a reliable impact indicator (French and Koeberl, 2010). In addition, the orientation and number of sets within one grain is related to the shock pressure and can thus give information about the impact itself (Grieve et al., 1996). Although PDFs can often be easily identified using light microscopy, other, non-shock features (e.g. tectonic deformation lamellae or growth features) can have similar appearances in light microscopy and might be mistaken for PDFs (table 5.1) (French and Koeberl, 2010). Other methods, such as scanning electron microscopy (SEM) cathodoluminescence (CL) imaging of sectioned grains or transmission electron microscopy (TEM) are thus necessary to confirm the true nature of planar deformation features (French and Koeberl, 2010; Hamers and Drury, 2011). Mahaney et al. (2010a) however, only imaged whole grains using SEM, showing parallel surface features spaced 0.5-1.0 μm apart. Although the spacing of these features is consistent

Table 5.1. Properties of PDFs compared to other shock features (planar fractures) and non-shock features (tectonic deformation lamellae and growth lines).

	Planar deformation features	Planar fractures	Tectonic deformation lamellae	Growth lines
shape	straight, parallel	straight, parallel	often slightly curved	straight, parallel, sometimes with zigzag
width	< 2-3 μm (typically < 1 μm	3-10 μm	> 2 μm (typically > 10-20 μm)	narrow
spacings	< 10 μm (typically < 2 μm)	> 15 μm	> 5 μm	close, irregular
sets/grain	≥ 1 (typically ≥ 3)	2-3	1-2 (typically 1)	1
orientation	parallel to specific planes	specific angles to c-axis	broad range of low angles to basal plane	often different from PDFs
CL imaging	red / non luminescent sharp / well-defined		red / blue luminescent hard to define	
impact shock pressure	10-30 GPa	< 8 GPa	not applicable	not applicable

with the spacing of PDFs, more information is necessary to distinguish these features from non-shock features. In a follow-up study on the same site Mahaney et al. (2010b) focus on the presence of closely spaced fractures oriented parallel to the surface of the quartz grains, highly disrupted grain surfaces and extreme brecciation. These features are, however, not considered as indicative of high shock pressures related to an extraterrestrial impact (French and Koeberl, 2010). Furthermore, Mahaney et al. (2010b) reported that they found no irrefutable PDFs.
The presence of extensive shocked quartz at the Allerød-Younger Dryas boundary would be a clear indication that an extraterrestrial impact occurred. An absence of shocked quartz, on the other hand, would not dismiss the impact hypothesis since no shocked quartz is expected if the Younger Dryas impact event consisted of airbursts or occurred over the ocean. This chapter reports the results on the search for shocked quartz grains in European palaeosols and peat layers that were at the surface at the time of the proposed Younger Dryas impact event and should thus have collected any impact related ejecta.

5.2 Study area

Samples from the Allerød-Younger Dryas boundary at nine locations in the European coversand area, and one from the Black Mat in North America were investigated(figure 5.1 and 5.2). In the coversand area, the Allerød-Younger Dryas boundary is often marked by either the Usselo horizon or the Finow soil (§1.2.2). The formation of both types of palaeosols is thought to have started during the Allerød, when aeolian activity ceased and the landscape stabilized, until the soil was buried by renewed aeolian activity during the Younger Dryas cold period (Kaiser et al., 2009). In the wetter parts of the landscape, peat started to develop during the Allerød, which formed layers that were also subsequently buried during the Younger Dryas (Kaiser et al., 2006). Both the Usselo and Finow palaeosols and the sampled peat layers would have been at the surface at the time of the proposed Younger Dryas impact event and should thus have collected any impact related material reaching Europe. Any material found, however, could have been incorporated in the palaeosols at any time during their formation period and analysis of these horizons will thus only give an indication of whether an impact event occurred during the end of the Lateglacial period (figure 1.1). The North American Black Mat differs in that these wet soils and algal mats did not form until the start of the Younger Dryas (§1.2.1, see also figure 1.1), and the Black Mat would thus cover any material related to the Younger Dryas impact event. In order to ensure that all sampled layers were at the surface at the Allerød-Younger Dryas transition and would have received any impact-related material, only previously dated sites were selected for investigation (table 5.2). Additional radiocarbon ages were obtained for three of the sites in this study (table 5.3). Three of the sites in this study have been previously investigated for impact markers (Firestone et al., 2007; Tian et al., 2011; van Hoesel et al., 2012), namely Murray Springs (Arizona), Lommel Maatheide (Belgium) and Geldrop Aalsterhut (The Netherlands).

5.2.1 Altdarss

The Altdarss site (Germany) contains a buried catena consisting of different palaeosol types – from dry soils to wet peat – in glaciolacustrine sands covered by aeolian sand. The dry palaeosols are similar to the Usselo horizon. Pollen analysis and optically stimulated luminescence (OSL) dating suggests that the palaeosols were formed during the late Allerød and were covered by aeo-

lian sands during the Younger Dryas (Kaiser et al., 2006). A thin peat layer (figure 5.2a) on top of a histic gleysol (profile ADO 39 in Kaiser et al., 2006) was sampled. This peat layer has been dated to 10,600 ± 55 ^{14}C yrs BP (12,615-12,435 cal[2]. yrs BP, n=3[3]), Kaiser et al. (2006), however, suggest that their radiocarbon dates might be contaminated with younger carbon.

5.2.2 Blankenförde

Blankenförde (Germany) is a site with a Lateglacial dune complex containing a weakly developed cambisol (figure 5.2b), which was interpreted as a Finow soil (Küster and Preusser, 2009). The sediment in which the paleosoil is formed has been dated using OSL to 15.5 ± 1 ka and was covered by aeolian sands that were OSL dated to 13.5 ± 0.5 ka (n=2) (Küster and Preusser, 2009).

5.2.3 Dybowo

Dybowo (Poland) contains a Finow soil in aeolian sand. Using conventional radiocarbon dating, the soil horizon was dated to 9,550 ± 220 ^{14}C yrs BP (11,400-10,2040 cal. yrs BP) (Jankowski, 2002). The dated charcoal might, however, have been contaminated with carbonate deposition or younger roots. Using accelerator mass spectrometry (AMS) radiocarbon dating, we obtained an age of 10,390 ± 50 ^{14}C yrs BP (12,385-12,125 cal. yrs BP) for a charcoal particle from the Finow soil. This is a few centuries younger than the Allerød-Younger Dryas boundary. However, soil formation takes time and considering the age of the palaeosols at nearby Katarzynka (table 5.2), it is possible that the Finow soil at Dybowo was already at the surface at the onset of the Younger Dryas. Nevertheless, the charcoal is younger than the Allerød-Younger Dryas boundary, so the wildfires that created the charcoal cannot have been related to a Younger Dryas impact event.

Figure 5.1. Location of the fieldsites in Europe and North America (inset).

[2]All radiocarbon ages have been callibrated using the IntCal13 calibraton curve (Reimer et al. 2013) and the online OxCal v4.2 calibration software (Bronk Ramsey, 2009)

[3]When the reported age is based on the average of multiple dates, n indicates the number of dates averaged

Table 5.2. Information of the different Allerød-Younger Dryas boundary layers investigated for the occurrence of shocked quartz. See figure 5.1 for the locations of the site and figure 5.2 for photos of the sampled layers.

Site name	Type of boundary layer	# of samples	Age	Archaeology	Reported markers	References
Altdarss 39 (DE)	peat layer	1	10,600 ± 55 ^{14}C yrs BP* (12,660-12,540 cal. yrs BP)			Kaiser et al. 2006
Blankenförde (DE)	Finow soil	1	between 15.5 ± 1 ka and 13.5 ± 0.7/13.8 ± 0.9 ka			Küster and Preusser 2009
Dybowo (PL)	Finow soil	1	10,390 ± 50 ^{14} yrs BP 12,390-12,160 cal. yrs BP)			Jankowski, 2002 this study
Geldrop Aalsterhut (NL)	Usselo horizon	4 + bg	10,845 ± 15 ^{14}C yrs BP (12,740-12,710 cal. yrs BP)	Federmesser, Ahrensburg	nanodiamonds	van Hoesel et al. 2012
Katarzynka (PL)	Usselo horizon Finow soil	3	11,100 ± 270 ^{14}C yrs BP* (13,195-12,725 cal. yrs BP)			Jankowski et al. 2012
Lommel Maatheide (BE)	Usselo horizon peat layer	2	11,480 ± 100 ^{14}C yrs BP (13,430-13,235 cal. yrs. BP); between 13.5 C 0.9 ka and 11.3 ± 0.8 ka	Federmesser, Early Mesolithic	nanodiamonds, iridium, magnetic spherules	Firestone et al. 2007 Tian et al. 2010 Derese et al. 2012 Wittke et al. 2013
Lommel Molse Nete (BE)	Usselo horizon	1	11,480 ± 35 ^{14}C yrs BP* (13,370-13,285 cal. yrs BP)	Federmesser, Early Mesolithic		van Montfoort et al. 2010 this study
Lutterzand (NL)	peat layer	3	11,480 ± 70 ^{14}C yrs BP (12,560-12,240 cal. yrs BP); between 13.8 ± 1.0 ka and 12.7 ± 0.9 ka			van den Berghe et al. 2013
Murray Springs (USA)	Black Mat	2	10,885 ± 50 ^{14}C yrs BP* (12,785-12,715 cal. yrs BP)		nanodiamonds, iridium, magnetic spherules, glass-like carbon	Waters and Stafford 2007 Firestone et al. 2007 Kennett et al. 2009
Rosenberg (DE)	Finow soil	2	between 15.71 ± 1.40 ka and 11.03 ± 1.20 ka*			Hilgers 2007

*based on multiple dates

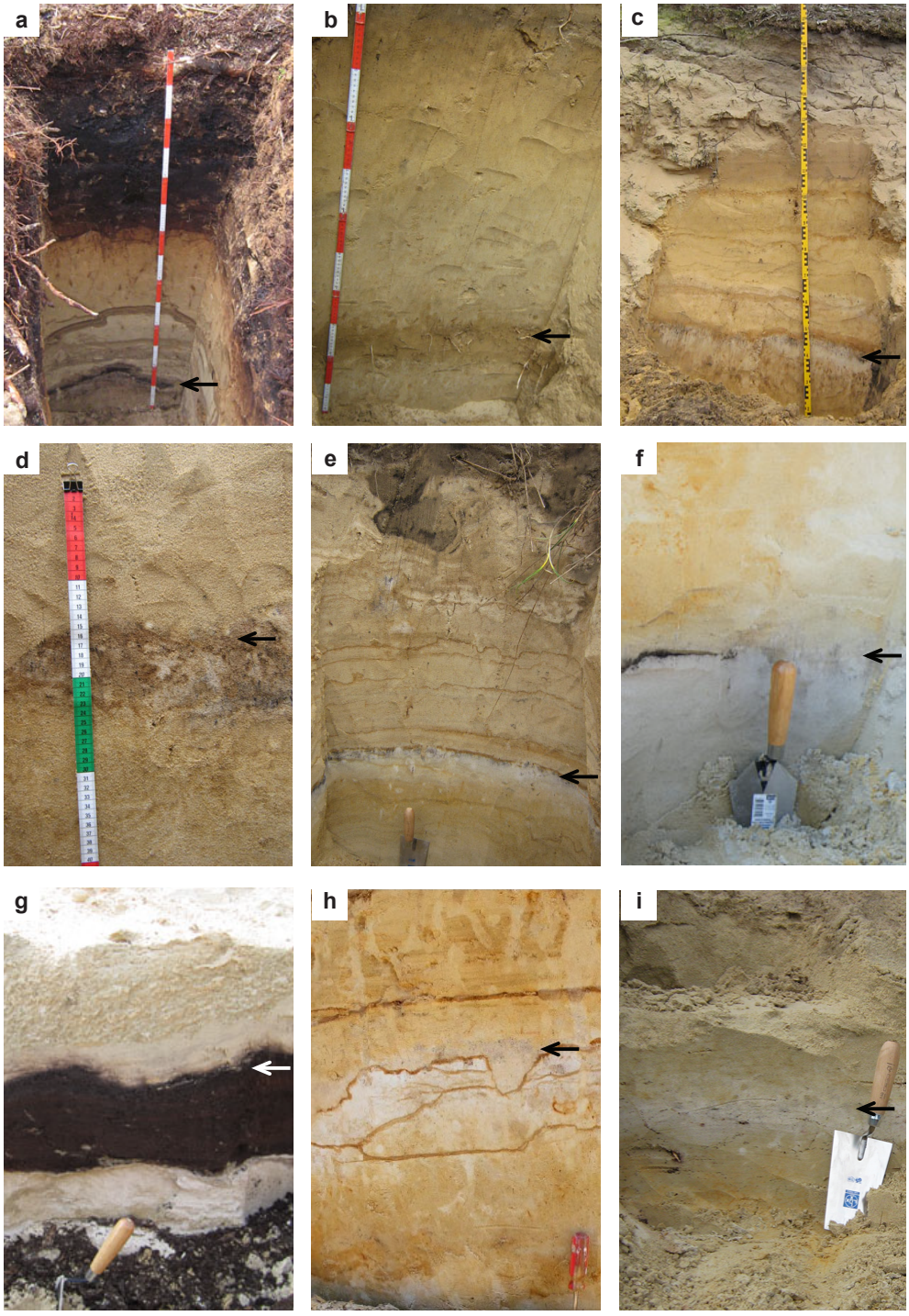
a
b
c
d
e
f
g
h
i

Figure 5.2. Photos of sampled layers at the field locations given in figure 1. Arrows indicate the location of the sampled layers a. Thin Allerød peat layer at Altdarss. b. Finow soil at Blankenförde. c. Usselo horizon at Geldrop Aalsterhut. d. Finow soil at Katarzynka. e. Usselo horizon at Katarzynka. f. Usselo horizon at Lommel Maatheide. The Usselo horizon is visible as grey specks and a thin black organic rich layer in the top of the white coversand. g. Thick Allerød peat bed at Lommel Maatheide. The undulating top of the peat suggests that the layer has been eroded. h. Usselo horizon at Lommel Maatheide. i. Usselo horizon at Lutterzand. This horizon was only radiocarbon dated in this study. j. Thin Allerød peat layer at Lutterzand. k. Black Mat at Murray Springs (photo: A. Andronikov). l. Black Mat at Murray Springs (photo: A. Andronikov). m. Finow horizon at Rosenberg (photo: N. Schlaak).

5.2.4 Geldrop-Aalsterhut

Geldrop Aalsterhut (the Netherlands) is an archaeological site in the coversand area containing artefacts of the Federmesser and the Ahrensburg cultures. The Federmesser culture, which occupied the Netherlands during the Allerød, had mostly disappeared from the Benelux near the end of the Younger Dryas (De Bie and Vermeersch, 1998; Riede, 2008; Vermeersch, 2011) and at Geldrop Aalsterhut its occupation horizon coincides with the Usselo horizon (figure 5.2c, see also figure 3.1). The Ahrensburg occupation horizon at Geldrop, positioned about 10 cm above the Usselo horizon, has been dated within 10,600 - 9,800 ^{14}C yrs BP (Vermeersch, 2011). The Usselo horizon at this location contains abundant charcoal and has been AMS radiocarbon dated to 10,845 ± 15 ^{14}C yrs BP (12,760 – 12,640 cal. yrs BP, n=14) (van Hoesel et al., 2012), consistent with previous conventional radiocarbon dates (De Vries et al., 1958). The charcoal slightly postdates the Allerød-Younger Dryas boundary, suggesting that the nanodiamonds found in the glass-like carbon from the Usselo horizon cannot be directly associated with the Younger Dryas impact hypothesis (van Hoesel et al., 2012). Geldrop-Aalsterhut is located approximately 25 km northeast of Lommel, which was part of the original Firestone et al. (2007) study.

Table 5.3. AMS radiocarbon dates of individual charcoal particles from the paleosoil at different locations.

Sample name	Site	Sample nr. for AMS	^{14}C age BP	Cal. age BP
Dyb-1	Dybowo	GrA-55464	10,930 ± 50	12,390 - 12,260
LZ-02	Lutterzand	GrA-55486	11,460 ± 50	13,380 - 13,255
LZB-01	Lutterzand	GrA-55616	10,930 ± 70	12,860 - 12,715
LZB-2	Lutterzand	GrA-55619	10,880 ± 50	12,785 - 12,710
LMN-01	Lommel Molse Nete	GrA-55466	11,050 ± 50	12,990 - 12,835
LMN-2	Lommel Molse Nete	GrA-55618	11,740 ± 110	13,710 - 13,465
LMN-3	Lommel Molse Nete	GrA-55621	11,930 ± 55	13,830 - 13,615

5.2.5 Katarzynka

Katarzynka (Poland) is located in the European sand belt and contains a Late Glacial palaeocatena (Jankowski, 2012). In its uppermost position the paleosoil has been dated to 11,100 ± 270 ^{14}C yrs BP (13,220 – 12,715 cal. yrs BP) and resembles the Finow soils (figure 5.2d). On the slope an Usselo horizon is present (figure 5.2e). The gleysol at the bottom of the sequence has been dated to 11,100 ± 230 ^{14}C yrs BP (13,180 – 12,735 cal. yrs BP). Based on the weak stage of development, Jankowski et al. (2012) suggest that the palaeosols were formed in a short period of time, existing at the land surface only during the Allerød.

5.2.6 Lommel

At Lommel (Belgium) samples were taken from two archaeological sites containing Federmesser artefacts (Vanmontfort et al., 2010a; Derese et al., 2012): Lommel Maatheide (figure 5.2f,g) and Lommel Molse Nete (figure 5.2h). Several Younger Dryas impact markers, including nanodiamonds, have been reported at Lommel, probably from the Maatheide site (Firestone et al. 2007; Tian et al. 2010; Wu et al. 2013). At the Maatheide site, there is an Usselo horizon present consisting of a thin black organic horizon on top of a thicker bleached horizon. Over a relatively short distance, with a slight decrease in elevation, the Usselo horizon grades into a relatively thick peat layer (ca. 20 cm in thickness). OSL dating of the over and underlying sediments shows that the Usselo horizon at this location must have formed between 13.5 ± 0.9 ka (n=4) and 11.3 ± 0.8 ka (n=2) (Derese et al., 2012). A charcoal particle from the Usselo horizon at Maatheide has been dated to 11,480 ± 100 ^{14}C yrs BP (13,435-13,245 cal. yrs BP, Wittke et al. 2013), which is consistent with the OSL age constraints. The Molse Nete site is situated at a coversand ridge bordering a small river valley. At some locations an Usselo horizon is present in the coversand, but not everywhere (Vanmontfort et al., 2010b). The Usselo horizon does not contain a clear black layer above a bleached horizon such as found at Maatheide, but rather a relatively thin irregular bleached horizon with charcoal and organic material distributed in the top part, similar to the Usselo horizon found at Geldrop Aalsterhut. AMS radiocarbon dating of three charcoal particles at Maatheide (table 5.3) yields an age of 11,480 ± 35 ^{14}C yrs BP (13,385-13,288 cal. yrs BP). These radiocarbon ages suggest that wildfires at both sites near Lommel were synchronous, but somewhat older than the wildfires at the nearby Geldrop Aalsterhut (~25km, van Hoesel et al. 2012) and Korhaan (15 km, Vanmontfort et al., 2010a) sites.

5.2.7 Lutterzand

Lutterzand (the Netherlands) is a classic type locality for the north western European coversand stratigraphy. The sections are exposed by the Dinkel river and contain the Usselo horizon (figure 5.2i) grading into a thin peat bed (figure 5.2j) associated with the Usselo horizon (Bateman and Van Huissteden, 1999, northern and southern profile; Vandenberghe et al., 2013, profile 4 and profile 1). To avoid dilution of possible shock quartz grains by the coversand, we sampled the thin peat layer. This layer contained no datable charcoal, but our radiocarbon dates (table 2) of three charcoal particles from the Usselo horizon yield an average age of 11,120 ± 35 ^{14}C yrs BP (13,100-12,950 cal. yrs BP), consistent with the radiocarbon age obtained by Van den Berghe et al. (2013). A charcoal particle from the thin peat bed was dated to 10,480 ± 70 ^{14}C yrs BP (12,560-12,220 cal. yrs BP) (UtC-14913, Vandenberghe et al., 2013), possibly suggesting a slightly younger age for the peat bed as compared to the Usselo horizon. OSL dating of the sediments above and below the layers put the formation of the Usselo horizon between 14.8 ± 1.2 ka and 13.0 ± 1.0 and the peat layer between 13.8 ± 1.1 ka and 12.7 ± 0.9 ka (Vandenberghe et al., 2013). These OSL ages are consistent with the radiocarbon ages as well as an earlier OSL study of the sediments (Bateman and Van Huissteden, 1999).

5.2.8 Murray Springs

Murray Springs is an archaeological site in Arizona, USA. The occupation horizon contains multiple Clovis artefacts in direct association with bone remains from different animals, and is covered by the Black Mat (Haynes et al., 2010). Charcoal from Clovis hearths has been dated to 10,885 ± 70 ^{14}C yrs BP (12,915 - 12,620 cal. yrs BP, n=8) (Waters and Stafford, 2007). The Black Mat itself (figure 5.2k,l) has been dated to 10,700 – 9,700 ^{14}C yrs BP (12,620-11,170 cal. yrs BP) (Haynes et al., 2010), which is consistent with a Younger Dryas age. Several research groups reported impact markers at the contact between the Clovis occupation horizon and the Black Mat (Firestone et al., 2007; Fayek et al., 2012; Kennett et al., 2009a), while others could not confirm the results or attributed observed concentrations to natural variation in fluvial systems (Paquay et al., 2009; Haynes et al., 2010).

5.2.9 Rosenberg

At the Rosenberg site, just north of the town of Melchow (Germany) a Finow soil (figure 5.2m) has been found in a Late Glacial dune (Hilgers et al., 2000). OSL dating shows that the soil must have formed between 15.71 ± 1.40 ka and 11.03 ± 1.20 (n=2) (Hilgers, 2007). Charcoal from the nearby Finow soil at the Melchow site has been dated to 10,840 ± 355 ^{14}C yrs BP (13,180-12,230 cal. yrs BP) (Kaiser et al., 2009), which is consistent with the OSL range. Charcoal from the horizon of reworked humic material higher in the profile has been dated to 1180 ± 80 ^{14}C yrs BP (965-730 cal. yrs BP) (Hilgers, 2007).

5.3 Methods

Subsamples from each site were treated with HCl, H_2O_2 and/or repeated rinsing to remove carbonates and organic matter when necessary, and sieved to remove the smallest (<20 μm)

and largest grains (>500 μm). To isolate the quartz grains, density separation was performed using a Loc50 centrifuge and diiodemethane heavy liquid (of 2.62 g/cm^3, 2.64 g/cm^3, 2.66 g/cm^3) at the Mineral Separation Laboratory at the VU Amsterdam. As most samples were rich in quartz grains and shocked quartz can have a slightly lower density than average (Langenhorst and Deutsch, 1994), the 2.62-2.64 g/cm3 fraction was used for further analysis. This fraction was embedded in epoxy resin and polished to 1 μm finish with Al_2O_3 using a standard polishing procedure. All fractions were inspected visually for the occurrence of PDFs using transmitted light microscopy (LM).
After carbon coating, grains with planar microstructures were analysed using scanning electron microscopy (SEM) cathodoluminescence (CL) imaging (see Hamers and Drury, 2011) using a Philips XL30S FEG-SEM with a KE Developments Centaurus CL 8 detector attached, which has a wavelength detection range of 300-650 nm with a peak at 420 nm. For some grains, additional SEM-CL images were taken using an FEI Nova Nanolab 600 SEM with a Gatan PanaCL detector, which is more or less panchromatic and has a detection range of 185-850 nm. Three images were taken with this detector, using a red (595-850 nm), green (495-575 nm), and blue (185-510 nm) filter and subsequently combined in a composite RGB image. In addition, on the XL30S FEG-SEM grains were analysed using forescatter electron (FSE) imaging, also known as orientation contrast imaging, and electron backscatter diffraction (EBSD) mapping using a Nordlys CCD EBSD camera, with two FSE detectors attached in the lower corners of the camera. For this analysis the samples were first polished using 50 nm colloidal silica.
A thin foil for transmission electron microscopy (TEM) analysis was prepared using the FEI Nova Nanolab instrument and analysed using a FEI Tecnai 20 FEG TEM operated at 200 kV. All electron microscopes are located at the Electron Microscopy Laboratory Utrecht (EMU).

5.4 Results

All samples contained grains with tectonic deformation lamellae and fractures in various, small amounts (figure 5.3). Three grains with multiple sets of lamellae were also observed (figure 5.3g-i, figure 5.4). The wavy nature of the lamellae of the first grain (figure 5.3g) clearly indicates that these are tectonic deformation lamellae. The other two grains, although not convincing as PDFs in transmitted LM (figure 5.4a,d), do show some features similar to PDFs in the SEM-CL images taken with the Centaurus detector (figure 5.3b,e). These features appear thin (<1-2 μm), closely spaced (<2 μm and 5-10 μm) and relatively straight. Colour filtered CL imaging, on the other hand, shows that the features are relatively thick (8-15 μm) bands bound by thin, irregular red luminescent lines and are thus not PDFs.

Two of the sites, Murray Springs and Lutterzand contained a few small grains, often feldspar, with one set of thin (<1-2 μm), closely spaced (<10 μm) planar microfeatures visible in LM. Interestingly, one of these grains (figure 5.5) closely resembled shocked quartz in SEM-CL imaging. FSE imaging and EBSD mapping shows that the thin microfeatures visible in CL are, however, twin boundaries rather than PDFs, which can also form in feldspar (Huffman et al., 1993; Huffman and Reimold, 1996; French, 1998).

One grain, from the Usselo horizon at Geldrop Aalsterhut, shows two sets of thin, closely spaced planar microfeatures in transmitted LM (figure 5.6a) with a north-south and northeast-

southwest orientation. The grain is relatively rounded and looks very similar to known shocked quartz grains (e.g. figure 3A in Langenhorst and Deutsch, 2012). When the microscope is focused slightly below the surface a third set of lamellae is visible with a northwest-southeast orientation (figure 5.6b). SEM-CL imaging shows that the lamellae are mostly red luminescent and are sometimes lined by pores (figure 5.6c,d), suggesting that they are healed PDFs (Hamers, 2013). A fourth set of lamellae, not visible in LM, can be seen in the bottom part of the grain

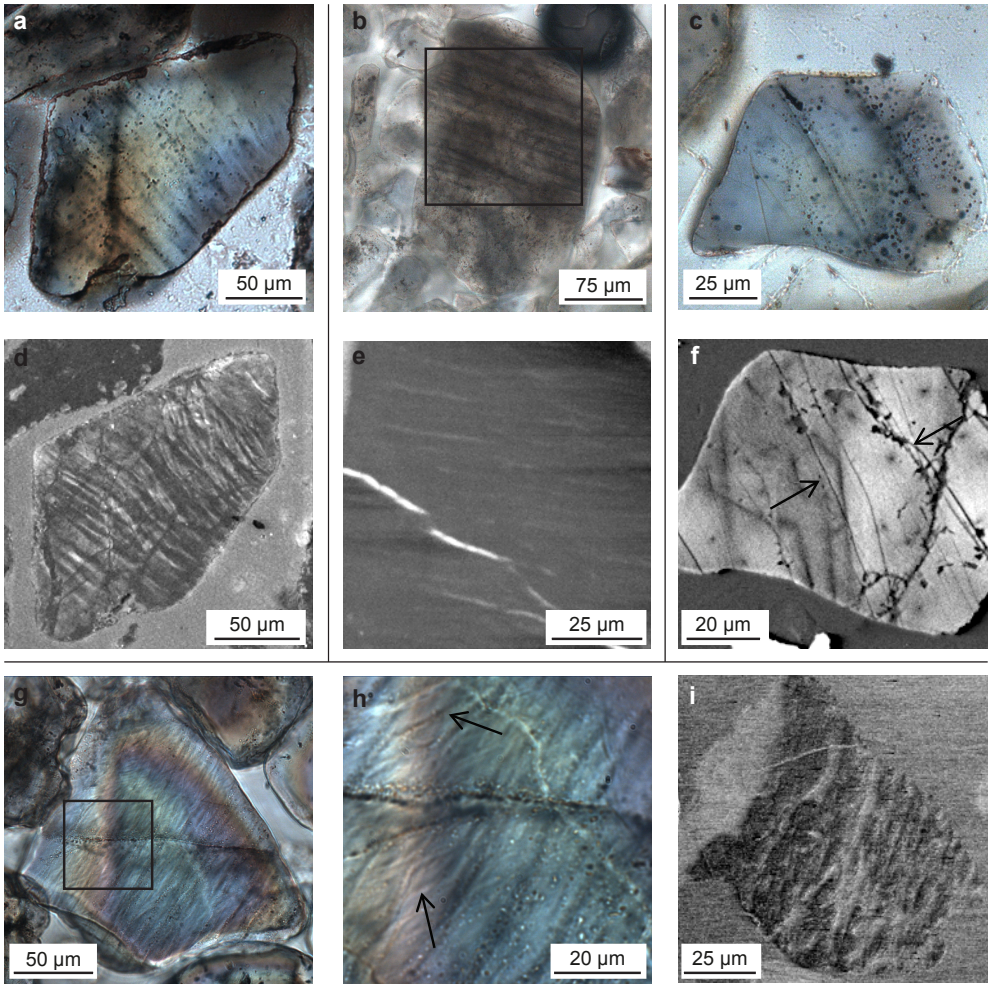

Figure 5.3. Examples of polished surfaces of grains with different kinds of (sub)planar microfeatures. a. Transmitted light microscopy (TLM) image of a grain with poorly defined subplanar microfeatures from the coversand underlying the Usselo horizon at Geldrop Aalsterhut. b. TLM image of a grain with relatively wide planar microstructures from the Usselo horizon at Geldrop Aalsterhut. c. TLM image of a grain with a few sharp (sub)planar microfeatures from the Finow soil at Rosenberg. d. SEM-CL image of the grain in (a) (boxed region) showing microstructures characteristic of tectonic deformation lamellae. e. SEM-CL image of the grain in (b) showing weak contrast from tectonic deformation lamellae. f. SEM-CL image of the grain in (c) showing narrow, irregular non-luminescent features (arrows), possibly healed fractures. g. TLM image of a grain with closely spaced wavy tectonic deformation lamellae from the Usselo horizon at Lommel Maatheide. h. Higher magnification TLM image of the grain in (g) (boxed region) showing a second set of deformation lamellae (arrows). i. SEM-CL image of grain in (g) showing weak contrast from relatively wide features, compared to the narrow features visible in the TLM.

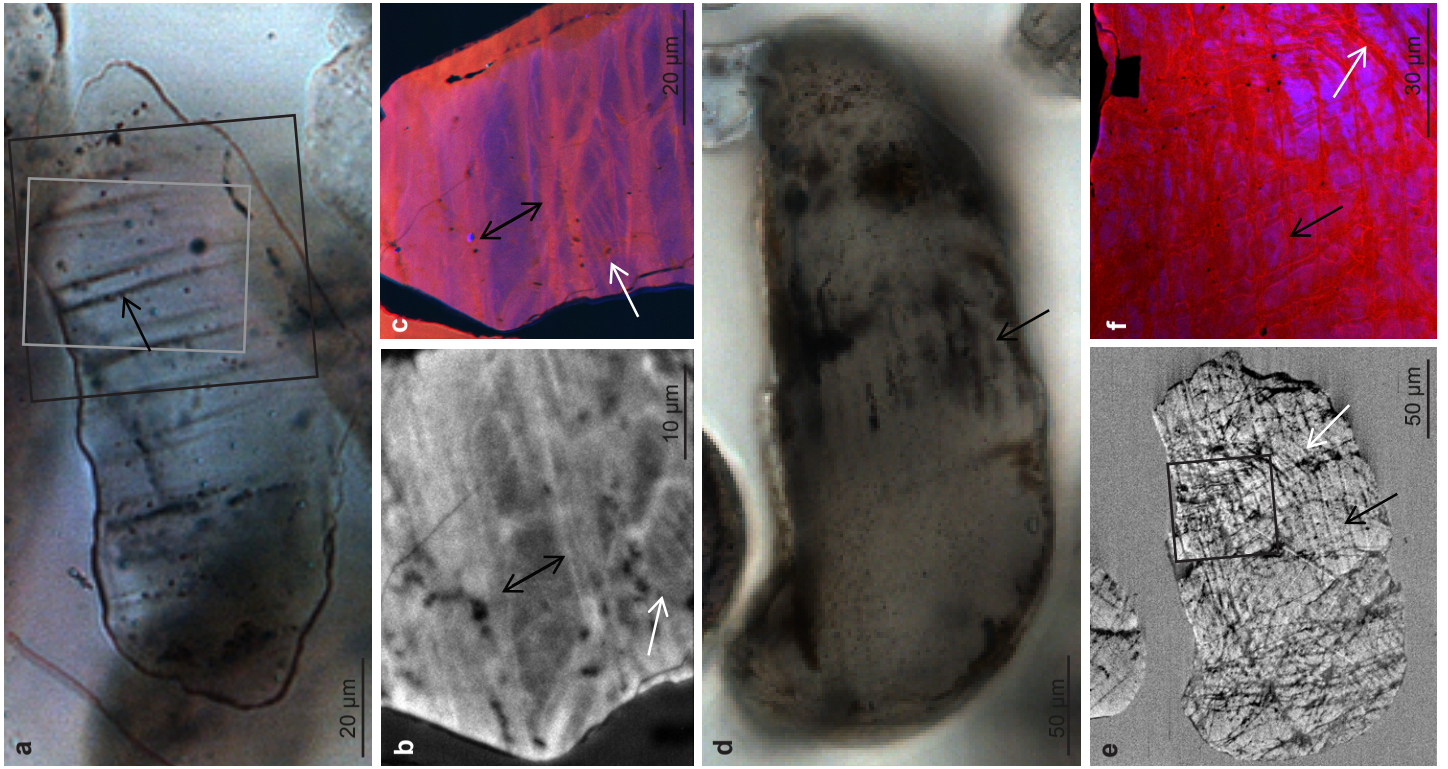

Figure 5.4. Polished surfaces of quartz grain from the Usselo horizon at Geldrop Aalsterhut (a-c) and Katarzynka (d-f). TLM images (a, d) show (sub-)planar microstructures that are not visible throughout the entire grain. Black and white SEM-CL images (b, e) of each grains show one set of thin, closely spaced microstructures that occur through most of the grain (black arrows) and a second set in some part of the grain (white arrows). Composite colour CL images (c, f) however, show that these microstructures consist of slightly thicker bands bounded by thin, irregular red-luminescent lines. The grey and black boxes in a show the location of b and c respectively. Note that c and c are rotated anti-clockwise compared to a. The black box in e shows the location of f.

and has a north-northeast to south-southwest orientation. No planar features with an orientation corresponding to the third set as seen in LM (figure 5.6b) were observed in the SEM-CL images, suggesting that this set is only present in the part of the grain that is below the polished surface. The pores along the lamellae are best visible in the FSE images (figure 5.7). The FSE images show trails of pores following the direction of the PDFs as well as two or three other orientations not seen in the LM or SEM-CL image, one of these other orientations is visible in figure 5.7a, where they often appear as a bright line or thin band. The EBSD pattern quality map (figure 5.7b) shows that the bright band in the FSE image has a less well ordered or amorphous crystal structure. Coesite or stishovite, which are denser phases of SiO_2 forms during high shock pressures, might also show up bright in the FSE image. These high pressure phases of SiO_2 would, however, show up brighter in the BSE image compared to quartz (Stähle et al., 2008), while the features in our grain do not (figure 5.7c). The bright lines observed in the FSE image (figure 5.7a) are thus most likely related to charging of PDFs (Hamers, 2013). The BSE image shows that the bright band in the FSE image actually consists of two converging lines creating a narrow lens-shaped feature. Curved crack-like features connect the pores along the converging lines.
The orientation map shows that the darker grey areas in the FSE and BSE image are Dauphiné

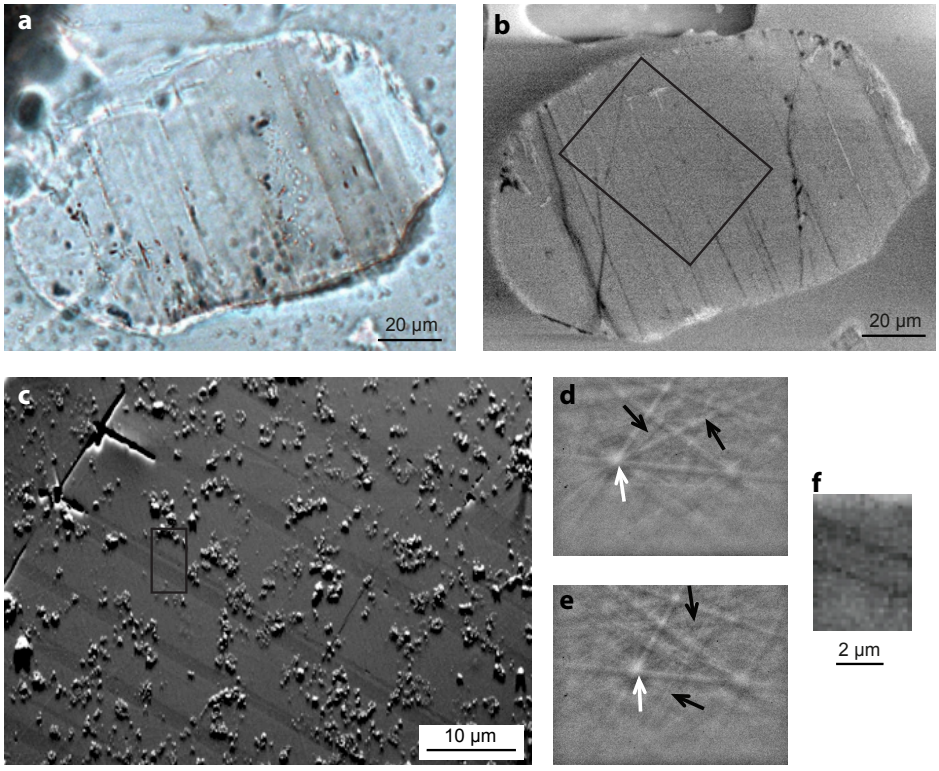

Figure 5.5. Feldspar grain from the Usselo horizon at Lutterzand showing one set of thin, well-defined, closely spaced planar microfeatures that cross the entire grain. a. TLM image. b. SEM-CL image of the grain showing the microfeatures as thin, non-luminescent lamellae resembling PDFs. c. FSE image of part of the grain showing dark-grey bands of varying thickness with a different orientation, also visible in the EBSD patterns of the dark bands (d) and the matrix (e). f. Pattern quality map showing thin lines of lower pattern quality. These thin lines of lower pattern quality occur at the boundaries between the two crystal orientations and might correspond to the thin features in the SEM-CL image.

twins (figure 5.7b), with a 60° rotation around the c-axis. Most Dauphiné twin boundaries in the grain are related to the orientation of the planar microfeatures. Dauphiné twins are known to occur in shocked quartz, but their origin and relation to the PDFs is not completely understood (French and Koeberl, 2010; Hamers, 2013).

Using FIB-SEM a rectangular TEM foil was created with its short side perpendicular to the grain surface and its long side perpendicular to one of the PDF sets within the shocked quartz grain (see figure 5.6a and 5.7a for its location). TEM imaging of this thin foil shows the planar microfeatures as thin lines of high dislocation density (with an east-west orientation in figure 5.8). No amorphous phase was detected, suggesting that the features are healed PDFs. The orientation of the PDF traces is parallel to the short side of the TEM foil and thus perpendicular to the polished surface of the grain (imaged in LM and SEM). Because the thin foil was sectioned perpendicular to the trace of the PDFs, the PDFs are orientated edge on in the thin foil. Analysis

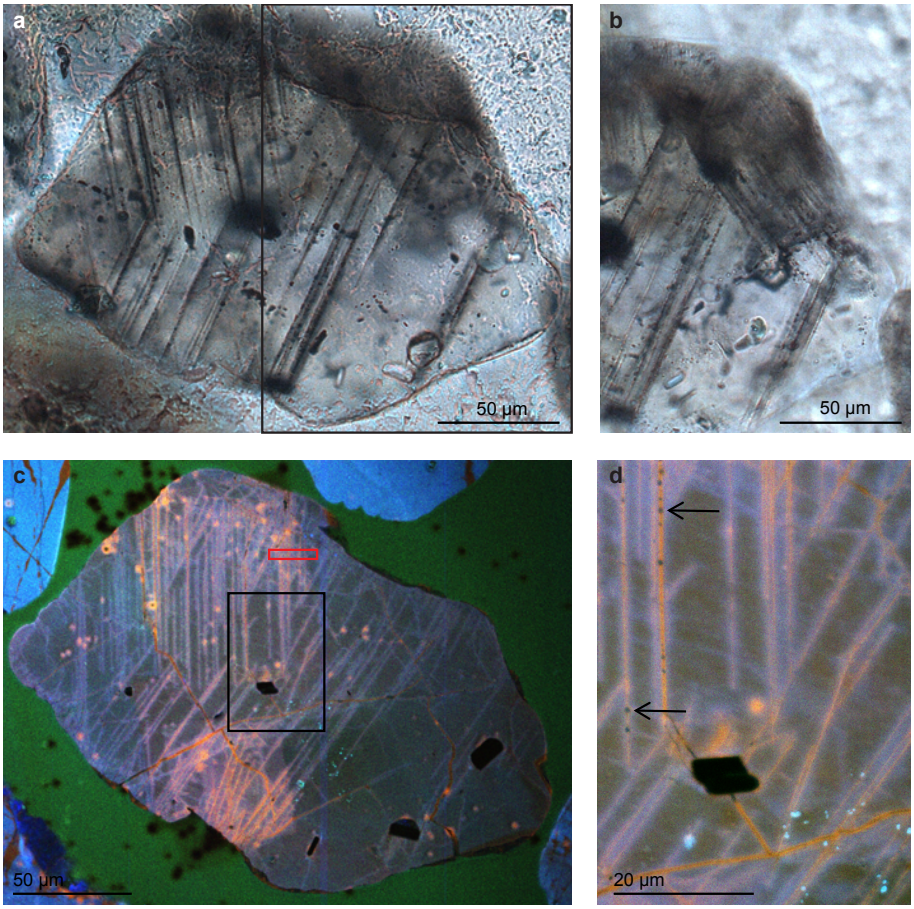

Figure 5.6. Quartz grain containing PDFs from the Usselo horizon at Geldrop Aalsterhut. a. TLM image showing two sets of thin, closely spaced planar microfeatures. b. A third set of planar microfeatures is visible slightly below the surface of the polished section. c. Composite colour CL-image of the grain showing that the microfeatures are mostly red-luminescent. A fourth orientation is visible in the bottom part of the grain. The black features are small feldspar inclusions. Red rectangle indicates the location of the TEM foil. d. Higher magnification composite colour CL-image showing some pores or fluid inclusions (arrows) along the PDFs. The irregular orange-luminescent feature is probably a healed fracture.

of the diffraction patterns (figure 5.8b) show that the PDFs are parallel to {10$\bar{1}$4}. EBSD data shows that the other two sets of planar microfeatures, which were not sampled by FIB for TEM analysis, have traces consistent with {10$\bar{1}$2} and {10$\bar{1}$3} planes, both common PDF orientations (Ferrière et al., 2009). Although most PDFs are straight, TEM shows that some of the PDFs deviate towards the edge of the pores. When tilted off zone, areas of different brightness are seen in part of the grain, suggesting that these areas have a somewhat different crystal orientation. This difference in orientation also explains the slight streaking in the diffraction pattern (figure 5.8b).
The shocked quartz grain also contains several K-feldspar inclusions (10-20 μm in diameter), visible as dark particles in the SEM-CL image (figure 5.6c). SEM-BSE images show the presence of even smaller (up to 2 μm) inclusions in some of the pores aligning the PDFs (best visible in the top of figure 5.7d). Due to the small size of the inclusions, the EDX spectra includes information of the surrounding quartz. The inclusions generally consist of sulphur, often in combination with iron or titanium (figure 5.7e). Inclusions with only iron or sulfur in combination with calcium were also observed.

5.5 Discussion

5.5.1 Identification of planar deformation features

Tectonic deformation lamellae are often easily distinguishable from PDFs in light microscopy (e.g. figure 5.3a). Although sometimes tectonic deformation lamellae are visible as one set of relatively well defined, parallel features (e.g. figure 5.3b) which might be confused with PDFs in light microscopy. Using SEM-CL images (e.g. figure 5.3d,e), however, these tectonic deformation lamellae are still distinguishable from PDFs as PDFs are sharp and well-defined in SEM-CL imaging, whereas tectonic deformation lamellae are not (Hamers and Drury, 2011). Although the occurrence of multiple sets of (sub)planar features is often seen as typical of PDFs (table 5.1), several non-shocked grains with more than one set of planar features can be observed (e.g. Drury, 1993; this chapter) (figure 5.3g-i, figure 5.4). For identifying the nature of the features in figure 4, color filtered CL-imaging proved to be better in distinguishing between PDFs and other features than the limited wavelength of greyscale CL imaging. Although transmitted LM of polished sections gives a good indication for the occurrence of PDFS, SEM-Cl imaging (preferably color filtered) of the polished sections and/or TEM analysis is thus necessary to convincingly identify PDFs. Analysis of the grain surface only, as done by Mahaney et al. (2010a), cannot be used to convincingly identify PDFs (French and Koeberl, 2010).
Due to the overlapping density of feldspar and quartz, the density separation did not yield a pure quartz fraction but also included some feldspar grains. As observed in this study, these feldspar grains sometimes contain thin, closely spaced planar features so that they look very similar to quartz with PDFs in both LM and SEM-CL imaging (figure 5.5). When relying solely on (greyscale) SEM-CL imaging, these grains can thus be mistaken for shocked quartz. Despite the density separation it is thus still necessary to check whether any possible shocked quartz grains are indeed quartz, either in light microscopy or by using EDX in the SEM. Although shocked feldspar can also contain PDFs (Huffman et al., 1993; Huffman and Reimold, 1996; French, 1998), the grain in question (figure 5.5) contained twinning and is therefore not a shocked feld-

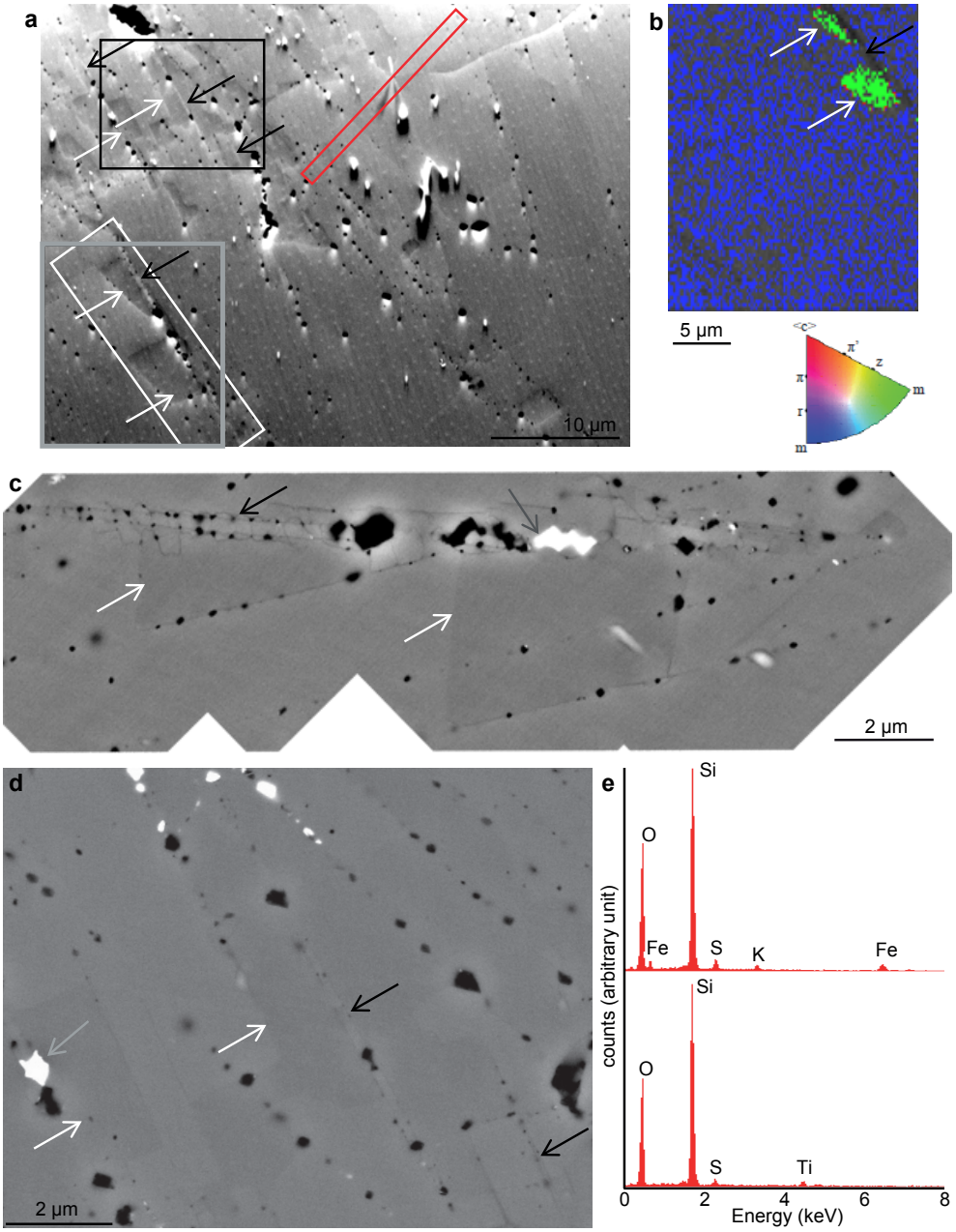

Figure 5.7 a. FSE image of part of the quartz grain shown in figure 5.6 clearly showing the planar microfeatures as trails of pores in multiple orientations. Darker and lighter grey areas, partly bound by the PDFs, are visible. At some locations a thin bright line is visible along the planar microfeatures (white arrows). Red rectangle indicates the location of where the TEM-foil was created. b. Pattern quality map and inverse pole figure map of the grey box in (a) showing that the dark areas in (a) are Dauphiné twins and that the planar microfeature is characterised by lower pattern quality (the feature is visible as a dark line) and thus a less well organised or possibly amorphous crystal structure (black arrow). The EBSD map has been distorted as a result of charging and was digitally stretched to match the geometry of the FS image. c. BSE image of the two Dauphiné twins and the bright planar microfeature in the white box in (a).

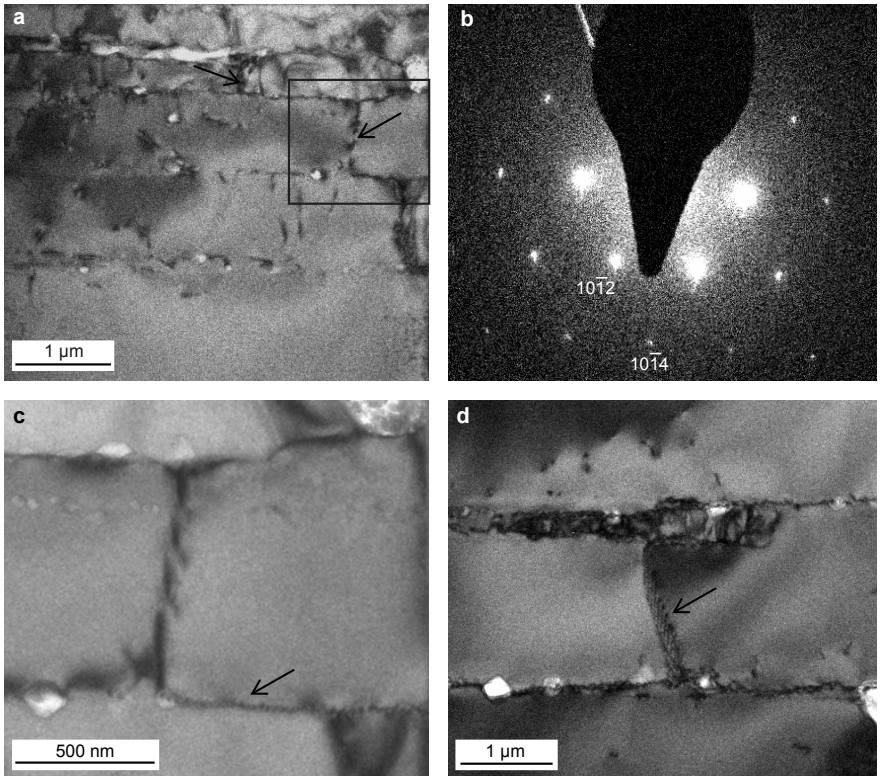

Figure 5.8 (above). TEM images of the FIB prepared TEM thin foil that was sectioned perpendicular to the trace of one of the PDF sets in the grain, see figure 5.6c and 5.7a (red rectangle). The right and left hand sides in the TEM image are parallel to the polished grain surface. a. TEM BF image detail of part of the top of the thin foil (corresponding to the bottom left corner of the red rectangle in 5.6a and 5.7c). Traces of the PDFs (east-west in the image) are approximately edge on and parallel to $\{10\bar{1}4\}$ as shown in the corresponding diffraction pattern in (b)., Features perpendicular to the PDFs (north-south orientation, see arrows) are also observed and might be twin boundaries.. c. Higher resolution image of part of the thin foil tilted slightly off zone, showing that the PDFs consist of lines of dislocations (arrow). d. TEM BF image of a different part of the thin foil, at a different tilt, showing a dislocation network (arrow) between two PDFs.

Figure 5.7 (continued) The Dauphiné twins are visible as blocky darker areas (white arrows). The band corresponding to the bright planar microfeature in the FSE image is bounded by two lines of pores (black arrow) that converge towards each other near the edge of the image. The pores in each line are connected by small curved lines, which are possibly thin cracks. The bright white feature (grey arrow) is an inclusion containing iron. d. BSE image of the area in the black rectangle in (a), showing the twin boundaries (white arrows). The bright features in the FSE image (black arrows) are again visible as two lines that converge towards each other in both directions. e. EDX spectra of two of the inclusions in the pores aligning the PDFs (grey arrows in c and d). The top spectrum shows the composition of the S-, Fe- and K-rich inclusion in (c). The bottom spectrum shows the inclusion in (d), which is Ti- and S-rich. Because of their small size, the EDX spectra are dominated by the X-rays of the surrounding quartz.

spar grain. Although SEM-CL imaging might provide a promising method to identify PDFs in quartz (Hamers and Drury, 2011), research on the application of SEM-CL imaging to identify PDFs in feldspar has not yet been done.

5.5.2 Origin of the shocked quartz grain

Among the quartz grains we studied from eleven Lateglacial paleosol and peat layers containing the Allerød-Younger Dryas transition, only one shocked quartz grain was found. Unless the sample was somehow contaminated, there are several questions when attempting to relate this grain to the Younger Dryas impact event. The more recent version of the Younger Dryas impact hypothesis favors multiple airbursts occurring across the world (Bunch et al., 2012). However, to our knowledge there is no evidence that airbursts produce shocked quartz. An alternative scenario initially suggested for the Younger Dryas impact event consisted of multiple small objects striking the Laurentide ice sheet (Firestone et al., 2007). If these objects penetrated the ice or also hit the unglaciated surface, shocked quartz could have formed and ejected into the atmosphere and subsequently have been incorporated in the Allerød-Younger Dryas boundary layer. The shocked grain found in the Usselo horizon in the present study is, however, relatively large (~200x150 μm) compared to, for example, the average size of shocked quartz grains found in the K/T boundary in Europe (~100 μm, Morgan et al., 2006). In addition, no crater related to the Allerød-Younger Dryas boundary has been found thus far, suggesting that if there was an actual impact rather than an airburst, the impact might have been small. If so, then it is also unlikely that such a large grain would travel from North America to Europe. Although it has been suggested that the 4 km diameter Corossol structure in the Gulf of Saint Lawrence might be an impact crater related to the Younger Dryas impact event (Israde-Alcántara et al., 2012), the Corossol structure is possibly much older (Higgins et al., 2011). The two other suggested Younger Dryas impact craters, Charity Shoal crater in Lake Ontario and the Bloody Creek structure in Nova Scotia (Wu et al., 2009), are however too old (Holcombe et al., 2013), or have not been dated (Spooner et al., 2009) respectively.

Although the more recent version of the Younger Dryas impact hypothesis considers multiple airbursts occurring around the globe (Bunch et al., 2012), it is possible that one of the objects entering the Earth's atmosphere did not explode in an airburst but actually hit the ground. In 1997 a small extraterrestrial object created the 15 m diameter Carancas crater (Kenkmann et al., 2009; Tancredi et al., 2009). Researchers reported the occurrence of shocked quartz in samples taken from the crater (Tancredi et al., 2009). Such a small crater would have easily been eroded or filled in by aeolian activity during the Younger Dryas or the Holocene. A small, local impact might also explain the occurrence of nanodiamond at the site. However, the orientations of the observed PDF suggest that the grain experienced a shock pressure of at least 17.5 GPa (Grieve et al., 1996; Ferrière et al., 2009), whereas peak pressures inferred from the Carancas impact crater were only up to a few GPa (Tancredi et al., 2009), suggesting that the shocked grain is related to a larger event. Also, no disturbances in the Usselo horizon, indicative of a small local impact, have been found at the Geldrop Aalsterhut site, although they could have been present at the non-excavated parts of the site. Most importantly, relating the grain to the proposed age of the Younger Dryas impact event would be difficult because the Usselo horizon in which the grain was found was at the surface during most of the Allerød and the early Younger Dryas (at least for several centuries) and formed in older sediments. The grain could have been incorporated into the top of the Usselo horizon anytime during this time window, and not necessarily at the

onset of the Younger Dryas. If it is assumed that the nanodiamond found in glass-like carbon from the Usselo horizon at the same site was also formed during the impact, and if the nanodiamond can be related to the charcoal (van Hoesel et al., 2012), the shocked quartz grain might also be dated to 10,845 ± 15 ^{14}C yrs BP (12,760 – 12,640 cal. yrs BP, n=14). Nanodiamonds in distal ejecta layers are, however, not considered diagnostic evidence for an extraterrestrial impact event and might have a different origin (French and Koeberl, 2010; Glass and Simonson, 2012; Reimold and Jourdan, 2012). Assuming a small local impact, it is also possible that this event occurred prior to the formation of the Usselo horizon and was incorporated into the coversand at an earlier stage, in which case the grain could be hundreds to thousands of years older.

One way to assess whether the shocked quartz found in the Usselo horizon formed recently is to identify amorphous PDFs, as these only occur in relatively young impact material. The PDFs in the grain, however, are aligned with pores or fluid inclusions, are red-luminescent and consist of dislocation arrays rather than amorphous material, which suggest that the PDFs are healed and the grain thus experienced post-impact alteration (Stöffler and Langenhorst, 1994; Trepmann and Spray, 2006; Hamers, 2013). Although healing can occur immediately following the impact, healed PDFs are more common in older impact material (i.e. several million years), where no amorphous PDFs are found (Grieve et al., 1996; French and Koeberl, 2010). Shocked quartz grains can be eroded from older craters or distal ejecta layers and incorporated into the sediment (Cavosie et al., 2010). It is thus possible that the shocked grain is related to a much older impact event. The rounded shape of the grain also suggests that it has been transported, although this rounding could have occurred prior to the impact which caused the PDFs. The coversands in the Netherlands are mostly of local sedimentary origin (Crommelin, 1964) originally from older fluvial deposits in the southern Netherlands from the Meuse river system. The K/T boundary (65 Ma) has been found in the Meuse catchment (Smit and Brinkhuis, 1996), although no shocked quartz was found (Hamers, 2013) and shocked quartz grains found in the K/T boundary in Europe are usually smaller (Morgan et al., 2006). The Ries and Steinheim craters in southern Germany (15 Ma) are located in close proximity to the (current) catchment of the river Rhine, which could have transported material from the ejecta layer to the Netherlands. There are also several craters in Scandinavia, which might be the source of the shocked quartz grain as the glacial ice could have eroded the craters and transported the material south. It is however unlikely that this material reached the southern Netherlands although the glacial ice and its meltwater never reached this part of the country.

The K-feldspar inclusions in the shocked grain can also give some constraints on the age of the grain of the grain, although sample volume is likely too small for K/Ar dating. In addition, the result would only indicate how old the grain is, not when it was shocked and thus only provide a maximum age for the shock event.

The S-, Fe- and Ti- rich inclusions found along the PDFs might give some indication of the conditions during the impact event. Previously, magnetite inclusions along PDFs have been observed in shocked quartz from the Vredefort crater (Cloete et al., 1999; Hart et al., 2000) and experiments have shown that during an impact, shocked quartz might get enriched in material from the impactor (Ebert et al., 2013, note that that no inclusions were reported). However, the inclusions along the PDFs could also have formed well after the impact, for example through the precipitation from fluids that might have entered the grain.

In summary, in our LM study of the quartz fraction of the Usselo horizon from multiple sites in Europe and the Black Mat in North America we found several grains that showed planar features

similar to those of shocked quartz. However, SEM imaging shows that only one of these grains contained contains PDFs indicative of a shock event. This grain came from the Usselo horizon at Geldrop Aalsterhut, where nanodiamond of early Younger Dryas age has been found (van Hoesel et al., 2012). Although the shocked grain was found in the Usselo horizon, which was at the surface during the onset of the Younger Dryas, the healed nature of the PDFs suggests that the grain is probably older. Because only one grain was found at only one of the sites, we suggest that the shocked grain might have been eroded from an older impact layer and transported to the southern Netherlands, where it was eventually incorporated in the coversand in which the Usselo horizon was formed. Alternatively, assuming that the shocked grain was found in-situ, the grain could have been deposited in the Usselo horizon at any point in time during its formation period (14,000~12,000 years ago) and not just at the Younger Dryas onset. Further studies searching for shocked quartz in the Allerød-Younger Dryas boundary at sites with better dating resolution, preferably in relation to the reported lechatelierite or magnetic spherules at other sites (Bunch et al., 2012; Wittke et al., 2013), are necessary before the shocked quartz grain at Geldrop Aalsterhut can be related to a Late Glacial impact event. Failure to find shocked quartz, however, does not invalidate the Younger Dryas impact hypothesis as airbursts are not likely to result in the necessary shock pressures at the surface.

5.6 Conclusions

One shocked quartz grain was found in the Usselo horizon at Geldrop Aalsterhut, which is a palaeosol that formed during the Allerød and early Younger Dryas. Based on the current evidence, however, it is not possible to determine whether this shocked quartz grain is related to the Younger Dryas impact event. The grain could also have been formed during a small-scale local impact in the vicinity of the site during the Lateglacial period or earlier, or eroded from an older impact layer and re-deposited into the source sediment for the coversand in which the Usselo horizon was formed. Although the PDFs in the grain must have been formed during an extraterrestrial impact, the shocked quartz grain at this moment cannot be unequivocally used to support the Younger Dryas impact hypothesis.

Chapter 6

Synthesis: was there an extaterreestrial impact at the onset of the Younger Dryas

The Younger Dryas impact hypothesis suggests that one or more extraterrestrial airbursts or impacts resulted in the Younger Dryas climate cooling. A wide range of markers has been put forward as evidence for the impact, of which some are ambiguous or not reproducible. This chapter discusses the evidence for the Younger Dryas impact hypothesis in the light of the nanodiamond and shocked quartz studies presented in the previous chapters. Unlike the use of shocked quartz, the use of nanodiamonds as an impact indicator is still ambiguous and different hypotheses for the origin of the Allerød-Younger Dryas boundary nanodiamonds will be discussed in the light of the TEM results on charcoal.

In addition, the timing of the Younger Dryas impact is addressed, a topic which, despite its importance, has not gained much attention thus far. There are three challenges related to the timing of the event: accurate age control for some of the sites that are reported to provide evidence for the impact, linking these sites to the onset of the Younger Dryas and, most importantly, an apparent age discrepancy of up to two centuries between different sites associated with the proposed impact event.

Part of this chapter was published in: van Hoesel, A., Hoek, W.Z., Pennock, G.M., Drury, M.R. (2014) The Younger Dryas impact hypothesis: a critical review. Quaternary Science Reviews, 83, 95-114.

6.1 Introduction

To find support for the Younger Dryas impact hypothesis researchers have investigated the Allerød-Younger Dryas boundary at a large number of sites, predominantly in North America but also in Europe, South America and the Middle East (Firestone et al., 2007; Mahaney et al., 2010a; Wittke et al., 2013b). Initial impact evidence included peak concentrations of the following markers: magnetic grains with iridium, magnetic microspherules, charcoal, soot, carbon spherules, glass-like carbon containing nanodiamonds, and fullerenes with ET helium (Firestone et al., 2007). Subsequent studies have focused on the magnetic spherules, nanodiamonds and scoria-like objects with lechatelierite (Bunch et al., 2012; Israde-Alcántara et al., 2012; Wittke et al., 2013b) and a peak in platinum concentrations has been reported in one of the Greenland ice cores (Petaev et al., 2013). However, as shown in chapter 2, these markers, especially the first two, are ambiguous as impact indicators and there have been some problems related to their reproducibility.

This thesis reports on the occurrence of nanodiamonds and shocked quartz in the Usselo horizon at Geldrop Aalsterhut. Although the original study reporting nanodiamonds as well as the occurrence of lonsdaleite in the Allerød-Younger Dryas boundary is disputed (Daulton et al., 2010; Daulton, 2012), nanodiamonds have been reported in several other studies (Kurbatov et al., 2010; Tian et al., 2011; Israde-Alcántara et al., 2012). However, with the exception of the Geldrop Aalsterhut site, no nanodiamonds were found at the investigated Allerød-Younger Dryas boundary layers in this study, including the Murray Springs and Lommel sites, where nanodiamond had been reported before (see Kennett et al. 2009a; Tian et al. 2011). Furthermore, dating of multiple charcoal particles in the Usselo horizon at Geldrop Aalsterhut shows that these particles were formed two centuries later than those at Arlington Canyon, were nanodiamonds were also reported (Kennett et al., 2009b). Considering that these nanodiamonds were reported in glass-like carbon and carbon spherules respectively, both potential wildfire products, it is reasonable to assume that the nanodiamonds were formed during the same event as the charcoal and that the ^{14}C data are indicative of their age.

Unlike the nanodiamonds, the single shocked quartz grain found at Geldrop Aalsterhut cannot be related to wildfires and thus to the ^{14}C ages. This would not be a problem if nanodiamonds are diagnostic of an impact, in which case it is feasible that the shocked quartz formed at the same age as the nanodiamonds. However, the formation mechanism of nanodiamonds is not fully understood and their presence cannot be used to convincingly identify a distal ejecta layer (French and Koeberl, 2010). If the shocked quartz was not already part of the coversand, the grain could thus have been incorporated in the Usselo horizon at any time during the period of soil formation, in other words: any time during the Allerød or early Younger Dryas period. Furthermore, no shocked quartz grains were found in the other Allerød-Younger Dryas boundary layers investigated, not even at nearby Lommel, and only one grain was found at Geldrop Aalsterhut. Finding multiple grains at the Geldrop Aalsterhut site would be an indication that the shocked quartz might have been found in-situ, whereas finding shocked quartz at multiple Lateglacial sites might indicate a (regional) impact event within that time window. Based on the current evidence, however, it is not possible to state whether the shocked quartz grain is related to the Younger Dryas impact event, a small-scale impact during the Lateglacial period or earlier, or eroded from an older impact layer and re-deposited into the source sediment for the coversand in which the Usselo horizon was formed (see also the discussion in §5.4).

The discussion above illustrates thee problems related to the Younger Dryas impact hypothesis:

the absence of convincing evidence for the occurrence of the event (as discussed in chapter 2), a lack of understanding of the origin of some of the impact markers, and issues related to the dating of the markers. This chapter further explores the possible origins of the nanodiamonds and their use as an impact indicator, followed by a discussion of some challenges related to linking the reported markers to the onset of the Younger Dryas. Finally, the implications that the reported findings have for the Younger Dryas impact hypothesis are discussed.

6.2 Use of nanodiamonds as an impact indicator

Although micrometer to millimeter-sized shock-produced diamonds in craters have been used to establish an impact origin, no distal ejecta layers have been diagnosed based on nanodiamonds (< 5 nm) alone. Instead, the use of these nanodiamonds as a definite impact criterion is still debated since their formation mechanisms are still not always clear (French and Koeberl, 2010). Within the Younger Dryas impact debate lonsdaleite was presented as a clear impact proxy as lonsdaleite is mostly known in relation to meteorites or impact craters, and it is often seen as a shock indicator (Kennett et al., 2009b). However, lonsdaleite can also form through other, non-shock, processes, such as carbon vapour deposition (Frenklach et al., 1989; Daulton et al., 1996; Erlich and Hausel, 2002) and is found in a number of other environments on Earth (Shibata et al., 1993; Erlich and Hausel, 2002; McCall, 2009; Dubinchuk et al., 2010). Furthermore, the occurrence of lonsdaleite in impact craters has been challenged (Koeberl et al., 1997; Gilmour, 1998; Masaitis, 1998).
Because the exact formation mechanisms for nanodiamonds, including lonsdaleite, are still unclear, it is also necessary to look at other hypotheses for the origin of these nanodiamonds in order to establish whether the nanodiamonds found in the Allerød- Younger Dryas boundary sediments are evidence for an impact,. The nanodiamonds could either be extraterrestrial in origin (1), arriving at Earth through continuous meteoritic rain or as part of an impacting body. They could also have been formed during an impact (2), either through shock deformation of carbon-rich target rock or during a carbon vapour deposition (CVD) mechanism following an airburst or 'atmospheric impact'. Finally, a terrestrial origin should be considered (3).

(1) Certain types of meteorites, micrometeorites and interplanetary dust particles are known to be carriers of nanodiamonds (Hanneman et al., 1967; Dai et al., 2002; Aoki and Akai, 2008; Ferroir et al., 2010). Shortly after the Younger Dryas impact hypothesis was proposed, Pinter and Ishman (2008) suggested that the evidence put forward by Firestone et al. (2007) was not related to an impact but the result of the accumulation of meteoritic rain over time. Although this is a plausible mechanism to explain the nanodiamonds found in sediments (Kennett et al., 2009a; Kurbatov et al., 2010; Tian et al., 2011; Israde-Alcántara et al., 2012), meteoritic rain does not explain how nanodiamonds ended up within carbon spherules, carbon elongates or glass-like carbon (Kennett et al., 2009b; van Hoesel et al., 2012). Furthermore, accumulation of meteoritic rain would result in a continuous background concentration, rather than the clear peak in nanodiamond concentration found in the Greenland ice sheet or Lake Cuitzeo (Kurbatov et al., 2010; Israde-Alcántara et al., 2012). This peak in nanodiamond concentration could be explained if the nanodiamonds had arrived in a larger impacting body. However, other traces of an impactor are absent and the nanodiamond concentrations reported are too large to have come from a small impactor body (French, 1998). Furthermore, Tian et al. (Tian et al., 2011) show that the carbon

isotope and C/N ratios of the bulk material from the Usselo horizon at Lommel are more indicative of a terrestrial origin for the carbon material. Considering the above, it seems unlikely that the nanodiamonds arrived in an impactor body or through meteoritic rain.

(2) Diamonds (up to mm-sized) occur in impact craters (Hough et al., 1995; Koeberl et al., 1997; Masaitis, 1998; Smith and Godard, 2009) and in distal ejecta layers (Carlisle and Bramant, 1991; Gilmour et al., 1992; Hough et al., 1997). Impact diamonds can form in two ways: through the shock transformation of graphite in the target rock, in which case they are associated with a crater, and during a carbon vapour deposition (CVD) process in the fireball following an airburst or atmospheric impact similar to the Tunguska event (Svetsov and Shuvalov, 2008). A CVD-like process, in which the nanodiamonds grow from a carbon rich vapour, is also consistent with the rounded shape and non-linear twins found in some of the round Allerød-Younger Dryas boundary nanodiamonds (Daulton et al., 1996; Tian et al., 2011; Israde-Alcántara et al., 2012), but might be less consistent with the plate-like diamonds reported by others (Tian et al., 2011; van Hoesel et al., 2012), or the occurrence of large amounts of lonsdaleite (Kennett et al., 2009b).

(3) On Earth, diamond is often associated with kimberlitic volcanic settings or metamorphic rocks in, for example, Norway. Sub-micron diamonds have also been found in a xenolith within Hawaiian tuff as well as in fluid inclusions in alkalic lavas (Wirth and Rocholl, 2003; Frezzotti and Peccerillo, 2007). The Hawaiian magmas are relatively similar to the volcanic region in the Eifel, suggesting a hypothetical regional source for the European nanodiamonds. However, nanodiamonds in the (older) volcanic rocks would be rare and if eroded and transported they are not expected to occur in a distinct layer. An eruption, on the other hand, would allow for the dispersion of nanodiamonds in a single layer. Nanodiamonds, however, would still be rare and likely to be locked up in xenoliths. In addition, Israde-Alcantára et al. (2012) failed to find any nanodiamonds in samples of tephra from the Laacher See volcanic eruption.
Another, more common, process that might hypothetically create nanodiamonds is wildfire. Some of the Allerød-Younger Dryas boundary nanodiamonds have been found in carbon spherules and glass-like carbon (Kennett et al., 2009b; van Hoesel et al., 2012), both of which are considered wildfire products (Hunt and Rushworth, 2005; McParland et al., 2010; Scott et al., 2010). Paquay et al. (2009) speculated that high temperatures, low oxygen levels and a source of carbon, all necessary conditions for diamond formation through CVD, can also be present in natural wildfires. Indeed, artificial nanodiamonds have been grown using low pressure CVD at temperatures as low as 450 °C (Frenklach et al., 1989; Daulton et al., 1996; Cowley et al., 2004). Moreover, nano-particles with a 3C diamond structure have been found in wood that was experimentally charred at 700 °C and subsequently cooled in a nitrogen atmosphere (Ishimaru et al., 2001). In addition, carbon onion structures, which can serve as nanoscopic pressure cells for diamond formation (Banhart and Ajayan, 1996; Banhart, 1997; Tomita et al., 2000), have been observed in charcoal (Hata et al., 2000; Ishimaru et al., 2001; Cohen-Ofri et al., 2007) and in the Allerød-Younger Dryas boundary layer (Tian et al., 2011; Israde-Alcántara et al., 2012). Nanodiamonds (<5 nm) have recently also been discovered in a candle flame as well as in a natural gas flame (Su et al., 2011). Although most of these nanodiamonds burn up in the flame, this discovery suggests it might be possible for nanodiamonds to form during a combustion-type process under normal atmospheric conditions.
These observations all suggest that it might be possible for the Allerød-Younger Dryas boundary nanodiamonds to have formed through wildfire. However, no nanodiamonds were found

in recent charcoal and glass-like carbon particles (Chapter 4). Estimated charring temperatures for these particles are 500-600 °C (table 4.2), at least 100 °C lower than the artificially charred particle in which nanodiamond was identified (Ishimaru et al., 2001). It might be that nanodiamonds in charcoal are only formed under certain experimental conditions or at higher (>600 °C) temperatures, but this would not explain why nanodiamond was found in the Usselo horizon at Geldrop Aalsterhut and Lommel, for which the inferred temperature was even lower (~420 °C). Although these observations do not completely rule out wildfire as an origin for the nanodiamonds, wildfire, at this point in time, does not seem a likely source.

As shown above, the formation of nanodiamonds is not yet completely understood and there are multiple hypotheses for the origin of the nanodiamonds in the Allerød-Younger Dryas boundary. Although little research has been done on nanodiamonds in the sedimentary record, nanodiamonds have been found in carbon spherules from present day forest soils in Europe (Yang et al., 2008) and possibly in a Holocene soil horizon in North America (Bement et al., 2013). Further research on nanodiamonds in the sedimentary record is necessary to assess how common they are, and whether they indeed occur in particular types of deposits or deposits of certain ages. Learning more about where and when nanodiamonds were deposited might provide insight in their origin and whether they might be used as marker to link different records.

6.3 Timing of the event

One important part of the Younger Dryas impact hypothesis that has not gained much attention in the literature so far is the timing of the event. In order to claim that a single impact event (be it multiple airbursts or just one impactor) caused the Younger Dryas, all sites at which impact markers have been found must be synchronous and date to the onset of the Younger Dryas. This synchronous-site requirement presents five challenges to the Younger Dryas impact hypothesis, which are discussed below.

Firstly, the exact timing of the Younger Dryas onset is still uncertain (Fiedel, 2010; Fiedel, 2011). The originally proposed Younger Dryas impact age of 12,900 ± 100 yrs ago (Firestone et al., 2007) fits relatively well (within uncertainties) with the onset of the Younger Dryas according to the Greenland ice cores and the Cariaco record (table 6.1). The Younger Dryas was, however, originally defined as a biostratigraphic zone in the Scandinavian region (Mangerud et al. 1974) and later recognised in other records in north-western Europe (Hoek 2008). Because of the transgressive nature of climate change and vegetation response in Europe the timing of the onset of the Younger Dryas differs between the different European record (see Björck et al., 1998; Hoek, 2008; Lowe et al., 2008). Still, many terrestrial European records (e.g. Goslar et al., 2000; Brauer et al., 2008; Hajdas and Michczyñski, 2010) place the onset of the Younger Dryas up to two centuries later then the ice core record. This is likely related to a lag between cooling and extensive hydrological and environmental changes in the region (Rach et al., 2014).
It must be noted here that Wittke et al. (2013b) propose an age of 12,800 ± 150 cal. yrs BP (IntCal09 calibrated) for the Younger Dryas impact event. They obtained this date by calibrating a radiocarbon age of 10,900 ± 145 ^{14}C yrs BP, which they suggest was the date originally reported for the impact event (Wittke et al., 2013b), although this ^{14}C age is not mentioned in Firestone et al. (2007). Using the recently published IntCal13 calibration curve (Reimer et al.,

Table 6.1. Onset of the Younger Dryas (or equivalent) according to different records.

Record	Type of Record	Calendar age (yrs ago*)	Radiocarbon age (^{14}C yrs BP)	Reference
GICC05 (Greenland, GRIP/NGRIP)	ice core	12,846 ± 138 (max error)		Rasmussen et al. 2006
GISP2 (Greenland)	ice core	12,890 ± 260 (max error)		Meese et al. 1997 Stuiver et al. 1995
Cariaco varves (Venezuela)	marine sediments	12,820 ± 30		Lea et al. 2003
Hulu Cave	stalagmites	12,823 ± 60		Wang et al. 2001
Meerfelder Maar (Germany)	varved lake	12,679		Brauer et al. 2008
Holzmaar (Germany)	varved lake	12,606		Brauer et al. 2008
Soppensee (Switzerland)	varved lake	12,593 ± 93		Hajdas and Michczinski, 2010
Swedisch time scale	varved lake	12,500-12,700		Wohlfarth 1996
Lake Gosciaz / Perespilno (Poland)	varved lakes	12,650	~11,000	Goslar 1995, 2000
Late Glacial Pine (LGP) Record	tree rings (floating)	12,950	10,950	Kromer et al. 2004
LGP + Huon Pine	tree rings	12,760	10,950	Hua et al. 2009
Original YD onset (Scandinavia)	biostratigraphy		11,000	Mangerud et al. 1974
The Netherlands	biostratigraphy		10,950 ± 50	Hoek 1997
Black Mat (North America)	palaeosoil/algal mat		10,900 ± 50	Haynes 2008
Radiocarbon cliff	multiple records		~11,000	Fiedel 2011

*On same time scale as radiocarbon years, 1950=0

2013), the radiocarbon age cited by Wittke et al. (2013b) for the age of the Younger Dryas impact event gives a calibrated age of 12,950-12,700 cal. yrs BP (68% confidence interval, median 12,830 cal. yrs BP) or 12,820 ± 130 cal. yrs BP. Compared to the age proposed by Wittke et al. (2013b), which was calculated using the IntCal09 calibration curve, the latest radiocarbon calibration curve places the Younger Dryas impact event almost a century earlier and reduces the uncertainty by two decades.

Secondly, many of the terrestrial sites where Younger Dryas impact markers have been found have been dated using radiocarbon (^{14}C) dating (table 6.2), which can introduce additional uncertainties. For instance, when dating charcoal, the "old wood" or "inbuilt age" effect arises when the wood was burned decades after it was formed in a growing tree (Schiffer, 1986; Gavin, 2001). Additional uncertainties arise when calibrating the radiocarbon ages to calendar years or when comparing ages calibrated using different calibration curves (box 3.1). These additional uncertainties are introduced because of uncertainties in the ^{14}C calibration curve, especially beyond the dendrochronologically calibrated part of the curve (0-12,550 cal. yrs BP, Reimer et al., 2009; Blockley et al., 2012). The latter uncertainties can be avoided by directly comparing radiocarbon ages rather than calibrated values, although age differences will not be directly comparable to calibrated years. When looking at radiocarbon ages of the Younger Dryas onset in terrestrial records, most dates are in the range of 11,000 – 10,950 ^{14}C yrs BP, although ages as young as

10,900 ^{14}C yrs BP are also considered a possibility (table 6.1). It is considered unlikely that the Younger Dryas started before 11,000 ^{14}C yrs BP, as the Laacher See eruption, which probably took place two centuries before the onset of the Younger Dryas (Brauer et al., 1999; Wulf et al., 2013), is dated to 11,063 ± 13 ^{14}C yrs BP (Stuiver et al., 1995; Litt et al., 2003). The range of 11,000 – 10,900 ^{14}C yrs BP adopted here for the timing of the Younger Dryas onset, roughly corresponds to the timing of the Younger Dryas impact event as adopted by Wittke et al. (2013b).
Thirdly, not all sites have been directly dated or their dates have a high uncertainty. Of the ten Clovis sites reported by Firestone et al. (2007), only six have been directly dated, sometimes with a large uncertainty in their age (table 6.2). In addition, the age Firestone et al. (2007) use for the Usselo horizon at the Lommel site (Belgium), does not appear in the literature they cited (van Geel et al., 1989; Hoek, 1997). However, recent optically stimulated luminescence (OSL) dates at Lommel give an age of 12,400 ± 900 yrs ago (Derese et al., 2012), which, within uncertainty, is still consistent with the proposed age for the Younger Dryas impact. Wittke et al. (2013b) acquired an age of 11,480 ± 100 ^{14}C yrs BP on charcoal from the Usselo horizon at Lommel, considerably older than the age they proposed for the Younger Dryas impact (10,900 ± 145 ^{14}C yrs BP).
The identification of the Allerød-Younger Dryas boundary layer in the Greenland ice sheet near Kangarlussuaq was based on a visible dust layer (Kurbatov et al., 2010) and Pinter et al. (2011) argue that the oxygen isotopes given by Kurbatov et al. (2010) are more typical for Holocene values than for Younger Dryas values. Although Pinter et al. (2011) do not give any information about the records on which their argument is based, their observation is consistent with the GISP2 and NGRIP ice core oxygen isotopes (Stuiver et al., 1995; Steffensen et al., 2008). On the other hand, Kurbatov et al. (2010, table 1) show that the oxygen isotope values vary greatly between different records depending on their location. In addition, (Kurbatov et al., 2010) argue that the record should be compared to the Dye-3 ice core instead, which has a similar accumulation area as Kangarlussuaq (Kurbatov et al., 2010) and values more consistent with their own record. The 'Black Mat' at the Mucubají site (Venezuela) has also not been dated directly. The correlation to the onset of the Younger Dryas is based on stratigraphy and radiocarbon age of a peat bed 20 cm below the black mat (Mahaney et al., 2010a). Some of the sites presented by Wittke et al. (2013b), namely Kimbel Bay (USA) and Lingen (Germany), were also only indirectly dated.
At Lake Cuitzeo (Mexico) the proposed Allerød-Younger Dryas boundary layer has been directly dated to 27,360 ± 130 ^{14}C yrs BP, which is considerably older than the Allerød-Younger Dryas boundary (Israde-Alcántara et al., 2012). According to the authors, however, the radiocarbon dates are erroneously old as a result of reworking of organic material. Using an age-depth model based on a known tephra layer and several radiocarbon ages, excluding the anomalously old dates, the peak in markers was dated to approximately 12,900 cal. yrs BP (calibrated by Israde-Alcántara et al., 2012 using IntCal04). However, if the organic matter in the layer is reworked, it is also possible that the markers in the layer are also reworked and thus from a different moment in time. In addition, Blaauw et al. (2012) find no reason to assume that the dates from the Lake Cuitzeo Allerød-Younger Dryas boundary layer are anomalously old. In the age model of Blaauw et al. (2012), which includes all dates of the section, the marker layer is placed >16,000 cal. yrs BP (IntCal09). Considering the above, the markers found at Lake Cuitzeo might not be related to the Allerød-Younger Dryas boundary but a layer of different age.
Bunch et al. (2012) investigated the Allerød-Younger Dryas boundary for markers at 18 different sites in North America, Europe and the Middle East, eight of which have been reported in

Table 6.2. Reported age for the Allerød Younger Dryas Boundary sites investigated for impact markers in the light of the Younger Dryas impact hypothesis. For comparison, radiocarbon ages are calibrated according to the IntCal04 calibration curve, used in the earlier Younger Dryas impact hypothesis studies, the IntCal09 calibration curve, used in the later Younger Dryas impact hypothesis studies, as well as the recent IntCal13 calibration curve. All ages are given within one standard deviation and rounded to their nearest 5 yrs.

Site	Location	Type	^{14}C age (^{14}C yrs BP)	IntCal04 (cal. yrs BP)
Abu Hureyra	Syria	Archaeological mound	11,070 ± 40	13,040-12,935
Arlington Canyon	California (US)	Black Mat	11,135 ± 10	13,085-13,000
Barber Creek	North Carolina (US)	Transition fluvial-aeolian		
Big Eddy	Missouri (US)	Alluvial		
Blackville	South Carolina (US)	Carolina Bay rim		
Blackwater Draw	New Mexico (US)	Black Mat	11,040 ± 500	13,565-12,385
Carolina Bay rims	eastcoast US	Carolina Bay		
Chobot	Alberta (CA)	Black Mat		
Daisy Cave	California (US)	Black Mat	11,180 ± 130	13,185-12,965
Gainey	Michigan (US)	Transition till-alluvium		
Geldrop Aalsterhut	The Netherlands	Usselo horizon	10,845 ± 15	12,860-12,853
GISP2	Greenland	Ice core		
Kangerlussuaq	Greenland	Dust layer in ice		
Kimbel Bay	North Carolina (US)	Carolina Bay		
Lake Cuitzeo	Central Mexico	Lake sediments	27,360 ± 130	
Lake Hind	Manitoba (CA)	Black Mat	10,610 ± 25	12,760-12,660
Lingen	Germany	Usselo horizon	< 11,310 ± 60	< 13,195
Lommel	Belgium	Usselo horizon	11,480 ± 100	13,420-13,240
Melrose	Pensylvania (US)	Colluvium		
Morley	Alberta (CA)	Black Mat		
Mucubaji	Venezuela	Black Mat like layer	< 11,440 ± 100	< 13,300
Murray Springs	Arizona (US)	Black Mat	10,885 ± 50	12,890-12,840
Newtonville	New Jersey (US)	Ash-gray layer in top of coversand		
Ommen	The Netherlands	Usselo horizon	11,440 ± 40	13,330-13,345
Sheridan Cave	Ohio (US)	Black Mat	10,919 ± 25	12,895-12,860
Talega	California (US)	Alluvial channel fill	11,070 ± 50	13,045-12,930
Topper	South Carolina	Colluvial sand		
Wally's Beach	Alberta (CA)	Alluvium	10,980 ± 80	12,975-12,855

IntCal09 (cal. yrs BP)	**IntCal13** (cal. yrs BP)	**Age** (yrs ago*)	**Note**	**References**
13,085-12,900	13,015-12,865		Also biostratigraphic control	Bunch et al. 2013
13,105-12,965	13,060-13,010		Average of 12 ^{14}C dates	Kennett et al. 2008.2009
		12,100 ± 700	OSL	Wittke et al. 2013
		~12,800	Age model based on ^{14}C dates	Wittke et al. 2013
		12,960 ± 1200	OSL	Bunch et al. 2012
13,565-12,390	13,545-12,390			Firestone et al. 2007 Haynes 1995
			No age control presented	Firestone et al. 2007
			~AYDB based on archaeology	Firestone et al. 2007
13,220-12,915	13,155-12,865			Firestone et al. 2007 Erlandson et al. 1996
		12,400 ± 1000	TSL	Firestone et al. 2007
12,760-12,635	12,740-12,710		Average of 14 ^{14}C dates	van Hoesel et al. 2012
		12,900-12,880	Pt peak, GISP2 timescale	Petaev et al. 2013
			~AYDB based on stratigraphy surface ice	Kurbatov et al. 2010
		~12,900 / ~20,000	Logarithmic interpolation / rough linear interpolation of ^{13}C dates	Wittke et al. 2013
31,575-31,345	31,330-31,130	~13,000	Age depth model dismissing the 'anomalous' dates of the layer	Israde-Alcántara et al. 2012
12,600-12,550	12,635-12,565			Firestone et al. 2007
< 13,205	< 13,165		Taken 9 cm below the sample	Wittke et al. 2013
13,435-13,245	13,460-13,325		Stratigraphy, dated in later study	Firestone et al. 2007 Wittke et al. 2013
		9000-14,000	Age-depth model based on one OSL date	Bunch et al. 2012
		~13,000	Deglaciation	Firestone et al. 2007 Boyce and Eyles 1991
< 13,305	< 13,280		Date of peat 20 cm below sample	Mahaney et al. 2010
12,830-12,660	12,755-12,720		Average of 8 ^{14}C dates on Clovis charcoal	Firestone et al. 2007 Waters and Stafford 2007
		< 16,800 ± 1700	OSL date of frost crack beneath the sampled layer	Wu et al. 2013
13,365-13,255	13,330-13,225			Wittke et al. 2013
12,860-12,700	12,790-12,735		Average of 3 ^{14}C dates	Wittke et al. 2013
13,085-12,895	13,015-12,855			Wittke et al. 2013
		13,200 ± 1300	OSL date	Firestone et al. 2013
12,955-12,710	12,930-12,755			Firestone et al. 2007 Kooyman et al. 2001

earlier studies and three of which (where scoria-like objects and lechatelierite were found) are discussed in depth in their supporting information. For seven sites investigated by Bunch et al. (2012), no information on dating, stratigraphy or sampling is presented at all, except for their approximate location, although information on these sites was recently published in a different paper (Wittke et al., 2013b). Age control at two of the three sites where lechatelierite was found (Bunch et al., 2012) also raises some questions. OSL dating of the Allerød-Younger Dryas boundary at Blackville (USA) gave an age of 12,960 ± 1200 yrs ago, almost coinciding with the proposed timing of the impact (Bunch et al., 2012). However, one of the other two OSL dates from the same site, taken 30 cm above the inferred Allerød-Younger Dryas boundary layer, has a much older age of 18,540 ± 1680 yrs ago. Bunch et al. (2012) reasoned that this older OSL age should be excluded from their age-depth model "because of the large magnitude of the age reversal, i.e., older sediments lying stratigraphically higher than younger sediments" (Bunch et al., 2012). This reasoning can however easily be inverted: why not exclude the OSL date at the Allerød-Younger Dryas boundary because younger sediments cannot lie stratigraphically lower than older sediments? In that case, linear interpolation of the two other OSL dates would yield a much older age (>20,000 yrs ago) for the layer containing the markers. At Melrose (USA) only one OSL age, from 5 cm below the inferred Allerød-Younger Dryas boundary layer, is reported. Based on linear interpolation between the OSL date and the surface, assuming a modern age for the surface, Bunch et al. (2012) date the layer to exactly the time of the proposed impact. No validation for the assumption of a linear model and modern age of the surface are presented. In addition, for the other two sites investigated for the occurrence of scoria-like objects, 28 m and 28 km from Melrose, no age control is presented at all. Instead, even though the sediment consists of colluvium and there is no clear marker horizon visible, the same depth interval was sampled. There is thus no guarantee that these different locations near Melrose where scoria-like objects are reported, are of the same age.

Fourthly, at several sites the sampling thickness or the thickness of the peak in markers leads to a large uncertainty in sample age. For example, Bunch et al. (2012) present an age of 12,900 ± 1600 yrs ago for the Allerød-Younger Dryas boundary at Melrose. From figure S5 in their work, assuming their age-model is correct, it can however be inferred that the top of the 10 cm thick layer marked as the Allerød-Younger Dryas boundary is 9000 yrs old while the bottom of the Allerød-Younger Dryas boundary is 14,000 yrs old, a 5000 year range. At Lake Cuitzeo, the 10 cm wide peak in markers (Israde-Alcántara et al., 2012) might reflect almost 5900 yrs of deposition (Israde-Alcántara et al., 2010). Given these wide age ranges, any markers at these three sites could have been deposited well before or after the onset of the Younger Dryas.
In addition, many of the other Allerød-Younger Dryas boundary sites which have been investigated featured either a Black Mat or, in the case of the European sites, the Usselo horizon. The Black Mat is generally considered to be a wet paleosoil or algal mat deposited during the Younger Dryas. The sediment directly below the Allerød-Younger Dryas boundary, the 'Clovis surface', would have been at the surface for several decades near the end of the Allerød (Haynes Jr., 2008) before the Black Mat was deposited during the Younger Dryas. There is thus a small hiatus between the top of the Clovis surface and the bottom of the Black Mat. Compared to the Black Mat, the Usselo horizon (a Late-Glacial paleosoil formed in the dry aeolian sandbelt in North-Western and Northern-Central Europe during the late Allerød to early Younger Dryas) comprises a longer lasting hiatus in sedimentation, probably lasting several centuries (Kasse, 2002; Kaiser et al., 2009; Jankowski, 2012). Any material found in the Black Mat and especially

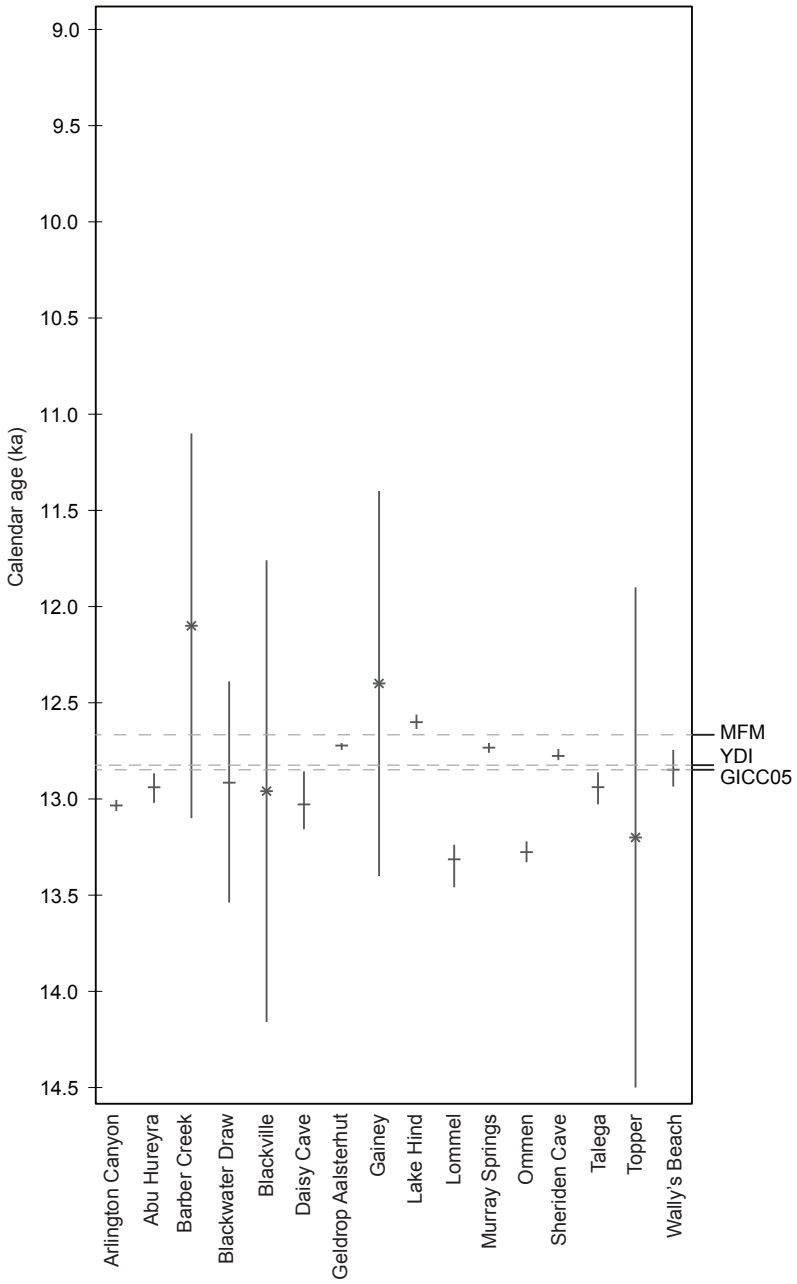

Figure 6.1. Calendar age for the different locations investigated in relation to the Younger Dryas impact (YDI) hypothesis where the marker layer has been directly dated (Firestone et al., 2007; Kennett et al., 2009b; Bunch et al., 2012; van Hoesel et al., 2012; Wittke et al., 2013b). Ages are given within one standard deviation (OSL/TL; mean indicated with an asterix) or within the 68% confidence interval (IntCal13 calibrated radiocarbon ages; median indicated with a short horizontal stripe). The proposed age of the Younger Dryas impact (Wittke et al., 2013b) is indicated as well as the onset of the Younger Dryas according to the Greenland Ice Core Chronology 2005 (GICC05, Rasmussen et al., 2006) and the Meerfelder Maar varved lake record (MFM, Brauer et al., 2008).

the Usselo horizon could thus come from a large interval of time, and increased values of cosmic material are expected due to relative enrichment as a result of non-deposition of sediments. Unless markers are related to dated material such as charcoal, it is thus difficult to pinpoint the exact time of deposition.

Lastly, there is an age discrepancy between different sites related to the Younger Dryas impact hypothesis table 6.2). Figure 6.1 shows the different age estimates for all sites investigated for Younger Dryas impact markers. Although some of the locations clearly overlap in time, others show a significant difference. Due to the radiocarbon cliff and additional uncertainties introduced through calibration, as well as the large scale range needed to present all the data in figure 6.1, some of the differences in age are more clearly visible in the radiocarbon ages, as shown in figure 6.2. Four main age-groups can be distinguished in figure 6.2. According to the ^{14}C ages, Daisy Cave, Abu Hureyra, Talega and Arlington Canyon cluster just before the early limit for the onset of the Younger Dryas (figure 6.2). Lommel and Ommen, two sites containing the Usselo horizon, are even older. Murray Springs and Geldrop Aalsterhut, on the other hand, likely date to the early Younger Dryas. Lake Hind is a single younger outlier. Only Sheriden Cave, Wally's Beach and Blackwater Draw date to the approximate time of the Younger Dryas onset, the latter, however, has a very high uncertainty. The marker horizons dated using OSL or thermoluminescence (TL) - Barber Creek, Blackville, Gainy and Topper - all have large uncertainties and overlap with most radiocarbon dated sites (figure 6.1), As the marker horizons found at different sites have ages that differ by up to two centuries, these markers may not be related to the same event. Some caution must, however, be taken into account when interpreting the age data. As mentioned in our second point, the "old wood" effect plays a role in interpreting radiocarbon ages. Kennett et al. (2008; 2009b) left out some of the older radiocarbon dates for Arlington Canyon, attributing them to old wood. Interestingly, these older dates were obtained from a carbon spherule, a glassy carbon particle and a carbon elongate (Kennett et al., 2008), all particles in which nanodiamonds have been reported and which are said to have formed within the fireball following the impact (Firestone et al., 2007; Kennett et al., 2009b). Fiedel (2010) argues that the age of these particles shows that the event must have occurred 100 or even 500 years before the onset of the Younger Dryas. Wittke et al. (2013a) even suggest that the radiocarbon ages of Arlington Canyon should not be used to date the nanodiamonds because of the old wood effect, even though the radiocarbon was used to date the layer in the original studies (Kennett et al., 2008; Kennett et al., 2009b). Although the older dates at Arlington Canyon may have originated from the pith of very old trees, similar reasoning should apply to all other radiocarbon-dated sites. It can, for example, easily be argued that the Younger Dryas impact layer at Murray Springs must be up to a century younger than indicated by the average radiocarbon ages, as the impact supposedly happened after the Clovis occupation, which was dated (Waters and Stafford, 2007), and the Clovis people could have burned older re-used wood. Invoking the old wood effect might therefore even increase the age discrepancy, rather than reducing it. Some of the age discrepancy could be explained by the occurrence of hiatuses or large sample intervals, as discussed earlier. However, this explanation only applies to some sites and only when the markers are not related to the dated material. Hiatuses, or large sampling intervals, therefore cannot eliminate the age discrepancy for all sites.

The age discrepancy thus poses a problem to the Younger Dryas impact hypothesis. If the impact hypothesis is valid, the chronology of some of the sites must be erroneous. If, on the other

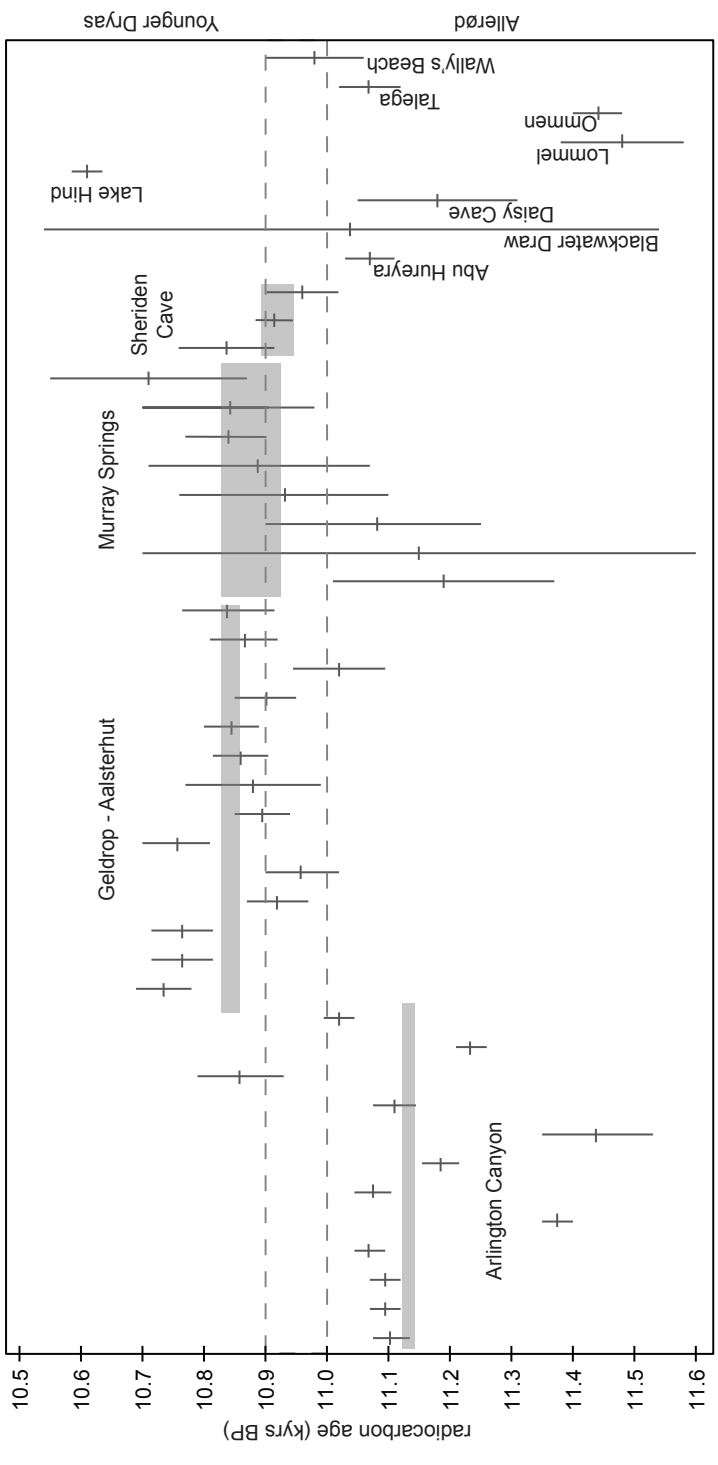

Figure 6.2. Reported uncalibrated radiocarbon ages (1σ) for the different locations investigated in relation to the Younger Dryas impact hypothesis where the marker layer has been directly dated (Firestone et al., 2007; Kennett et al., 2009b; Bunch et al., 2012; van Hoesel et al., 2012; Wittke et al., 2013b). Weighted averages (1σ) for sites with multiple 14C ages are indicated as grey bars. The estimated timing for the Younger Dryas onset (11,000 – 10,900 14C yrs BP) is indicated with the two dotted lines.

hand the age discrepancy is real, then there are three possibilities to explain the age difference between sites:

- The age discrepancy could indicate that there is no impact origin for the markers that have been reported. Pigati et al. (2012), for example, give a plausible explanation for the occurrence of magnetic spherules and iridium anomaly, leaving only the nanodiamonds, Pt peak and possibly the lechatelierite unexplained.

- It is possible that the markers correspond to several smaller impacts or airbursts spaced several decades to centuries apart. However, in this case it is unlikely that the multiple impacts are the cause of the Younger Dryas climate change, megafaunal extinctions or changes in human culture, as multiple smaller impacts would only have had local effects.

- Some of the markers or sites might be unrelated to an impact event of any size, whereas others are related to one or more impact events.

6.4 Implications for the Younger Dryas impact event and climate change.

Meteorite impacts produce a wide range of deformation features and ejecta. Only a few of these features are considered unique to an impact and can be used as conclusive evidence when analysing an impact structure. Namely shatter cones, diagnostic shock-metamorphic effects (e.g. shocked quartz), and chemical or isotopic traces of the impactor (French and Koeberl, 2010; Koeberl et al., 2012; Langenhorst and Deutsch, 2012; Reimold and Jourdan, 2012). Distal ejecta layers are often thin and insubstantial, and can most easily be recognised by the occurrence of (formerly molten) sand-sized spherules, including dumbbell and teardrop shapes (Glass and Simonson, 2012). Although indicative of an extraterrestrial impact, the presence of shock-metamorphic effects or traces of the impactor are still necessary to establish an impact origin for the layer (French and Koeberl, 2010; Glass and Simonson, 2012). For example the impact origin of the 1-5 mm thick Jeerinah spherule layer (Australia, 2.63 Ga) has been established on the basis of an Ir anomaly (>1-2 ppb) and one shocked quartz grain (Rasmussen and Koeberl, 2004). Finding a shocked quartz grain in-situ in a suspected crater structure would also be a good indication of an impact origin. However, finding a single shocked quartz grain in loose sediment without a clear relation to other impact markers – such as the grain found in the Usselo horizon at Geldrop Aalsterhut – is not a good indication of an impact, as the grain might have originated elsewhere (see discussion in §5.4).

In the case of an airburst, as was suggested for the Younger Dryas impact event (Firestone et al., 2007; Bunch et al., 2012; Wittke et al., 2013b), no shock metamorphism is expected to occur (unless it is accompanied by small crater-forming impacts of projectile fragments (Wittke et al., 2013b)) and the only way to conclusively identify an impact origin would be through traces of the projectile. Although magnetic spherules have been reported in the Allerød-Younger Dryas boundary at more than 20 sites (Wittke et al., 2013b), no unambiguous geochemical extraterrestrial signature accompanying these spherules has been reported so far. Lechatelierite is also seen as a good indication of an extraterrestrial impact (French and Koeberl, 2010) and Bunch et

al. (2012) reported the occurrence of scoria-like objects and lechatelierite at three of the 18 sites they investigated. As discussed above, only one of these sites (Abu Hureyra, Syria), has been accurately dated to the Allerød-Younger Dryas boundary: however, analyses for projectile traces or nanodiamonds have not been reported for this site. Finding projectile traces would confirm the impact nature of the lechatelierite while finding the nanodiamonds would strengthen the case for a possible impact origin of the Allerød-Younger Dryas boundary nanodiamonds reported elsewhere.

The confirmation of impact related lechatelierite, would show that there was a meteorite impact or airburst in the vicinity of Abu Hureyra (as suggested by Bunch et al., 2012). However, a relatively small impact or airburst in this region is unlikely to have triggered the Younger Dryas climate change. For an impact to have triggered the Younger Dryas climate change through meltwater input effecting the ocean circulation, it would have to be located at or near the ice sheet, most likely in North America. At this moment, there is no convincing evidence that an impact occurred in North America region at the onset of the Younger Dryas. More research would thus be necessary to confirm an impact event occurred at the onset of the Younger Dryas.

Chapter 7

Main conclusions

This thesis tests the hypothesis that an extraterrestrial impact event is responsible for the climate change at the onset of the Younger Dryas. Based on the combination of the analysis of several Allerød-Younger Dryas boundary layers in western Europe for nanodiamonds and shocked quartz using electron microscopy analysis, careful radiocarbon dating, and an assessment of the use of nanodiamonds as impact markers, the main findings can be summarized as follows.

Nanodiamonds have remained one of the main lines of evidence put forward to support the Younger Dryas impact hypothesis. Although some of the nanodiamonds have been reported in carbon spherules and glass-like carbon, suggesting they might have been formed during wildfires, no evidence for nanodiamonds was found in charcoal, carbon spherules or glass-like carbon of different ages.

In this study nanodiamonds were found only at one site, namely in glass-like carbon from the Usselo horizon at Geldrop Aalsterhut. Radiocarbon dating of charcoal particles has shown that these nanodiamonds probably post-date the Allerød-Younger Dryas transition.

One shocked quartz grain, a well-known impact indicator, was also found in the Usselo horizon at Geldrop Aalsterhut but not at other Allerød-Younger Dryas boundary sites. However, based on the current evidence it is not possible to determine whether this shocked grain was found in-situ and, if so, whether the possible impact is also related to the nanodiamonds found or occurred earlier. However, several aspects of the shocked quartz grain indicate that it was derived by re-deposition from an older crater or ejecta layer.

Most critically, there is an age discrepancy of up to two centuries between sites where Younger Dryas impact markers have been found. This leads to three possibilities:

- the reported markers are not related to an impact event;
- some of the markers are related to the Younger Dryas impact event, whereas others are not;
- the markers correspond to several smaller impacts or airbursts spaced several decades to centuries apart rather than one large-scale impact event.

Thus far there is no convincing evidence for the occurrence of a large-scale impact event at the Allerød-Younger Dryas boundary. More research is necessary to establish whether or not one or more impacts or airburst occurred at the onset of the Younger Dryas before making any further link with the climate cooling can be confirmed. If multiple smaller impacts, or airbursts, occurred at different points in time, as the age discrepancy between different sites might suggest, then it is unlikely that the impact events are responsible for the Younger Dryas cold period. The change in ocean circulation that has been held responsible for the Younger Dryas climate cooling thus probably had a more common, terrestrial trigger.

7.1 Suggestions for further research

It is crucial that a supposed consequence of any type of event can only be attributed to that event if there is a clear and causal relation between the timing of the event and the supposed impact. This has been advocated as such by the INTIMATE project group for the impact of abrupt climate changes, such as the transition from Allerød to Younger Dryas (Lowe et al., 2001; Lowe et al., 2008). It is very important in these kinds of studies to select suitable sedimentary archive that have enough time-resolution and, ideally, no hiatuses. Furthermore, these ideal archives should have the possibility of applying independent dating techniques in order to establish a reliable chronology. In many cases, the evidence used by, for example, Firestone et al. (2007) to support the Younger Dryas impact hypothesis does not meet these criteria.

Reproducibly analysing various well-dated annually laminated records containing the Allerød-Younger Dryas transition, preferably with one or more independent marker horizons that link the records, might shed light on the apparent age discrepancy between different sites. This type of analysis would show whether the markers are found exactly at the Allerød-Younger Dryas boundary and whether the markers at different locations point to the same point in time. In addition, analysing longer records, where available, would show whether the markers only occur at the Allerød-Younger Dryas boundary or are a more common phenomenon, regardless of their origin. For example, if nanodiamonds turn out to be more common in sediments than previously thought, it would bring the use of nanodiamonds as an impact indicator further into question. If, on the other hand, nanodiamonds are only found at one single point in time in several records, this would indicate that probably some sort of event took place and might provide an additional marker that can be used to link different records. Furthermore, we suggest that both the stratigraphy of the sedimentary archive and the methods used to analyse it, as well as the results are documented in detail. Sampling across the Allerød-Younger Dryas boundary and the rest of the record should be continuous rather than taken at intervals, and sample thickness should be equal for all samples, preferably representing an equal amount of time. This methodology insures that no peaks in markers at non- Allerød-Younger Dryas boundary levels are missed and concentrations across the profile are comparable.

A good example of such a record would be the Greenland ice cores, which also have the advantage that there is no dilution by terrestrial sediments. Thus far only the GISP2 ice core has been investigated, which showed a Pt peak at the Allerød-Younger Dryas boundary (Petaev et al., 2013). If possible, it would be good to investigate the same samples for other markers, such as nanodiamonds to determine whether these markers might be related. In addition, it is necessary to test whether the Pt peak is a local or a wide-spread phenomenon by investigating

other records. Although in terrestrial records the Pt signal, if present, might be diluted by the sediment. If the Pt signal is related to a single event and can be found in multiple records in a wide area, it could provide a useful marker to link different sedimentary records.

Currently, the best evidence far for an impact event at the Allerød-Younger Dryas boundary currently seems to come from the well-dated Abu Hureyra site in Syria, in the form of lechatelierite (Bunch et al., 2012). Ideally the Allerød-Younger Dryas boundary at this site, and others in the region, should be investigated for other markers, preferably diagnostic impact indicaters, in order to confirm the impact origin of the material and establish the extent of the event. However, unless it was a large event, an extraterrestrial impact or airburst in the Middle East cannot have triggered the Younger Dryas climate change. For the impact event to have triggered the Younger Dryas climate cooling, it would have had to be near one of the northern hemisphere ice caps. Therefore further research, focussing on the Mid- and South Atlantic Regions in the United States, is suggested. Here lechatelierite has been reported at two sites but without good age control (Bunch et al., 2012). As it would probably be difficult to date these sites more accurately it would be best to select nearby sites with a wellestablished chronology. These selected sedimentary records should be thoroughly analysed for lechatelierite, geochemical traces of the impactor and shock indicators. Additional analysis for other markers such as nanodiamonds and magnetic spherules could also provide insight in the event.
Although shocked quartz is a well-known indicator and has been found in the Usselo horizon at Geldrop Aalsterhut, further research in the western European region is less vital. This study has already shown that shocked quartz was not found at other sites and also that nanodiamonds do not seem common in this region. In addition, this site is situated south of the Scandinavian ice sheet rather than the Laurentide ice sheet, which is commonly seen as the source of the meltwater input that triggered the Younger Dryas cold period (Carlson and Clark, 2012).

This project has shown that nanodiamonds are rare and can be difficult/time consuming to detect. These practical aspects make it difficult to test the competing hypothesis for the origin of the Allerød-Younger Dryas boundary. Further research on nanodiamonds in the sedimentary record, possibly combining electron microscopy with other techniques, is necessary to assess how common nanodiamonds actually are, and whether they occur in particular types of deposits or deposits of certain ages. Learning more about where and when nanodiamonds were deposited might provide insight into their origin and whether they might be used as time marker to link different records. If, on the other hand, nanodiamonds prove to be common in the sedimentary record, this would suggest that they cannot be used as an impact indicator. Analysing the samples where high Pt concentrations or lechatelierite has been found (Bunch et al., 2012; Petaev et al., 2013) for nanodiamond would also show whether the nanodiamonds at the Allerød-Younger Dryas boundary are related to these markers.

References

Alley R.B., 2000. The Younger Dryas cold interval as viewed from central Greenland. Quaternary Science Reviews 19 (1-5), 213-226.

Anderson D.G., Meeks S.C., Goodyear A.C. and Miller D.S., 2008. Southeastern data inconsistent with Paleoindian demographic reconstruction. Proceedings of the National Academy of Sciences 105 (50), 108.

Andronikov A.V., Lauretta D.S., Andronikova I.E. and Maxwell R.J., 2011. On the possibility of a Late Pleistocene extraterrestrial impact: LA-ICP-MS analysis of the Black Mat and Usselo horizon samples. 74th Annual Meteoritical Society Meeting, 5008.

Aoki T. and Akai J., 2008. Carbon materials in Antarctic and nonAntarctic carbonaceous chondrites: high-resolution transmission electron microscopy. Journal of Mineralogical and Petrological Sciences 103 (3), 173-182.

Baker A.G., Bhagwat S.A. and Willis K.J., 2013. Do dung fungal spores make a good proxy for past distribution of large herbivores? Quaternary Science Reviews 62, 21-31.

Banhart F. and Ajayan P.M., 1996. Carbon onions as nanoscopic pressure cells for diamond formation. Nature 382 (6590), 433-435.

Banhart F., 1997. The transformation of graphitic onions to diamond under electron irradiation. Journal of Applied Physics 81 (8), 3440-3445.

Barnosky A.D., 2008. Megafauna biomass tradeoff as a driver of Quaternary and future extinctions. Proceedings of the National Academy of Sciences 105 (Suppl. 1), 11543-11548.

Bateman M.D. and Van Huissteden J., 1999. The timing of last-glacial periglacial and aeolian events, Twente, eastern Netherlands. Journal of Quaternary Science 14 (3), 277-283.

Bement L., C, Andrew S., Carter B.J., Simms A., Swindle A.L., Alexander H.M., Fine S. and Benamara M., 2013. Nanodiamond quantification in pre-Younger Dryas to recent age deposits along Bull Creek, Oklahoma, USA. GSA Annual Meeting 45 (7), 306-8.

Björck S., Walker M.J., Cwynar L.C., Johnsen S., Knudsen K., Lowe J.J. and Wohlfarth B., 1998. An event stratigraphy for the Last Termination in the North Atlantic region based on the Greenland ice-core record: a proposal by the INTIMATE group. Journal of Quaternary Science 13 (4), 283-292.

Blaauw M., Holliday V.T., Gill J.L. and Nicoll K., 2012. Age models and the Younger Dryas Impact Hyptohesis. Proceedings of the National Academy of Sciences 109 (34), E2240.

Bland P.A. and Artemieva N.A., 2006. The rate of small impacts on Earth. Meteoritics and Planetary Science 41 (4), 607-631.

Blockley S.P.E., Lane C.S., Hardiman M., Rasmussen S.O., Seierstad I.K., Steffensen J.P., Svensson A., Lotter A.F., Turney C.S.M. and Bronk Ramsey C., 2012. Synchronisation of palaeoenvironmental records over the last 60,000 years, and an extended INTIMATE event stratigraphy to 48,000 b2k. Quaternary Science Reviews 36, 2-10.

Boggs S. J., Krinsley D.H., Goles G.G., Seyedolali A. and Dyvik H., 2001. Identification of shocked quartz by scanning cathodoluminescence imaging. Meteoritics and Planetary Science 36 (6), 783-791.

Boslough M., Nicoll K., Holliday V., et al. , 2012. Arguments and Evidence Against a Younger Dryas Impact Event. In: L. Giosan, D. Q. Fuller, K. Nicoll, R. K. Flad, and P. D. Clift. (Eds.), Climates, Landscapes, and Civlizations. Geophysical Monograph Series 198, 13-26.

Braadbaart F., 2008. Carbonisation and morphological changes in modern dehusked and husked Triticum dicoccum and Triticum aestivum grains. Vegetation History and Archaeobotany 17 (1), 155-166.

References

Braadbaart F. and Poole I., 2008. Morphological, chemical and physical changes during charcoalification of wood and its relevance to archaeological contexts. Journal of Archaeological Science 35 (9), 2434-2445.

Braadbaart F., Poole I. and van Brussel A.A., 2009. Preservation potential of charcoal in alkaline environments: an experimental approach and implications for the archaeological record. Journal of Archaeological Science 36 (8), 1672-1679.

Bradley R.S. and England J.H., 2008. The Younger Dryas and the Sea of Ancient Ice. Quaternary Research 70 (1), 1-10.

Brakenridge G.R., 2011. Core-collapse supernovae and the Younger Dryas/terminal Rancholabrean extinctions. Icarus 215 (1), 101-106.

Brauer A., Haug G.H., Dulski P., Sigman D.M. and Negendank J.F.W., 2008. An abrupt wind shift in western Europe at the onset of the Younger Dryas cold period. Nature Geoscience 1 (8), 520-523.

Goslar A., Endres C., Günter C., Litt T., Stebich M. and Negendank J.F.W., 1999. High resolution sediment and vegetation responses to Younger Dryas climate change in varved lake sediments from Meerfelder Maar, Germany. Quaternary Science Reviews 18 (3), 321-329.

Boyce J.I. and Eyles N., 1991. Drumlins carved by deforming till streams below the Laurentide ice sheet. Geology 19 (8), 787-790.

Broecker W.S., Kennett J.P., Flower B.P., Teller J.T., Trumbore S., Bonani G. and Wolfli W., 1989. Routing of meltwater from the Laurentide Ice Sheet during the Younger Dryas cold episode. Nature 341 (6240), 318-321.

Broecker W.S., Bond G., Klas M., Bonani G. and Wolfli W., 1990. A salt oscillator in the glacial Atlantic? 1. The concept. Paleoceanography 5 (4), 469-477.

Broecker W.S., Denton G.H., Edwards R.L., Cheng H., Alley R.B. and Putnam A.E., 2010. Putting the Younger Dryas cold event into context. Quaternary Science Reviews 29, 1078-1081.

Bronk Ramsey C., 2009. Bayesian analysis of radiocarbon dates. Radiocarbon 51 (1), 337-360.

Brooks M.J., Taylor B.E. and Ivester A.H., 2010. Carolina bays: Time capsules of culture and climate change. Southeastern Archaeology 29 (1), 146-163.

Brown P., Spalding R.E., ReVelle D.O., Tagliaferri E. and Worden S.P., 2002. The flux of small near-Earth objects colliding with the Earth. Nature 420 (6913), 294-296.

Buchanan B., Collard M. and Edinborough K., 2008. Paleoindian demography and the extraterrestrial impact hypothesis. Proceedings of the National Academy of Sciences 105 (33), 11651-11654.

Buettner K.M. and Valentine A.M., 2011. Bioinorganic chemistry of titanium. Chemical reviews 112 (3), 1863-1881.

Bunch T.B., Kennet J. and Kennet D.K., 2008. Comment on 'Impacts, mega-tsunami, and other extraordinary claims'. GSA Today 18 (6), 11.

Bunch T.E., West A., Firestone R.B., Kennett J.P., Wittke J.H., Kinzie C.R. and Wolbach W.S., 2010. Geochemical data reported by Paquay et al. do not refute Younger Dryas impact event. Proceedings of the National Academy of Sciences 107 (15), E58.

Bunch T.E., Hermes R.E., Moore A.M.T., Kennett D.J., Weaver J.C., Wittke J.H., DeCarli P.S., Bischoff J.L., Hillman G.C., Howard G.A., Kimbel D.R., Kletetschka G., Lipo C.P., Sakai S., Revay Z., West A., Firestone R.B. and Kennett J.P., 2012. Very high-temperature impact melt products as evidence for cosmic airbursts and impacts 12,900 years ago. Proceedings of the National Academy of Sciences 109 (28), 1903-1912.

Carlisle D.B. and Bramant D.R., 1991. Nanometre-size diamonds in the Cretaceous/Tertiary boundary clay of Alberta. Nature 352 (6337), 708-709.

Carlson A.E. and Clark P.U., 2012. Ice sheet sources of sea level rise and freshwater discharge during the last deglaciation. Reviews of Geophysics 50 (4)

Carlson A.E., 2008. Why there was not a Younger Dryas-like event during the Penultimate Deglaciation. Quaternary Science Reviews 27 (9-10), 882-887.

Cavosie A.J., Quintero R.R., Radovan H.A. and Moser D.E., 2010. A record of ancient cataclysm in modern sand: Shock microstructures in detrital minerals from the Vaal River, Vredefort Dome, South Africa. Geological Society of America Bulletin 122 (11-12), 1968-1980.

Cheng H., Edwards R.L., Broecker W.S., Denton G.H., Kong X., Wang Y., Zhang R. and Wang X., 2009. Ice age terminations. Science 326 (5950), 248-252.

Cloete M., Hart R.J., Schmid H.K., Drury M., Demanet C.M. and Sankar K.V., 1999. Characterization of magnetite particles in shocked quartz by means of electron-and magnetic force microscopy: Vredefort, South Africa. Contributions to mineralogy and petrology 137 (3), 232-245.

Cody G.D., Alexander C.M.O. and Tera F., 2002. Solid-state (1H and 13C) nuclear magnetic resonance spectroscopy of insoluble organic residue in the Murchison meteorite: A self-consistent quantitative analysis. Geochimica et Cosmochimica Acta 66 (10), 1851-1865.

Cohen-Ofri H., Popovitz-Biro R. and Weiner S., 2007. Structural characterization of modern and fossilized charcoal produced in natural fires as determined by using electron energy loss spectroscopy. Chemistry - A European Journal 13 (8), 2306-2310.

Colledge S. and Conolly J., 2010. Reassessing the evidence for the cultivation of wild crops during the Younger Dryas at Tell Abu Hureyra, Syria. Environmental Archaeology 15 (2), 124-138.

Condron A. and Winsor P., 2012. Meltwater routing and the Younger Dryas. Proceedings of the National Academy of Sciences 109 (49), 19928-19933.

Cowley J.M., Mani R.C., Sunkara M.K., O'Keeffe M. and Bonneau C., 2004. Structures of carbon nanocrystals. Chemistry of Materials 16 (24), 4905-4911.

Crommelin R.D., 1964. A contribution to the sedimentary petrology and provenance of young Pleistocene cover sand in the Netherlands. Geologie en Mijnbouw 43 (9), 389-402.

Dadsetani M., Titantah J.T. and Lamoen D., 2010. Ab initio calculation of the energy-loss near-edge structure of some carbon allotropes: Comparison with n-diamond. Diamond and Related Materials 19 (1), 73-77.

Dai Z.R., Bradley J.P., Joswiak D.J., Brownlee D.E., Hill H.G.M. and Genge M.J., 2002. Possible in situ formation of meteoritic nanodiamonds in the early Solar System. Nature 418 (6894), 157-159.

Dalton R., 2009. Impact theory under fire once more. Nature News 461, 861.

Dalton R., 2007. Archaeology: Blast in the past? Nature 447 (7142), 256-257.

Daniau A.L., Harrison S.P. and Bartlein P.J., 2010. Fire regimes during the Last Glacial. Quaternary Science Reviews 29 (21-22), 2918-2930.

Daulton T.L., Eisenhour D.D., Bernatowicz T.J., Lewis R.S. and Buseck P.R., 1996. Genesis of presolar diamonds: Comparative high-resolution transmission electron microscopy study of meteoritic and terrestrial nano-diamonds. Geochimica et Cosmochimica Acta 60 (23), 4853-4872.

Daulton T.L., Pinter N. and Scott A.C., 2010. No evidence of nanodiamonds in Younger–Dryas sediments to support an impact event. Proceedings of the National Academy of Sciences 107 (37), 16043-16047.

Daulton T.L., 2012. Suspect cubic diamond "impact" proxy and a suspect lonsdaleite identification. Proceedings of the National Academy of Sciences 109 (34), E2242.

De Bie M. and Vermeersch P.M., 1998. Pleistocene-Holocene transition in Benelux. Quaternary International 49-50, 29-43.

De Vries H., Barendsen G.W. and Waterbolk H.T., 1958. Groningen radiocarbon dates II. Science 127, 129-137.

Denton G.H., Anderson R.F., Toggweiler J.R., Edwards R.L., Schaefer J.M. and Putnam A.E., 2010. The Last Glacial Termination. Science 328 (5986), 1652-1656.

Derese C., Vandenberghe D.A.G., Van Gils M., Mees F., Paulissen E. and van den Haute P., 2012. Final Palaeolithic settlements of the Campine region (NE Belgium) in their environmental context: Optical age constraints. Quaternary International 251, 7-21.

Dubinchuk V.T., Simakov S.K. and Pechnikov V.A., 2010. Lonsdaleite in diamond-bearing metamorphic rocks of the Kokchetav massif. Doklady Earth Sciences 430 (1), 40-42.

Dumon J. and Ernst W., 1988. Titanium in plants. Journal of Plant Physiology 133 (2), 203-209.

Durda D.D. and Kring D.A., 2004. Ignition threshold for impact-generated fires. Journal of Geophysical Research E: Planets 109 (8), 1-14.

Ebert M., Hecht L., Deutsch A. and Kenkmann T., 2013. Chemical modification of projectile residues and target material in a MEMIN cratering experiment. Meteoritics & Planetary Science 48 (1), 134-149.

Edington J.W., 1975. Electron diffraction in the electron microscope. 2, 122.

Eric S., 2010. Extinctions, scenarios, and assumptions: Changes in latest Pleistocene large herbivore abundance and distribution in western North America. Quaternary International 217 (1-2), 225-239.

References

Erlandson J.M., Kennett D.J., Ingram B.L., Guthrie D.A., Morris D.P., Tveskov M.A., West G.J. and Walker P.L., 1996. An archaeological and paleontological chronology for Daisy Cave (CA-SMI-261), San Miguel Island, California. Radiocarbon 38 (2), 355-373.

Erlich E.I. and Hausel W.D., 2002. Diamond deposits: origin, exploration, and history of discovery. Society of Mining, Metallurgy, and Exploration Littleton, 374p.

Fayek M., Anovitz L.M., Allard L.F. and Hull S., 2012. Framboidal iron oxide: Chondrite-like material from the black mat, Murray Springs, Arizona. Earth and Planetary Science Letters 319–320, 251-258.

Ferrière L., Morrow J.R., Amgaa T. and Koeberl C., 2009. Systematic study of universal-stage measurements of planar deformation features in shocked quartz: Implications for statistical significance and representation of results. Meteoritics and Planetary Science 44 (6), 925-940.

Ferroir T., Dubrovinsky L., El Goresy A., Simionovici A., Nakamura T. and Gillet P., 2010. Carbon polymorphism in shocked meteorites: Evidence for new natural ultrahard phases. Earth and Planetary Science Letters 290 (1-2), 150-154.

Fiedel S.J. , 2009. Sudden deaths: The chronology of terminal Pleistocene megafaunal extinction. In: Haynes G. (Eds.), American megafaunal extinctions at the end of the Pleistocene. Springer, Netherlands, 21-37.

Fiedel S.J. , 2010. Did a bolide impact trigger the Younger Dryas and wipe out American megafauna? In: Mainwaring A.B., Giegengack R. and Vita-Finzi C. (Eds.), Lightning Rod Press volume 6: Climate crises in human history. American Philosophical Society, Philadelphia, 83-109.

Fiedel S.J., 2011. The mysterious onset of the Younger Dryas. Quaternary International 242 (2), 262-266.

Firestone R.B., 2002. Resonse to the Comments by J.R. Southon and R.E. Taylor. Mammoth Trumpet 17 (2), 14-17.

Firestone R.B., 2009. The Case for the Younger Dryas Extraterrestrial Impact Event: Mammoth, Megafauna, and Clovis Extinction, 12,900 Years Ago. Journal of Cosmology 2, 256-285.

Firestone R.B. and Topping W., 2001. Terrestrial evidence of a nuclear catastrophe in paleoindian times. 16 (2), 9-16.

Firestone R.B., West A., Kennett J.P., Becker L., Bunch T.E., Revay Z.S., Schultz P.H., Belgya T., Kennett D.J., Erlandson J.M., Dickenson O.J., Goodyear A.C., Harris R.S., Howard G.A., Kloosterman J.B., Lechler P., Mayewski P.A., Montgomery J., Poreda R., Darrah T., Que Hee S.S., Smitha A.R., Stich A., Topping W., Wittke J.H. and Wolbach W.S., 2007. Evidence for an extraterrestrial impact 12,900 years ago that contributed to the megafaunal extinctions and the Younger Dryas cooling. Proceedings of the National Academy of Sciences 104 (41), 16016-16021.

Fitz Gerald J., Pennock G. and Taylor G., 1991. Domain structure in MP (mesophase pitch)-based fibres. Carbon 29 (2), 139-164.

Franceschi V.R. and Nakata P.A., 2005. Calcium oxalate in plants: formation and function. Annu.Rev.Plant Biol. 56, 41-71.

Franke C., von Dobeneck T., Drury M.R., Meeldijk J.D. and Dekkers M.J., 2007. Magnetic petrology of equatorial Atlantic sediments: Electron microscopy results and their implications for environmental magnetic interpretation. Paleoceanography 22 (4), PA4207.

Franzén L.G. and Cropp R.A., 2007. The peatland/ice age hypothesis revised, adding a possible glacial pulse trigger. Geografiska Annaler: Series A, Physical Geography 89 (4), 301-330.

French B.M., 1998. Traces of catastrophe: A handbook of shock-metamorphic effects in terrestrial meteorite impact structures. LPI Contribution No. 954, 120.

French B.M. and Koeberl C., 2010. The convincing identification of terrestrial meteorite impact structures: What works, what doesn't, and why. Earth-Science Reviews 98 (1-2), 123-170.

Frenklach M., Kematick R., Huang D., Howard W., Spear K.E., Phelps A.W. and Koba R., 1989. Homogeneous nucleation of diamond powder in the gas phase. Journal of Applied Physics 66 (1), 395-399.

Frezzotti M.L. and Peccerillo A., 2007. Diamond-bearing COHS fluids in the mantle beneath Hawaii. Earth and Planetary Science Letters 262 (1-2), 273-283.

Frost R.L. and Weier M.L., 2004. Thermal treatment of whewellite—a thermal analysis and Raman spectroscopic study. Thermochimica Acta 409 (1), 79-85.

Fuhrer K., Neftel A., Anklin M., Staffelbach T. and Legrand M., 1996. High-resolution ammonium ice core record covering a complete glacial-interglacial cycle. Journal of Geophysical Research D: Atmospheres 101 (D2), 4147-4164.

Gardner J.E., Carey S. and Sigurdsson H., 1998. Plinian eruptions at Glacier Peak and Newberry volcanoes, United States: Implications for volcanic hazards in the Cascade Range. Bulletin of the Geological Society of America 110 (2), 173-187.

Gavin D.G., 2001. Estimation of inbuilt age in radiocarbon ages of soil charcoal for fire history studies. Radiocarbon 43 (1), 27-44.

Gill J.L., Williams J.W., Jackson S.T., Lininger K.B. and Robinson G.S., 2009. Pleistocene megafaunal collapse, novel plant communities, and enhanced fire regimes in North America. Science 326 (5956), 1100-1103.

Gilmour I., Russell S.S., Arden J.W., Lee M.R., Franchi I.A. and Pillinger C.T., 1992. Terrestrial carbon and nitrogen isotopic ratios from Cretaceous-Tertiary boundary nanodiamonds. Science 258 (5088), 1624-1626.

Gilmour I., 1998. Geochemistry of carbon in terrestrial impact processes. Geological Society Special Publication (140), 205-216.

Glass B.P., 1990. Tektites and microtektites: key facts and inferences. Tectonophysics 171 (1-4), 393-404.

Glass B.P. and Simonson B.M., 2012. Distal impact ejecta layers: Spherules and more. Elements 8 (1), 43-48.

Goslar T., Arnold M., Bard E., Kuc T., Pazdur M.F., Ralska-Jasiewiczowa M., Rózański K., Tisnerat N., Walanus A., Wicik B. and Wi□ckowski K., 1995. High concentration of atmospheric 14C during the Younger Dryas cold episode. Nature 377 (6548), 414-417.

Goslar T., Arnold M., Tisnerat-Laborde N., Hatté C., Paterne M. and Ralska-Jasiewiczowa M., 2000. Radiocarbon calibration by means of varves versus 14C ages of terrestrial macrofossils from Lake Gościa□ż and Lake Perespilno, Poland. Radiocarbon 42 (3), 335-348.

Grebennikov A.V., 2011. Silica-metal spherules in ignimbrites of southern Primorye, Russia. Journal of Earth Science 22 (1), 20-31.

Grebennikov A.V., Shcheka S.A. and Karabtsov A.A., 2012. Silicate-metallic spherules and the problem of the ignimbrite eruption mechanism: The Yakutinskaya volcanic depression. Journal of Volcanology and Seismology 6 (4), 211-229.

Grieve R.A.F., Langenhorst F. and Stöffler D., 1996. Shock metamorphism of quartz in nature and experiment: II. Significance in geoscience. Meteoritics and Planetary Science 31 (1), 6-35.

Hajdas I., Bonani G., Bodén P., Peteet D.M. and Mann D.H., 1998. Cold reversal on Kodiak Island, Alaska, correlated with the European Younger Dryas by using variations of atmospheric 14C content. Geology 26 (11), 1047-1050.

Hajdas I. and Michczyński A., 2010. Age-depth model of lake Soppensee (Switzerland) based on the high-resolution 14C chronology compared with varve chronology. Radiocarbon 52 (3), 1027-1040.

Hamers M.F., 2013. Identifying shock microstructures in quartz from terrestrial impacts: new scanning electron microscopy methods. Utrecht studies in Earth Sciences 32, 191.

Hamers M.F. and Drury M.R., 2011. Scanning electron microscope-cathodoluminescence (SEM-CL) imaging of planar deformation features and tectonic deformation lamellae in quartz. Meteoritics and Planetary Science 46 (12), 1814-1831.

Hamilton M.J. and Buchanan B., 2009. Archaeological and Paleobiological Problems with the Case for the Extraterrestrial Younger Dryas Impact Event. Journal of Cosmology 2, 289-292.

Hammen T.v.d., 1951. Late-glacial flora and periglacial phenomena in the Netherlands.

Hanneman R.E., Strong H.M. and Bundy F.P., 1967. Hexagonal diamonds in meteorites: Implications. Science 155 (3765), 995-997.

Harris P.J.F., 2004. Fullerene-related structure of commercial glassy carbons. Philosophical magazine 84 (29), 3159-3167.

Harris P.J.F., 2005. New perspectives on the structure of graphitic carbons. Critical Reviews in Solid State and Materials Sciences 30 (4), 235-253.

Harris P.J.F., 2013. Fullerene-like models for microporous carbon. Journal of Materials Science 48 (2), 565-577.

Hart R., Connell S., Cloete M., Mare L., Drury M. and Tredoux M., 2000. 'Super magnetic' rocks generated by shock metamorphism from the centre of the Vredefort impact structure, South Africa. South African Journal of Geology 103 (2), 151-155.

Hata T., Imamura Y., Kobayashi E., Yamane K. and Kikuchi K., 2000. Onion-like graphitic particles observed in wood charcoal. Journal of Wood Science 46 (1), 89-92.

References

Haynes Jr. C.V., Stanford D.J., Jodry M., Dickenson J., Montgomery J.L., Shelley P.H., Rovner I. and Agogine G.A., 1999. A Clovis well at the type site 11,500 B.C.: The oldest prehistoric well in America. Geoarchaeology 14 (5), 375-479.

Haynes Jr. C.V., 2008. Younger Dryas "black mats" and the Rancholabrean termination in North America. Proceedings of the National Academy of Sciences 105 (18), 6520-6525.

Haynes C.V., Boerner J., Domanik K., Lauretta D., Ballenger J. and Goreva J., 2010. The Murray Springs Clovis site, Pleistocene extinction, and the question of extraterrestrial impact. Proceedings of the National Academy of Sciences 107 (9), 4010-4015.

Higgins M.D., Lajeunesse P., St-Onge G., Locat J., Duschesne M., Ortiz J. and Sanfacon R., 2011. Bathymetric and petrological evidence for a young (Pleistocene?) 4-km diameter impact crater in the Gulf of Saint Lawrence, Canada. 42nd Lunar and Planetary Science Conference, abstract 1504.

Hilgers A., Murray A.S., Schlaak N. and Radtke U., 2000. The potential of optically stimulated luminescence for dating Late Glacial and Holocene dune sands–a case study from Brandenburg, Germany. Geolines 11, 79-83.

Hilgers A., 2007. The chronology of Late Glacial and Holocene dune development in the northern Central European lowland reconstructed by optically stimulated luminescence (OSL) dating PhD Thesis, University of Cologne, 440p.

Hirai H. and Kondo K., 1991. Modified Phases of Diamond Formed Under Shock Compression and Rapid Quenching. Science 253 (5021), 772-774.

Hoek W.Z., 1997. Late-glacial and early Holocene climatic events and chronology of vegetation development in the Netherlands. Vegetation History and Archaeobotany 6 (4), 197-213.

Hoek W.Z. and Bohncke S.J.P., 2002. Climatic and environmental events over the Last Termination, as recorded in The Netherlands: A review. Geologie en Mijnbouw/Netherlands Journal of Geosciences 81 (1), 123-137.

Hoek W.Z., 2008. The Last Glacial-Interglacial Transition. Episodes 31 (2), 226-229.

Holcombe T.L., Youngblut S. and Slowey N., 2013. Geological structure of Charity Shoal crater, Lake Ontario, revealed by multibeam bathymetry. Geo-Marine Letters 33 (4), 245-252.

Hough R.M., Gilmour I., Pillinger C.T., Arden J.W., Gilkes K.W.R., Yuan J. and Milledge H.J., 1995. Diamond and silicon carbide in impact melt rock from the Ries impact crater. Nature 378 (6552), 41-44.

Hough R.M., Gilmour I., Pillinger C.T., Langenhorst F. and Montanari A., 1997. Diamonds from the iridium-rich K-T boundary layer at Arroyo el Mimbral, Tamaulipas, Mexico. Geology 25 (11), 1019-1022.

Hua Q., Barbetti M., Fink D., Kaiser K.F., Friedrich M., Kromer B., Levchenko V.A., Zoppi U., Smith A.M. and Bertuch F., 2009. Atmospheric ^{14}C variations derived from tree rings during the early Younger Dryas. Quaternary Science Reviews 28 (25-26), 2982-2990.

Huffman A.R., Brown J.M., Carter N.L. and Reimold W.U., 1993. The microstructural response of quartz and feldspar under shock loading at variable temperatures. Journal of Geophysical Research: Solid Earth 98 (B12), 22171-22197.

Huffman A.R. and Reimold W.U., 1996. Experimental constraints on shock-induced microstructures in naturally deformed silicates. Tectonophysics 256 (1-4), 165-217.

Hunt C.O. and Rushworth G., 2005. Cultivation and human impact at 6000 cal yr B.P. in tropical lowland forest at Niah, Sarawak, Malaysian Borneo. Quaternary Research 64 (3), 460-468.

Ishimaru K., Vystavel T., Bronsveld P., Hata T., Imamura Y. and De Hosson J., 2001. Diamond and pore structure observed in wood charcoal. Journal of Wood Science 47 (5), 414-416.

Israde-Alcántara I., Velázquez-Durán R., García M.S.L., Bischoff J., Vázquez G.D. and Monroy V.H.G., 2010. Evolución Paleolimnológica del Lago Cuitzeo, Michoacán durante el Pleistoceno-Holoceno (Paleolimnologic evolution of Lake Cuitzeo, Michoacán, during the Pleistocene-Holocene). Boletín de la Sociedad Geológica Mexicana 62 (3), 345-357.

Israde-Alcántara I., Bischoff J.L., Domínguez-Vázquez G., Li H., DeCarli P.S., Bunch T.E., Wittke J.H., Weaver J.C., Firestone R.B., West A., Kennett J.P., Mercer C., Xie S., Richman E.K., Kinzie C.R. and Wolbach W.S., 2012. Evidence from central Mexico supporting the Younger Dryas extraterrestrial impact hypothesis. Proceedings of the National Academy of Sciences 109 (13), E738-E747.

Itambi A.C., Von Dobeneck T., Dekkers M.J. and Frederichs T., 2010. Magnetic mineral inventory of equatorial Atlantic Ocean marine sediments off Senegal-glacial and interglacial contrast. Geophysical Journal International 183 (1), 163-177.

Jankowski M. , 2002. Buried soils of the Torun Basin. In: Manikowska B., Konecka-Betley K. and Bednarek R. (Eds.), Paleopedology Problems in Poland. Lodzkie Towarzystwo Naukowe (Lodz) 233-252.

Jankowski M., 2012. Lateglacial soil paleocatena in inland-dune area of the Toruń Basin, Northern Poland. Quaternary International 265, 116-125.

Jessen K. and Jonassen H., 1935. The composition of the forests in Northern Europe in Epipalaeolithic time. Biologiske Meddelelser 12, 1-64.

Jones N., 2013. Evidence found for planet-cooling asteroid. Nature News, doi:10.1038/nature.2013.13661.

Jones T.L., 2008. California archaeological record consistent with Younger Dryas disruptive event. Proceedings of the National Academy of Sciences 105 (50), 109.

Kaiser K., Hilgers A., Schlaak N., Jankowski M., Kühn P., Bussemer S. and Przegietka k., 2009. Palaeopedological marker horizons in northern central Europe: characteristics of Lateglacial Usselo and Finow soils. Boreas 38, 591-609.

Kaiser K., Barthelmes A., Czakó Pap S., Hilgers A., Janke W., Kühn P. and Theuerkauf M., 2006. A Lateglacial palaeosol cover in the Altdarss area, southern Baltic Sea coast (northeast Germany): Investigations on pedology geochronology and botany. Geologie en Mijnbouw/Netherlands Journal of Geosciences 85 (3), 197-220.

Kaiser K.F., Friedrich M., Miramont C., Kromer B., Sgier M., Schaub M., Boeren I., Remmele S., Talamo S., Guibal F. and Sivan O., 2012. Challenging process to make the Lateglacial tree-ring chronologies from Europe absolute – an inventory. Quaternary Science Reviews 36, 78-90.

Karczemska A., Szurgot M., Kozanecki M., Szynkowska M.I., Ralchenko V., Danilenko V.V., Louda P. and Mitura S., 2008. Extraterrestrial, terrestrial and laboratory diamonds - differences and similarities. Diamond and Related Materials 17 (7-10), 1179-1185.

Kasse C., 2002. Sandy aeolian deposits and environments and their relation to climate during the Last Glacial Maximum and Lateglacial in northwest and central Europe Progress in Physical Geography 26 (4), 507-532.

Kenkmann T., Artemieva N.A., Wünnemann K., Poelchau M.H., Elbeshausen D. and Prado H.N.D., 2009. The Carancas meteorite impact crater, Peru: Geologic surveying and modeling of crater formation and atmospheric passage. Meteoritics and Planetary Science 44 (7), 985-1000.

Kennett J., Mayewski P.A., West A., Bunch T.E., Stafford T.W. and Wolbach W.S., 2009. Evidence for widespread biomass-burning at the Younger Dryas boundary. Eos Transactions AGU 90 (82), Fall Meeting Supplement, Abstract PP31D-1397.

Kennett D.J., Kennett J.P., West G.J., Erlandson J.M., Johnson J.R., Hendy I.L., West A., Culleton B.J., Jones T.L. and Stafford Jr. T.W., 2008. Wildfire and abrupt ecosystem disruption on California's Northern Channel Islands at the Ållerød-Younger Dryas boundary (13.0-12.9 ka). Quaternary Science Reviews 27 (27-28), 2530-2545.

Kennett D.J., Kennett J.P., West A., Mercer C., Que Hee S.S., Bement L., Bunch T.E., Sellers M. and Wolbach W.S., 2009a. Nanodiamonds in the Younger Dryas boundary sediment layer. Science 323 (5910), 94.

Kennett D.J., Kennett J.P., West A., West G.J., Bunch T.E., Culletona B.J., Erlandson J.M., Que Hee S.S., Johnson J.R., Mercer C., Shen F., Sellers M., Stafford Jr. T.W., Stich A., Weaver J.C., Wittke J.H. and Wolbach W.S., 2009b. Shock-synthesized hexagonal diamonds in Younger Dryas boundary sediments. Proceedings of the National Academy of Sciences 106 (31), 12623-12628.

Kennett J.P. and West A., 2008. Biostratigraphic evidence supports Paleoindian population disruption at ≈12.9 ka. Proceedings of the National Academy of Sciences 105 (50), E110-E110.

Kerr R.A., 2007. Mammoth killer impact gets mixed reception from Earth scientists. Science 316 (5829), 1264-1265.

Kerr R.A., 2008. Paleontology: Experts find no evidence for a mammoth-killer impact. Science 319 (5868), 1331-1332.

Kerr R.A., 2009. Did the mammoth slayer leave a diamond calling card? Science 323 (5910), 26.

Kerr R.A., 2010. Mammoth-Killer Impact Flunks Out. Science 329 (5996), 1140-1141.

Kieffer S.W., Phakey P.P. and Christie J.M., 1976. Shock processes in porous quartzite: Transmission electron microscope observations and theory. Contributions to Mineralogy and Petrology 59 (1), 41-93.

Kloosterman H., 1976. Apophoreta - 2. Catastrophist Geology 1 (2), 57.

Koeberl C., Claeys P., Hecht L. and McDonald I., 2012. Geochemistry of impactites. Elements 8 (1), 37-42.

Koeberl C., Masaitis V.L., Shafranovsky G.I., Gilmour I., Langenhorst F. and Schrauder M., 1997. Diamonds from the Popigai impact structure, Russia. Geology 25 (11), 967-970.

References

Konyashin I., Zern A., Mayer J., Aldinger F., Babaev V., Khvostov V. and Guseva M., 2001. A new carbon modification: 'n-diamond' or face-centred cubic carbon. Diamond and Related Materials 10 (1), 99-102.

Konyashin I., Khvostov V., Babaev V., Guseva M., Mayer J. and Sirenko A., 2006. A new hard allotropic form of carbon: Dream or reality? International Journal of Refractory Metals and Hard Materials 24 (1-2), 17-23.

Kromer B., Friedrich M., Hughen K.A., Kaiser F., Remmele S., Schaub M. and Talamo S., 2004. Late glacial 14C ages from a floating, 1382-ring pine chronology. Radiocarbon 46 (3), 1203-1209.

Kuehn S.C., Froese D.G., Carrara P.E., Foit Jr. F.F., Pearce N.J.G. and Rotheisler P., 2009. Major- and trace-element characterization, expanded distribution, and a new chronology for the latest Pleistocene Glacier Peak tephras in western North America. Quaternary Research 71 (2), 201-216.

Kurbatov A.V., Mayewski P.A., Steffenson J.P., West A., Kennett D.J., Kennett J.P., Bunch T.E., Handley M., Introne D.S., Que Hee S.S., Mercer C., Sellers M., Shen F., Smeed S.B., Weaver J.C., Wittke J.H., Stafford T.W., Donovan J.J., Xie S.R., J.J., Stitch A., Kinzie C.R. and Wolback W.S., 2010. Discovery of a nanodiamond-rich layer in the Greenland ice sheet. Journal of Glaciology 56 (199), 747-757.

Küster M. and Preusser F., 2009. Late Glacial and Holocene aeolian sands and soil formation from the Pomeranian outwash plain (Mecklenburg, NE-Germany). Quaternary Science Journal 58 (2), 156-163.

Kyte F.T., Zhou L. and Wasson J.T., 1988. New evidence on the size and possible effects of a late Pliocene oceanic asteroid impact. Science 241 (4861), 63-65.

Langenhorst F. and Deutsch A., 1994. Shock experiments on pre-heated α- and β-quartz: I. Optical and density data. Earth and Planetary Science Letters 125 (1-4), 407-420.

Langenhorst F., 2002. Shock metamorphism of some minerals: Basic introduction and microstructural observations. Vestnik Ceskeho Geologickeho Ustavu 77 (4), 265-282.

Langenhorst F. and Deutsch A., 2012. Shock metamorphism of minerals. Elements 8 (1), 31-36.

LaViolette P.A., 2011. Evidence for a solar flare cause of the Pleistocene mass extinction. Radiocarbon 53 (2), 303-323.

Lea D.W., Pak D.K., Peterson L.C. and Hughen K.A., 2003. Synchroneity of tropical and high-latitude Atlantic temperatures over the last glacial termination. Science 301 (5638), 1361-1364.

LeCompte M.A., Goodyear A.C., Demitroff M.N., Batchelor D., Vogel E.K., Mooney C., Rock B.N. and Seidel A.W., 2012. Independent evaluation of conflicting microspherule results from different investigations of the Younger Dryas impact hypothesis. Proceedings of the National Academy of Sciences 106 (43), 18155-18158.

Litt T., Schmincke H. and Kromer B., 2003. Environmental response to climatic and volcanic events in central Europe during the Weichselian Lateglacial. Quaternary Science Reviews 22 (1), 7-32.

Lohne Ø.S., Mangerud J., Birks, H.H., 2013. Precies ^{14}C ages of the Vedde and Saksunarvatn ashes and the Younger Dryas boundaries from western Norway and their comparison with the Greenland Ice Core (GICC05) chronology. Jounral of Quaternary Science 28 (5), 490-500.

Lowe J.J., Hoek W.Z. and INTIMATE group, 2001. Inter-regional correlation of palaeoclimatic records for the Last Glacial–Interglacial Transition: a protocol for improved precision recommended by the INTIMATE project group. Quaternary Science Reviews 20 (11), 1175-1187.

Lowe J.J., Rasmussen S.O., Björck S., Hoek W.Z., Steffensen J.P., Walker M.J.C. and Yu Z.C., 2008. Synchronisation of palaeoenvironmental events in the North Atlantic region during the Last Termination: a revised protocol recommended by the INTIMATE group. Quaternary Science Reviews 27 (1-2), 6-17.

Lowell T.V. and Kelly M.A., 2008. Climate: Was the Younger Dryas global? Science 321 (5887), 348-349.

Lowell T.V., Applegate P.J., Fisher T.G. and Lepper K., 2013. What caused the low-water phase of glacial Lake Agassiz? Quaternary Research 80 (3), 370-382.

Mahaney W.C., Kalm V., Krinsley D.H., Tricart P., Schwartz S., Dohm J., Kim K.J., Kapran B., Milner M.W., Beukens R., Boccia S., Hancock R.G.V., Hart K.M. and Kelleher B., 2010a. Evidence from the northwestern Venezuelan Andes for extraterrestrial impact: The black mat enigma. Geomorphology 116 (1-2), 48-57.

Mahaney W.C., Krinsley D. and Kalm V., 2010b. Evidence for a cosmogenic origin of fired glaciofluvial beds in the northwestern Andes: Correlation with experimentally heated quartz and feldspar. Sedimentary Geology 231 (1-2), 31-40.

Mahaney W.C., Krinsley D., Langworthy K., Kalm V., Havics T., Hart K.M., Kelleher B.P., Schwartz S., Tricart P. and Beukens R., 2011. Fired glaciofluvial sediment in the northwestern Andes: Biotic aspects of the Black Mat. Sedimentary Geology 237 (1-2), 73-83.

Mahaney W.C., Keiser L., Krinsley D., Kalm V., Beukens , Roelf and West A., 2013. New evidence from a black mat site in the northern Andes supporting a cosmic impact 12,800 years ago. The Journal of geology 121 (4), 309-325.

Mangerud J., Andersen S.T., Berglund B.E. and Donner J.J., 1974. Quaternary stratigraphy of Norden, a proposal for terminology and classification. Boreas 3 (3), 109-128.

Mangerud J., Gulliksen S. and Larsen E., 2010. 14C□ dated fluctuations of the western flank of the Scandinavian Ice Sheet 45–25 kyr BP compared with Bølling–Younger Dryas fluctuations and Dansgaard–Oeschger events in Greenland. Boreas 39 (2), 328-342.

Marguerie D. and Hunot J., 2007. Charcoal analysis and dendrology: data from archaeological sites in north-western France. Journal of Archaeological Science 34 (9), 1417-1433.

Marlon J.R., Bartlein P.J., Walsh M.K., Harrison S.P., Brown K.J., Edwards M.E., Higuera P.E., Power M.J., Anderson R.S., Briles C., Brunelle A., Carcaillet C., Daniels M., Hu F.S., Lavoie M., Long C., Minckley T., Richard P.J.H., Scott A.C., Shafer D.S., Tinner W., Umbanhowar Jr. C.E. and Whitlock C., 2009. Wildfire responses to abrupt climate change in North America. Proceedings of the National Academy of Sciences 106 (8), 2519-2524.

Marshal W., Head K., Clough R. and Fisher A., 2012. Exceptional iridium concentrations found at the Allerød-Younger Dryas transition in sediments from Bodmin Moor in southwest England. Quaternary International 279-280, 308.

Masaitis V.L., 1998. Popigai crater: Origin and distribution of diamond-bearing impactites. Meteoritics and Planetary Science 33 (2), 349-359.

Mayewski P.A., Meeker L.D., Whitlow S., Twickler M.S., Morrison M.C., Alley R.B., Bloomfield P. and Taylor K., 1993. The atmosphere during the Younger Dryas. Science 261 (5118), 195-197.

McCall G.J.H., 2009. The carbonado diamond conundrum. Earth-Science Reviews 93 (3-4), 85-91.

McParland L.C., Collinson M.E., Scott A.C. and Campbell G., 2009. The use of reflectance values for the interpretation of natural and anthropogenic charcoal assemblages. Archaeological and Anthropological Sciences 1, 249-261.

McParland L.C., Collinson M.E., Scott A.C., Campbell G. and Veal R., 2010. Is vitrification in charcoal a result of high temperature burning of wood? Journal of Archaeological Science 37 (10), 2679-2687.

Meese D.A., Gow A.J., Alley R.B., Zielinski G.A., Grootes P.M., Ram M., Taylor K.C., Mayewski P.A. and Bolzan J.F., 1997. The Greenland Ice Sheet Project 2 depth-age scale: methods and results. Journal of Geophysical Research 102 (C12), 26411-26423.

Melott A.L., Thomas B.C., Dreschhoff G. and Johnson C.K., 2010. Cometary airbursts and atmospheric chemistry: Tunguska and a candidate Younger Dryas event. Geology 38 (4), 355-358.

Mignan A., Grossi P. and Muir-Wood R., 2011. Risk assessment of Tunguska-type airbursts. Natural Hazards 56 (3), 869-880.

Mohling J.W., 2004. Exogenic fulgurites from Elko County, Nevada: A new class of fulgurite associated with large soil-gravel fulgurite tubes. Rocks & Minerals 79 (5), 334-340.

Mook W.G. and Streurman H.J., 1983. Physical and chemical aspects of radiocarbon dating. Pact Publications 8, 31-55.

Mook W.G. and van der Plicht J., 1999. Reporting 14C activities and concentrations. Radiocarbon 41, 227-239.

Morgan J., Lana C., Kearsley A., Coles B., Belcher C., Montanari S., Díaz-Martínez E., Barbosa A. and Neumann V., 2006. Analyses of shocked quartz at the global K-P boundary indicate an origin from a single, high-angle, oblique impact at Chicxulub. Earth and Planetary Science Letters 251 (3-4), 264-279.

Morrison D., 2010. Did a Cosmic Impact Kill the Mammoths? Sceptical Inquirer 43 (3), 14-18.

Murton J.B., Bateman M.D., Dallimore S.R., Teller J.T. and Yang Z., 2010. Identification of Younger Dryas outburst flood path from Lake Agassiz to the Arctic Ocean. Nature 464, 740-743.

Napier B. and Asher D., 2009. The Tunguska impact event and beyond. Astronomy & Geophysics 50 (1), 1.18-1.26.

Napier W.M., 2010. Palaeolithic extinctions and the Taurid Complex. Monthly Notices of the Royal Astronomical Society 405 (3), 1901-1906.

Overholt A.C. and Melott A.L., 2013. Cosmogenic nuclide enhancement via deposition from long-period comets as a test of the Younger Dryas impact hypothesis. Earth and Planetary Science Letters 377–378, 55-61.

Paquay F.S., Goderi S., Ravizzaa G., Vanhaeckc F., Boydd M., Surovelle T.A., Holliday V.T., Haynes Jr V.C. and Claeys P., 2009. Absence of geochemical evidence for an impact event at the Bølling–Allerød/Younger Dryas transition. Proceedings of the National Academy of Sciences 106 (51), 21505-21510.

References

Petaev M.I., Huang S., Jacobsen S.B. and Zindler A., 2013. Large Pt anomaly in the Greenland ice core points to a cataclysm at the onset of Younger Dryas. Proceedings of the National Academy of Sciences 110 (32), 12917-12920.

Phelps A.W., 1999. Interstellar Diamond: I. Condensation and Nucleation. Lunar and Planetary Science Conference XXX, 1749.

Pigati J.S., Latorre C., Rech J.A., Betancourt J.L., Martínez K.E. and Budahn J.R., 2012. Accumulation of impact markers in desert wetlands and implications for the Younger Dryas impact hypothesis. Proceedings of the National Academy of Sciences 109 (19), 7208-7212.

Pinter N. and Ishman S.E., 2008. Impacts, mega-tsunami, and other extraordinary claims. GSA Today 18 (1), 37-38.

Pinter N., Scott A.C., Daulton T.L., Podoll A., Koeberl C., Anderson R.S. and Ishman S.E., 2011. The Younger Dryas impact hypothesis: A requiem. Earth-Science Reviews 106, 247-264.

Qin L.C., Zhou D., Krauss A.R. and Gruen D.M., 1998. TEM characterization of nanodiamond thin films. Nanostructured Materials 10 (4), 649-660.

Rach O., Brauer A., Wilkes H., Sachse D., 2014. Delayed hydrological response to Greenland cooling at the onset of the Younger Dryas in western Europe. Nature Geoscience 7, 109-112.

Rasmussen S.O., Andersen K.K., Svensson A.M., Steffensen J.P., Vinther B.M., Clausen H.B., Siggaard-Andersen M.-., Johnsen S.J., Larsen L.B., Dahl-Jensen D., Bigler M., Roethlisberger R., Fischer H., Goto-Azuma K., Hansson M.E. and Ruth U., 2006. A new Greenland ice core chronology for the last glacial termination. Journal of Geophysical Research 111 (D06102), 1-16.

Rasmussen B. and Koeberl C., 2004. Iridium anomalies and shocked quartz in a Late Archean spherule layer from the Pilbara craton: New evidence for a major asteroid impact at 2.63 Ga. Geology 32 (12), 1029-1032.

Regev L., Eckmeier E., Mintz E., Weiner S. and Boaretto E., 2011. Radiocarbon concentrations of wood ash calcite: Potential for dating. Radiocarbon 53 (1), 117-127.

Reimer P.J., Baillie M.G.L., Bard E., Bayliss A., Beck J.W., Blackwell P.G., Ramsey C.B., Buck C.E., Burr G.S., Edwards R.L., Friedrich M., Grootes P.M., Guilderson T.P., Hajdas I., Heaton T.J., Hogg A.G., Hughen K.A., Kaiser K.F., Kromer B., McCormac F.G., Manning S.W., Reimer R.W., Richards D.A., Southon J.R., Talamo S., Turney C.S.M., van der Plicht J. and Weyhenmeyer C.E., 2009. IntCal09 and Marine09 radiocarbon age calibration curves, 0-50,000 years cal BP. Radiocarbon 51 (4), 1111-1150.

Reimer P.J., Bard E., Bayliss A., Beck J.W., Blackwell P.G., Bronk Ramsey C., Grootes P.M., Guilderson T.P., haflidason h., Hajdas I., Hatté C., Heaton T.J., Hoffmann D.L., Hogg A.G., Hughen K.A., Kaiser K.F., Kromer B., Manning S.W., Niu M., Reimer R.W., Richards D.A., Scott E.M., Southon J.R., Staff R.A., Turney C.S.M. and van der Plicht J., 2013. IntCal13 and Marine13 Radiocarbon Age Calibration Curves 0–50,000 Years cal BP. Radiocarbon 55 (4), 1869-1887.

Reimold W.U. and Jourdan F., 2012. Impact! - Bolides, craters, and catastrophes. Elements 8 (1), 19-24.

Renssen H., Geel B.V., van der Plicht J. and Magny M., 2000. Reduced solar activity as a trigger for the start of the Younger Dryas? Quaternary International 67-71, 373-383.

Revelle D.O., 1997. Historical detection of atmospheric impacts by large bolides using acoustic-gravity waves. Annals of the New York Academy of Sciences 822, 284-302.

Riede F., 2008. The Laacher See-eruption (12,920 BP) and material culture change at the end of the Allerød in Northern Europe. Journal of Archaeological Science 35 (3), 591-599.

Ruban D.A., 2009. The survival of megafauna after the end-Pleistocene impact: a lesson from the Cretaceous/Tertiary boundary. Geologos 15 (2), 129-132.

Sawlowicz Z., 1993a. Pyrite framboids and their development: a new conceptual mechanism. Geologische Rundschau 82 (1), 148-156.

Sawlowicz Z., 1993b. Iridium and other platinum-group elements as geochemical markers in sedimentary environments. Palaeogeography, Palaeoclimatology, Palaeoecology 104 (1-4), 253-270.

Schaub M., Büntgen U., Kaiser K.F., Kromer B., Talamo S., Andersen K.K. and Rasmussen S.O., 2008. Lateglacial environmental variability from Swiss tree rings. Quaternary Science Reviews 27 (1-2), 29-41.

Schiffer M.B., 1986. Radiocarbon dating and the "old wood" problem: The case of the Hohokam chronology. Journal of Archaeological Science 13 (1), 13-30.

Schmincke H.-., Park C. and Harms E., 1999. Evolution and environmental impacts of the eruption of Laacher See Volcano (Germany) 12,900 a BP. Quaternary International 61, 61-72.

Schulz M., Paul A. and Timmermann A., 2002. Relaxation oscillators in concert: A framework for climate change at millennial timescales during the late Pleistocene. Geophysical Research Letters 29 (24), 46-1.

Schwander M. and Partes K., 2011. A review of diamond synthesis by CVD processes. Diamond and Related Materials 20 (9), 1287-1301.

Scott A.C., Pinter N., Collinson M.E., Hardiman M., Anderson R.S., Brain A.P.R., Smith S.Y., Marone F. and Stampanoni M., 2010. Fungus, not comet or catastrophe, accounts for carbonaceous spherules in the Younger Dryas "impact layer". Geophysical Research Letters 37 (14), L14302.

Shibata K., Kamioka H., Kaminsky F.V., Koptil V.I. and Svisero D.P., 1993. Rare earth element patterns of carbonado and yakutite: evidence for their crustal origin. Mineralogical Magazine 57 (4), 607-611.

Sima A., Paul A. and Schulz M., 2004. The Younger Dryas - An intrinsic feature of late Pleistocene climate change at millennial timescales. Earth and Planetary Science Letters 222 (3-4), 741-750.

Smit J. and Brinkhuis H., 1996. The Geulhemmerberg Cretaceous/Tertiary boundary section (Maastrichtian type area, SE Netherlands); summary of results and a scenario of events. Geologie en Mijnbouw 75 (2-3), 283-293.

Smith D.C. and Godard G., 2009. UV and VIS Raman spectra of natural lonsdaleites: Towards a recognised standard. Spectrochimica Acta Part A: Molecular and Biomolecular Spectroscopy 73 (3), 428-435.

Southon J.R. and Taylor R.E., 2002. Brief comments on 'Terrestrial evidence of a nuclear catastrophy in palaeoindian times' by Richard B. Firestone and William Topping. Mammoth Trumpet 17 (2), 14-17.

Spooner I., Stevens G., Morrow J., Pufahl P., Grieve R., Raeside R., Pilon J., Stanley C., Barr S. and McMullin D., 2009. Identification of the Bloody Creek structure, a possible impact crater in southwestern Nova Scotia, Canada. Meteoritics & Planetary Science 44 (8), 1193-1202.

Stähle V., Altherr R., Koch M. and Nasdala L., 2008. Shock-induced growth and metastability of stishovite and coesite in lithic clasts from suevite of the Ries impact crater (Germany). Contributions to Mineralogy and Petrology 155 (4), 457-472.

Steffensen J.P., Andersen K.K., Bigler M., Clausen H.B., Dahl-Jensen D., Fischer H., Goto-Azuma K., Hansson M., Johnsen S.J., Jouzel J., Masson-Delmotte V., Popp T., Rasmussen S.O., Röthlisberger R., Ruth U., Stauffer B., Siggaard-Andersen M.-., Sveinbjörnsdóttir Á.E., Svensson A. and White J.W.C., 2008. High-resolution Greenland ice core data show abrupt climate change happens in few years. Science 321 (5889), 680-684.

Stöffler D. and Langenhorst F., 1994. Shock metamorphism of quartz in nature and experiment: I. Basic observation and theory. Meteoritics 29 (2), 155-181.

Stroud R.M., Chisholm M.F., Heck P.R., Alexander C.M.O. and Nittler L.R., 2011. Supernova shock-wave-induced co-formation of glassy carbon and nanodiamond. Astrophysical Journal Letters 738 (2), L.27.

Stuiver M., Grootes P.M. and Braziunas T.F., 1995. The GISP2 $\delta^{18}O$ Climate record of the past 16,500 years and the role of the sun, ocean, and volcanoes. Quaternary Research 44 (3), 341-354.

Su Z., Zhou W. and Zhang Y., 2011. New insight into the soot nanoparticles in a candle flame. Chemical Communications 47, 4700-4702.

Surovell T.A., Holliday V.T., Gingerich J.A.M., Ketron C., Haynes Jr. C.V., Hilman I., Wagner D.P., Johnson E. and Claeyes P., 2009. An independent evaluation of the Younger Dryas extraterrestrial impact hypothesis. Proceedings of the National Academy of Sciences 106 (43), 18155-18158.

Svetsov V. , 2008. Terminal radiation and fires after impacts of cosmic objects. In: Adushkin V.V. and Nemchinov I.V. (Eds.), Catastrophic events caused by cosmic objects. Springer, 207-226.

Svetsov V. and Shuvalov V. , 2008. Tunguska Catastrophe of 30 June 1908. In: Adushkin V. and Nemchinov I. (Eds.), Catastrophic events caused by cosmic objects. Springer, 227-266.

Tagle R. and Hecht L., 2006. Geochemical identification of projectiles in impact rocks. Meteoritics and Planetary Science 41 (11), 1721-1735.

Tancredi G., Ishitsuka J., Schultz P.H., Harris R.S., Brown P., Revelle D.O., Antier K., Pichon A.L., Rosales D., Vidal E., Varela M.E., Sánchez L., Benavente S., Bojorquez J., Cabezas D. and Dalmau A., 2009. A meteorite crater on Earth formed on September 15, 2007: The Carancas hypervelocity impact. Meteoritics and Planetary Science 44 (12), 1967-1984.

References

Tarasov L. and Peltier W.R., 2005. Arctic freshwater forcing of the Younger Dryas cold reversal. Nature 435 (7042), 662-665.

Tarasov L. and Peltier W.R., 2006. A calibrated deglacial drainage chronology for the North American continent: evidence of an Arctic trigger for the Younger Dryas. Quaternary Science Reviews 25 (7-8), 659-688.

Teller J.T., Boyd M., Yang Z., Kor P.S.G. and Mokhtari Fard A., 2005. Alternative routing of Lake Agassiz overflow during the Younger Dryas: new dates, paleotopography, and a re-evaluation. Quaternary Science Reviews 24 (16-17), 1890-1905.

Teller J.T., 2013. Lake Agassiz during the Younger Dryas. Quaternary Research 80 (3), 361-369.

Tian H., Schryvers D. and Claeys P., 2011. Nanodiamonds do not provide unique evidence for a Younger Dryas impact. Proceedings of the National Academy of Sciences 108 (1), 40-44.

Tollmann A., 2001. Kosmische gross-impakte der Jung- und Nacheiszeit (Cosmic Mega-Impacts During the Late- and Post-Pleistocene). Sitzungsberichte Abt. I - Ostenreichische Akademie der Wissenschaften 208, 3-13.

Tomita S., Fujii M., Hayashi S. and Yamamoto K., 2000. Transformation of carbon onions to diamond by low-temperature heat treatment in air. Diamond and Related Materials 9 (3), 856-860.

Trepmann C.A. and Spray J. G., 2006. Shock-induced crystal-plastic deformation and post-shock annealing of quartz microstructural evidence from crystalline target rocks of the Charlevoix impact structure, Canada. European Journal of Mineralogy 18 (2), 161-173.

van der Hammern T., 1951. Late-Glacial flora and periglacial phenomena in The Netherlands. PhD thesis, Leidse Geologische Mededelingen 17.

van der Hammen T. and van Geel B., 2008. Charcoal in soils of the Allerød-Younger Dryas transition were the result of natural fires and not necessarily the effect of an extra- terrestrial impact. Geologie en Mijnbouw/Netherlands Journal of Geosciences 87 (4), 359-361.

van der Plicht J., Wijma A., Aerts A.T., Pertuisot M.H.P. and Meijer H.A.J., 2000. The Groningen AMS facility: status report. Nuclear Instruments and Methods in Physics Research B172, 58-65.

van Geel B., Coope G.R. and van der Hammen T., 1989. Palaeoecology and stratigraphy of the lateglacial type section at Usselo (the Netherlands). Review of Palaeobotany and Palynology 60 (1-2), 25-129.

van Hoesel A., Hoek W.Z., Braadbaart F., van der Plicht J., Pennock G.M. and Drury M.R., 2012. Nanodiamonds and wildfire evidence in the Usselo horizon postdate the Allerød-Younger Dryas boundary. Proceedings of the National Academy of Sciences 109 (20), 7648-7653.

van Hoesel A., Hoek W.Z., van der Plicht J., Pennock G.M. and Drury M.R., 2013. Cosmic impact or natural fires at the Allerød–Younger Dryas boundary: A matter of dating and calibration. Proceedings of the National Academy of Sciences 110 (41), E3896.

van Hoesel A., Hoek W.Z., Pennock G.M. and Drury M.R., 2014. The Younger Dryas impact hypothesis: a critical review. Quaternary Science Reviews 83, 95-114

Vandenberghe D.A.G., Derese C., Kasse C. and Van den Haute P., 2013. Late Weichselian (fluvio-)aeolian sediments and Holocene drift-sands of the classic type locality in Twente (E Netherlands): A high-resolution dating study using optically stimulated luminescence. Quaternary Science Reviews 68, 96-113.

Vanmontfort B., van Gils M., Paulissen E., Bastiaens J., de Bie M. and Meirsman E., 2010a. Human occupation of the Late and Early Post-Glacial environments in the Liereman Landscape (Campine, Belgium). Journal of archaeology in the low countries. 2 (2), http://dpc.uba.uva.nl/jalc/02/nr02/a02.

Vanmontfort B., Yperman W., Lambrechts B., van Gils M. and Geerts F., 2010b. Een finaalpaleolithisch en meslotisch sitecomplex the Lommel, Molste Nete. Opgravingscampagne 2010. Notae Praehistoricae 30, 29-34.

Vermeersch P.M., 2011. The human occupation of the Benelux during the Younger Dryas. Quaternary International 242 (2), 267-276.

Voldman G.G., Genge M.J., Albanesi G.L., Barnes C. and Ortega G., 2012. Cosmic spherules from the Ordovician of Argentina. Geological Journal 48 (2-3), 222-235.

Waters M.R. and Stafford T.W., 2007. Redefining the Age of Clovis: Implications for the Peopling of the Americas. Science 315 (5815), 1122-1126.

Weixin Xu, Van Der Voo R. and Peacor D.R., 1994. Are magnetite spherules capable of carrying stable magnetizations? Geophysical Research Letters 21 (7), 517-520.

Wirth R. and Rocholl A., 2003. Nanocrystalline diamond from the Earth's mantle underneath Hawaii. Earth and Planetary Science Letters 211 (3-4), 357-369.

Wittke J.H., Bunch T.E., Kennett J.P., Kennett D.J., Culleton B.J., Tankersley K.B., Daniel I.R., Kloosterman J.B., Kletetschka G., West A. and Firestone R.B., 2013a. Reply to van Hoesel et al.: Impact-related Younger Dryas boundary nanodiamonds from The Netherlands. Proceedings of the National Academy of Sciences 110 (41), E3897-E3898.

Wittke J.H., Weaver J.C., Bunch T.E., Kennett J.P., Kennett D.J., Moore A.M.T., Hillman G.C., Tankersley K.B., Goodyear A.C., Moore C.R., Daniel I.R., Ray J.H., Lopinot N.H., Ferraro D., Israde-Alcántara I., Bischoff J.L., DeCarli P.S., Hermes R.E., Kloosterman J.B., Revay Z., Howard G.A., Kimbel D.R., Kletetschka G., Nabelek L., Lipo C.P., Sakai S., West A. and Firestone R.B., 2013b. Evidence for deposition of 10 million tonnes of impact spherules across four continents 12,800 y ago. Proceedings of the National Academy of Sciences 110 (23), E2088-E2097.

Wohlfarth B., 1996. The chronology of the last termination: A review of radiocarbon-dated, high-resolution terrestrial stratigraphies. Quaternary Science Reviews 15 (4), 267-284.

Wolbach W.S., Lewis R.S. and Anders E., 1985. Cretaceous extinctions: Evidence for wildfires and search for meteoritic material. Science 230 (4722), 167-170.

Wood J.R. and Wilmshurst J.M., 2013. Accumulation rates or percentages? How to quantify Sporormiella and other coprophilous fungal spores to detect late Quaternary megafaunal extinction events. Quaternary Science Reviews 77, 1-3.

Wu Y., Sharma M., LeCompte M.A., Demitroff M.N. and Landis J.D., 2013. Origin and provenance of spherules and magnetic grains at the Younger Dryas boundary. Proceedings of the National Academy of Sciences 110 (38), E3557-E3566.

Wulf S., Ott F., Słowiński M., Noryśkiewicz A.M., Dräger N., Martin-Puertas C., Czymzik M., Neugebauer I., Dulski P., Bourne A.J., Błaszkiewicz M. and Brauer A., 2013. Tracing the Laacher See Tephra in the varved sediment record of the Trzechowskie palaeolake in central Northern Poland. Quaternary Science Reviews 76, 129-139.

Yang Z.Q., Verbeeck J., Schryvers D., Tarcea N., Popp J. and Rösler W., 2008. TEM and Raman characterisation of diamond micro- and nanostructures in carbon spherules from upper soils. Diamond and Related Materials 17 (6), 937-943.

Publications

Published

van Hoesel, A., Hoek, W.Z., Braadbaart, F., van der Plicht, J., Pennock. G.M., and Drury, M.R. (2012). *Nanodiamonds and wildfire evidence post-date the Allerod-Younger Dryas boundary.* Proceedings of the National Academy of Sciences 109 (20), 7648-7653.

van Hoesel, A. , Hoek, W.Z., van der Plicht, J., Pennock. G.M., and Drury, M.R. (2013) *Cosmic impact or natural fires at the Allerod-Younger Dryas boundary: a matter of dating and calibration.* Proceedings of the National Academy of Sciences 110 (41), E3896.

van Hoesel, A., Hoek, W.Z., Pennock, G.M., and Drury, M.R. (2014) *The Younger Dryas impact hypothesis: a critical review.* Quaternary Science Reviews 83, 95-114.

In prep.

van Hoesel, A., Hoek, W.Z., Pennock, G.M., Kaiser., K., O. Plümper, M. Jankowski, M.F. Hamers, N. Schlaak, M. Küster, A.V. Andronikov and Drury M.R.. *Shocked quartz in the Usselo horizon.*

van Hoesel, A., Braadbaart, F., Pennock, G.M., and Drury, M.R.. *Charcoal and glass-like carbon: a TEM study.*

Curriculum Vitae

On July 5th, 1986 Annelies van Hoesel was born in Meppel as the oldest of two sisters. After spending her first four years living in Steenwijk, her parents decided to move to the town of Duiven, where she finished her primary school, montessorischool De Groene Ring, in 1998. In 2004 she got her high school diploma from the Lorentz College in nearby Arhnem, where she had taken bilingual classes. Having a wide interest in not only science but also subjects such as philosophy, theology, or ancient culture and mythology Annelies was not entirely sure which direction to take after high school. That is, until a kind biologist at a university open day, suggested she should take a look at the Geoarchaeology stand. There she was suddenly surrounded by a horde of enthusiastic earth scientists, and it did not take her long to decide that this discipline was perfect for her (in retrospect the favourite book on volcanoes and random stones in her bedroom should have been a hint). With an interest in maps, (river) patterns, the recent geological past, the hands on of fieldwork and the logic of modelling, she got her bachelor in Physical Geography (cum laude) at Utrecht University in 2007. In 2009 she finished the System Earth Modelling Master (also cum laude). Working as a junior researcher on the sand-depth map of Gelderland project at the department of Physical Geography during the summer, she decided that she wanted to stay in research. Having finished her master thesis on modelling the opening of the Dover Strait it was again time to study a big event and she applied for a PhD position on the Younger Dryas impact hypothesis. Staying in Utrecht, moving back to the Earth Sciences department to learn about microstructures, electron microscopy and meteorite impacts, she worked on the project from late 2009 until early 2014. Realising just how interesting charcoal and fire are, Annelies is now conducting on a short research project on burned materials for the Human Origins group at Leiden University, Faculty of Archaeology, mostly working in the lab of Dutch Cultural Heritage Agency in Amsterdam.

Acknowledgements
Dankwoord

Great, you have made it to the end of my thesis! Or you just started with what is known as the most-read part of most PhD dissertations, which is also fine. Doing a PhD is a long journey that takes you along a varying landscape of beautiful sunny mountain tops, shadowy valleys and sometimes long monotonous plains. Along the road, there are many people to help you find the way, repair your gear, walk along for some time or sit down with you during a rest stop. Without those people I would have stranded somewhere in the middle of nowhere rather than finishing the trip with this booklet to prove it. In this section I would like to thank all these people for all their help and support.

First I would like to thank my advisors and 'tourguides' of my journey. Martyn, it was great working with you, you were never too unimaginative to see a crater somewhere. Unfortunately I'm sorry could not find a Dutch impact layer for you. Maybe you'll have better luck with the Zuidwal volcano. You know what they say: driemaal is scheepsrecht. Thank you for letting me work in this project, and for your guidance and support. Wim, I did not see you as much as the other two as you were 'all the way' over in the other building. Thank you for our discussions and the fieldwork, somehow always near a place to eat. Thank you also for showing me that I had sometimes learned more already than I had thought, by having no clue what I was talking about when I was going on about some electron microscopy results. Gill, you were always willing to review my paper drafts in detail. I'll admit that I was not always happy with all your comments upon receiving them, but in the end they always helped to improve my work. Thank you for all your help, your kind words, (the home grown vegetables), our discussions and chats. Gill, you are an inspiration.
I would also like to use this space to thank my dissertation committee Achim Brauer, Christian Koeberl, Hans Renssen, Jan Smit, and Nick Schryvers, for making time to read my work and their valuable suggestions. For the published chapters, this also includes reviewer 1 and reviewer 2, you guys are great.

All the electron microscopy work presented in this thesis could not have been done without the help of the dynamic duo Hans and Chris, as well as Tilly and Mathijs. For (help with) the sample preparation I would like to thank Roel van Elsas for his help with the density separation of the quartz grains, Otto and Wynanda for doing part of the polishing, Olli for preparing the FIB-cut sample Mark and Tim Tijn for the magnetic separation, Natasja, Helen and Wendy Wolbach for help or advise with the chemical preparation, Freek Braadbaart for the reflectance measurements and Hans van der Plicht for the radiocarbon dating.

In order to get my samples I first needed to find suitable fieldsites. For showing me the Dutch and Belgium fieldsites I would like to thank Bart van Montfoort, Jan Willem de Kort, Jos Deeben, Kay Beets, Kees Kasse and Leo Tebbens. For the fieldwork in north-eastern Germany and Poland I greatly acknowledge Knut Kaiser. Not only for showing me his fieldsite, but also for inviting me to stay at his house and introducing me to Mathias Küster, Michal Jankowski, and Norbert Schlaak. The long drive to the east (and back again) would not have been possible without my field assistant Yvonne. Also Alexander Andronikov and Andy Lotter, thanks for letting me use your samples.
For their interest in my work and discussions on the topic I thank Alex, Freek, Hans, Jim Kennett, Joanne Ballard, Malcolm LeCompte, Mark Hardiman, Simon Blockley, and many others. Although we never met, I should maybe also mention George Howard here, thank you for making keeping up to date with the literature so much easier.

My four years (and three months) at the Earth Science department would not have been the same without my colleagues at the Structural Geology group. Including my first officemate and other extraterrestrial lady Maartje, thanks for the good time and the help with the shocked quartz and CL-imaging. Côme, Auke, Wouter and Herman, the spontaneous coffee breaks in our office were always fun. Cong, appearing in the group at the same time as me, it was good to have you back around for a while in the end. Reinoud, I'll miss you walking in at random times ranting about what ridiculous thing the students wrote this time. Olli, it was great having another practicing 'tem-er' in the group. Maartje 2, it was fun having you as my officemate during my last year, and you always seemed to have the relevant PhD comic at hand. Kalijn, our nextdoor office neighbour, thanks for the chats. And Magda, always ready to lend a helping hand for any administrative issues. Of course I should not forget my colleagues at the HPT-lab, the rest of Earth Sciences and of course at the Physical Geography department: Alejandro, Andre, Anne, Bart, Chris, Collin, Elisenda, Esther, Filip, Germari, Hans, Hans, Harm Jan, Inge Loes, Jan, Jasper, Jeroen, Jon, Juul, Kees, Kim, Maarten, Michiyo, Nelleke, Nico, Peter, Ross, Sander, Sabine, Sabrina, Sonja, Tim, Willem, Wietse, Wout, and others.

Doing a PhD would be a lot more difficult if not for having some life outside of university. For this I would like to thank my friends. First my two good friends and paranimphs: Mariëlle and Robert. Mariëlle, voormalig veldwerk- en stagepartner, tijdens de studie waren we zo onafscheidelijk dat schijnbaar niet iedereen wist wie van ons nou wie was. Doordat ik op de universiteit ben rond blijven hangen terwijl jij voor het echte leven koos zien we elkaar helaas wat minder. Bedankt voor alle gezellig keren avondeten, spelletjesmiddagen en theegeleut. Dear Robert, we did not meet until the second year of my research, when you were already entering your last. It seemed that we were both lost in that canyon, but together we got out. Thank you for your emotional support, your tem knowledge, our dinner chats and top of the hours. To use your own words against you: you are awesome. ;-)
Emma, het is altijd gezellig om met jou te kletsen, of het nu online of offline is. Samen met Annemiek, Debby, Gerlinde, en Nathalie, bedankt voor de leuke roleplay verhalen en de spelletjesmiddagen. André, aka the Portuguese guy, it was great seeing you again at the EGU. Good luck with your own PhD research back in the homeland. Verder wil ik nog even mijn sportvrienden, Agnes, Audri, Jem, Mark, Rick, Rox, Thijs, en de rest, bedanken voor de gezelligheid en de motivatie. Ook Anke, Birgit, Fred, Reb, Valleke en de andere frettenliefhebbers

bedankt, het is altijd fijn om een plek te hebben waar ook ruimte is om gewoon even lekker te klagen (of om over fretten en andere leuke dingen te kletsen).

Most importantly I would like to thank my family for their love and support during my journey. Mijn lieve opa's, die er helaas niet meer bij zijn, en mijn lieve oma's. Grootje, het was me een eer om de kleindochter te zijn die ook iets met die grondlagen deed die jij ook altijd al zo interessant vond. Tante Mar het was altijd gezellig als jij ook toevallig in Teck was. Lieve papa, bedankt voor je enthousiasme en interesse in mijn studierichting, het is altijd fijn om te weten dat je papers iniedergeval door één iemand gelezen worden. Lieve Mama, bedankt voor alle steun en een gezellig weekje zomervakantie. Lief zusje, het is altijd weer leuk om samen te kletsen (ring ring, helleu…), bedankt voor alle gezellige weekendjes (en niet alleen omdat de chaos in mijn huis daarna soms een stuk minder was). En last but definitely not the least (integendeel), mijn allerliefste vriend en rots in de branding Marc. Bedankt voor al je geduld en begrip als ik (weer eens) wat gestresst thuiskwam. Al die keren dat je avondeten voor me gekookt hebt, de heerlijke avondjes gewoon lekker samen bankhangen voor de tv, nog even een wandelingetje maken met het mooie weer of lekker samen sporten. Je weet me altijd weer aan het lachen te maken. Ik hou van je, zonder jou was het me nooit gelukt.